

**ASSOCIATION OF PLASTID LIPID METABOLISM WITH THE ACTIVATION OF  
SYSTEMIC ACQUIRED RESISTANCE IN *ARABIDOPSIS THALIANA***

by

KARTIKEYA KROTHAPALLI

B. Sc. (Agriculture), Acharya N.G. Ranga Agricultural University (ANGRAU), India, 2001

AN ABSTRACT OF A DISSERTATION

submitted in partial fulfillment of the requirements for the degree

DOCTOR OF PHILOSOPHY

Division of Biology  
College of Arts and Sciences

KANSAS STATE UNIVERSITY  
Manhattan, Kansas

2008

## Abstract

Localized inoculation of a plant with an avirulent pathogen results in the activation of systemic acquired resistance (SAR), a defense mechanism that confers enhanced resistance against a variety of pathogens. The activation of SAR requires the translocation of an unknown signal from the pathogen-inoculated organ to the other organs where defenses are primed to respond faster in response to a future attack by a pathogen. Previous studies with the *Arabidopsis thaliana* *dir1* (*defective in induced resistance1*) and *sfd1* (*suppressor of fatty acid desaturase deficiency1*) mutants implicated a role for plant lipids in the activation of SAR. *DIR1* encodes a putative lipid transfer protein and *SFD1* encodes a dihydroxyacetone phosphate (DHAP) reductase involved in plastid glycerolipid metabolism. To further evaluate the role of DHAP reductases and plastid lipids in SAR, the involvement of two additional putative DHAP reductase encoding genes (*AtGPDHp* and *AtGPDHc*) and the *SFD2* gene, which like *SFD1* is involved in plastid glycerolipid metabolism, in SAR was evaluated. Only *SFD2* was found to be essential for SAR. Although the lipid profile of the *sfd2* mutant was similar to that of the *fad5* (*fatty acid desaturase 5*) mutant, *sfd2* is not allelic with *fad5* and does not influence *FAD5* expression. The *SFD2* gene was mapped to an 85 kilo basepairs (kb) region on the third chromosome of *Arabidopsis*. The lipid composition defect of the *sfd2* mutant was partially complemented by two independent recombinant bacterial artificial chromosomes (BACs) that contained genomic DNA spanning the wild type *SFD2* locus. The role of plastid synthesized glycerolipids in the activation of SAR was further evaluated by characterizing SAR in additional *Arabidopsis* mutants that were deficient in plastid lipid metabolism. The requirement of *MGDI* (*MONOGALACTOSYLDIACYLGLYCEROL SYNTHASE 1*), *DGDI* (*DIGALACTOSYLDIACYLGLYCEROL SYNTHASE 1*) and *FAD7* (*FATTY ACID DESATURASE 7*) genes in SAR, confirmed the essential role of plastid glycerolipids, presumably a galactolipid-dependent factor, in signaling associated with the SAR.

**ASSOCIATION OF PLASTID LIPID METABOLISM WITH THE ACTIVATION OF  
SYSTEMIC ACQUIRED RESISTANCE IN *ARABIDOPSIS THALIANA***

by

KARTIKEYA KROTHAPALLI

B. Sc. (Agriculture), Acharya N.G. Ranga Agricultural University (ANGRAU), India, 2001

A DISSERTATION

submitted in partial fulfillment of the requirements for the degree

DOCTOR OF PHILOSOPHY

Division of Biology  
College of Arts and Sciences

KANSAS STATE UNIVERSITY  
Manhattan, Kansas

2008

Approved by:

Major Professor  
Dr. Jyoti Shah

# **Copyright**

KARTIKEYA KROTHAPALLI

2008

## Abstract

Localized inoculation of a plant with an avirulent pathogen results in the activation of systemic acquired resistance (SAR), a defense mechanism that confers enhanced resistance against a variety of pathogens. The activation of SAR requires the translocation of an unknown signal from the pathogen-inoculated organ to the other organs where defenses are primed to respond faster in response to a future attack by a pathogen. Previous studies with the *Arabidopsis thaliana* *dir1* (*defective in induced resistance1*) and *sfd1* (*suppressor of fatty acid desaturase deficiency1*) mutants implicated a role for plant lipids in the activation of SAR. *DIR1* encodes a putative lipid transfer protein and *SFD1* encodes a dihydroxyacetone phosphate (DHAP) reductase involved in plastid glycerolipid metabolism. To further evaluate the role of DHAP reductases and plastid lipids in SAR, the involvement of two additional putative DHAP reductase encoding genes (*AtGPDHp* and *AtGPDHc*) and the *SFD2* gene, which like *SFD1* is involved in plastid glycerolipid metabolism, in SAR was evaluated. Only *SFD2* was found to be essential for SAR. Although the lipid profile of the *sfd2* mutant was similar to that of the *fad5* (*fatty acid desaturase 5*) mutant, *sfd2* is not allelic with *fad5* and does not influence *FAD5* expression. The *SFD2* gene was mapped to an 85 kilo basepairs (kb) region on the third chromosome of *Arabidopsis*. The lipid composition defect of the *sfd2* mutant was partially complemented by two independent recombinant bacterial artificial chromosomes (BACs) that contained genomic DNA spanning the wild type *SFD2* locus. The role of plastid synthesized glycerolipids in the activation of SAR was further evaluated by characterizing SAR in additional *Arabidopsis* mutants that were deficient in plastid lipid metabolism. The requirement of *MGDI* (*MONOGALACTOSYLDIACYLGLYCEROL SYNTHASE 1*), *DGDI* (*DIGALACTOSYLDIACYLGLYCEROL SYNTHASE 1*) and *FAD7* (*FATTY ACID DESATURASE 7*) genes in SAR, confirmed the essential role of plastid glycerolipids, presumably a galactolipid-dependent factor, in signaling associated with the SAR.

## Table of Contents

List of Figures .....	xi
List of Tables .....	xiii
Acknowledgements .....	xiv
Dedication .....	xv
CHAPTER 1 - Introduction .....	1
The threat of plant diseases .....	1
Plant defense response .....	2
Innate Resistance .....	2
Gene-for-gene resistance .....	3
Defense signaling mechanisms .....	4
Salicylic acid .....	4
Salicylic acid binding proteins .....	6
NPR1 .....	6
Jasmonic acid .....	8
Cross talk between SA and JA signaling .....	10
Induced resistance .....	11
Induced systemic resistance (ISR) .....	11
Systemic acquired resistance (SAR) .....	12
Lipids in plant defense .....	14
Concluding remarks .....	16
Figure 1.1 SAR induction in plants .....	18
Figure 1.2 Schematic SAR signaling pathway .....	20
References .....	22
CHAPTER 2 - The role of dihydroxyacetone phosphate (DHAP) reductases in plant defense ...	41
Materials and methods .....	44
Results .....	48
Homology of SFD1 to AtGPDHp, AtGPDHc and At3g07690 .....	48

Identification of homozygous plants from T-DNA insertion lines of AtGPDHp and AtGPDHc .....	48
Analysis of the lipid composition of AtGPDHp and AtGPDHc.....	50
Basal defense phenotype of the insertion lines of AtGPDHp and AtGPDHc .....	50
AtGPDHp does not play a role in SAR.....	51
Discussion.....	52
References.....	54
Figure legends.....	58
Fig 2.1 Homology of SFD1 to the predicted DHAP reductases .....	58
Fig 2.2 Model for identification homozygous T-DNA insertion lines by PCR.....	58
Fig 2.3 Identification of homozygous plants from T-DNA insertion lines of AtGPDHp and AtGPDHc .....	59
Fig 2.4 RT-PCR analysis of gene expression .....	59
Fig 2.5 Basal defense phenotype of the insertion lines of AtGPDHp and AtGPDHc .....	60
Fig 2.6 Analysis of the SAR phenotype of the <i>atgpdhp</i> mutant plant .....	60
Fig 2.7 Analysis of the SAR phenotype of the <i>atgpdhpsfd1</i> double mutant plants .....	61
Table 2.1 lipid composition of AtGPDHp and AtGPDHc.....	61
Figures .....	62
Figure 2.1 Homology of SFD1 to the predicted DHAP reductases.....	62
Figure 2.2 Schematic for identification homozygous T-DNA insertion lines by PCR.....	64
Figure 2.3 Identification of homozygous plants from T-DNA insertion lines of AtGPDHp and AtGPDHc .....	65
Figure 2.4 RT-PCR analysis of gene expression .....	66
Figure 2.5 Basal defense phenotype of the insertion lines of AtGPDHp and AtGPDHc ....	67
Figure 2.6 Analysis of the SAR phenotype of the <i>atgpdhp</i> mutant plant .....	69
Figure 2.7 Analysis of the SAR phenotype of the <i>atgpdhp sfd1</i> double mutant plants .....	70
Table 2-1 Lipid composition of AtGPDHp and AtGPDHc .....	71
CHAPTER 3 - Involvement of galactolipids in SAR .....	72
Lipid biosynthesis in Arabidopsis plastids .....	72
Materials and methods .....	78
Results.....	81

SAR is compromised in suppressors of <i>ssi2</i> that also impact plastid glycerolipid metabolism .....	81
Arabidopsis genes involved in plastid galactolipid biosynthesis are required for SAR signaling.....	81
<i>ssi2</i> -conferred growth and defense phenotypes are suppressed by the <i>fad7</i> mutant allele ...	82
JA mutants <i>opr3</i> and <i>coi1</i> are not SAR compromised.....	83
Discussion.....	84
References.....	87
Figure Legends.....	95
Fig 3.1 A simplified overview of lipid biosynthesis in plastids .....	95
Fig 3.2 SAR is compromised in the <i>sfd2</i> mutant .....	95
Fig 3.3 SAR is compromised in the <i>act1</i> mutant .....	96
Fig 3.4 SAR is compromised in the <i>fad6</i> mutant.....	96
Fig 3.5 SAR is compromised in the <i>mdg1</i> mutant.....	97
Fig 3.6 SAR is compromised in the <i>dgd1</i> mutant.....	97
Fig 3.7 SAR is compromised in the <i>fad5</i> mutant.....	98
Fig 3.8 SAR is not compromised in the <i>fad4</i> mutant.....	98
Fig. 3.9 <i>ssi2</i> -conferred defense phenotypes are suppressed by <i>fad7</i> .....	99
Fig. 3.10 <i>ssi2</i> -conferred growth phenotypes are suppressed by <i>fad7</i> .....	100
Fig 3.11 SAR is not compromised in the <i>opr3</i> and <i>coi1</i> mutants .....	100
Fig 3.12 JA and SA content in the WT and <i>opr3</i> mutant plants .....	101
Fig 3.13 Lipid diagrams .....	101
Fig 3.14 Schematic of SAR signaling pathway .....	101
Figures .....	103
Figure 3.1 A simplified overview of lipid biosynthesis in plastids .....	103
Figure 3.2 SAR is compromised in the <i>sfd2</i> mutant .....	104
Figure 3.3 SAR is compromised in the <i>act1</i> mutant.....	105
Figure 3.4 SAR is compromised in the <i>fad6</i> mutant.....	106
Figure 3.5 SAR is compromised in the <i>mgd1</i> mutant.....	107
Figure 3.6 SAR is compromised in the <i>dgd1</i> mutant.....	109
Figure 3.7 SAR is compromised in the <i>fad5</i> mutant.....	110



Figure 3.8 SAR is not compromised in the <i>fad4</i> mutant.....	111
Figure 3.9 <i>ssi2</i> -conferred defense phenotypes are suppressed by <i>fad7</i> .....	112
Figure 3.10 <i>ssi2</i> -conferred growth phenotypes are suppressed by <i>fad7</i> .....	114
Figure 3.11 SAR is not compromised in the <i>opr3</i> and <i>coi1</i> mutants.....	116
Figure 3.12 JA and SA content in the WT and <i>opr3</i> mutant plants.....	118
Figure 3.13 Lipid diagrams.....	120
Figure 3.14 Schematic of SAR signaling pathway .....	122
CHAPTER 4 - Genetic characterization and mapping of <i>sfd2</i> .....	123
Introduction.....	123
Materials and Methods.....	125
Results.....	133
<i>sfd2</i> 's lipid profile resembles <i>fad5</i> .....	133
<i>FAD5</i> and <i>SFD2</i> are different genes .....	133
Mapping strategy and generation of the mapping population.....	134
Genetic and complementation analysis.....	135
Discussion.....	138
References.....	140
Figure legends.....	142
Fig 4.1 DGDG, MGDG and PG profiles of <i>fad5</i> and <i>sfd2</i> .....	142
Fig 4.2 34:6 MGDG content in leave of WT, <i>sfd2</i> , <i>fad5</i> , <i>sfd2/+</i> and <i>fad5/+ sfd2/+</i> plants .....	142
Fig 4.3 Real time PCR data for <i>FAD5</i> expression in the <i>sfd2</i> and <i>fad5</i> mutant and the corresponding wild type plants .....	142
Fig 4.4 Lipid profiles of WT, <i>sfd2</i> and <i>FAD5-sfd2</i> plants .....	143
Fig 4.5 Chromosome 3 of Arabidopsis with <i>FAD5</i> and <i>sfd2</i> region .....	143
Fig 4.6 34:6 MGDG content of WT, <i>sfd2</i> WT and <i>sfd2</i> plants.....	143
Fig 4.7 34:6 MGDG content of WT, WT- <i>sfd2</i> and <i>sfd2</i> plants .....	143
Table 4.1 Recombination data of <i>sfd2-2</i> X <i>Col-0</i> mapping population.....	143
Figures .....	145
Figure 4.1 Lipid profiles of WT, <i>fad5</i> and <i>sfd2</i> .....	145
Figure 4.2 Lipid profiles of WT, <i>sfd2</i> , <i>fad5-1</i> , <i>sfd2/+</i> and <i>fad5/+ sfd2/+</i> plants.....	149

Figure 4.3 Real time PCR data for <i>FAD5</i> expression in the <i>sfd2</i> and <i>fad5</i> mutants and the corresponding WT plants .....	150
Figure 4.4 Lipid profiles of WT, <i>sfd2</i> and <i>FAD5-sfd2</i> plants .....	151
Figure 4.5 Chromosome 3 of Arabidopsis with <i>FAD5</i> and <i>sfd2</i> region .....	152
Figure 4.6 34:6 MGDG content of WT, <i>sfd2</i> -WT and <i>sfd2</i> plants .....	153
Figure 4.7 34:6 MGDG content of WT, WT- <i>sfd2</i> and <i>sfd2</i> plants .....	155
Table 4-1 Recombination data of <i>sfd2</i> -2 X <i>Col-0</i> mapping population.....	156
CHAPTER 5 - Other Observations and Future directions.....	157
References.....	160
Appendix A - Lipid profiles.....	162

## List of Figures

Figure 1.1 SAR induction in plants.....	18
Figure 1.2 Schematic SAR signaling pathway .....	20
Figure 2.1 Homology of SFD1 to the predicted DHAP reductases.....	62
Figure 2.2 Schematic for identification homozygous T-DNA insertion lines by PCR .....	64
Figure 2.3 Identification of homozygous plants from T-DNA insertion lines of AtGPDHp and AtGPDHc .....	65
Figure 2.4 RT-PCR analysis of gene expression .....	66
Figure 2.5 Basal defense phenotype of the insertion lines of AtGPDHp and AtGPDHc.....	67
Figure 2.6 Analysis of the SAR phenotype of the <i>atgpdhp</i> mutant plant.....	69
Figure 2.7 Analysis of the SAR phenotype of the <i>atgpdhp sfd1</i> double mutant plants.....	70
Figure 3.1 A simplified overview of lipid biosynthesis in plastids .....	103
Figure 3.2 SAR is compromised in the <i>sfd2</i> mutant .....	104
Figure 3.3 SAR is compromised in the <i>act1</i> mutant.....	105
Figure 3.4 SAR is compromised in the <i>fad6</i> mutant.....	106
Figure 3.5 SAR is compromised in the <i>mgd1</i> mutant.....	107
Figure 3.6 SAR is compromised in the <i>dgd1</i> mutant.....	109
Figure 3.7 SAR is compromised in the <i>fad5</i> mutant.....	110
Figure 3.8 SAR is not compromised in the <i>fad4</i> mutant.....	111
Figure 3.9 <i>ssi2</i> -conferred defense phenotypes are suppressed by <i>fad7</i> .....	112
Figure 3.10 <i>ssi2</i> -conferred growth phenotypes are suppressed by <i>fad7</i> .....	114
Figure 3.11 SAR is not compromised in the <i>opr3</i> and <i>coi1</i> mutants.....	116
Figure 3.12 JA and SA content in the WT and <i>opr3</i> mutant plants.....	118
Figure 3.13 Lipid diagrams.....	120
Figure 3.14 Schematic of SAR signaling pathway .....	122
Figure 4.1 Lipid profiles of WT, <i>fad5</i> and <i>sfd2</i> .....	145
Figure 4.2 Lipid profiles of WT, <i>sfd2</i> , <i>fad5-1</i> , <i>sfd2/+</i> and <i>fad5/+ sfd2/+</i> plants.....	149

Figure 4.3 Real time PCR data for <i>FAD5</i> expression in the <i>sfd2</i> and <i>fad5</i> mutants and the corresponding WT plants .....	150
Figure 4.4 Lipid profiles of WT, <i>sfd2</i> and <i>FAD5-sfd2</i> plants .....	151
Figure 4.5 Chromosome 3 of Arabidopsis with <i>FAD5</i> and <i>sfd2</i> region .....	152
Figure 4.6 34:6 MGDG content of WT, <i>sfd2</i> -WT and <i>sfd2</i> plants .....	153
Figure 4.7 34:6 MGDG content of WT, WT- <i>sfd2</i> and <i>sfd2</i> plants .....	155

## List of Tables

Table 2-1 Lipid composition of AtGPDHp and AtGPDHc .....	71
Table 4-1 Recombination data of <i>sfd2-2</i> X <i>Col-0</i> mapping population.....	156
Table 5-1 Lipid profiles of WT (Col), <i>fad5</i> , WT (1/8E/5) and <i>sfd2</i> in mol % of total lipids ....	162
Table 5-2 Lipid profiles of WT (Col), <i>atgpdhc</i> and <i>atgpdhp</i> mutants in mol % of total lipids..	166

## **Acknowledgements**

First and foremost I would like to thank my major adviser, my guru, guide and philosopher Dr. Jyoti Shah. I am truly grateful for the way he nurtured me as a scientist, by always being by my side initially to help me start off and slowly weaning me away so that I could develop independently. I take this opportunity to express my heartfelt gratitude to Dr. Ruth Welti. She has always showed great faith in me even when I did not have it myself. For that and innumerable other things I will be ever grateful to her.

I would like to thank all the past and present members of the Shah lab, especially Dr. Ashis Nandi for his patient mentoring, guidance and friendship. I am thankful to Dr. Ratnesh Chaturvedi, Dr. Aparna Patankar and Dr. Ragiba Makandar for their friendship and advice. My fellow graduate students Dr. Venkatramana Pegadaraju, Vamsi Nalam, Vijay Singh, Joe Louis and Jessica Morton for their friendship and for the good times we had together.

I would also like to thank all the members of the Welti lab, especially Mary Roth for all her patient help with my lipid samples. I thank Pam Tamura, Dr. Richard Jeannotte, Alexis Sparks, Dr. Giorgis Isaac, Danny Wu and Joe Bloomfield for their help and friendship.

Lastly, I thank my parents and family for all the love they showered upon me, and my friends for always being there for me.

## **Dedication**

I dedicate this thesis to my parents and to the memory of my beloved uncle Shri. Vemuri Asokavardhan.

## CHAPTER 1 - Introduction

### The threat of plant diseases

An estimated 826 million people are underfed globally-792 million people in the developing world and 34 million in the developed world. Plant disease, responsible for about 10% of the loss of global food output, is one of the contributing factors (Strange and Scott, 2005). The irony is that the majority of the affected reside in rural regions, which are the very centers of food production (FAO, 2000).

Plant disease can also bring about fiscal devastation. The escalating cost of crop protection is the major reason for the ever increasing indebtedness of small and marginal farmers. Repeated occurrence of disease outbreaks causes further indigence, ultimately resulting in small and marginal farmers losing farm land and becoming landless agricultural laborers, joining the 1.3 billion who earn less than \$1 a day (Strange and Scott, 2005). The environmental consequence of crop protection with chemicals is still an open question. The worldwide crop protection market in 2005 was worth US \$33.6 billion, of which fungicides accounted for 23%, according to a 2006 Goldman Sachs report (nufarm.com)

Two great human tragedies in modern human history were due to plant diseases. The well-known Irish famine of 1840s resulted in a million deaths and the migration of an even larger number of people (Strange and Scott, 2005). The late blight disease of potato, caused by the fungus *Phytophthora infestans*, was the primary cause of this famine. The lesser known 1943 great Bengal famine in colonial India was triggered by the fungus *Cochliobolus miyabeanus*, which causes brown spot on rice (Padmanabhan, 1973). The resulting death toll of about 4 million was due to an abominable combination of depleted rice production and colonial neglect.

There are hundreds of viruses, bacteria, fungi, oomycetes, nematodes and parasitic plants able to cause diseases in plants. This, combined with the fact that human food consumption is largely based on about fourteen crops (Strange and Scott, 2005), puts global food security at a high risk.



Human population growth, increasing longevity, and an unprecedented demand for quality food have made it crucial for us to better understand the mechanisms of defense in plants.

Human interest in plant diseases and their control has ancient origins. Ancient Indian, Chinese and Egyptian manuscripts describe various plant disease symptoms and advise on control measures. Vrikshayurveda, a pre-10<sup>th</sup> century Indian text on plant science mentions many plant disease symptoms including chlorosis (pondurog) in trees and advises the use of specific decoctions to alleviate them (Nene, 2007). The first scientific chronicling of a plant disease epidemic caused by an infectious agent was done in 1861 (DeBary, 1861) in response to the Irish epidemic of late blight on potato. The first scientific description of a resistance phenomenon reported an 'immune' response of the host plant to a rust infection (Ward, 1902).

## **Plant defense response**

Plant defense to pathogens is a combination of innate and acquired resistance (Glazebrook, 2005). The innate part consists of both non-specific and specific resistance. As the name suggests, non-specific resistance is a general form of resistance and is effective against a wide variety of pathogens. *Au contraire*, specific resistance is directed against a particular pathogen. Acquired resistance is the subsequent resistance observed because of preconditioning by a prior infection. Systemic acquired resistance (SAR) and induced systemic resistance (ISR) are two forms of acquired or induced resistance mechanisms that are better characterized (Grant and Lamb, 2006). These two forms of defense responses differ on the basis of the regulatory pathways involved and the nature of the elicitor (Pieterse et al., 1996; Knoester et al., 1999; Maleck et al., 2000; van Wees et al., 2000). When simultaneously activated, ISR plus SAR have a concerted effect on plant resistance (Grant and Lamb, 2006).

## **Innate Resistance**

Constitutive barriers, non-host resistance and basal resistance to bacteria and fungus are all part of general innate resistance (Nürnberger and Lipka, 2005). Plants have constitutive barriers against easy entry and spread of pathogenic organisms. A waxy cuticle and thickened cell walls are structural barriers that hinder the ingress of pathogens. Preformed secondary metabolic antimicrobial compounds like saponins and glucosinolates are also part of this defense mechanism. These compounds may be sequestered in vacuoles in their active forms or as

inactive precursors, which are converted to their active forms by enzymes released upon attack. Non-host resistance is the term given to the phenomenon of most plant species being resistant to a large number of species of microbial invaders (Thordal-Christensen, 2003; Mysore and Ryu, 2004). Plants that are resistant to all isolates of a given pathogen species are referred to as non-host plants, while micro-organisms, which have the potential to be pathogenic, but are incapable of infecting a given plant species are referred to as heterologous pathogens (Nürnberger and Lipka, 2005). When these pathogens overcome structural barriers and enter a cell, they are recognized by host surveillance mechanisms. Microbe associated molecular patterns (MAMPs), present in many pathogens, are known to trigger receptor-mediated defense responses in non-host plants (Jones and Takemoto, 2004; Abramovitch et al., 2006). The N-terminal 22-mer fragment of eubacterial flagellin, flg22, and structural elements of lipopolysaccharide (LPS) from gram-negative bacteria are reported to be inducers of defense responses in various plant species (Felix et al., 1999; Newman et al., 2002).

### **Gene-for-gene resistance**

Some heterologous pathogens have evolved ‘virulence’ factors which enable them either to suppress or to evade non-host defenses (Abramovitch and Martin, 2004; Alfano and Collmer, 2004). The plant species now becomes a host to this particular pathogen subtype, which is now referred to as a homologous pathogen (Nürnberger and Lipka, 2005). Evolutionary selection pressure led to the development of resistance (*R*) genes in the host plants, which precisely recognize a particular strain of pathogen or race-specific factors and allow for the establishment of uniquely tailored defense mechanisms generally referred to as gene for gene interaction (Abramovitch and Martin, 2004; Jones and Takemoto, 2004). The pathogen, in this case is referred to as an avirulent pathogen. Such unique recognition mechanisms are part of specific resistance, which along with MAMP-induced non-host or general resistance and structural barriers, constitute innate resistance in plants. In many cases of plant-pathogen interaction, one of the dramatic features of this resistance response is the hypersensitive response (HR) which is accompanied by the rapid and localized induction of programmed cell death (PCD). HR creates a physical barrier to the spread of the pathogen and also denies nutrients to the invader due to the rapid dehydration of the dying tissue (Watanabe and Lam, 2006). A rapid production of reactive oxygen species (ROS) is also observed at the site of the HR. ROS detoxifying enzymes are

suppressed by salicylic acid (SA) and nitrous oxide (NO) that accumulate at the site of HR and allow the amassing of ROSs that promote PCD (Apel and Hirt, 2004).

## **Defense signaling mechanisms**

Turning on defenses constantly is “costly” for the plant (Bostock, 2005; Heil and Ton, 2008). Plants have evolved signaling mechanisms that activate defenses only in response to an attack. A number of components are involved in plant defense signaling, some of which are reviewed below.

## **Salicylic acid**

Salicylic acid (SA) derives its name from the Latin name of the white willow plant, *Salix alba*. The Greek physician Hippocrates recommended the use of the bitter powder extracted from the bark of the willow plant to relieve pain and fever (Weissman, 1991). The active ingredient in this powder was found to be salicin, which was isolated by French pharmacist Henry Leroux in the year 1828. The Italian chemist Raffaele Piria was able to convert salicin to the free acid, SA. In plants, SA can also be found in the form of SA-glucoside and methylsalicylate (MeSA). The role of SA in plant defense was first reported by White (1979), who demonstrated that application of acetyl salicylic acid (aspirin) to tobacco induced resistance against tobacco mosaic virus. This observation was later extended to other plant systems and pathogens (Schneider et al., 1996). Subsequent studies demonstrated that SA level increased in pathogen infected tissues and this accumulation of SA paralleled the expression of the SA-inducible *PATHOGENESIS RELATED (PR)* genes, some of which (e.g. *PR1*) are excellent markers for the activation of SA signaling (Malamy et al. 1990; Sitcher et al., 1997). Studies with transgenic plants expressing a salicylate hydroxylase encoded by the bacterial *nahG* gene, provided additional proof for the important role of SA in plant defense. Transgenic tobacco and Arabidopsis plants expressing this enzyme, were unable to accumulate elevated levels of SA and exhibited enhanced susceptibility to a number of pathogens (Chaturvedi and Shah, 2007). Application of a benzothiadiazole (BTH), a functional analog of SA that is not a substrate for the *nahG*-encoded enzyme, restored resistance in *nahG* plants, confirming that the heightened susceptibility to pathogens of the *nahG* transgenic plants was indeed due to SA deficiency. However

considering that catechol, the product of salicylate hydroxylase action on SA, can itself influence defense responses in some cases of plant-pathogen interaction (van Wees and Glazebrook, 2003), results based solely on effect of *nahG* on plant defense need to be interpreted with caution.

SA is synthesized by at least two pathways in plants, the phenylpropanoid pathway also called the eukaryotic SA-synthesizing pathway and the chorismate pathway known as the prokaryotic SA-synthesizing pathway (Métraux, 2002; Shah, 2003). The phenylpropanoid pathway is also involved in the synthesis of lignins, phytoalexins and coumarins (Métraux, 2002; Shah, 2003). Here phenylalanine is converted to trans-cinnamic acid by the action of the enzyme phenylalanine ammonia lyase (PAL). Trans-cinnamic acid is further hydroxylated to form *ortho*-coumaric acid, a precursor of SA; alternatively, it may be oxidized to yield benzoic acid, which may subsequently be converted to SA through the action of benzoic acid-2-hydroxylase (BA2H) (Sticher et al., 1997; Shah, 2003). In *Arabidopsis*, the inhibition of phenylalanine ammonia lyase (PAL) by 2-amino-indane-2-phosphonic acid (AIP) resulted in susceptibility to a normally avirulent race of *Peronospora parasitica*. Exogenous application of SA restored resistance in AIP treated *Arabidopsis* plants (Mauch-Mani and Slusarenko, 1996). This suggests an involvement of the phenylpropanoid pathway in defense against *P. parasitica*.

The chorismate pathway, however, is now thought to be the major pathway involved in SA biosynthesis in *Arabidopsis* (Métraux, 2002; Shah, 2003). In bacteria, SA biosynthesis occurs through the conversion of chorismate to isochorismate by the enzyme isochorismate synthase (ICS), which is then converted to SA, by the enzyme isochorismate pyruvate lyase (IPL) (Métraux, 2002; Shah, 2003). When both these enzymes were simultaneously overexpressed in *Arabidopsis*, the amount of free and conjugated SA was increased more than 20-fold above wild type level (Mauch et al., 2001). The *SID2* (*SALICYLIC ACID INDUCTION-DEFICIENT 2*) gene encodes an isochorismate synthase, with 57% identity with *Catharanthus roseus* ICS and approximately 20% identity with bacterial ICS (Wildermuth et al., 2001). The *SID2* gene has a putative plastid transit sequence and cleavage site consistent with its use of plastid-synthesized chorismate as substrate suggesting evolution from prokaryotic endosymbionts. Furthermore, the presence of an *ICS* gene in the chloroplast genome of the red algae *Cyanidium caldarium* supports a prokaryotic origin of *SID2*, also known as *ICS1* (Wildermuth et al., 2001). The SA level of infected *Arabidopsis sid2* plants was only 5-10% of the wild type level and a loss of

resistance was observed in the *sid2* mutants to *Erysiphe* spp. and *Pseudomonas syringae* (Wildermuth et al., 2001). All these observations together support the idea that the prokaryotic chorismate pathway is the major source of SA in Arabidopsis defense against pathogens. More recently, *ICS2*, which also encodes an isochorismate synthase, was also shown to contribute to SA synthesis (Garcion et al. 2008). Another gene that appears to be involved in SA biosynthesis is *EDS5* (*ENHANCED DISEASE SUSCEPTIBILITY 5*). It encodes a protein with homology to the multidrug and toxin extrusion (MATE) family of transporter proteins (Nawrath et al., 2002). Although the exact role of EDS5 in SA synthesis is not known, it may be involved in the transport of precursors or inducers of SA synthesis, across the chloroplast membrane.

### **Salicylic acid binding proteins**

Screens set up to identify the SA receptor resulted in the identification of many SA-binding proteins in tobacco. Catalase and ascorbate peroxidase, enzymes that are known to scavenge hydrogen peroxide were identified as proteins that bind to SA (Chen et al., 1993; Durner and Klessig, 1995). But these enzymes were found to have low affinity for SA. Moreover, SA was found to bind other iron-containing enzymes of plant and non-plant origin (Rüffer et al., 1995). SA binding protein 3 (SABP3), an enzyme with homology to carbonic anhydrase was identified in another screen. Although SABP3s affinity for SA was higher than that of Catalase and ascorbate peroxidase, it was still fairly low (Slaymaker et al., 2002). SA binding protein 2 (SABP2) was subsequently purified from tobacco leaves as a protein with high affinity for SA ( $K_d = 90$  nM) (Du and Klessig, 1997; Kumar and Klessig, 2003). Biochemical analysis of SABP2 demonstrated that it had an esterase activity that hydrolyzed methylsalicylate (MeSA) to yield SA (Forouhar et al., 2005; Park et al., 2007).

### **NPR1**

A number of genetic screens were conducted to identify genes involved in SA signaling. Several of these studies yielded mutant alleles of the *NPR1* (*NONEXPRESSOR OF PR GENES 1*) gene (Cao et al. 1994; Delaney et al., 1995; Glazebrook et al., 1996; Shah et al., 1997). The *npr1* mutants showed enhanced susceptibility to several pathogens and were compromised in their ability to express *PR* genes upon SA treatment or infection by pathogens (Dong, 2004; Durrant

and Dong, 2004). The NPR1 protein does not bind SA, confirming that it is not another SA-binding protein (Cao et al., 1997).

The NPR1 gene encodes a protein with regions of ankyrin repeats and BTB/POZ (Broad-Complex, Tramtrack, and Bric-a-brac/Pox virus and Zinc finger) domains (Cao et al., 1997; Ryals et al., 1997). The protein also has conserved Cys residues that are capable of forming inter or intra-molecular disulphide bonds. It is constitutively expressed, and upon treatment with SA, a two fold increase of transcript was observed (Cao et al., 1998). An NPR1–GFP (Green Fluorescent Protein) fusion protein accumulated in the nucleus upon induction by SA or INA (Kinkema et al., 2000). Overexpression of NPR1 and its alleles showed that the presence of high levels of protein alone did not result in constitutive high-level expression of *PR* genes (Cao et al., 1998; Friedrich et al., 2001). However, NPR1 overexpressing plants were primed to respond faster in response to pathogen attack and exhibited enhanced resistance to multiple pathogens. In uninfected plants, NPR1 protein was found to exist as a larger complex in the cytosol. However, in response to treatment with SA or its analog INA, NPR1 monomers were found to accumulate in the nucleus (Mou et al., 2003). Addition of DTT to proteins extracted from leaf tissue also resulted in monomerization of NPR1, suggesting that the interconversion between multimeric to monomeric form results from a change in NPR1s REDOX status (Mou et al., 2003). Treatment of INA induced plants with 6-aminonicotinamide (6-AN), an inhibitor of the pentose phosphate pathway (PPP), a pathway responsible for providing electrons for reductive reactions in the cell, led to the partial inhibition of NPR1 monomerization and decreased *PR1* gene expression. This suggested that NPR1 monomerization may be needed for *PR1* gene expression (Mou et al., 2003). Mutation of the two Cys residues C82 and C216 in the NPR1 protein led to constitutive monomerization, constitutive expression of *PR1* genes and constitutive nuclear localization of the NPR1 monomer (Mou et al., 2003). All this together implied that the Cys residues were responsible for the NPR1 oligomerization and upon change in the redox state of the cell to a more reduced state, the NPR1 oligomer monomerizes and moves into the nucleus.

Yeast two-hybrid screens have revealed that NPR1 interacts with members of the TGA family of basic domain/Leu zipper (bZIP) transcription factors (Zhang et al., 1999; Després et al., 2000; Niggeweg et al., 2000; Zhou et al., 2000; Chern et al., 2001). In transgenic Arabidopsis plants

overexpressing the carboxy-terminal domain of TGA2, the mutant TGA2 protein interacted with NPR1 but the DNA binding activity of the transcription factor was lost. This mutant protein acted as a dominant negative and led to the abolition of TGA activity in an NPR1 dependent manner; hence these transgenic plants had an *npr1* phenotype, i.e. they had an increased susceptibility to *Pseudomonas syringae* pv. *maculicola* and were compromised in their ability to express *PR* genes when treated with INA (Fan and Dong, 2002). Some TGAs such as TGA1 and TGA4 did not interact with NPR1 in yeast two hybrid assays but TGA1 were found to interact with NPR1 in Arabidopsis leaves upon SA treatment (Després et al., 2003). Mutations in the two Cys residues in TGA1 and TGA4, which were absent in TGAs that interact with NPR1 in yeast two hybrid assays, led to their ability to interact with NPR1 in yeast two hybrid assays (Després et al., 2003) implying that TGA function was also under redox regulation. TGA2 and TGA3 were recruited *in vivo* to SA-responsive elements in the *PR-I* promoter, in a SA- and NPR1-dependent manner, indicating that transcription factors were involved in the regulation of *PR* gene expression (Johnson et al., 2003).

NPR1 homologues have been identified in rice, tobacco, tomato, apple and orange (Chern et al., 2001; Durrant and Dong, 2004). This suggested that NPR1 was conserved across species. When the Arabidopsis NPR1 was constitutively expressed in monocotyledonous plants like rice and wheat, it conferred enhanced resistance to bacterial blight, caused by *Xanthomonas oryzae* (Chern et al., 2001) and scab disease caused by *Fusarium graminearum* (Makandar et al., 2006), respectively. Similarly, overexpression of NPR1 enhanced disease resistance in tomato (Lin et al., 2004). Taken together, these results indicate that NPR1 function is conserved amongst plants.

## **Jasmonic acid**

The plant hormone JA is another important player in plant defense signaling.

JA and its derivatives are involved in resistance to insect herbivores (McConn et al., 1997), in defense against necrotrophic pathogens (Thomma et al., 1998) and in induced systemic resistance (ISR) (Pieterse et al., 1998). Jasmonates are also required for anther dehiscence and pollen development (Feys et al., 1994; McConn and Browse, 1996), and protection against ozone stress (Rao et al., 2000). The essential oil of *Jasminum grandiflorum* was used to isolate

jasmonic acid methyl ester (MeJA) in the year 1962 (Demole et al., 1962). The biological relevance of JA and MeJA were first shown in studies where these metabolites were independently isolated as growth inhibitors (Dathe et al., 1981) and as senescence promoting compounds (Ueda and Kato, 1980). Subsequent studies demonstrated that jasmonates also regulate gene expression (Farmer and Ryan, 1990).

JA biosynthesis was described in 1984 (Vick and Zimmerman, 1984). JA biosynthesis starts in the chloroplast with  $\alpha$ -linolenic acid being oxidized by a 13-lipoxygenase (13-LOX) enzyme to 13-hydroperoxy linolenic acid. This is followed by the conversion of the 13-hydroperoxy linolenic acid by allene oxide synthase (AOS) to allene oxide. Subsequently, 12-oxophytodienoic acid (OPDA) is formed by the action of allene oxide cyclase (AOC) on allene oxide. This is reduced to 12-oxophytodienoic acid by 12-oxophytodienoic acid reductase (OPR) in the cytoplasm. Three subsequent  $\beta$ -oxidations in the peroxisome convert OPDA to JA. In addition to JA and MeJA, JA-amino acid derivatives and JA containing galactolipids have also been identified from plants (Wasternack, 2007).

The role of JA in defense against necrotrophic pathogens has been widely studied in *Arabidopsis* using a number of JA-insensitive and JA biosynthesis mutants. The first JA-insensitive mutant identified, *coi1* (*coronatine-insensitive1*), encodes for an F-box protein, which is part of the ubiquitin-mediated SCF proteasome pathway (Feys et al., 1994; Xie et al., 1998), and shows an increased susceptibility to *Erwinia carotovora* (Norman-Setterblad et al., 2000), *Alternaria brassicicola* and *Botrytis cinerea* (Thomma et al., 1998, 1999). *jar1* (*jasmonate resistant 1*), a JA insensitive mutant belongs to the superfamily of adenylate – forming enzymes, and the fatty acid desaturase deficient *fad3 fad7 fad8* triple mutant that lacks linolenic acid, a JA precursor, are reported to be susceptible to normally nonpathogenic oomycete *Pythium* (Staswick et al., 1998; Vijayan et al., 1998). Increasing endogenous MeJA levels by the overexpression of a JA carboxyl methyl transferase led to enhanced resistance to *Botrytis cinerea* (Seo et al., 2001).

Recently, JAZ (JASMONATE ZIM-DOMAIN) proteins were identified as substrates for the COI1-SCF (SCF<sup>COI1</sup>) complex that negatively regulates JA signaling (Chini et al., 2007; Thines et al., 2007). JAZ proteins repress the activity of transcription factors that positively regulate



early JA-response genes. The Arabidopsis JAZ3 protein directly interacted with the JIN1 (JASMONATE INSENSITIVE1) transcription factor and acted as a negative regulator of its function (Thines et al., 2007). JA has been shown to encourage direct interaction between the COI1 and JAZ proteins and cause the turn-over of JAZ proteins by the SCF<sup>COI1</sup> complex.

Evidently, JA might also act as a susceptibility factor to certain pathogens. The *coi1* mutant shows enhanced resistance to the bacterial pathogen *Pseudomonas syringae* (Feys et al., 1994; Kloeck et al., 2001). It appears that the pathogen exploits this trait to colonize the plant, especially during the early stages of pathogenesis, by turning on the JA signaling pathway with its type III effectors and coronatine, a phytotoxin, which structurally mimics JA-isoleucine conjugates (He et al., 2004). JAR1 was found to be a JA-amino acid synthetase that is required to activate JA for optimal signaling in Arabidopsis by forming JA- Isoleucine conjugates (Staswick and Tiryaki, 2004). It has been shown that the binding of COI1 to some JAZ proteins is promoted by JA- isoleucine conjugates (Chini et al., 2007). But as the *JAR1* gene was needed for basal resistance against *Xanthomonas campestris* (Ton et al., 2002); it appears that JA's role in promoting either resistance or susceptibility seems to depend on so far unknown factors.

### **Cross talk between SA and JA signaling**

Convergence of pathways that can positively or negatively regulate each other could be critical for defense as they allow for a fine tuning of the defense response to different types of pathogens. Interactions between JA and SA pathways, in general are antagonistic. SA and its analogs like BTH and INA are known to suppress JA synthesis and signaling (Doherty et al., 1988; Pena-Cortes et al., 1993; Bowling et al., 1997) and JA signaling is known to suppress SA synthesis in pathogen-infected plants (Kunkel and Brooks, 2002). WRKY70, a transcription factor, seems to affect the repression of JA responsible genes while acting as an activator of SA inducible genes (Li et al., 2004). Other evidence suggests that these two pathways can also act in synergy, as in case of the additive effect shown during induced resistance against *Pseudomonas syringae* (van Wees et al., 2000). Indeed expression profiling studies indicate an overlap between genes induced by both SA and JA signaling pathways (Schenk et al., 2000; Glazebrook et al., 2003).

The cross-talk between the two defense related SA and JA pathways seems to be regulated through NPR1 (Spoels et al., 2003). When wild type plants are treated with both SA and MeJA, no effect of MeJA is observed on the SA induced *PR1* transcript levels. On the other hand, JA responsive genes are suppressed by SA. However, in *npr1-1* mutant plants SA appears to be unable to suppress JA inducible gene expression, suggesting a role of NPR1 in cross-talk between SA and JA. Furthermore; NPR1 appears to be needed in the cytosol rather than in the nucleus to mediate this cross-talk (Spoels et al., 2003). Another study that used hierarchical clustering of microarray data found that in the *npr1-1* mutant, the expression of SA, JA and ethylene –mediated genes was affected (Glazebrook et al., 2003). But in case of the nuclear localization signal lacking mutant, *npr1-3*, expression of only SA mediated genes was affected (Glazebrook et al., 2003), suggesting a cytosolic role for NPR1.

## **Induced resistance**

Induced resistance is considered a physiological “state of enhanced defensive capacity” elicited by specific environmental stimuli, whereby the plant’s innate defenses are potentiated against subsequent biotic challenges (van Loon et al., 1998). This state of heightened resistance is effective against a broad range of pathogens like fungi, bacteria, viruses, nematodes and insect herbivores (Sticher et al., 1997; van Loon et al., 1998; Benhamou and Nicole, 1999; Kessler and Baldwin, 2002). Localized acquired resistance (LAR) is considered to be induced when only those tissues exposed to the primary pathogen become more resistant (Yarwood, 1960; Ross, 1961a). Cross protection is a term that also implies induced resistance and was described nearly a hundred years ago (N Bernard 1909, cited in Deverall, 1977).

## **Induced systemic resistance (ISR)**

Some forms of rhizobacteria that are present near the plant root surface help promote or stimulate plant growth. These are referred to as plant growth-promoting rhizobacteria (PGPR) (Kloepper et al., 1980). This increase in growth is a result of both a direct effect of the bacteria on plant growth and the suppression of soil born pathogens (Schippers et al., 1987). Fluorescent *Pseudomonas* spp. are known to effectively reduce soil-borne diseases in soils where disease incidence is low (Weller, 1988). Besides this, it has been demonstrated that these bacteria have

the ability to induce a systemic defense response in plants upon colonization of seeds or roots (van Peer et al., 1991; Wei et al., 1991). This kind of resistance is referred to as rhizobacteria mediated induced systemic resistance (ISR) and has been shown to be effective in a number of plant species e.g. Arabidopsis, bean, carnation, cucumber, tomato, tobacco, etc. In Arabidopsis colonization of the root by *P. fluorescens* led to resistance against bacterial pathogens *P. syringae*, *X. campestris*, fungal pathogens *A. brassicicola*, and *F. oxysporum*, and the oomycete *P. parasitica* (Pieterse et al., 1996; Ton et al., 2002). Induction of ISR requires specific recognition between the rhizobacteria and the plant e.g. *Pseudomonas putida* can trigger ISR in Arabidopsis, but not in carnation and radish.

When the Arabidopsis ethylene response mutant *etr1-1* and the JA response mutant *jar1-1* were tested for their ability to induce ISR upon root colonization by *P. fluorescens*, they were found to be unable to show induced resistance against *P. syringae* (Pieterse et al., 1998). This suggested that the ISR signal response required JA and ethylene. But there was no change in the levels of these hormones locally or systemically in plants infected with *P. fluorescens*, indicating that ISR was perhaps based on an enhanced sensitivity to these hormones rather than their increased availability (Pieterse et al., 2000). In support of this notion, it was found that the expression of the JA responsive gene *VSP* was enhanced in ISR induced plants compared to controls, but other JA response genes seemed unaffected, implying that ISR is associated with only a specific set of genes in that pathway (van Wess et al., 1999). In contrast, to JA and ethylene, studies with the *nahG* transgenic plants, indicated that SA accumulation was not important for ISR-conferred resistance (Pieterse et al., 1996). However, the NPR1 gene is required for the activation of ISR; the *npr1* mutant was unable to mount an ISR response (Pieterse et al., 1998). Subsequent studies indicated that cytosolic multimeric NPR1 is required for JA signaling as opposed to monomeric nuclear localized NPR1, which is required for mediating SA signaling (Spoels et al., 2003).

## **Systemic acquired resistance (SAR)**

Systemic acquired resistance (SAR) is an inducible defense mechanism that is activated throughout the plant subsequent to the localized inoculation of one or more leaves with a pathogen (Figure 1.1). In 1961, the existence of an acquired resistance that was systemic was demonstrated in tobacco against *Tobacco mosaic virus* (TMV) (Ross, 1961b). Since then SAR

has been reported in a number of diverse plant species including *Arabidopsis*, alfalfa, asparagus, barley, bean, carnation, cucumber, muskmelon, pearl millet, potato, radish, rape seed, rice, soybean, tobacco, tomato and watermelon (Sticher et al., 1997). SAR induces resistance to wide range of bacterial, fungal, oomycete and viral pathogens (Sticher et al., 1997; Durrant and Dong, 2004; Grant and Lamb, 2006). The establishment of SAR requires different time periods in different plant species and is dependent on the plant species and type of inducing organism involved (Sticher et al., 1997). It ranges from 7 hours after primary inoculation with *P. syringae* to 2-3 weeks in tobacco after infection with the oomycete *P. parasitica* (Cohen and Kuc, 1981; Smith and Métraux, 1991). It has been generally accepted that a local development of necrosis at the site of primary infection is a necessary condition for the development of SAR; but recent research suggests that this might not always be the case (Mishina and Zeier, 2007). SAR is characterized by a local and systemic increase in SA levels and expression of the *PR* genes. During SAR, an unknown signal translocates from the pathogen infected organs to rest of the plant where it primes defenses to respond faster in response to pathogen attack (Fig 1.2). The SAR signal was thought to be conducted through the vasculature. Girdling experiments in cucumber suggested that the signal travel to the systemic parts through the phloem (Ross, 1966; Guedes et al., 1980). Labeling experiments in *Arabidopsis* using radio-labeled sucrose, showed that SAR induction did not match the exact orthostichy of the plant, suggesting that a fraction of the signal may be using an alternate route (Kiefer and Slusarenko, 2003; Durrant and Dong, 2004). The observation that the endogenous level of SA increases locally and systemically in tobacco plants that were inoculated with TMV led to the hypothesis that SA could be the endogenous signal for SAR (Malamy et al., 1990; Sticher et al., 1997). The SAR deficiency of *nahG* plants supported this hypothesis (Gaffney et al., 1993; Delaney et al., 1994). However, grafting experiments with the *nahG* plants indicated that SA is not the mobile signal in SAR (Vernooij et al., 1994). Transgenic tobacco root stocks expressing the *nahG* gene, and hence unable to accumulate elevated SA levels, were fully capable of delivering a signal that primed non-transgenic scions to become resistant to future pathogen attacks. In contrast, reciprocal grafts containing non-transgenic root stocks and *nahG* scions were unable to express SAR, indicating that SA accumulation in the distal tissue is required for SAR. This effect of SA in the SAR expressing organs requires the NPR1 gene (Durrant and Dong, 2004; Shah, 2003). More recently, studies with the SABP2 protein have suggested that MeSA may be involved in SAR

associated systemic signaling in TMV-infected tobacco plants (Park et al. 2007). However, whether MeSA is also involved in long distance signaling associated with SAR in other plants is not known. One study in Arabidopsis has implicated JA as a long distance signaling molecule in SAR (Truman et al. 2007). However, this conclusion is debatable (Chaturvedi et al. 2008).

*dir1* (*defective in induced resistance1*) was the first Arabidopsis mutant identified that had normal basal or local resistance but was compromised in SAR (Maldonado et al., 2002). Petiole exudates from pathogen challenged leaves of *dir1* mutant plants were unable to activate SAR in naïve wild type plants (Maldonado et al., 2002; Chaturvedi et al., 2008). Conversely, petiole exudates from pathogen-challenged leaves of wild type plants were able to turn on SAR in naïve *dir1* mutant plants (Chaturvedi et al., 2008), implying that the *dir1* plants were compromised either in the generation or translocation of the SAR signal but not in its perception. The *DIR1* gene encodes a putative apoplastic lipid transfer protein with homology to non-specific lipid transfer proteins (LTP). In Arabidopsis LTPs form a multigene family with 71 predicted members (Beisson et al., 2003). This suggested that the SAR signal could be a lipid or lipid derived molecule. Further evidence for a lipid or lipid-derived molecule as the SAR signal came from the identification of the *sfd* (*suppressors of fatty acid desaturase deficiency*) mutants (Nandi et al., 2003) that successfully suppressed the constitutive SAR phenotype of the *ssi2* mutant. The *sfd1* mutant plants, like the *dir1* plants, were also compromised in SAR but had normal basal defense phenotypes (Nandi et al., 2004). Similarly petiole exudates from the mutant were unable to turn on SAR in wild type plants, but the mutants were responsive to exudates from wild type plants (Chaturvedi et al., 2008), suggesting that the *SFD1* gene was involved in the generation or translocation of the SAR signal. The *SFD1* gene codes for a plastidic dihydroxyacetone phosphate (DHAP) reductase (Nandi et al., 2004). The galactolipid lipid composition of the *sfd1* mutant plants was altered as compared to wild type composition, implying a role for galactolipid-dependent factors in SAR signaling. Fig. 1.2 provides a schematic linking the signaling mechanisms involved in the activation of SAR.

## **Lipids in plant defense**

Lipids are vital components of cells. They help compartmentalize the cell by forming membranes and act as a repository for energy storage. Lipids play a role in almost all major

activities of the plant e.g. growth and development, photosynthesis, response to environmental stimuli, signaling, defense, etc. (Laxalt and Munnik, 2002; Wang, 2004; Shah, 2005). In plants, lipids are synthesized in two compartments the plastids and the endoplasmic reticulum (Somerville et al., 2000). These two are also referred to as the prokaryotic and the eukaryotic lipid biosynthetic pathways. The prokaryotic pathway is characterized by the addition of 16:0 fatty acids at the sn-2 position of lysophosphatidic acid (LPA). The eukaryotic pathway is characterized by the addition of 18 carbon fatty acids in the sn-2 position of LPA. Initial reactions between the prokaryotic and eukaryotic paths are similar, except for localization of the components involved. Glycerol 3-phosphate is acylated by a transferase to form LPA. Subsequently, a second acyl chain is added to LPA to yields phosphatidic acid (PA). In the plastids and ER, acyl-ACP (acyl carrier protein) and acyl-CoA are the acyl donors, respectively. PA can be converted into different types of lipids by the addition of different head groups and by the action of desaturases. Other pathways lead to the synthesis of waxes, sphingolipids and sterols (Somerville et al., 2000).

Lipids have varied roles in plant interaction with pathogens. For example, one of the first barriers that a pathogen encounters when it lands on the plant surface is the epidermal waxy cuticle, which is largely composed of cutin and cutan. Cutin, the more abundant of the two, is made of hydroxyl fatty acids interlinked by ester bonds. The cuticle can provide protection against pathogens as seen in case of the *Arabidopsis att1* mutant, which has a 70% reduction in its cutin content and shows enhanced susceptibility to *Pseudomonas syringae* (Xiao et al., 2004). In other cases of plant-pathogen interaction for example rice and the rice blast fungus *Magnaporthe grisea*, cutin monomers are a host factor that is recognized by the pathogen resulting in the activation of appressoria formation (Gilbert et al., 1996). Plant lipids also provide a surface on which a variety of defense signaling proteins are localized and where interaction between plant proteins and pathogen-derived elicitors occurs, resulting in the activation of downstream signaling (Shah, 2005).

Lipids like PA can themselves function as signaling molecules by binding to proteins and modulating their activities. PA levels increase in response to stress (Wang et al., 2006), and application of PA to plant cells results in an oxidative burst and cell death (Sang et al., 2001; de

Jong et al., 2004). Fatty acids are also suggested to participate in plant defense. Levels of fatty acids such as linolenic acid and hexadecatrienoic acid increase rapidly in avirulent pathogen inoculated *Arabidopsis* leaves, and polyunsaturated fatty acids when applied to tobacco suspension cells activate an oxidative burst (Yaeno et al., 2004). Changes in composition of fatty acids also impact defenses. For example, mutations in the *SSI2*-encoded stearyl-ACP desaturase, which is involved in the conversion of stearyl ACP (18:0-ACP) to oleoyl-ACP (18:1-ACP), resulted in enhanced resistance to bacterial, oomycete and viral pathogens (Kachroo et al., 2001; Shah et al., 2001; Sekine et al., 2004; Nandi et al., 2005) and enhanced susceptibility to *Botrytis cinerea*, a fungal pathogen, thus Polyunsaturated fatty acids also serve as precursors of a variety of oxylipins, for example, JA, which is involved in plant defense signaling. In addition, a number of other oxylipins have been reported to have antimicrobial activities (Prost et al., 2005). The first step in the synthesis of oxylipins and other lipid-derived volatiles is catalyzed by LOXs (lipoxygenases), which add amolecular oxygen fatty acids (Feussner and Wasternack, 2002; Shah, 2005). LOX-derived products have been shown to provide race specific resistance to *Phytophthora parasitica* var. *nicotianae* in tobacco (Rancé et al., 1998). Genetic studies indicate that LOX-derived products can also be utilized for pathogenicity by other microbes and hence function as susceptibility factor (Gao et al., 2007). Lipases are a larger group of enzymes that catalyze the hydrolysis of lipids. Several lipases are associated with plant-pathogen interaction (Shah, 2005). For example, several putative lipases were induced by microbial elicitors and by pathogens in tobacco (Dhondt et al., 2002). Genetic studies have confirmed the involvement of the AtPLA1 and GLIP1 encoded lipases in plant defense against pathogens (Seok et al., 2005; Yang et al., 2007). In addition, the *Arabidopsis* the DGL (DONGLE) and DAD1 (DEFECTIVE IN ANTHOR DEHICENCE 1) proteins were shown to have phospholipase A activity that are involved in JA biosynthesis (Hyun et al., 2008).

## Concluding remarks

Figure 1.2 summarizes the current working model of SAR related signaling. A number of questions remain to be answered. As mentioned earlier, *SFD1* codes for a DHAP reductase. The *sfd1* mutant had altered lipid composition and is SAR compromised. There are four other DHAP reductases in *Arabidopsis* and their role in lipid metabolism and SAR remains to be analyzed. Furthermore, although studies with the *sfd1* mutant suggest that plastid lipids may have a role in

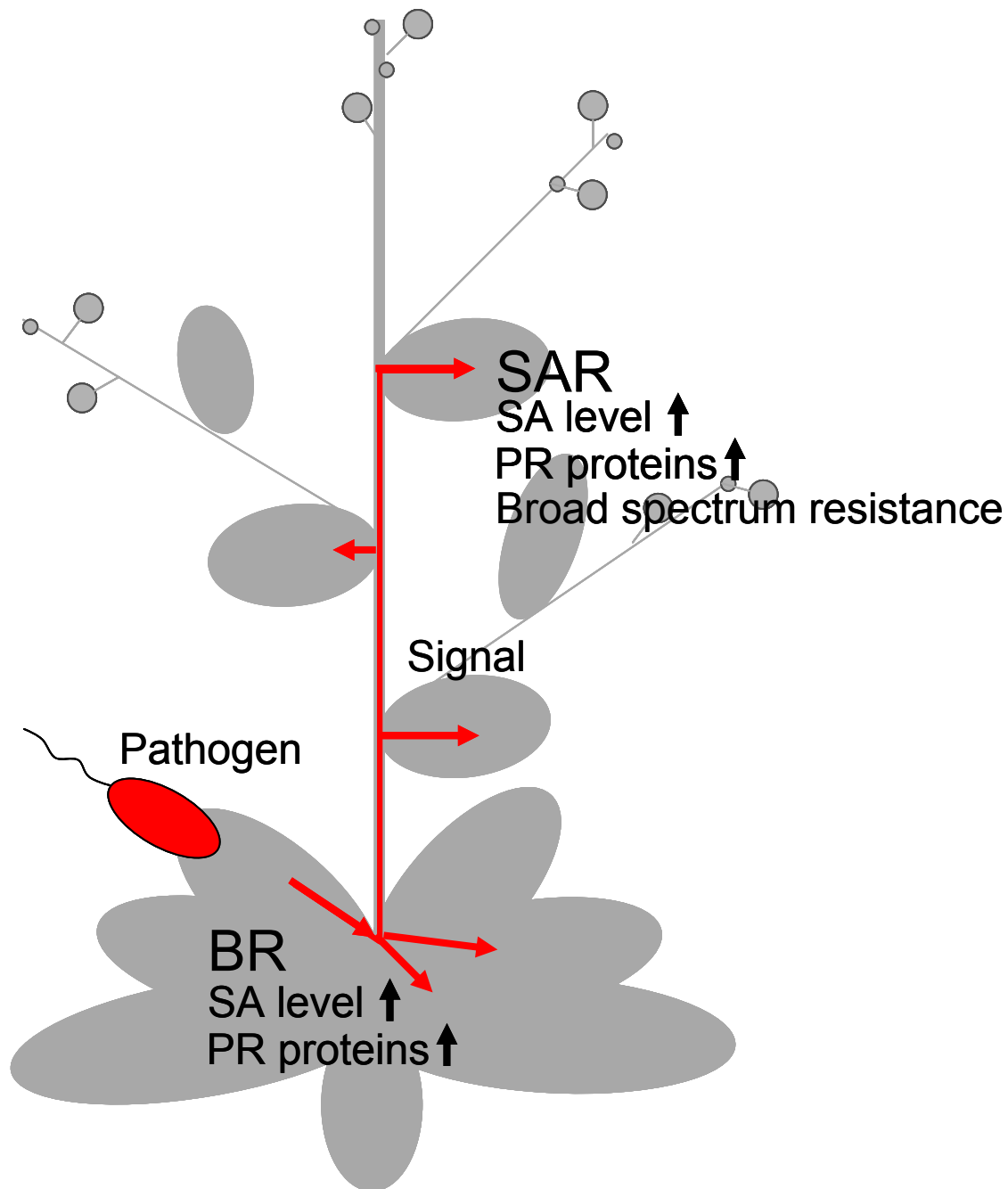
SAR, the role of the different plastidic glycerolipids in SAR is yet to be deciphered. In the following chapters I provide evidence indicating that plastid galactolipids have an important role in SAR and that unlike SFD1 two other DHAP-reductases do not have important roles in plant lipid metabolism and SAR.



**Figure 1.1 SAR induction in plants.**

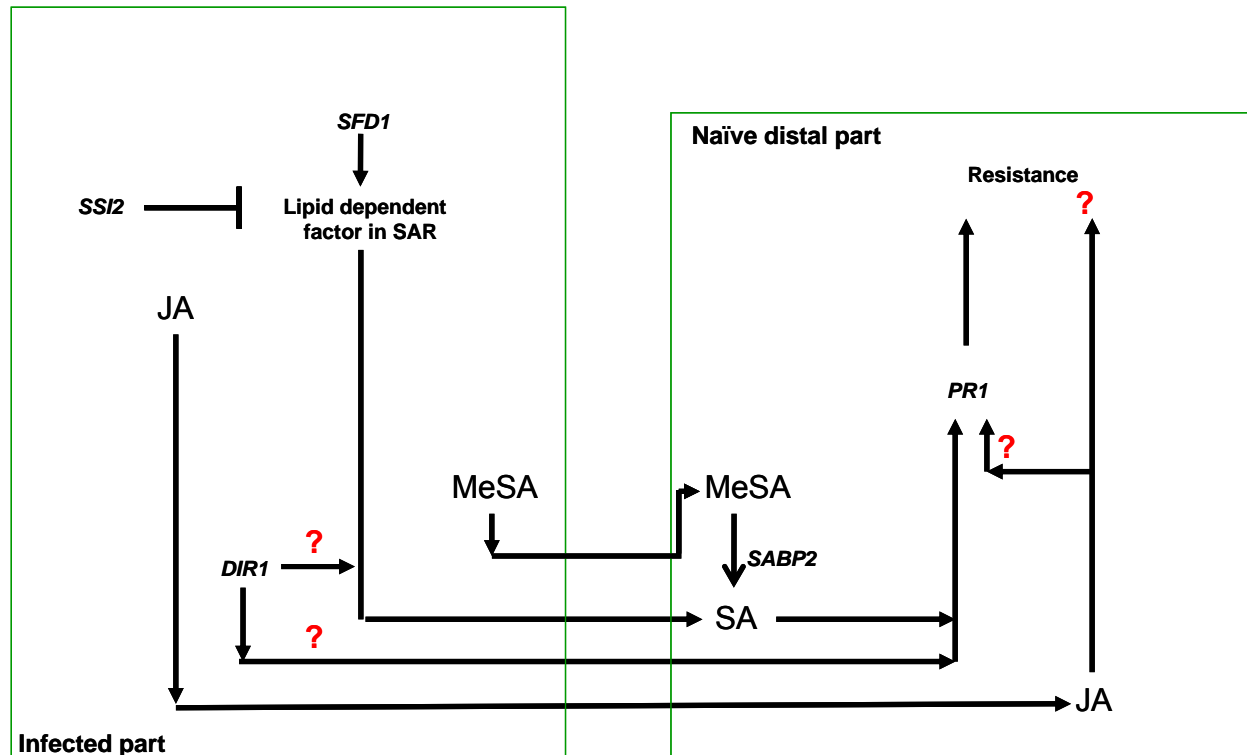
BR: Basal resistance, SAR: Systemic acquired resistance

PR: Pathogenesis related proteins, SA: Salicylic acid



Infection of one or more leaves with a pathogen stimulates SA accumulation and expression of the *PR* genes in the pathogen-inoculated organs, wherein they contribute to basal resistance (BR). Simultaneously, an unknown signal is translocated from the pathogen inoculated organs to the uninfected organs where it primes defenses to respond faster in response to a pathogen attack, a phenomenon termed systemic acquired resistance (SAR), which confers enhanced resistance against a broad-spectrum of pathogens (Durrant and Dong, 2004; Shah, 2005; Chaturvedi and Shah, 2007).

**Figure 1.2 Schematic SAR signaling pathway**



Steps leading to the activation of SAR in the naïve distal parts are shown here. SA levels increase in the pathogen inoculated and the distal leaves of plants exhibiting SAR. In tobacco infected with TMV, MeSA also accumulates in petiole exudates and the distal leaves, suggesting that MeSA may move from the pathogen inoculated to the distal organs during SAR (Park et al. 2007). The tobacco SABP2 encoded esterase likely releases SA from MeSA in the distal organs expressing SAR. JA accumulates in the petiole exudates of infected leaves and JA signaling is activated in the distal leaves of plants in which SAR is activated (Truman et al. 2007), suggesting that JA moves from the infected to the uninfected leaves. *SFD1* codes for a dihydroxyacetonephosphate (DHAP) reductase that provides glycerol-3-phosphate (G3P) for glycerolipids synthesis in the plastids and is required for the accumulation of a SAR-inducing factor/activity in petiole exudates of a pathogen-inoculated leaf. In contrast, *SSI2* which encodes a stearyl-ACP desaturase suppresses the activation of SAR. Genetic studies indicate that the

*sfd1* allele is epistatic to the *ssi2* mutant allele (Nandi et al. 2003). *DIR1* encodes a putative lipid transfer protein that may or may not bind to the SAR-activating factor/activity, but is required for the activation of SAR in the naïve distal parts. Petiole exudates from avirulent pathogen-inoculated *sfd1* mutant complement the SAR defect of the similar petiole exudates collected from the *dir1* mutant, suggesting that the SFD1-dependent factor and DIR1 are required together in petiole exudates for the activation of SAR. The *NPRI* gene is required for the expression of SAR in the distal organs.

## References

- Abramovitch, R. B., Anderson, J. C., and Martin, G. B.** (2006). Bacterial elicitation and evasion of plant innate immunity. *Nat. Rev. Mol. Cell Biol.* **7**, 601-611.
- Abramovitch, R. B., and Martin, G. B.** (2004). Strategies used by bacterial pathogens to suppress plant defenses. *Curr. Opin. Plant. Biol.* **7**, 356-364.
- Alfano, J. R., and Collmer, A.** (2004). Type III secretion system effector proteins: double agents in bacterial disease and plant defense. *Annu. Rev. Phytopathol.* **42**, 385-414.
- Apel, K., and Hirt, H.** (2004). Reactive oxygen species: Metabolism, oxidative stress and signal transduction. *Annu. Rev. Plant Biol.* **55**, 373-399.
- Beisson, F., Koo, A. J. K., Ruuska, S., Schwender, J., Pollard, M., Thelen, J. J., Paddock, T., Salas, J. J., Savage, L., Milcamps, A., Mhaske, V. B., Cho, Y., and Ohlrogge, J. B.** (2003). Arabidopsis genes involved in acyl lipid metabolism. A 2003 census of the candidates, a study of the distribution of expressed sequence tags in organs, and a web-based database. *Plant Physiol.* **132**, 681-697.
- Benhamou, N., and Nicole, M.** (1999). Cell biology of plant immunization against microbial infection: The potential of induced resistance in controlling plant diseases. *Plant Physiol. Biochem.* **37**, 703-719.
- Bostock, R. M.** (2005). Signaling crosstalk and induced resistance: Straddling the line between cost and benefit. *Annu. Rev. Phytopathol.* **43**, 545-580.
- Bowling, S. A., Clarke, J. D., Liu, Y., Klessig, D. F., and Dong, X.** (1997). The *cpr5* mutant of Arabidopsis expresses both NPR1-dependent and NPR1-independent resistance. *Plant Cell* **9**, 1573-1584.

**Cao, H., Bowling, S. A., Gordon, A. S., and Dong, X.** (1994). Characterization of an Arabidopsis mutant that is nonresponsive to inducers of systemic acquired resistance. *Plant Cell* **6**, 1583-1592.

**Cao, H., Glazebrook, J., Clark, J. D., Volko, S., and Dong, X.** (1997). The Arabidopsis *NPR1* gene that controls systemic acquired resistance encodes a novel protein containing ankyrin repeats. *Cell* **88**, 57-63.

**Cao, H., Xin, L., and Dong, X.** (1998). Generation of broad-spectrum disease resistance by overexpression of an essential regulatory gene in systemic acquired resistance. *Proc. Natl. Acad. Sci. USA* **95**, 6531-6536.

**Chaturvedi, R., Krothapalli, K., Makandar, R., Nandi, A., Sparks, A. A., Roth, M. R., Welti, R., and Shah, J.** (2008). Plastid omega-3-fatty acid desaturase-dependent accumulation of a systemic acquired resistance inducing activity in petiole exudates of *Arabidopsis thaliana* is independent of jasmonic acid. *Plant J.* **54**, 106-117.

**Chaturvedi, R., and Shah, J.** (2007). Salicylic acid in plant disease resistance. In "Salicylic Acid-A Plant Hormone" ed. S. Hayat and A. Ahmad, pp 335-370, Springer, Dordrecht, The Netherlands

**Chen, Z., Silva, H. and Klessig, D. F.** (1993). Active oxygen species in the induction of plant systemic acquired resistance by salicylic acid. *Science* **262**, 1883-1886.

**Chern, M. S., Fitzgerald, H. A., Yadav, R. C., Canlas, P. E., Dong, X., and Ronald, P. C.** (2001). Evidence for a disease-resistance pathway in rice similar to the NPR1-mediated signaling pathway in Arabidopsis. *Plant J.* **27**, 101-113.

**Chini, A., Fonseca, S., Fernandez, G., Adie, B., Chico, J. M., Lorenzo, O., Garcia-Casado, G., Lopez-Vidriero, I., Lozano, F. M., Ponce, M. R., Micol, J. L., Solano, R.** (2007). The JAZ family of repressors is the missing link in jasmonate signalling. *Nature* **448**, 666-671.

**Cohen, Y., and Kuc, J.** (1981). Evaluation of systemic acquired resistance to blue mold induced in tobacco leaves by prior stem inoculation with *Peronospora hyoscyami* f.sp. *tabacina*. *Phytopathology*. **71**, 783-787.

**Dathe, W., Rönsch, H., Preiss, A., Schade, W., Sembdner, G., and Schreiber, K.** (1981). Endogenous plant hormones of the broad bean, *Vicia faba* L. (–)-Jasmonic acid, a plant growth inhibitor in pericarp. *Planta* **155**, 530-535.

**de Jong, C., F., Laxalt, A. M., Bargmann, B. O. R., deWit, P. J. G. M., Joosten, M. H. A. J., and Munnik, T.** (2004). Phosphatidic acid accumulation is an early response in the Cf-4/Avr4 interaction. *Plant J.* **39**, 1-12.

**DeBary, A.** (1861). Die gegenwärtig herrschende Kartoffelkrankheit, ihre Ursache und ihre Verhütung (Leipzig, Germany: Felix Verlag).

**Delaney, T. P., Uknes, S., Vernooij, B., Friedrich, L., Weymann, K., Negrotto, D., Gaffney, T., Gut-Rella, M., Kessmann, H., Ward, E., and Ryals, J. A.** (1994). A Central Role of Salicylic Acid in Plant Disease Resistance. *Science* **266**, 1247-1250.

**Delaney, T. P., Friedrich, L., and Ryals, J.A.** (1995). Arabidopsis signal transduction mutant defective in chemically and biologically induced disease resistance. *Proc. Natl. Acad. Sci. USA* **92**, 6602-6606.

**Demole, E., Lederer, E., and Mercier, D.** (1962). Isolement et détermination de la structure du jasmonate de méthyle, constituant odorant caractéristique de l'essence de jasmin. *Helvetica Chimica. Acta.* **45**, 675–685.

**Després, C., Chubak, C., Rochon, A., Clark, R., Bethune, T., Desveaux, D., and Fobert, P. R.** (2003). The Arabidopsis NPR1 disease resistance protein is a novel cofactor that confers

redox regulation of DNA binding activity to the basic domain/leucine zipper transcription factor TGA1. *Plant Cell* **15**, 2181-2191.

**Després, C., DeLong, C., Glaze, S., Liu, E., and Fobert, P. R.** (2000). The Arabidopsis NPR1/NIM1 protein enhances the DNA binding activity of a subgroup of the TGA family of bZIP transcription factors. *Plant Cell* **12**, 279-290.

**Deverall, B. J.** (1977). *Defense mechanisms of plants*, P. Brian, W., Pringle, J, W, S., ed (Cambridge: Cambridge University Press;).

**Dhondt, S., Gouzerh, G., Müller, A., Legrand, M., and Heitz, T.** (2002). Spatio-temporal expression of patatin-like lipid acyl hydrolases and accumulation of jasmonates in elicitor-treated tobacco leaves are not affected by endogenous levels of salicylic acid. *Plant J.* **32**, 749-762.

**Doherty, H. M., Selvendran, R. R., and Bowles, D. J.** (1988). The wound response of tomato plants can be inhibited by aspirin and related hydroxy-benzoic acids. *Physiol. Mol. Plant Pathol.* **33**, 377-384.

**Dong, X.** (2004). NPR1, all things considered. *Curr. Opin. Plant Biol.* **7**, 547-552.

**Du, H., and Klessig, D. F.** (1997). Identification of a soluble, high-affinity salicylic acid binding protein in tobacco. *Plant Physiol.* **113**, 1319-1327.

**Durner, J., and Klessig, D. F.** (1995). Inhibition of ascorbate peroxidase by salicylic acid and 2, 6-dichloroisonicotinic acid, two inducers of plant defense responses. *Proc. Natl. Acad. Sci. USA* **92**, 11312-11316.

**Durrant, W. E., and Dong, X.** (2004). Systemic acquired resistance. *Annu. Rev. Phytopathol.* **42**, 185-209.



**Fan, W., and Dong, X.** (2002). In vivo interaction between NPR1 and transcription factor TGA2 leads to salicylic acid-mediated gene activation in Arabidopsis. *Plant Cell* **14**, 1377-1389.

**F. A. O.** (2000). The state of food insecurity in the world (SOFI ). (Rome,Italy: FAO, UN).

**Farmer, E. E., and Ryan, C. A.** (1990). Interplant communication: airborne methyl jasmonate induces synthesis of proteinase inhibitors in plant leaves. *Proc. Natl. Acad. Sci. USA* **87**, 7713–7716.

**Felix, G., Duran, J. D., Volko, S., and Boller, T.** (1999). Plants have a sensitive perception system for the most conserved domain of bacterial flagellin. *Plant J.* **18**, 265-276.

**Feussner, I., and Wasternack, C.** (2002). The lipoxygenase pathway. *Annu. Rev. Plant Biol.* **53**, 275-297.

**Feys, B. J. F., Benedetti, C. E., Penfold, C. N., and Turner, J. G.** (1994). Arabidopsis mutants selected for resistance to the phytotoxin coronatine are male sterile, insensitive to methyl jasmonate and resistant to a bacterial pathogen. *Plant Cell* **6**, 751–759.

**Forouhar, F., Yang, Y., Kumar, D., Chen, Y., Fridman, E., Park, S. W., Chiang, Y., Acton, T. B., Montelione, G. T., Pichersky, E., Klessig, D. F., and Tong, L.** (2005). Structural and biochemical studies identify tobacco SABP2 as a methyl salicylate esterase and implicate it in plant innate immunity. *Proc. Natl. Acad. Sci. USA* **102**, 1773-1778.

**Friedrich, L., Lawton, K., Dietrich, R., Willits, M., Cade, R., and Ryals, J.** (2001). NIM1overexpression in Arabidopsis potentiates plant disease resistance and results in enhanced effectiveness of fungicides. *Mol. Plant Microbe Interact.* **14**, 1114-1124.

**Gaffney, T., Friedrich, L., Vernooij, B., Negrotto, D., Nye, G., Uknes, S., Ward, E., Kessmann, H., and Ryals, J.** (1993). Requirement of salicylic acid for the induction of systemic acquired resistance. *Science* **261**, 754-756.

**Gao, X., Shim, W-B., Gobel, C., Kunze, S., Feussner, I., Meeley, R., Balint-Kurti, P., and Kolomiets, M.** (2007). Disruption of a maize 9-lipoxygenase results in increased resistance to fungal pathogens and reduced levels of contamination with mycotoxin fumonisin. *Mol. Plant Microbe Interact.* **20**, 922-933.

**Garcion, C., Lohmann, A., Lamodière, E., Catinot, J., Buchala, A., Doermann, P., and Métraux, J-P.** (2008). Characterization and biological function of the *ISOCHORISMATE SYNTHASE 2* gene of Arabidopsis. *Plant Physiol.* **147**, 1279-1287.

**Gilbert, R. D., Johnson, A. N., and Dean, R. A.** (1996). Chemical signals responsible for appressorium formation in the rice blast fungus *Magnaporthe grisea*. *Physiol. Mol. Plant Pathol.* **48**, 335-346.

**Glazebrook, J.** (2005). Contrasting mechanisms of defense against biotrophic and necrotrophic pathogens. *Annu. Rev. Phytopathol.* **43**, 205-227.

**Glazebrook, J., Chen, W. J., Estes, B., Chang, H. S., Nawrath, C., Metraux, J. P., Zhu, T., and Katagiri, F.** (2003). Topology of the network integrating salicylate and jasmonate signal transduction derived from global expression phenotyping. *Plant J.* **34**, 217-228.

**Glazebrook, J., Rogers, E. E., and Ausubel, F. M.** (1996). Isolation of Arabidopsis mutants with enhanced disease susceptibility by direct screening. *Genetics* **143**, 973-982.

**Grant, M., and Lamb, C.** (2006). Systemic immunity. *Curr. Opin. Plant. Biol.* **9**, 414-420

**Guedes, M. E. M., Richmond, S., and Kuc, J.** (1980). Induced systemic resistance to anthracnose in cucumber as influenced by the location of the inducer inoculation with *Colletotrichum lagenarium* and the onset of flowering and fruiting. *Physiol. Plant Pathol.* **17**, 229-233.

**He, P., Chintamanani, S., Chen, Z. Y., Zhu, L., Kunkel, B. N., Alfano, J. R., Tang, X., and Zhou, J. M.** (2004). Activation of a COI1-dependent pathway in Arabidopsis by *Pseudomonas syringae* type III effectors and coronatine. *Plant J.* **37**, 589-602.

**Heil, M., and Ton, J.** (2008). Long-distance signalling in plant defense. *Trends Plant Sci.* **13**, 264-272.

**Hyun, Y., Choi, S., Hwang, H. J., Yu, J., Nam, S. J., Ko, J., Park, J. Y., Seo, Y. S., Kim, E. Y., Ryu, S. B., Kim, W. T., Lee, Y-H., Kang, H., and Lee, I.** (2008). Cooperation and functional diversification of two closely related galactolipase genes for jasmonate biosynthesis. *Dev. Cell* **14**, 183-192.

**Johnson, C., Boden, E., and Arias, J.** (2003). Salicylic acid and NPR1 induce the recruitment of trans-activating TGA factors to a defense gene promoter in Arabidopsis. *Plant Cell* **15**, 1846-1858.

**Jones, D. A., and Takemoto, D.** (2004). Plant innate immunity—direct and indirect recognition of general and specific pathogen-associated molecules. *Curr. Opin. Immunol.* **16**, 48-62.

**Kachroo, P., Shanklin, J., Shah, J., Whittle, E. J., and Klessig, D. F.** (2001). A fatty acid desaturase modulates the activation of defense signaling pathways in plants. *Proc. Natl. Acad. Sci. USA* **98**, 9448-9453.

**Kessler, A., and Baldwin, I. T.** (2002). Plant responses to insect herbivory: The emerging molecular analysis. *Annu. Rev. Plant Biol.* **53**, 299-328.

**Kiefer, I. W., and Slusarenko, A. J.** (2003). The pattern of systemic acquired resistance induction within the Arabidopsis rosette in relation to the pattern of translocation. *Plant Physiol.* **132**, 840-847.

**Kinkema, M., Fan, W., and Dong, X.** (2000). Nuclear localization of NPR1 is required for activation of *PR* gene expression. *Plant Cell* **12**, 2339-2350.

**Kloek, A. P., Verbsky, M. L., Sharma, S. B., Schoolz, J. E., Vogel, J., Klessig, D. F., and Kunkel, B. N.** (2001). Resistance to *Pseudomonas syringae* conferred by an *Arabidopsis thaliana coronatine-insensitive (coi1)* mutation occurs through two distinct mechanisms. *Plant J.* **26**, 509-522.

**Kloepper, J. W., Leong, J., Teintze, M., and Schroth, M. N.** (1980). Enhanced plant growth by siderophores produced by plant growth-promoting rhizobacteria. *Nature* **286**, 885-886.

**Knoester, M., Pieterse, C. M. J., Bol, J. F., and Van Loon, L. C.** (1999). Systemic resistance in *Arabidopsis* induced by rhizobacteria requires ethylene-dependent signaling at the site of application. *Mol. Plant Microbe Interact.* **12**, 720-727.

**Kumar, D., and Klessig, D. F.** (2003). High-affinity salicylic acid-binding protein 2 is required for plant innate immunity and has salicylic acid-stimulated lipase activity. *Proc. Natl. Acad. Sci. USA* **100**, 16101-16106.

**Kunkel, B.N. and Brooks, D.M.** (2002) Cross talk between signaling pathways in plant defense. *Curr. Opin. Plant Biol.* **5**, 325-331.

**Laxalt, A., and Munnik, T.** (2002). Phospholipid signaling in plant defense. *Curr. Opin. Plant Biol.* **5**, 332-338.

**Li, J., Brader, G., and Palva, E. T.** (2004). The WRKY70 transcription factor: a node of convergence for jasmonate-mediated and salicylate-mediated signals in plant defense. *Plant Cell* **16**, 319-331.

**Lin, W. C., Lu, C. F., Wu, J. W., Cheng, M. L., Lin, Y. M., Yang, N. S., Black, L., Green, S. K., Wang, J. F., and Cheng, C. P.** (2004). Transgenic tomato plants expressing the *Arabidopsis*

*NPR1* gene display enhanced resistance to a spectrum of fungal and bacterial diseases. Transgenic Res. **13**, 567-581.

**Makandar, R., Essig, J. S., Schapaugh, M. A., Trick, H. N., and Shah, J.** (2006) Genetically engineered resistance to Fusarium head blight in wheat by expression of *Arabidopsis* NPR1. Mol. Plant Microbe Interact. **19**, 123-129

**Malamy, J., Carr, J. P., Klessig, D. F., and Raskin, I.** (1990). Salicylic acid a likely endogenous signal in the resistance response of tobacco to viral infection. Science **250**, 1002-1004.

**Maldonado, A. M., Doerner, P., Dixon, R. A., Lamb, C. J., and Cameron, R. K.** (2002). A putative lipid transfer protein involved in systemic resistance signaling in Arabidopsis. Nature **419**, 399-403.

**Maleck, K., Levine, A., Eulgem, T., Morgan, A., Schmid, J., Lawton, K. A., Dangl, J. L., and Dietrich, R. A.** (2000). The transcriptome of *Arabidopsis thaliana* during systemic acquired resistance. Nat. Genet. **26**, 403-410.

**Mauch, F., Mauch-Mani, B., Gaille, C., Kull, B., Haas, D., and Reimmann, C.** (2001). Manipulation of salicylate content in *Arabidopsis thaliana* by the expression of an engineered bacterial salicylate synthase. Plant J. **25**, 67-77.

**Mauch-Mani, B., and Slusarenko, A. J.** (1996). Production of salicylic acid precursors is a major function of phenylalanine ammonia-lyase in the resistance of Arabidopsis to *Peronospora parasitica*. Plant Cell **8**, 203-212.

**McConn, M., and Browse, J.** (1996). The critical requirement for linolenic acid is pollen development, not photosynthesis, in an Arabidopsis mutant. Plant Cell **8**, 403-416.

- McConn, M., Creelman, R. A., Bell, E., Mullet, J. E., and Browse, J.** (1997). Jasmonate is essential for insect defense. *Proc. Natl. Acad. Sci. USA* **94**, 5473–5477.
- Métraux, J-P .** (2002). Recent breakthroughs in the study of salicylic acid biosynthesis. *Trends Plant Sci.* **7**, 332-334.
- Mishina, T. E., and Zeier, J.** (2007). Pathogen-associated molecular pattern recognition rather than development of tissue necrosis contributes to bacterial induction of systemic acquired resistance in *Arabidopsis*. *Plant J.* **50**, 500-513.
- Mou, Z., Fan, W., and Dong, X.** (2003). Inducers of plant systemic acquired resistance regulate NPR1 function through redox changes. *Cell* **113**, 935-944.
- Mysore, K. S., and Ryu, C-M.** (2004). Nonhost resistance: how much do we know? *Trends Plant Sci.* **9**, 97-104.
- Nandi, A., Krothapalli, K., Buseman, C. M., Li, M., Welti, R., Enyedi, A., and Shah, J.** (2003). *Arabidopsis sfd* mutants affect plastidic lipid composition and suppress dwarfing, cell death, and the enhanced disease resistance phenotypes resulting from the deficiency of a fatty acid desaturase. *Plant Cell* **15**, 2383-2398.
- Nandi, A., Moeder, W., Kachroo, P., Klessig, D. F., and Shah, J.** (2005). The *Arabidopsis ssi2*-conferred susceptibility to *Botrytis cinerea* is dependent on *EDS5* and *PAD4*. *Mol. Plant-Microbe Interact.* **18**, 363-370.
- Nandi, A., Welti, R., and Shah, J.** (2004). The *Arabidopsis thaliana* dihydroxyacetone phosphate reductase gene *SUPPRESSOR OF FATTY ACID DESATURASE DEFICIENCY 1* is required for glycerolipid metabolism and for the activation of systemic acquired resistance. *Plant Cell* **16**, 465-477.

- Nawrath, C., Heck, S., Parinthewong, N., and Métraux, J-P.** (2002). *EDS5*, an essential component of salicylic acid-dependent signaling for disease resistance in *Arabidopsis*, is a member of the MATE transporter family. *Plant Cell* **14**, 275-286.
- Nene, Y. L.** (2007). A Glimpse at Viral Diseases in the Ancient Period. *Asian Agri-History* **11**, 33-46
- Newman, M., A., von Roepenack-Lahaye, E., Parr, A., Daniels, M. J., and Dow, M. J.** (2002). Prior exposure to lipopolysaccharide potentiates expression of plant defenses in response to bacteria. *Plant J.* **29**, 487-495.
- Niggeweg, R., Thurow, C., Weigel, R., Pfitzner, U., and Gatz, C.** (2000). Tobacco TGA factors differ with respect to interaction with NPR1, activation potential and DNA-binding properties. *Plant Mol. Biol.* **42**, 775-788.
- Norman-Setterblad, C., Vidal, S., and Palva, T. E.** (2000). Interacting signal pathways control defense gene expression in *Arabidopsis* in response to cell wall-degrading enzymes from *Erwinia carotovora*. *Mol. Plant-Microbe Interact.* **13**, 430-438.
- Nurnberger, T., and Lipka, V.** (2005). Non-host resistance in plants: new insights into an old phenomenon. *Mol Plant Pathol* **6**, 335–345
- Padmanabhan, S. Y.** (1973). The great Bengal famine. *Annu. Rev. Phytopathol.* **11**, 11-24.
- Park, S-W., Kaimoyo, E., Kumar, D., Mosher, S., and Klessig, D. F.** (2007). Methyl salicylate is a critical mobile signal for plant systemic acquired resistance. *Science* **318**, 113-116.
- Pena-Cortes, H., Albrecht, T., Prat, S., Weiler, E. W., and Willmitzer, L.** (1993). Aspirin prevents wound-induced gene expression in tomato leaves by blocking jasmonic acid biosynthesis. *Planta* **191**, 123-128.

**Pieterse, C. M. J., Pelt, J. A., Ton, J., Parchmann, S., Mueller, M. J., Buchala, A. J., Mettraux, J-P, and Loon, L. C.** (2000). Rhizobacteria-mediated induced systemic resistance (ISR) in *Arabidopsis* requires sensitivity to jasmonate and ethylene but is not accompanied by an increase in their production. *Physiol Mol Plant Patho* **57**, 123-134.

**Pieterse, C. M. J., Wees, S. C. M., Pelt, J. A., Knoester, M., Laan, R., Gerrits, N., Welsbeek, P. J., and Loon, L. C.** (1998). A novel signaling pathway controlling induced systemic resistance in *Arabidopsis*. *Plant Cell* **10**, 1571-1580.

**Pieterse, C. M. J., Van Wees, S. C. M., Hoffland, E., van Pelt, J. A., and van Loon, L. C.** (1996). Systemic resistance in *Arabidopsis* induced by biocontrol bacteria is independent of salicylic acid accumulation and pathogenesis-related gene expression. *Plant Cell* **8**, 1225-1237.

**Prost, I., Dhondt, S., Rothe, G., Vicente, J., Rodriguez, M. J., Carbonne, F., Griffiths, G., Esquerre-Tugaye, M. T., Rosahl, S., Castresana, C., Hamberg, M., and Fournier, J.** (2005). Evaluation of the antimicrobial activities of plant oxylipins supports their involvement in defense against pathogens. *Plant Physiol.* **139**, 1902-1913.

**Rancé, I., Fournier, J., and Esquerre-Tugaye, M. T.** (1998). The incompatible interaction between *Phytophthora parasitica* var. *nicotianae* race 0 and tobacco is suppressed in transgenic plants expressing antisense lipoxygenase sequences. *Proc. Natl. Acad. Sci. USA* **95**, 6554-6559.

**Rao, M. V., Lee, H., Creelman, R. A., Mullet, J. E., and Davis, K. R.** (2000). Jasmonic acid signalling modulates ozone-induced hypersensitive cell death. *Plant Cell* **12**, 1633-1646.

**Ross, A. F.** (1961a). Localized acquired resistance to plant virus infection in hypersensitive hosts. *Virology* **14**, 329-339.

**Ross, A. F.** (1961b). Systemic acquired resistance induced by localized virus infections in plants. *Virology* **14**, 340-358.



**Ross, A. F.** (1966). Systemic effects of local lesion formation. In *Viruses of Plants*, A. Beemster, B. R., Dijkstra, J., ed ( Amsterdam: North-Holland), pp. 127-150.

**Rüffer, M., Steipe, B., and Zenk, M. H.** (1995). Evidence against specific binding of salicylic acid to plant catalase. *FEBS Lett.* **377**, 175-180.

**Ryals, J., Weymann, K., Lawton, K., Friedrich, L., Ellis, D., Steiner, H. Y., Johnson, J., Delaney, T. P., Jesse, T., Vos, P., and Uknes, S.** (1997). The Arabidopsis NIM1 protein shows homology to the mammalian transcription factor inhibitor I[kappa]B. *Plant Cell* **9**, 425-439.

**Ryu, S. B.** (2004). Phospholipid-derived signaling mediated by phospholipase A in plants. *Trends Plant Sci.* **9**, 229-235.

**Sang, Y., Cui, D., and Wang, X.** (2001). Phospholipase D and phosphatidic acid-mediated generation of superoxide in Arabidopsis. *Plant Physiol.* **126**, 1449-1458.

**Schenk, P. M., Kazan, K., Wilson, I., Anderson, J. P., Richmond, T., Somerville, S. C., and Manners, J. M.** (2000). Coordinated plant defense responses in Arabidopsis revealed by microarray analysis. *Proc. Natl. Acad. Sci. USA* **97**, 11655-11660.

**Schippers, B., Bakker, A. W., and Bakker, P. A. H. M.** (1987). Interactions of deleterious and beneficial rhizosphere microorganisms and the effect of cropping practices. *Annu. Rev. Phytopathol* **25**, 339-358.

**Schneider, M., Schweizer, P., Meuwly, P., and Métraux, J-P.** (1996). Systemic acquired resistance in plants. *Int. J. Cytol.* **168**, 303-340.

**Sekine, K. T., Nandi, A., Ishihara, T., Hase, S., Ikegami, M., Shah, J., and Takahashi, H.** (2004). Enhanced resistance to Cucumber mosaic virus in the *Arabidopsis thaliana* *ssi2* mutant is mediated via an SA-independent mechanism. *Mol. Plant-Microbe Interact.* **17**, 623-632.

**Seo, H. S., Song, J. T., Cheong, J.-J., Lee, Y. H., Lee, Y. W., Hwang, I., Lee, J. S., and Chol, Y. D.** (2001). Jasmonic acid carboxyl methyltransferase: A key enzyme for jasmonate-regulated plant responses. *Proc. Natl. Acad. Sci. USA* **98**, 4788-4793.

**Seok, O. H., Park, A. R., Bae, M. S., Kwon, S. J., Kim, Y. S., Lee, J. E., Kang, N. Y., Lee, S., Cheong, H., Park, O. K.** (2005). Secretome analysis reveals an Arabidopsis lipase involved in defense against *Alternaria brassicicola*. *Plant Cell* **17**, 2832-2847.

**Shah, J.** (2003). The salicylic acid loop in plant defense. *Curr. Opin. Plant. Biol.* **6**, 365-371.

**Shah, J.** (2005). Lipids, lipases, and lipid-modifying enzymes in plant disease resistance. *Annu. Rev. Phytopathol.* **43**, 229-260.

**Shah, J., Kachroo, P. K., Nandi, A., and Klessig, D. F.** (2001). A recessive mutation in the Arabidopsis *SSI2* gene confers SA- and *NPR1*-independent expression of *PR* genes and resistance against bacterial and oomycete pathogens. *Plant J.* **25**, 563-574.

**Shah, J., Tsui, F., and Klessig, D. F.** (1997). Characterization of a salicylic acid-insensitive mutant (*sai1*) of *Arabidopsis thaliana*, identified in a selective screen utilizing the SA-inducible expression of the *tms2* gene. *Mol. Plant Microbe Interact.* **10**, 69-78.

**Slaymaker, D. H., Navarre, D. A., Clark, D., del Pozo, O., Martin, G. B., and Klessig, D. F.** (2002). The tobacco salicylic acid-binding protein 3 (SABP3) is the chloroplast carbonic anhydrase, which exhibits antioxidant activity and plays a role in the hypersensitive defense response. *Proc. Natl. Acad. Sci. USA* **99**, 11640-11645.

**Smith, J. A., and M'ettraux, J. P.** (1991). *Pseudomonas syringae* pv. *syringae* induces systemic resistance to *Pyricularia oryzae* in rice. *Physiol. Mol. Plant Pathol.* **39**, 451-461.

**Somerville, C., Browse, J., Jaworski, J. G., and Ohrologge, J. B.** (2000). Lipids. In *Biochemistry and molecular biology of plants*. B.

Buchanan, W. Gruissem, and R. Jones, eds (Rockville, MD: American Society of Plant Biologists), pp. 456–527.

**Spoels, H. S., Koornneef, A., Claessens, S., Korzelius, J. P., Van Pelt, J. A., Mueller, M. J., Buchala, A. J., Métraux, J. P., Brown, R., Kazan, K., Van Loon, L. C., Dong, X., and Pieterse, C. M. J.** (2003). NPR1 modulates cross-talk between salicylate- and jasmonate-dependent defense pathways through a novel function in the cytosol. *Plant Cell* **15**, 760-770.

**Staswick, P. E., Yuen, G. Y., and Lehman, C. C.** (1998). Jasmonate signaling mutants of *Arabidopsis* are susceptible to the soil fungus *Pythium irregulare*. *Plant J.* **15**, 747-754.

**Staswick, P. E., and Tiryaki, I.** (2004). The oxylipin signal jasmonic acid is activated by an enzyme that conjugates it to isoleucine in *Arabidopsis*. *Plant Cell* **16**, 2117-2127

**Sticher, L., Mauch-Mani, B., and Métraux, J-P.** (1997). Systemic acquired resistance. *Anal. Rev. Phytopathol.* **35**, 235-270.

**Strange, R. N., and Scott, P. R.** (2005). Plant disease: A threat to global food security. *Annu. Rev. Phytopathol.* **43**, 83-116.

**Thines, B., Katsir, L., Melotto, M., Niu, Y., Mandaokar, A., Liu, G., Nomura, K., He, S. Y., Howe, G. A., Browse, J.** (2007). JAZ repressor proteins are targets of the SCFCOI1 complex during jasmonate signalling. *Nature* **448**, 661-665.

**Thomma, B. P. H. J., Eggermont, K., Penninckx, I. A. M. A., Mauch-Mani, B., Vogelsang, R., Cammue, B. P. A., and Broekaert, W. F.** (1998). Separate jasmonate-dependent and salicylate-dependent defense-response pathways in *Arabidopsis* are essential for resistance to distinct microbial pathogens. *Proc. Natl. Acad. Sci. USA* **95**, 15107-15111.

- Thomma, B. P. H. J., Eggermont, K., Tierens, K. F. M.-J., and Broekaert, W. F.** (1999). Requirement of functional *ethylene-insensitive 2* gene for efficient resistance of Arabidopsis to infection by *Botrytis cinerea*. *Plant Physiol.* **121**, 1093–1101.
- Thordal-Christensen, H.** (2003). Fresh insights into processes of nonhost resistance. *Curr. Opin. Plant Biol.* **6**, 351-357.
- Ton, J., Van Pelt, J. A., Van Loon, L. C., and Pieterse, C. M. J.** (2002). Differential effectiveness of salicylate-dependent and jasmonate/ethylene-dependent induced resistance in Arabidopsis. *Mol. Plant Microbe Interact.* **15**, 27-34.
- Truman, W., Bennett, M. H., Kubigsteltig, I., Turnbull, C., Grant, M.** (2007). Arabidopsis systemic immunity uses conserved defense signaling pathways and is mediated by jasmonates. *Proc. Natl. Acad. Sci. USA* **104**, 1075-1080.
- Ueda, J., and Kato, J.** (1980). Isolation and identification of a senescence-promoting substance from wormwood (*Artemisia absinthium* L.). *Plant Physiol.* **66**, 246–249.
- van Loon, L. C., Bakker, P. A. H. M., and Pieterse, C. M. J.** (1998). Systemic resistance induced by rhizosphere bacteria. *Annu. Rev. Phytopathol.* **36**, 453-483.
- van Peer, R., Niemann, G. J., and Schippers, B.** (1991). Induced resistance and phytoalexin accumulation in biological control of fusarium wilt of carnation by *Pseudomonas* sp. strain WCS417r. *Phytopathology.* **81**, 728-734.
- van Wees, S. C. M., and Glazebrook, J.** (2003). Loss of non-host resistance of Arabidopsis *NahG* to *Pseudomonas syringae* pv. *phaseolicola* is due to degradation products of salicylic acid. *Plant J.* **33**, 733-742.

**van Wees, S. C. M., De Swart, E. A. M., Van Pelt, J. A., van Loon, L. C., and Pieterse, C. M. J.** (2000). Enhancement of induced disease resistance by simultaneous activation of salicylate- and jasmonate-dependent defense pathways in *Arabidopsis thaliana*. Proc. Natl. Acad. Sci. USA **97**, 8711-8716.

**van Wess, S. C. M., LUIjendilk, M., Smoorenburg, I., Van Loon, L. C., and Pieterse, C. M. J.** (1999). Rhizobacteria-mediated induced systemic resistance (ISR) in *Arabidopsis* is not associated with direct effect on expression of known defense-related genes but stimulates the expression of the jasmonate-inducible gene *Atvsp* upon challenge. Plant Mol. Biol. **41**, 537-549.

**Vernooij, B., Friedrich, L., Morse, A., Reist, R., Kolditz-Jawhar, R., Ward, E., Uknes, S., Kessmann, H., and Ryals, J.** (1994). Salicylic acid is not the translocated signal responsible for inducing systemic acquired resistance but is required in signal transduction. Plant Cell **6**, 959-965.

**Vick, B. A., and Zimmerman, D. C.** (1984). Biosynthesis of jasmonic acid by several plant species. Plant Physiol. **75**, 458-461.

**Vijayan, P., Shockey, J., Levesque, C. A., Cook, R. J., and Browse, J.** (1998). A role for jasmonate in pathogen defense of *Arabidopsis*. Proc. Natl. Acad. Sci. USA **95**, 7209-7214.

**Wang, X.** (2004). Lipid signaling. Curr. Opin. Plant Biol. **7**, 329-336.

**Wang, X., Devaiah, S. P., Zhang, W., and Welti, R.** (2006). Signaling functions of phosphatidic acid. Prog. Lipid Res. **45**, 250-278.

**Ward, H. M.** (1902). On the relations between host and parasite in the bromes and their brown rust, *Puccinia dispersa* (Erikss.). Ann Bot **16**, 233-315.

**Wasternack, C.** (2007) Jasmonates: an update on biosynthesis, signal transduction and action in plant stress response, growth and development. Annal. Bot. **100**, 681–697.

**Watanabe, N., and Lam, E.** (2006). The hypersensitive response in plant disease resistance. In multigenic and induced systemic resistance in plants, S. Tuzun, and Bent, E., ed (New York: Springer), pp. 83-111.

**Wei, G., Kloepper, J. W., and Tuzun, S.** (1991). Induction of systemic resistance of cucumber to *Colletotrichum orbiculare* by select strains of plant growth-promoting rhizobacteria. *Phytopathology*. **81**, 1508-1512.

**Weissman, G.** (1991). Aspirin. *Scientific American* **264**, 84-90.

**Weller, D. M.** (1988). Biological control of soil-borne plant pathogens in the rhizosphere with bacteria. *Annu. Rev. Phytopathol* **26**, 379-407.

**White, R. F.** (1979). Acetyl salicylic acid (aspirin) induces resistance to tobacco mosaic virus in tobacco. *Virology* **99**, 410-412.

**Wildermuth, M. C., Dewdney, J., Wu, G., and Ausubel, F. M.** (2001). Isochorismate synthase is required to synthesize salicylic acid for plant defence. *Nature* **414**, 562-565.

**Xiao, F., Goodwin, S. M., Xiao, Y., Sun, Z., Baker, D., Tang, X., Jenks, M. A., and Zhou, J. M.** (2004). Arabidopsis *CYP86A2* represses *Pseudomonas syringae* type III genes and is required for cuticle development. *EMBO J.* **23**, 2903-2913.

**Xie, D. X., Feys, B. F., James, S., Nieto-Rostro, M., and Turner, J. G.** (1998). *COI1*: an Arabidopsis gene required for jasmonate-regulated defense and fertility. *Science* **280**, 1091–1094.

**Yang, W., Devaiah, S. P., Pan, X., Isaac, G., Welti, R., and Wang, X.** (2007). *AtPLAI* is an acylhydrolase involved in basal jasmonic acid production and Arabidopsis resistance to *Botrytis cinerea*. *J. Biol. Chem.* **282**, 18116-18128.

**Yaeno, T., Matsuda, O., and Iba, K.** (2004). Role of chloroplast trienoic fatty acids in plant disease defense responses. *Plant J* **40**, 931-941.

**Yarwood, C. E.** (1960). Localized acquired resistance to tobacco mosaic virus. *Phytopathology*. **50**, 741-744.

**Zhang, Y., Fan, W., Kinkema, M., Li, X., and Dong, X.** (1999). Interaction of NPR1 with basic leucine zipper protein transcription factors that bind sequences required for salicylic acid induction of the *PR-1* gene. *Proc. Natl. Acad. Sci. USA*. **96**, 6523-6528.

**Zhou, J-M., Trifa, Y., Silva, H., Pontier, D., Lam, E., Shah, J., and Klessig, D.F.** (2000). NPR1 differentially interacts with members of the TGA/OBF family of transcription factors that bind an element of the *PR-1* gene required for induction by salicylic acid. *Mol. Plant Microbe Interact.* **13**, 191-202.

## **CHAPTER 2 - The role of dihydroxyacetone phosphate (DHAP) reductases in plant defense**

A mutation in the *SSI2* gene, which encodes a plastid-localized stearyl-acyl carrier protein (ACP) desaturase (Kachroo et al., 2001), resulted in the spontaneous development of lesions, dwarfing, constitutive expression of the *PATHOGENESIS-RELATED (PR)* genes and heightened resistance to a wide spectrum of pathogens (Kachroo et al., 2001; Shah et al., 2001; Sekine et al., 2004; Nandi et al., 2005). Both, NPR1-dependent SAR and an NPR1-independent defense mechanism were hyperactive in the *ssi2* mutant plant (Shah et al., 2001). All *ssi2* allele associated phenotypes were suppressed by loss-of-function mutations in the *SFD1* (*SUPPRESSOR OF FATTY ACID DESATURASE DEFICIENCY 1*) gene (Nandi et al., 2003, 2004). The *sfd1* mutant was found to have a characteristic defense phenotype. Basal resistance to bacteria was not affected in the *sfd1* mutant. However, compared to the WT, *sfd1* mutants were compromised in SAR induced by prior exposure to an avirulent pathogen (Nandi et al., 2004). *Sfd1* mutants were subsequently found to lack the ability to accumulate a SAR activating signal in their petiole exudates (Chaturvedi et al., 2008).

*SFD1* (annotated as At2g40690 gene) encodes a 420 amino acid protein with a putative plastid localization signal sequence at its N-terminal end (Nandi et al., 2004). The predicted SFD1 protein exhibits high homology to eukaryotic glycerol-3-phosphate (G3P) dehydrogenases /dihydroxyacetone phosphate (DHAP) reductases. SFD1 contains a highly conserved NAD(P)H-dependent glycerol-3-phosphate dehydrogenase multi domain (PRK00094, gpsA) (Marchler-Bauer et al., 2007) which extends from the amino acid position 89 to 413. A recombinant SFD1 protein complemented the glycerol deficiency of an *Escherichia coli* G3P-dehydrogenase mutant, suggesting that it encodes a functional enzyme. In case of the *sfd1-2* mutant the amino acid Ala, at position 381 in this multidomain, was replaced by Thr (Nandi et al., 2004).



DHAP reductases are involved in the conversion of DHAP to G3P. DHAP, a product of glycolysis, is converted to G3P with the utilization of NADH as proton donor. The reverse reaction, i.e. the conversion of G3P to DHAP is catalyzed by G3P dehydrogenases, which were first identified in animal tissue (Lin, 1977). In higher plants and algae, the G3P dehydrogenases are referred to as DHAP reductases because at physiological pH and substrate concentrations the enzymes are essentially inactive as dehydrogenases (Gee et al., 1988; Kirsch et al., 1992). There are two forms of DHAP reductases in plants (Gee et al., 1988; Kirsch et al., 1992), plastidic and cytosolic. G3P provide the C backbone for glycerolipid synthesis, in addition to C for other metabolic processes.

Glycerolipid biosynthesis is initiated by an acylation reaction that transfers a fatty acid from plastidic acyl-ACP (acyl carrier protein) or the cytoplasmic acyl-CoA, to G3P to yield lysophospholipid (LPA). LPA is subsequently acylated to yield phosphatidic acid (PA). In the plastids, PA is further utilized for the synthesis of a variety of glycerolipids (Somerville et al., 2000). The *sfd1* mutant contains an alteration in its lipid composition, in particular plastidic lipids (Nandi et al., 2003, 2004). MGDG (monogalactosyldiacylglycerol) is the most abundant form of glycerolipid in Arabidopsis, which is found in the plastids. Its levels are largely represented by two of its chief species 34:6 (18:3 + 16:3)-MGDG and 36:6 (18:3 + 18:3)-MGDG. The level of the 34:6 (18:3 + 16:3) MGDG was 45% lower and the level of 36:6 (18:3+18:3) MGDG was 2-fold higher in the leaves of the *sfd1* mutant than the WT plant (Nandi et al., 2004), confirming a role for SFD1 in synthesizing precursors needed for MGDG synthesis.

The Arabidopsis database (<http://www.arabidopsis.org>) has five genes listed as encoding a putative DHAP reductases. These genes are annotated as At2g40690 (*SFD1*), At5g40610 (AtGPDHp), At2g41540 (AtGPDHc), At3g07690 and At3g10370. At5g40610 (AtGPDHp) encodes a 400 amino acid protein with a NAD(P)H-dependent G3P dehydrogenase multidomain (PRK00094, *gpsA*) which extends from the amino acid position 54 to 395. At2g41540 (AtGPDHc) encodes a 462 amino acid protein with a NAD(P)H-dependent G3P dehydrogenase multidomain (PRK00094, *gpsA*) extending from position 43 to 384. At3g07690 codes for a 466 amino acid protein with a similar domain from position 36 to 422. Lastly, At3g10370 codes for a 629 amino acid protein with two domains, a G3P dehydrogenase multidomain (COG0578,

GlpA) (Marchler-Bauer et al., 2007) extending from amino acids 64 to 615 and a FAD dependent oxidoreductase multidomain (pfam01266, DAO) between amino acid residues 75 and 307.

Although At5g40610 (AtGPDHp) was described as a plastid-localized DHAP reductase (Wei et al., 2001), its contribution to glycerolipid biosynthesis or its role in plant defense has not been identified. Similarly, At2g41540 (AtGPDHc) was shown to encode a cytosolic DHAP reductase (Shen et al., 2006), but its role in glycerolipid metabolism or plant defense is not known.

I identified the DHAP reductases with highest similarity to *SFDI* (Fig 2.1) and examined their role in glycerolipid biosynthesis through the analysis of their knock out lines. I demonstrate that glycerolipid composition is not affected in the *gpdhc* mutant (Table 2.1), which contains a T-DNA insertion in the At2g41540 gene, although basal resistance against *P. syringae* pv *maculicola* was higher in the mutant compared to the WT plant (Fig 2.5 B). In contrast, in comparison to the WT, glycerolipid composition was slightly altered in the *gpdhp* mutant (Table 2.1), which contains a T-DNA insertion in the At5g40610 gene. However, plant defense was not affected in the *gpdhp* mutant plant (Fig 2.5 A, 2.6 A).

## **Materials and methods**

### **Cultivation of plants and pathogens**

Arabidopsis plants were cultivated at 22°C in a tissue-culture chamber programmed for a 14 h light (100 µE/m/s) and 10 h dark cycle. Seeds were germinated either in soil or on Murashige-Skoog (MS) (Sigma, St. Louis) agar supplemented with 1% sucrose. Ten days post germination, seedlings were transplanted to soil-filled pots and cultivated as described above. *Pseudomonas syringae* pv. *maculicola* ES4326 was propagated at 28°C on King's B medium (King et al., 1954) containing streptomycin (100 µg/ml). An overnight culture was used for infecting plants. *Pseudomonas syringae* pv. *tomato* DC3000 V288 containing *avrRpt2* was propagated at 28°C on King's B medium (King et al., 1954) containing kanamycin (25 µg/ml) and rifampicin (100 µg/ml).

### **Arabidopsis mutants**

The Arabidopsis T-DNA insertion lines (SALK collection <http://signal.salk.edu>) were obtained from the Arabidopsis Biological Resource Center (ABRC) located at the Ohio State University. The lines Salk\_062006 and Salk\_020444 contained T-DNA insertions within the At5g40610 (AtGPDHp) and At2g41540 (AtGPDHc) genes, respectively.

### **Bacterial inoculations**

Four week-old soil grown plants were used for inoculation. The overnight grown bacterial strain cultures were harvested and resuspended in 10 mM MgCl<sub>2</sub> at an optical density specific to each experiment. A 1 ml syringe without a needle was used to infiltrate the bacterial suspension in to the abaxial surface of the leaf.

Basal resistance was monitored by inoculating 4-5 leaves per plant with a suspension of *Pseudomonas syringae* pv. *maculicola* ES4326 grown to an OD<sub>600nm</sub> = 0.0001. The growth of the bacteria was measured 3 days after inoculation. 20 (5 replications of 4 leaves in each sample) leaf discs (0.28 cm<sup>2</sup>) were harvested and samples ground in 1 ml of 10 mM MgCl<sub>2</sub> and appropriate dilutions were plated on King's B medium containing streptomycin (100 µg/ml).

Plates were incubated at 28°C for 2 days before counting the bacterial colonies. Bacterial counts are expressed as colony-forming units per leaf disc.

SAR was activated by inoculating 3-4 lower leaflets (1° challenge), keeping the orthostichy of the Arabidopsis rosette in consideration, with a suspension ( $OD_{600nm} = 0.01$ ) of *Pseudomonas syringae* pv. *tomato* DC3000 V288 containing the *avrRpt2* avirulence gene in 10 mM  $MgCl_2$ . In parallel, plants that were inoculated with 10 mM  $MgCl_2$  (mock challenge) provided the negative controls. The activation of SAR was monitored by monitoring expression of *PR1* and quantifying the bacterial growth in the uninoculated naive leaves of mock and Avirulent pathogen treated plants. 3-4 naive leaves were challenged (2° challenge) 3 d after 1° challenge or mock challenge with a suspension of *Pseudomonas syringae* pv. *maculicola* ES4326 ( $OD_{600nm} = 0.00025$ ) and the growth of the bacteria was measured 3 d after 2° challenge. 20 (5 replications of 4 leaves in each sample) leaf discs ( $0.28\text{ cm}^2$ ) were harvested and samples ground in 1 ml of 10 mM  $MgCl_2$  at and appropriate dilutions were plated on King's B medium containing streptomycin (100  $\mu\text{g/ml}$ ). Plates were incubated at 28°C for 2 days before counting the bacterial colonies. Bacterial counts are expressed as colony-forming units per leaf disc.

### **Lipid Extraction**

Two to three leaves of about 4 week old plants are used per each sample. The leaves are immersed into 3 ml of isopropanol with 0.01% butylated hydroxytoluene at 75°C. After 15 minutes; 1.5 ml of chloroform and 0.6 ml of water were added to the above. The tubes were shaken for about an hour, followed by removal of the extract, which is collected separately. The leaves were re-extracted with 4 ml chloroform/methanol (2:1) with 0.01% butylated hydroxytoluene four times with 30 min of agitation each time except the last round which was left overnight, until all of the leaves appeared colorless. The remaining leaves were heated overnight at 105°C and weighed to obtain the dry weight of the tissue used. The combined extracts were washed once with 1 ml of 1 M KCl by vortexing. The mix was then centrifuged and the upper phase was discarded. The wash was repeated with 2 ml of water and the upper phase was discarded. The remaining solvent was evaporated under nitrogen, and the lipid extract was dissolved in 1 ml of chloroform. Standards were added and the ESI-MS/MS mass spectrometric analysis was performed as previously described (Walti et al., 2002).

### **RNA extraction and RT-PCR analysis**

Leaf tissue was ground under liquid nitrogen, and RNA was extracted using acid guanidinium thiocyanate-phenol-chloroform as previously described (Chomczynski and Sacchi, 1987). The isolated RNA was purified and used in the two step reverse-transcription polymerase chain reactions (RT-PCR). 2 µg total RNA was mixed with oligo(dT) primers (Promega), and the final volume was made up to 15 µl with water. This mixture was incubated at 70°C for 5 min, and then chilled on ice for 1-2 min. To the above mix, 5 µl of M-MLV RT buffer (Promega), 1.25 µl dNTP mix (10 nM each), 1 µl M-MLV reverse transcriptase (Promega) and 2.75 µl of water were added. cDNA synthesis allowed to proceed at 37°C for 1 – 1.5 h. 1 µl aliquots of this cDNA were used in subsequent PCR. The PCR primers used for the ACT8 gene (*At1g49240*) were ACT8-F 5'-ATGAAGATTAAGGTCGTGGCA-3' and ACT8-R 5'-CCGAGTTTGAAGAGGCTAC-3'. The AtGPDH<sub>p</sub> -RTF 5'- GCCCTCAAGCTTCCTTCTTT-3' and AtGPDH<sub>p</sub> -RTR 5'- ATGTTTGCGCCCATAGAAGAAC -3'primers were used for amplification of AtGPDH<sub>p</sub> (*At5g40610*), and the AtGPDH<sub>c</sub> -RTF 5'-CATGGTACGGTCAAATGCTG -3' and AtGPDH<sub>c</sub> -RTR 5'- TAGAATGCATGGCTCTGTGC -3'primers were used for amplification of AtGPDH<sub>c</sub> (*At2g41540*). The PCRs were performed with the following conditions: 95°C for 5 min followed by 25 cycles of 95°C for 30 sec, 60°C for 45 sec, 72°C for 1 min, with final extension at 72°C for 10 min. The At-PR1-F 5'-CTCTTGTAAGGTGCTCTTGTTTC-3' and At-PR1-R 5'-CAGCTCTTATTTGTATTATTG-3'primers were used for PCR amplification of *PR1* (*At2g14610*). The PCR was performed with the following conditions: 95°C for 5 min followed by 25 cycles of 95°C for 30 sec, 60°C for 45 sec, 72°C for 1 min, with final extension at 72°C for 10 min.

### **DNA extraction and PCR analysis**

*Arabidopsis* genomic DNA from leaf tissue was isolated as previously described (Konieczny and Ausubel, 1993). A medium sized leaf (approx 30 mg) was put in a 1.5 ml microfuge tube and frozen in liquid nitrogen. A plastic pestle was used to grind the frozen sample. 200 µl of extraction buffer (200 mM Tris-HCl pH 7.5, 250 mM NaCl, and 25 mM EDTA pH 8.0, 0.5% SDS) was added to the still frozen ground sample. 100 µl of Tris-saturated phenol: chloroform (1:1) solution was then added. After thorough mixing, the sample was centrifuged at 13,000 rpm

for 10 min. The supernatant was transferred to a 1.5 ml microfuge tube that contained 150 µl of isopropanol and the contents thoroughly mixed. After centrifugation at 13,000 rpm for 10 min the supernatant was discarded and the pellet, which contains the DNA, was washed with 70% ethanol. The washed DNA pellet was suspended in 200 µl of HPLC grade water.

### **Identification of homozygous T-DNA insertion mutant Arabidopsis plants**

The transgenic Arabidopsis lines Salk\_020444 and Salk\_062006 contain T-DNA insertions within the AtGPDHc and AtGPDHp genes, respectively. Seeds from these lines were germinated and DNA extracted from individual plants was analyzed by PCR to identify plants that were homozygous for the T-DNA insertion allele. Two sets of PCR were conducted. The first PCR used gene specific primers to detect the presence of the WT allele in each plant. The primers AtGPDHc-F 5'-AACTGCTCTTGAACCAGTTCC-3' plus AtGPDHc-R 5'-AGATGTGAAACTACCCCTTCC-3' were used to detect the WT AtGPDHc allele, and the primers AtGPDHp-F 5'-TCCCACATAACTCTACTCCTTC-3' plus AtGPDHp-R 5'-AAGCTCATTGCTTCTAATGCC-3' were used for detecting WT AtGPDHp allele. The PCR conditions used were 95°C for 5 min followed by 30 cycles of 95°C for 30 s, 50°C for 30 s and 72°C for 1 min with a final extension of 72°C for 5 min. A second PCR was conducted to identify plants that contained the T-DNA insertional allele. A cocktail of the forward and reverse gene specific primers along with the T-DNA left border primer 5'-GCGTGGACCGCTTGCTGCAAC-3' was used in the PCR. The PCR conditions used were 95°C for 5 min followed by 30 cycles of 95°C for 30s, 55°C for 30 s and 72°C for 1 min with a final extension of 72°C for 5 min. Homozygous T-DNA allele bearing plants were identified as those that yielded a PCR product in the second set of PCR reaction, but none in the first set of PCR. As opposed to the homozygous T-DNA plants, hemizygous plants yielded a PCR product in both reactions, and plants that lacked the T-DNA insertion yielded a product only in the first PCR reaction with the gene-specific primer.

## Results

### Homology of SFD1 to AtGPDHp, AtGPDHc and At3g07690

A Basic Local Alignment Search Tool (BLASTp) analysis of the SFD1 protein sequence revealed close homology to three Arabidopsis proteins, At5g40610 (AtGPDHp), At2g41540 (AtGPDHc) and At3g07690. At5g40610 (AtGPDHp) exhibited 29% (101 of 343 amino acids) identity and 46% (158 of 343 amino acids) similarity with SFD1 (Fig 2.1 A). At2g41540 (AtGPDHc) exhibited 25% (61/244) identity and 43% (107/244) similarity to SFD1 (Fig 2.1 B). Lastly, At3g07690 shared 23% (67/299) identity and 40% (121/299) similarity with SFD1 (Fig 2.1 C). This homology was along the highly conserved NAD(P)H-dependent glycerol-3-phosphate dehydrogenase multidomain (PRK00094, *gpsA*) which extends from the amino acid position 89 to 413, 54 to 395, 43 to 384 and 36 to 422 for SFD1, AtGPDHp, AtGPDHc and At3g07690, respectively.

The role of the At5g40610 (AtGPDHp) and At2g41540 (AtGPDHc) genes, which encode proteins with highest homology to SFD1, in lipid metabolism and plant defense was characterized. At5g40610 and At2g41540 encode plastidic and cytosolic DHAP reductases, respectively (Wei et al., 2001; Shen et al., 2006).

### Identification of homozygous plants from T-DNA insertion lines of AtGPDHp and AtGPDHc

T-DNA insertion lines, Salk\_062006 and Salk\_020444 were obtained from the ABRC. Seeds were ordered through The Arabidopsis Information Resource (TAIR; <http://www.arabidopsis.org>). Salk\_062006 and Salk\_02044 contain T-DNA insertions in the At5g40610 (AtGPDHp) and At2g41540 (AtGPDHc) genes, respectively. As the seeds obtained were from an F<sub>2</sub> segregating generation, the population had to be screened for homozygous T-DNA insertion lines. In order to identify homozygous T-DNA insertion, F<sub>2</sub> progeny plants for each of these Salk insertion lines were grown and genomic DNA isolated from leaves. A set of primers were developed from areas flanking the predicted T-DNA insertion region for each of the Salk lines (Fig 2.2). Genomic DNA from WT allele when amplified with gene-specific primers that flank the T-DNA insertion site is expected to produce a gene specific PCR product

with these primer sets. However, a T-DNA insertion in the region results in an increase in the length of the region flanked by these two primers. This large region will not yield a PCR product with the two gene-specific primers due to the short amplification time used for PCR. However, depending on the orientation of the T-DNA, a primer designed to the left border of the T-DNA when used in combination with one of the gene-specific primers should result in a PCR product with the T-DNA insertion allele, indicating presence of the T-DNA insertion allele. When a cocktail of the two gene specific primers and the T-DNA left border primer are used for PCR, the presence of a PCR product corresponding to the T-DNA mutant allele and the simultaneous absence of the PCR product corresponding to the WT allele indicates homozygosity for the mutant allele at this locus. Presence of only the PCR product corresponding to the WT allele indicates lack of the T-DNA allele in the diploid plant and presence of both PCR products indicates the plant is hemizygous (contains one mutant and one WT allele).

Forward and reverse gene specific primer sets, AtGPDHc- F&R for At5g40610 and AtGPDHp- F&R for At2g41540, flanking the predicted T-DNA insertion were designed. DNA was obtained from leaves of each progeny plant. The first round of PCR was done with the gene specific primer sets for each gene (Fig 2.3 A lanes 1-6, Fig 2.3 B lanes 1-4). The absence of a band in lanes 2 and 6 in Fig 2.3 A and lane 3 in Fig 2.3 B suggests that the gene in these plants had been most-likely disrupted by the T-DNA insertion. This was confirmed by the second round of PCR that contained a gene specific primer sets plus the T-DNA left border primer (Fig 2.3 A lanes 7-12, Fig 2.3 B lanes 5-8). The presence of the band, corresponding to the product of the left border primer and a gene specific primer, in lanes that lack a gene-specific product (Fig 2.3 A lanes 8 and 12, Fig 2.3 B lane 7) confirms the presence of a T-DNA insertion disrupting that specific gene.

To confirm the homozygosity of the selected insertion line plants, and ensure the disruption of the transcript expression, RT-PCR analysis was conducted on RNA extracted from the homozygous T-DNA allele bearing lines. mRNA specific primers were designed for each gene and expression of each gene was assessed. RNA extracted from WT plants showed presence of the corresponding WT transcripts (Fig 2.4 A lane 1, Fig 2.4 B lane 1) while the homozygous T-



DNA insertion lines did not (Fig 2.4 A lane 2, Fig 2.4 B lane 2), thus confirming that expression of the corresponding gene had been knocked out in the homozygous T-DNA insertion bearing lines.

### **Analysis of the lipid composition of AtGPDHp and AtGPDHc**

To determine whether AtGPDHp and AtGPDHc have a role in Arabidopsis lipid metabolism, glycerolipid profiles of the *gpdhp* and *gpdhc* homozygous mutant plants were compared with the WT. Lipids from four week old leaves of the insertion lines, along with the WT, were extracted and subjected to the ESI-MS/MS analysis (Walti et al., 2002). Results in Table 2.1 indicate that compared to the WT, the *gpdhp* mutant plants had marginally lower levels of 34:6 (18:3 + 16:3) monogalactosyldiacylglycerol (MGDG), while the *gpdhc* mutant plants did not show any significant change (Table 2.1). There was no significant difference between the WT and homozygous mutants for AtGPDp and AtGPDHc for the other major MGDG species, 36:6 (18:3 + 18:3) MGDG and other lipids (Supplementary Table 1). This suggests that the AtGPDHp gene, which has the highest homology to SFD1, has a minor contribution to leaf glycerolipid composition. AtGPDHc, on the other hand, appears not to be involved in glycerolipid metabolism; glycerolipid composition was comparable between the WT and the *gpdhc* mutant plants.

### **Basal defense phenotype of the insertion lines of AtGPDHp and AtGPDHc**

Leaves of four week old insertion line and WT plants were inoculated with a suspension of the virulent bacterial pathogen *Pseudomonas syringae* pv. *maculicola* ES4326. Bacterial numbers were monitored at 3 dpi. Bacterial numbers were comparable between the *atgpdhp* mutant and WT plants (Fig 2.5 A). This implies that ATGPDHp is not essential for basal resistance to *P. syringae* pv. *maculicola*. On the other hand, in comparison to the WT, bacterial growth was reproducibly observed to be lower in the *gpdhc* mutant, suggesting that the mutant plant is more resistant to the pathogen than the WT (Fig 2.5 B).

## **AtGPDHp does not play a role in SAR**

To determine whether the *gpdhp* mutant impacts the activation of SAR, growth of *P. s. maculicola* was monitored in the distal leaves of the mutant and WT plants, which were previously treated with an avirulent strain of *P. s. tomato* on the lower leaves. The *sfd1* mutant plant, which is defective in SAR, was used as a control for these experiments. As previously demonstrated, SAR-conferred heightened resistance to *P. syringae* pv. *maculicola* was prevalent in the WT but not in the *sfd1* mutant. However, SAR-conferred protection was comparable between the WT and the *gpdhp* mutant, suggesting that AtGPDHp gene is dispensable for the manifestation of SAR (Fig 2.6 A). To determine if the presence of *SFD1* allele masked any contribution of AtGPDHp in SAR, the *atgpdhp sfd1* double mutant was generated. SAR was compromised in the double mutant plant to a level comparable to that in the *sfd1* single mutant (Fig 2.7), suggesting that AtGPDHp and *SFD1* are unlikely to have overlapping function in SAR.

An increase in the accumulation of the transcript of *PATHOGENESIS-RELATED1 (PRI)* gene is also a strong indicator of the activation of SAR (van Loon and van Kammen, 1970; Durrant and Dong, 2004). RT-PCR was performed on the RNA collected from the naïve leaves of, initially mock and avirulent pathogen challenged wild type and *gpdhp* insertion line plants. Lanes 2 and 4 (Fig 2.6 B) show a comparable increase in the accumulation of *PRI* transcript in the WT (Fig 2.6 B lane 2) and the *gpdhp* mutant (Fig 2.6 B lane 4) that were pre-inoculated on other leaves with an avirulent pathogen, further supporting the conclusion that AtGPDHp is not involved in SAR.

## Discussion

The discovery of the *sfd1* mutant that was compromised in SAR but was unaffected in basal resistance implicated a role for plastid lipid metabolism in SAR (Nandi et al., 2004). I searched the Arabidopsis database to identify genes encoding proteins with similarity to SFD1 to determine their contribution to leaf lipid composition and plant defense, in particular SAR.

Of the five Arabidopsis encoded proteins with similarity to the SFD1 protein, AtGPDHp, a plastidic DHAP reductase (Wei et al., 2001) with a 29% (101 of 343 amino acids) identity and a 46% (158 of 343 amino acids) similarity (Fig 3.1 A) to SFD1, and AtGPDHc, a cytosolic DHAP reductase (Shen et al., 2006) with 25% (61/244) identity and a 43% (107/244) similarity with SFD1 were characterized for their role in lipid metabolism and plant defense.

Leaf glycerolipid composition was comparable between the *atgpdhc* mutant and the WT, suggesting that this gene does not contribute to Arabidopsis leaf lipid composition, or alternatively, is redundant with other similar activities. In contrast, a slight reduction in levels of 34:6 (18:3 + 16:3) MGDG (Table 2.1) were observed in leaves of the *atgpdhp* mutant compared to the WT leaves, implying that AtGPDHp contributes to plastid glycerolipid metabolism. Thus SFD1 and AtGPDHp may have overlapping roles in plastid glycerolipid metabolism, with SFD1 providing the major source of G3P for glycerolipid synthesis in plastids.

The *Atgpdhc* mutant however, did impact plant resistance to the bacterial pathogen, *P. s. maculicola*. Bacterial growth in the mutant plant was lower compared to that in the WT plant (Fig 2.5 B), suggesting AtGPDHc, which is a cytosolic protein contributes to host susceptibility to this pathogen. It was recently demonstrated that the basal levels of reactive active species (ROS) was higher in the *atgpdhc* mutant than the WT plant, suggesting that the mutant plant is impaired in maintaining cellular redox homeostasis (Shen, 2006). ROS are known for their role in basal and induced plant defense responses (Bolwell, 1999; Apel and Hirt, 2004; Glazebrook, 2005). *R* gene-mediated resistance is generally accompanied by a rapid production of reactive oxygen species (ROS) also called an oxidative burst. ROS production is also required for the hypersensitive response (HR), a type of programmed cell death that is thought to limit the access of the pathogen to water and nutrients in the host (Bolwell, 1999; Apel and Hirt, 2004;

Glazebrook, 2005). AtGPDHc acts as the cytosolic component of a glycerol-3-phosphate (G3P) shuttle (Shen et al., 2006). Mitochondrial G3P shuttles channel cytosolic reducing equivalent to the mitochondria for respiration through the oxidoreduction of G3P (Shen et al., 2006). Alternatively, since G3P is an important contributor of C to a number of metabolites (Aubert et al., 1994) and the establishment and maintenance of a metabolic sink is a crucial aspect of plant pathogenesis (Solomon et al., 2003; Oliver et al., 2004), of the AtGPDHc gene could have altered the availability of plant metabolites that are required for pathogenesis, leading to the resistance phenotype in the *atgpdhc* mutant.

*atgpdhp*, like *sfd1*, had an unaltered basal defense phenotype (Fig 2.5 A). But when its SAR phenotype was examined, unlike *sfd1*, it was similar to the WT (Fig 2.6). AtGPDHp, though the most similar to SFD1, did not appear to play a role in SAR. The slight reduction in the levels of 34:6 (18:3 + 16:3) MGDG were apparently not significant enough to alter the plants SAR phenotype. The comparable SAR-defect in both, the *atgpdhp sfd1* double mutant and the *sfd1* single mutant further rule out the possibility that AtGPDHp and SFD1 have overlapping functions in SAR.

In conclusion although there are other DHAP reductases in Arabidopsis that share similarity with SFD1, they appear not to be involved in SAR related signaling. Despite the genetic evidence presented in the next chapter that indicates that a plastid-synthesized glycerolipid is required for SAR, whether the DHAP reductase activity of SFD1 is required for SAR needs to be determined.

## References

- Apel, K., and Hirt, H.** (2004). REACTIVE OXYGEN SPECIES: metabolism, oxidative stress, and signal transduction. *Annu. Rev. Phytopathol.* **55**, 373-399.
- Aubert, S., Gout, E., Bligny, R., and Douce, R.** (1994). Multiple effects of glycerol on plant cell metabolism. Phosphorus-31 nuclear magnetic resonance studies. *J. Biol. Chem.* **269**, 21420-21427.
- Bolwell, P.** (1999). Role of active oxygen species and NO in plant defence responses. *Curr. Opin. Plt. Biol.* **2**, 287-294.
- Chaturvedi, R., Krothapalli, K., Makandar, R., Nandi, A., Sparks, A. A., Roth, M. R., Welti, R., and Shah, J.** (2008). Plastid omega-3-fatty acid desaturase-dependent accumulation of a systemic acquired resistance inducing activity in petiole exudates of *Arabidopsis thaliana* is independent of jasmonic acid. *Plant J.* **54**, 106-117.
- Chomczynski, P., and Sacchi, N.** (1987). Single-step method of RNA isolation by acid guanidinium thiocyanate-phenol-chloroform extraction. *Anal. Biochem.* **162**, 156-159.
- Durrant, W. E., and Dong, X.** (2004). Systemic acquired resistance. *Annu. Rev. Phytopathol.* **42**, 185-209.
- Gee, R. W., Byerrum, R. U., Gerber, D. W., and Tolbert, N. E.** (1988). Dihydroxyacetone phosphate reductase in plants. *Plant Physiol.* **86**, 98-103.
- Glazebrook, J.** (2005). Contrasting mechanisms of defense against biotrophic and necrotrophic pathogens. *Annu. Rev. Phytopathol.* **43**, 205-227.
- Kachroo, P., Shanklin, J., Shah, J., Whittle, E. J., and Klessig, D. F.** (2001). A fatty acid desaturase modulates the activation of defense signaling pathways in plants. *Proc. Natl. Acad. Sci. USA* **98**, 9448-9453.

**King, E. O., Ward, M. K., and Raney, D. E.** (1954). Two simple media for the demonstration of phycocyanin and fluorescein. *J. Lab. Clin. Med.* **44**, 301-307.

**Kirsch, T., Gerber, D. W., Byerrum, R. U., and Tolbert, N. E.** (1992). Plant dihydroxyacetone phosphate reductases. *Plant Physiol.* **100**, 352-359.

**Konieczny, A., and Ausubel, F. M.** (1993). A procedure for mapping Arabidopsis mutations using co-dominant ecotype-specific PCRbased markers. *Plant J.* **4**, 403-410.

**Lin, E. C. C.** (1977). Glycerol utilization and its regulation in mammals. *Ann. Rev. Biochem.* **46**, 765-795.

**Maldonado, A. M., Doerner, P., Dixon, R. A., Lamb, C. J., and Cameron, R. K.** (2002). A putative lipid transfer protein involved in systemic resistance signaling in Arabidopsis. *Nature* **419**, 399-403.

**Marchler-Bauer, A., Anderson, J. B., Derbyshire, M. K., DeWeese-Scott, C., Gonzales, N. R., Gwadz, M., Hao, L., He, S., Hurwitz, D. I., Jackson, J. D., Ke, Z., Krylov, D., Lanczycki, C. J., Liebert, C. A., Liu, C., Lu, F., Lu, S., Marchler, G. H., Mullokandov, M., Song, J. S., Thanki, N., Yamashita, R. A., Yin, J. J., Zhang, D., Bryant, S. H.** (2007) CDD: a conserved domain database for interactive domain family analysis. *Nucleic Acids Res.* **35**: D237-240

**Nandi, A., Krothapalli, K., Buseman, C. M., Li, M., Welti, R., Enyedi, A., and Shah, J.** (2003). Arabidopsis *sfd* mutants affect plastidic lipid composition and suppress dwarfing, cell death, and the enhanced disease resistance phenotypes resulting from the deficiency of a fatty acid desaturase. *Plant Cell* **15**, 2383-2398.

**Nandi, A., Moeder, W., Kachroo, P., Klessig, D. F., Shah, J.** (2005). The Arabidopsis *ssi2*-conferred susceptibility to *Botrytis cinerea* is dependent on EDS5 and PAD4. *Mol. Plant-Microbe Interact.* **18**, 363-370.

**Nandi, A., Welti, R., and Shah, J.** (2004). The *Arabidopsis thaliana* dihydroxyacetone phosphate reductase gene *SUPPRESSOR OF FATTY ACID DESATURASE DEFICIENCY 1* is required for glycerolipid metabolism and for the activation of systemic acquired resistance. *Plant Cell* **16**, 465-477.

**Oliver, R. P., and Ipcho, S. V. S.** (2004). Arabidopsis pathology breathes new life into the necrotrophs-vs.-biotrophs classification of fungal pathogens. *Mol. Plant Pathol.* **5**, 347-352.

**Sekine, K. T., Nandi, A., Ishihara, T., Hase, S., Ikegami, M., Shah, J., and Takahashi, H.** (2004). Enhanced resistance to Cucumber mosaic virus in the *Arabidopsis thaliana* *ssi2* mutant is mediated via an SA-independent mechanism. *Mol. Plant-Microbe Interact.* **17**, 623-632.

**Shen, W., Wei, Y., Dauk, M., Tan, Y., Taylor, D. C., Selvaraj, G., and Zou, J.** (2006). Involvement of a glycerol-3-phosphate dehydrogenase in modulating the NADH/NAD<sup>+</sup> ratio provides evidence of a mitochondrial glycerol-3-phosphate shuttle in Arabidopsis. *Plant Cell* **18**, 422-441.

**Solomon, P. S., Tan, K. C., and Oliver, R. P.** (2003). The nutrient supply of pathogenic fungi; a fertile field for study. *Mol. Plant Pathol.* **4**, 203-210.

**Van Loon, L. C., and Van Kammen, A.** (1970). Polyacrylamide disc electrophoresis of the soluble leaf proteins from *Nicotiana tabacum* var. 'Samsun' and 'Samsun NN'. II. Changes in protein constitution after infection with tobacco mosaic virus. *Virology* **40**, 199-211.

**Wei, Y., Periappuram, C., Datla, R., Selvaraj, G., and Zou, J.** (2001). Molecular and biochemical characterization of a plastidic glycerol-3-phosphate dehydrogenase from Arabidopsis. *Plant Physiol. Biochem.* **39**, 841-848.

**Welti, R., Li, W., Li, M., Sang, Y., Biesiada, H., Zhou, H-E., Rajashekar, C. B., Williams, T. D., and Wang, X.** (2002). Profiling membrane lipids in plant stress response. Role of

phospholipase D alpha in freezing-induced lipid changes in Arabidopsis. J. Biol. Chem **277**, 31994-32002.



## Figure legends

### Fig 2.1 Homology of SFD1 to the predicted DHAP reductases

Dashed and dotted lines above the SFD1 sequence mark the predicted NAD<sup>+</sup> and substrate binding domains, respectively.

#### (A) Homology of SFD1 to AtGPDHp

The other plastid-localized DHAP reductase AtGPDHp At5g40610 had 29% (101/343) identity and 46% (158/343) similarity with the SFD1 protein. SFD1 is a 420 amino acid protein with a highly conserved NAD(P)H-dependent glycerol-3-phosphate dehydrogenase multidomain (PRK00094, *gpsA*) which extends from the amino acid position 89 to 413. The AtGPDHp protein too has a similar multidomain which extends from amino acid position 54 to 395.

#### (B) Homology of SFD1 to AtGPDHc

The cytoplasm localized DHAP reductase AtGPDHc (At2g41540) is a 462 amino acid protein with a SFD1 like NAD(P)H-dependent glycerol-3-phosphate dehydrogenase multidomain (PRK00094, *gpsA*) extending from position 43 to 384. At2g41540 (AtGPDHc) had 25% (61/244) identity and 43% (107/244) similarity to SFD1 in this region.

#### (C) Homology of SFD1 to At3g07690

At3g07690 codes for a 466 amino acid protein with a NAD(P)H-dependent glycerol-3-phosphate dehydrogenase multidomain (PRK00094, *gpsA*) from position 36 to 422. At3g07690 shared 23% (67/299) identity and 40% (121/299) identity with SFD1 in this region.

### Fig 2.2 Model for identification homozygous T-DNA insertion lines by PCR

A two round PCR-based strategy to obtain homozygous plants from the T-DNA insertion lines was setup. T-DNA insertion lines, Salk\_062006 and Salk\_02044 were obtained for the genes At5g40610 (AtGPDHp) and At2g41540 (AtGPDHc). A set of primers were developed from areas flanking the predicted T-DNA insertion region for each of the Salk lines. The WT undisrupted gene would produce a gene specific PCR product with these primer sets. But a T-DNA insertion in the region between the gene specific primer sets will not result in a PCR product, as the insertion will lead to the disruption of the gene. A cocktail of the gene-specific primer set and the T-DNA left border primer was used on each Salk plant DNA, where the

absence of the PCR product from the region between the gene specific primer set will signify the disruption of the specific gene and the PCR product between the left border primer and a gene-specific primer will ensure the presence of the T-DNA insertion.

### **Fig 2.3 Identification of homozygous plants from T-DNA insertion lines of AtGPDHp and AtGPDHc**

#### **(A) Identification of homozygous plants from T-DNA insertion lines of AtGPDHp**

The lanes 1-6 show the first round of PCR screening based on the usage of AtGPDHp gene specific primers to detect the presence of the WT gene in any of the plants. Lanes 2 and 6 do not show a gene specific product. Lanes 7-12 show the second round of screening with a cocktail of AtGPDHp gene specific primers and T-DNA left border primer, lanes 8 and 12 have no gene specific product but a smaller band corresponding to the product of the left border primer and a gene specific primer.

#### **(B) Identification of homozygous plants from T-DNA insertion lines of AtGPDHc**

The lanes 1-4 show the first round of PCR screening based on the usage of AtGPDHc gene specific primers to detect the presence of the WT gene in any of the plants. Lane 3 does not show a gene specific product. Lane 5-8 show the second round of screening with a cocktail of AtGPDHc gene specific primers and T-DNA left border primer, lane 7 has no gene specific product but a smaller band corresponding to the product of the left border primer and a gene specific primer.

### **Fig 2.4 RT-PCR analysis of gene expression**

#### **(A) RT-PCR analysis of expression of AtGPDHp**

RT-PCR analysis of AtGPDHp from expression in leaves of the wild type (lane1) and *atgpdhp* lines (lane2).

#### **(B) RT-PCR analysis of expression of AtGPDHc**

RT-PCR analysis of AtGPDHc expression in leaves of the wild type (lane1) and *atgpdhc* lines (lane2). *ACT8* expression served as a control for RNA quality in the RT-PCR reaction. These experiments were repeated twice and RNA used in each experiment was isolated independently.

## **Fig 2.5 Basal defense phenotype of the insertion lines of AtGPDHp and AtGPDHc**

### **(A) Basal defense phenotype of *atgpdhp* mutant plant**

Comparison between the colony forming unit (CFU) per leaf disk numbers of the bacterial pathogen *Pseudomonas syringae* pv. *maculicola* ES4326, on 4 week old wild type and *atgpdhp* insertion lines. Each bar represents the average *Psm* count in 12 leaf discs  $\pm$  SD.

### **(B) Basal defense phenotype of *atgpdhc* mutant plant**

Comparison between the colony forming unit (CFU) per leaf disk numbers of the bacterial pathogen *Pseudomonas syringae* pv. *maculicola* ES4326, on 4 week old wild type and *atgpdhc* insertion lines. Each bar represents the average *Psm* count in 12 leaf discs  $\pm$  SD. The different letters above the bars indicate values that are significantly different from each other upon a student's *t*-test ( $P < 0.05$ ).

## **Fig 2.6 Analysis of the SAR phenotype of the *atgpdhp* mutant plant**

### **(A) SAR phenotype of the *atgpdhp* mutant plant**

Growth of the virulent pathogen *P. syringae* pv. *maculicola* (*Psm*) in wild type (WT), *atgpdhp* insertion line plants. *Pseudomonas syringae* pv. *tomato* DC3000 carrying the *avrRpt2* avirulence gene was infiltrated into three lower leaves of wild type and *atgpdhp* insertion line plants. Plants similarly treated with 10 mM  $MgCl_2$  provided controls. Three days later, three to four upper leaves in each plant were infiltrated with *Psm* and the bacterial growth was monitored 3 days post-inoculation (dpi). Each bar represents the average *Psm* count in 15 leaf discs  $\pm$  SD. White bars: Primary inoculation with 10 mM  $MgCl_2$ ; Black bars: primary inoculation with Avr pathogen. The different letters above the bars indicate values that are significantly different from each other upon a student's *t*-test ( $P < 0.05$ ).

### **(B) RT-PCR analysis of *PR1* expression in the systemic leaves of the *atgpdhp* mutant plant**

Reverse transcription-PCR analysis for *PR1* expression in the upper leaves of WT and *atgpdhp* insertion line plants, 2 days post-infiltration of three lower leaves with 10 mM  $MgCl_2$  (Mock) or the avirulent pathogen (Avr).

### **Fig 2.7 Analysis of the SAR phenotype of the *atgpdhpsfd1* double mutant plants**

Growth of the virulent pathogen *P. syringae* pv. *maculicola* (*Psm*) in wild type (WT), *sfd1* and *atgpdhp sfd1* double mutant plants. *Pseudomonas syringae* pv. *tomato* DC3000 carrying the *avrRpt2* avirulence gene was infiltrated into three lower leaves of wild type, *sfd1* and *atgpdhp sfd1* double mutant plants. Plants similarly treated with 10 mM MgCl<sub>2</sub> provided controls. Three days later, three to four upper leaves in each plant were infiltrated with *Psm* and the bacterial growth was monitored 3 days post-inoculation (dpi). Each bar represents the average *Psm* count in 15 leaf discs  $\pm$  SD. White bars: Primary inoculation with 10 mM MgCl<sub>2</sub>; Black bars: primary inoculation with Avr pathogen. The different letters above the bars indicate values that are significantly different from each other upon a student's *t*-test ( $P < 0.05$ ).

### **Table 2.1 lipid composition of AtGPDH<sub>p</sub> and AtGPDH<sub>c</sub>**

The table shows the average and standard deviation of the mol % of the chief glycerolipid species monogalactosyldiacylglycerol (MGDG) in the leaves of WT, *atgpdhc* and *atgpdhp* lines. The *atgpdhp* insertion line plants had lower levels of 34:6 (18:3 + 16:3) MGDG and total MGDG compared to the WT. The asterisk above the number indicates values that are significantly different from the WT upon a student's *t*-test ( $P < 0.05$ ).

## Figures

**Figure 2.1 Homology of SFD1 to the predicted DHAP reductases**

### (A) Homology of SFD1 to AtGPDHp

Score = 114 bits (286), Expect = 2e-25, Method: Compositional matrix adjust.  
Identities = 101/343 (29%), Positives = 158/343 (46%), Gaps = 28/343 (8%)

SFD1	89	KVVVLGGSGFTAMAAHVARRKEGL-----EVNMLVRDSFVCQS-----INENHHNCKY	137
AtGpDHP	56	KVTVVGSGNWGSVAAKLIASNALKLPSFHDVVRMWVFEEVLPNGEKLNDVINKTNENVKY	115
-----			
SFD1	138	FPEHKLPENVIATTDAAKALLDADYCLHAVPVQFSSSFLEGIADYVDPGLPFISLSKGLE	197
AtGpDHP	116	LPGIKLGGRNVVADPDLENVAVKDNMLVFVTPHQFMDGICKKLDGKITGDVEAISLVKGME	175
-----			
SFD1	198	LNTLR--MMSQIIPIALKNRPQPFVALSGPSFALEL-MNNLPTAMVVASKDKKLANAVQQ	254
AtGpDHP	176	VKKEGPCMISSLIS--KQLGINCCVLMGANIANEIAVEKFSEATVGYRGSREIADTWVQ	232
-----			
SFD1	255	LLASSYLRLNTSSDVTGVEIAGALKNVLAIAAGIVDGMNLGNNSMAALVSQGCSEIRWLA	314
AtGpDHP	233	LFSTPYFMVTPVHDVEGVLCGTCLKNVVAIAAGFVDGLEMGNNTKAAIMRIGLREMKALS	292
-----			
SFD1	315	TKM--GAKPTTITGLSGTGDIMLTFCFVNLNRNRTVGVRLGSG---ETLDDILTSM--NQV	367
AtGpDHP	293	KLLFPSVKDSTFFESCGLVADVITTCGL--GRNRRVAEAFKSRGKRSFDELEAEMLQGGQK	350
-----			
SFD1	368	AEGVATAGAVIALAQK--YVVKLPVLTAVAKIIDNELTPTKAV	408
AtGpDHP	351	LQGVSTAREVYEVCLKHCGWLEMPFLFSTVHQICTGRLQPEAIV	393

### (B) Homology of SFD1 to AtGPDHc

Score = 58.9 bits (141), Expect = 1e-08, Method: Compositional matrix adjust.  
Identities = 61/244 (25%), Positives = 107/244 (43%), Gaps = 29/244 (11%)

SFD1	151	TDAAKALLDADYCLHAVPVQFSSSFLEGIADYVDPGLP---FISLSKGLE-----L	198
AtGpDHC	150	TNMQEAVWDADIVVNGLPSTETREVFEEISKYWKERITVPIIISLSKGIETALEPVPPII	209
-----			
SFD1	199	NTLRMSQIIPIALKNRPQPFVALSGPSFALELMN-NLPTAMVVASKDKKLANAVQQLLA	257
AtGpDHC	210	TPTKMIHQATGVPIDN----VLYLGGPNIAAEIYNKEYANARICGAA--KWRKPLAKFLR	263
-----			
SFD1	258	SSYLRLNTSSDVTGVEIAGALKNVLAIAAGIVDGM-NLGNNSMAALVSQGCSEIRWLATK	316
AtGpDHC	264	QPHFIVWDNSDLVTHEVMGGLKNVYAIGAGMVAAALTNESATSKSVYFAHCTSEMIFITHL	323
-----			
SFD1	317	MGAKPTTITGLSGTGDIMLTFCFVNL--SRNRTVGVRLGSGETLDDILTSMN--QVAEGVA	372
AtGpDHC	324	LAEEPEKL-----AGPLLADTYVTLKGRNAWYQMLAKGEINRDMGDSISGKGMIQGVV	378
-----			
SFD1	373	TAGA	376
AtGpDHC	379	AVGA	382

### (C) Homology of SFD1 to At3g07690

Score = 48.9 bits (115), Expect = 1e-05, Method: Compositional matrix adjust.  
Identities = 67/299 (22%), Positives = 121/299 (40%), Gaps = 46/299 (15%)

```

-----
SFD1      151  TDAKAALLDADYCLHAVPVQFSSSFLEGIADYVDPGLP---FISLSKGLELN-----TLR  202
              T+ + A+ DAD ++ +P + I+ Y + ISL+KG+E +
3g07690   143  TNLQEAVWDADIVINGLPSTETFQVFNEISKYWKERVNAPVVIISLAKGVEAEFEPHPRIV  202
              -----

SFD1      203  MMSQIIPIALKNPRQPFVALSGPSFALELMN-NLPTAMVVASKDKKLANAVQQLLASSYL  261
              +Q+I A P + + L GP+ A E+ N A + S+ K + + L S+
3g07690   203  TPTQMIHRATGIPILENILYLGGPNIASEVYNKEYANARICGSE--KWRKPLGKFLRQSHF  260
              -----

SFD1      262  RINTSSDVTGVEIAGALKNVLAIAAGIVDGMNLGNNMAALVSQGC-----SEI  310
              + +SD+ E+ G LKNV AI A V +A L + SE+
3g07690   261  IVWDNSDLITHEVMGGLKNVYAIGAVFVLAFLYSTGMVATLTKE SATSKSVYFAHCTSEM  320
              -----

SFD1      311  RWLATKMGAKPTTITGLSGTDIMLTCTFVNL--SRNRTVGVRGSGETLDDILTSM--NQ  366
              ++ + +P + G ++ +V L RN G +L GE ++ S+
3g07690   321  IFITHLLAKEPEKL-----AGPLLADTYVTLLKGRNAWYGQKLAKGELSLEMGDSIKGKG  375
              -----

SFD1      367  VAEGVATAGAVIALAQKYNVKL-----PVLTA VAKIIDNELTPTKAVLE  410
              + +GV+ A L + ++ L P+L + +I+ +A+LE
3g07690   376  MIQGVSAVKAFFELLNQSSLQHPPEGKPVTPAELCPILKMLYRILITREFSCEAILE  434
              -----

```

**Figure 2.2 Schematic for identification homozygous T-DNA insertion lines by PCR**

A- AtGPDHp- F

B- AtGPDHp- R

C- AtGPDHc- F

D- AtGPDHc- R

L- T-DNA left border primer

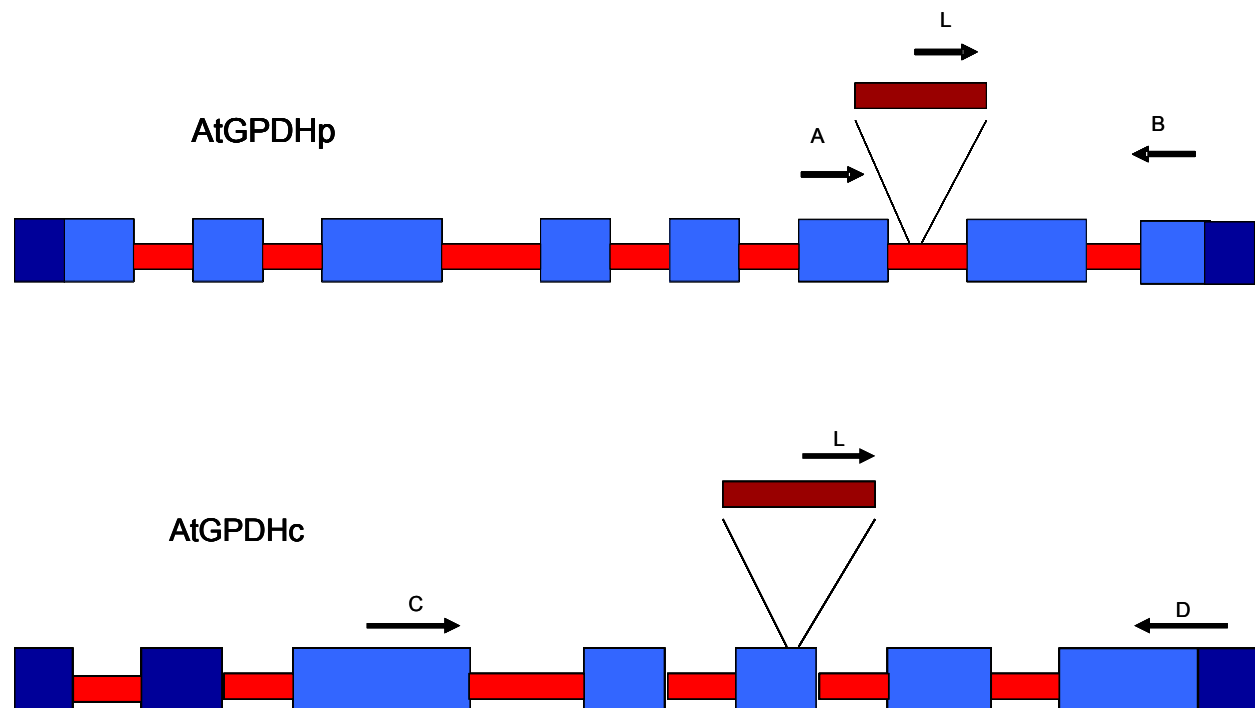
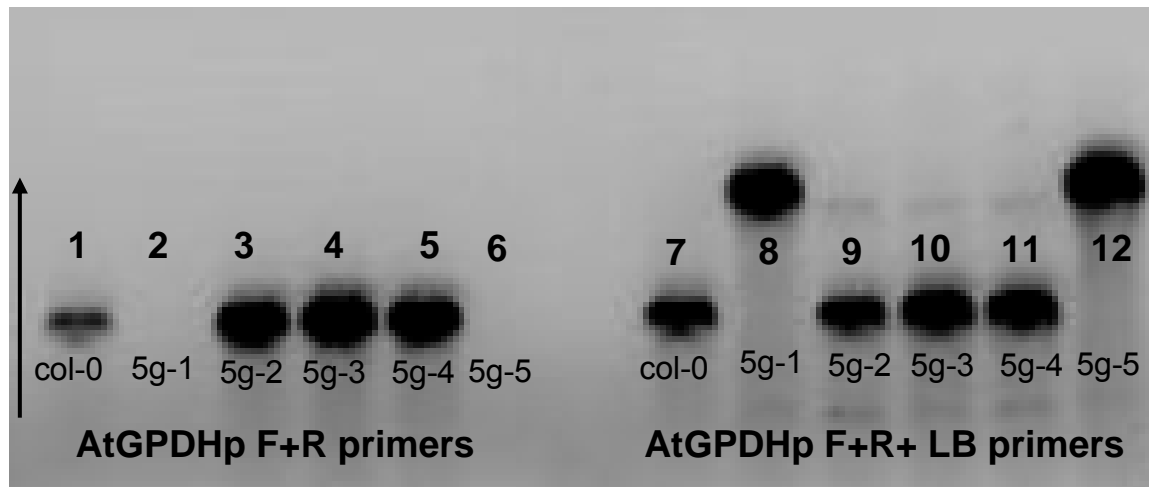


**Figure 2.3 Identification of homozygous plants from T-DNA insertion lines of AtGPDHp and AtGPDHc**

**(A) Identification of homozygous plants from T-DNA insertion lines of AtGPDHp**



**(B) Identification of homozygous plants from T-DNA insertion lines of AtGPDHc**

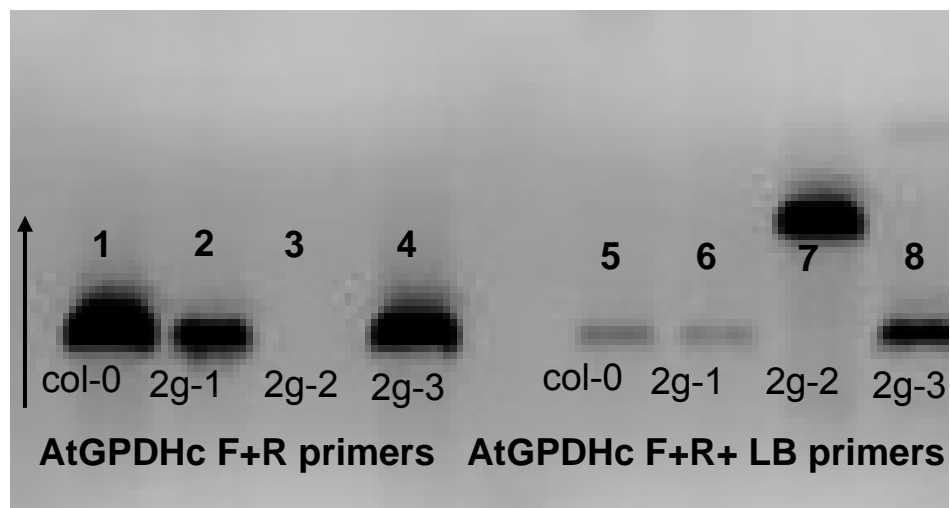
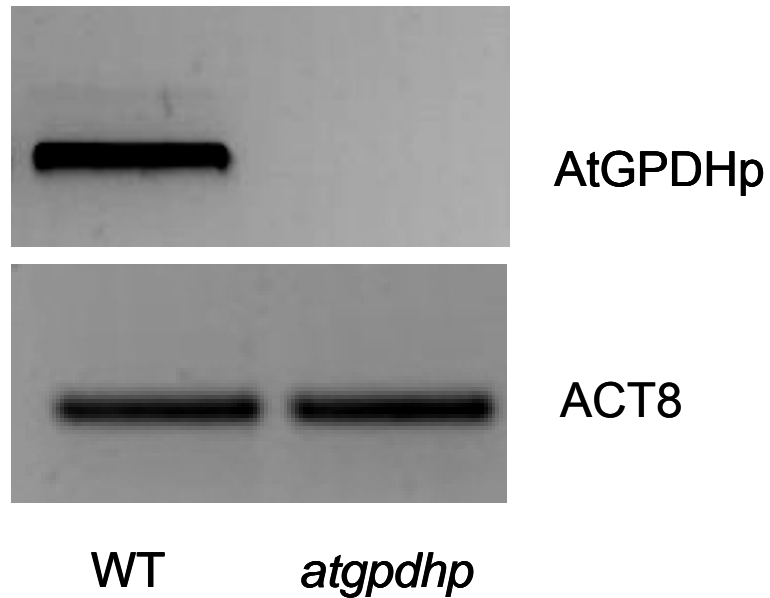




**Figure 2.4 RT-PCR analysis of gene expression**

**(A) RT-PCR analysis of expression of AtGPDHp**



**(B) RT-PCR analysis of expression of AtGPDHc**

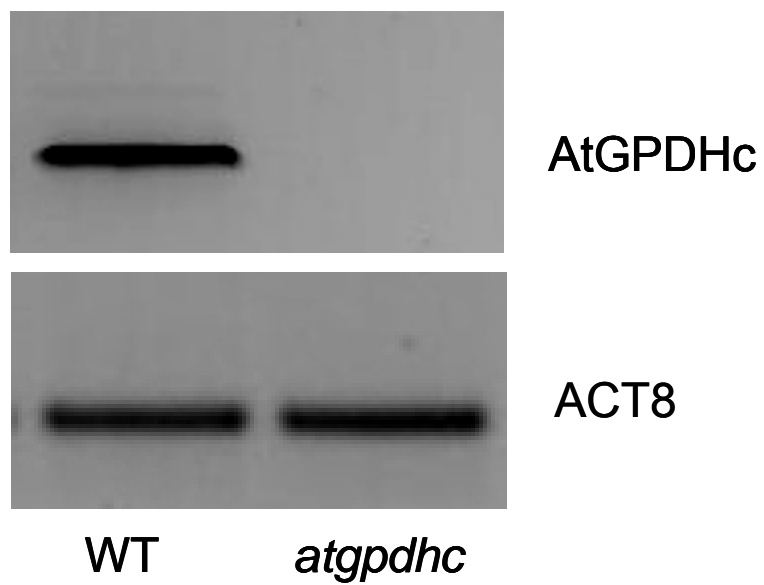
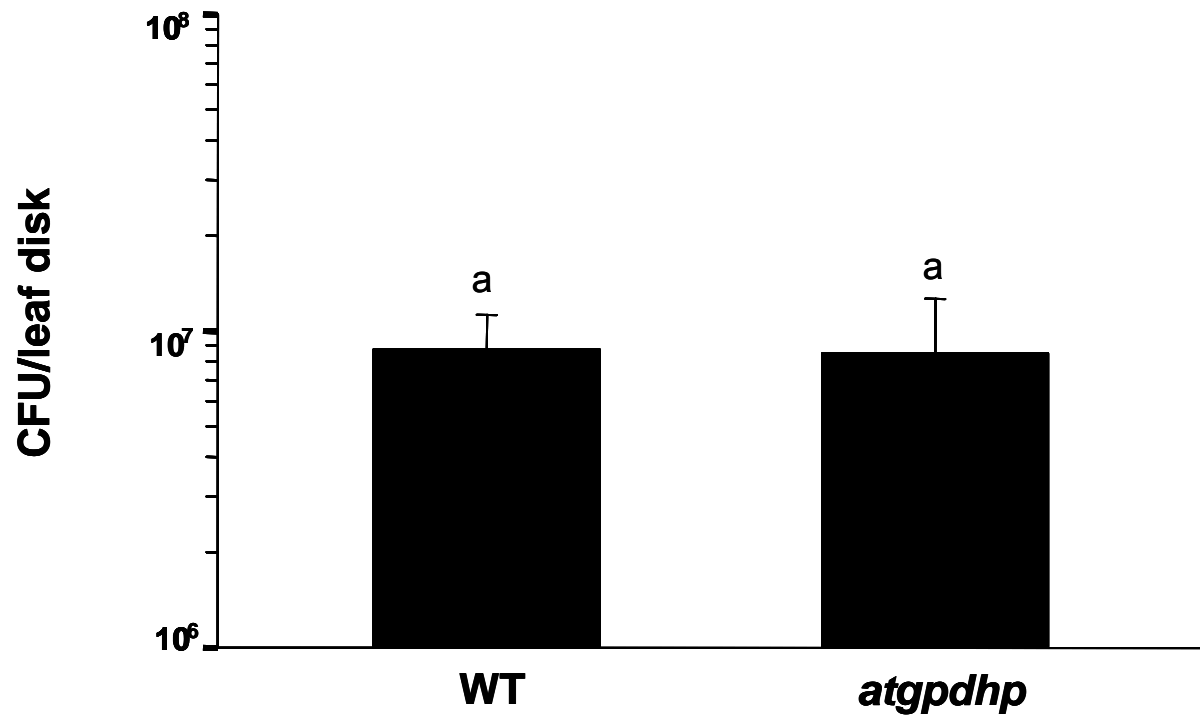


**Figure 2.5 Basal defense phenotype of the insertion lines of AtGPDHp and AtGPDHc**

**(A) Basal defense phenotype of *atgpdhp* mutant plant**



**(B) Basal defense phenotype of the *atgpdhc* mutant plant**

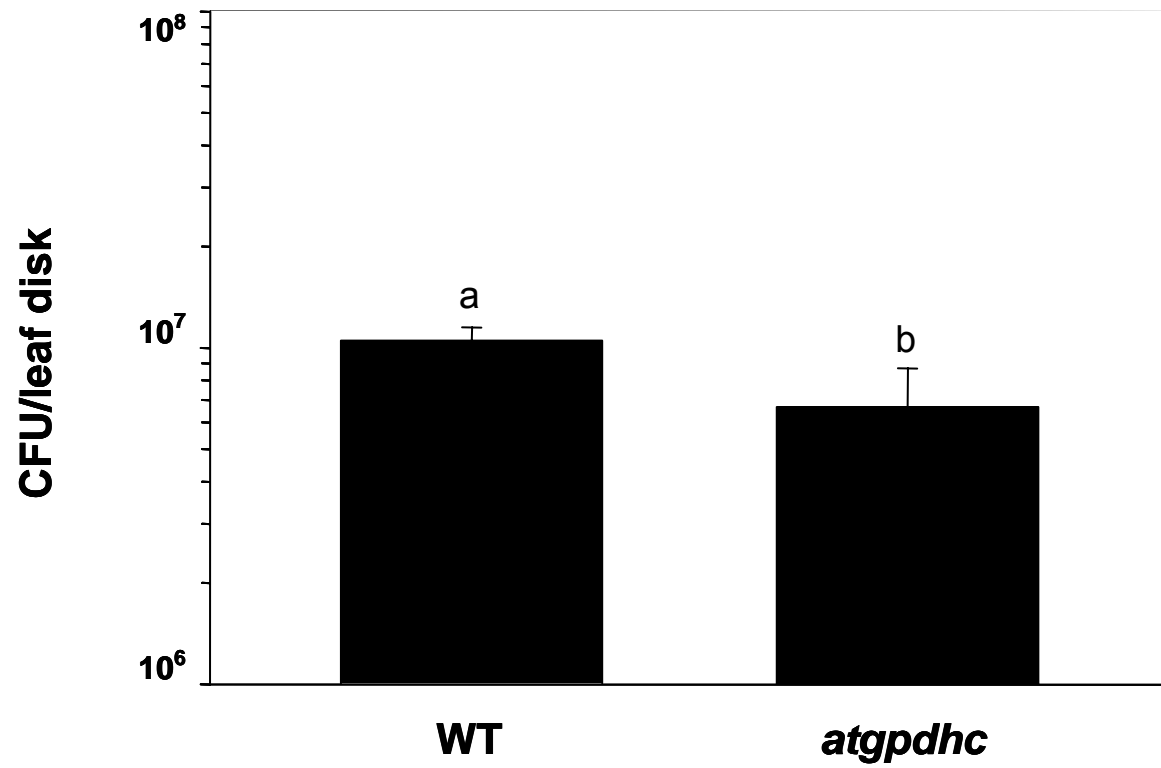
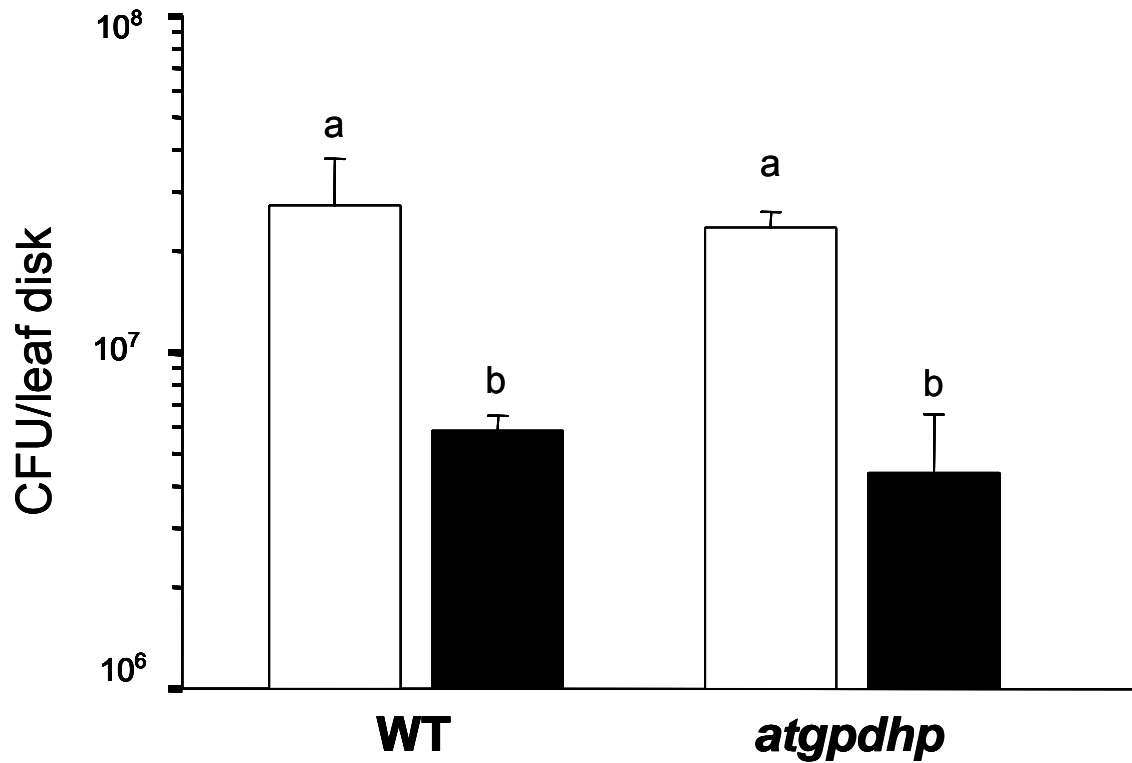


**Figure 2.6 Analysis of the SAR phenotype of the *atgpdhp* mutant plant**

**(A) SAR phenotype of the *atgpdhp* mutant plant**



**(B) RT-PCR analysis of *PR1* expression in the systemic leaves of the *atgpdhp* mutant plant**

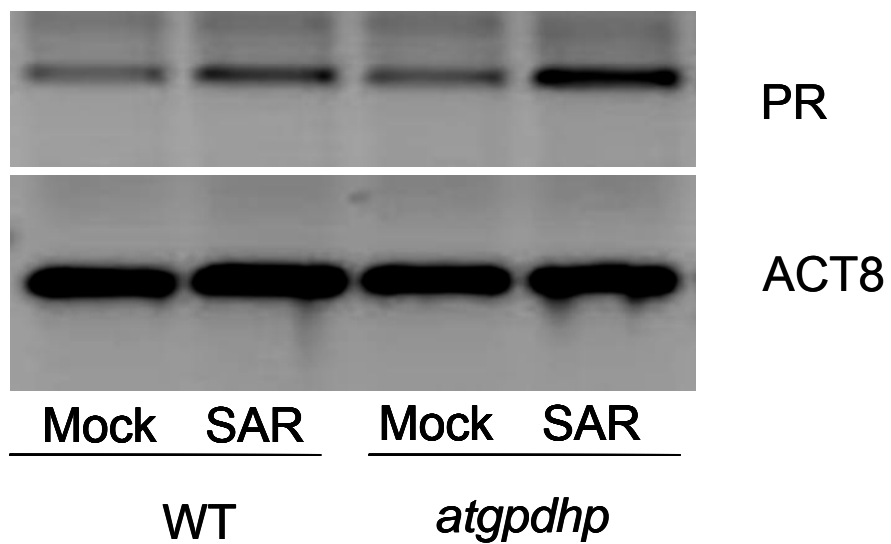


**Figure 2.7** Analysis of the SAR phenotype of the *atgpdhp sfd1* double mutant plants

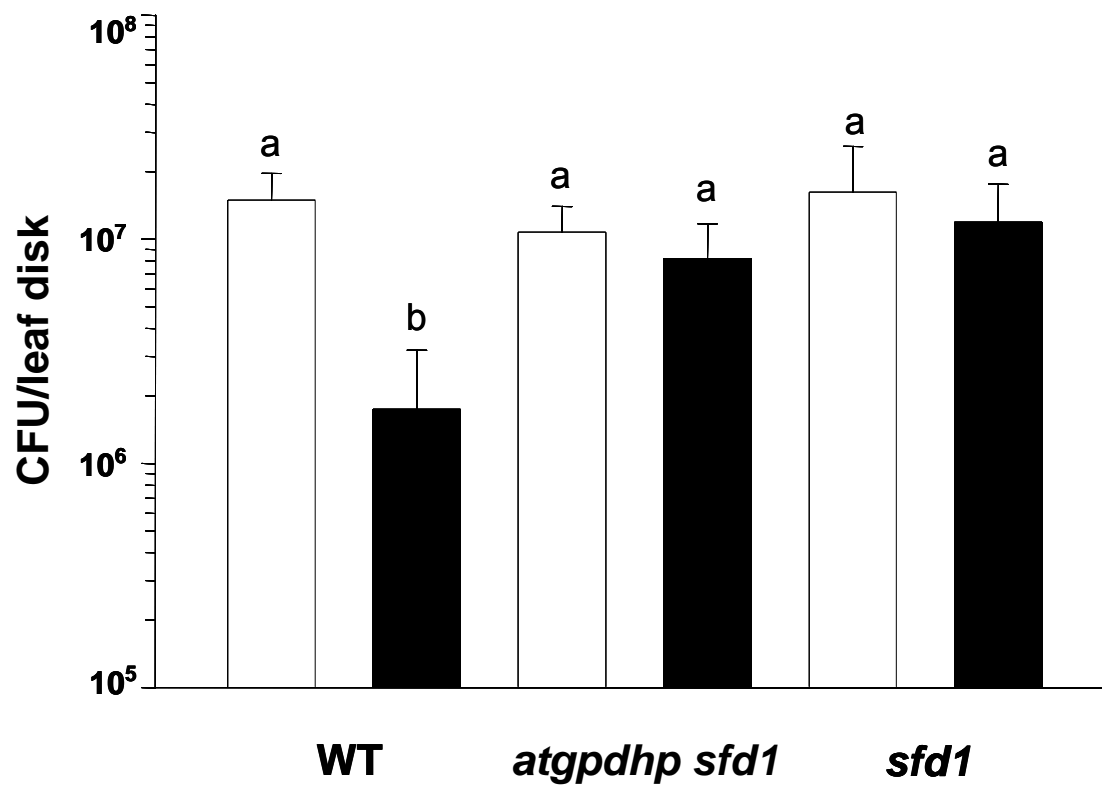


**Table 2-1 Lipid composition of AtGPDHp and AtGPDHc**

	Wild type		AtGPDHc		AtGPDHp	
	average	stdev	average	stdev	average	stdev
<b>MGDG 34:6</b>	39.112	2.353	35.845	3.434	34.405*	1.720
<b>MGDG 34:5</b>	0.000	0.000	0.000	0.000	0.000	0.000
<b>MGDG 34:4</b>	0.987	0.129	0.961	0.148	1.013	0.148
<b>MGDG 34:3</b>	0.367	0.044	0.286	0.103	0.340	0.076
<b>MGDG 34:2</b>	0.182	0.042	0.110	0.088	0.177	0.082
<b>MGDG 34:1</b>	0.095	0.099	0.141	0.106	0.126	0.075
<b>MGDG 36:6</b>	7.437	0.483	8.642	1.429	7.531	0.531
<b>MGDG 36:5</b>	0.006	0.014	0.068	0.113	0.005	0.010
<b>MGDG 36:4</b>	0.663	0.163	0.723	0.276	0.772	0.092
<b>MGDG 36:3</b>	0.031	0.031	0.042	0.071	0.057	0.055
<b>MGDG 36:2</b>	0.002	0.005	0.000	0.000	0.022	0.020
<b>MGDG 36:1</b>	0.001	0.002	0.000	0.000	0.003	0.006
<b>MGDG 38:6</b>	0.000	0.000	0.000	0.000	0.000	0.000
<b>MGDG 38:5</b>	0.001	0.002	0.000	0.000	0.000	0.000
<b>MGDG 38:4</b>	0.042	0.021	0.062	0.106	0.063	0.065
<b>MGDG 38:3</b>	0.006	0.013	0.008	0.018	0.000	0.000
<b>Total</b>	<b>48.932</b>	<b>1.902</b>	<b>46.888</b>	<b>3.260</b>	<b>44.511*</b>	<b>1.841</b>
<b>MGDG</b>						

## CHAPTER 3 - Involvement of galactolipids in SAR

### Lipid biosynthesis in Arabidopsis plastids

The Arabidopsis plastidic glycerolipid biosynthetic pathway generates three kinds of lipids. The first group is composed of galactolipids represented by monogalactosyldiacylglycerol (MGDG) and digalactosyldiacylglycerol (DGDG), while the other two groups consist of the sulpholipid, sulfoquinovosyldiacylglycerol (SQDG), and the phospholipid, phosphatidylglycerol (PG). In the leaves of Arabidopsis, synthesis in the plastids account for about 76% of the total glycerolipids, while the remaining 24% is derived from the endoplasmic reticulum (ER) (Somerville et al., 2000). Galactolipids constitute about 60% of the total lipids present in the leaf. They are synthesized and localized in the plastid and are characterized by the presence of one or more galactose moieties in the head group. Monogalactosyldiacylglycerol (MGDG) and digalactosyldiacylglycerol (DGDG) are the two major groups of galactolipids (Somerville et al., 2000). The *MGD1* gene encodes a MGDG synthase that catalyzes the transfer of a D-galactose moiety from UDP-galactose to diacylglycerol to synthesize MGDG in the plastids (Jarvis et al., 2000; Awai et al., 2001). MGDG content was 75% lower in leaves of the *mgd1* mutant compared to the wild type (WT). Two other genes, MGD2 and MGD3 also contribute to MGDG synthesis in Arabidopsis (Awai et al., 2001). DGDG is synthesized from MGDG by the action of a DGDG synthase encoded by the *DGD1* gene; DGDG content was 90% lower in the *dgd1* mutant compared to the corresponding WT plant (Dormann et al., 1995). The *FAD4*, *FAD5*, *FAD6* and *FAD7*-encoded enzymes catalyze various acyl chain desaturation steps in glycerolipids. For example, the *FAD4*-encoded desaturase catalyzes the desaturation of 16:0 acyl chains in PG to 16:1 (Somerville et al., 2000). In contrast, the *FAD5*-encoded desaturase is responsible for the desaturation of 16:0 acyl chain in galactolipids to 16:1. *FAD6* and *FAD7* on the other hand encode  $\omega$ 6 and  $\omega$ 3 desaturases that catalyze the conversion of monoenoic (16:1 and 18:1) and dienoic (16:2 and 18:2) acyl chains in glycerolipids to dienoic and trienoic (16:3 and 18:3) species, respectively. Thus, for example, leaves of the *fad7* mutant contain elevated levels of 34:4- and 36:4-MGDG at the expense of 34:6- and 36:6-MGDG, while the *fad6* mutant contains elevated levels of 34:2 MGDG and lower levels of the MGDG species with higher levels of

desaturation compared to the WT plant. The glycerol backbone of glycerolipids is derived from G3P. Two rounds of acylation of G3P yield phosphatidic acid (PA), which feeds into synthesis of other glycerolipids. Genetic and biochemical evidence indicates that *SFD1*, which encodes a DHAP reductase, is the major provider of G3P for glycerolipid synthesis in the plastids (Nandi, et al. 2004), and the *ACT1* (*ATSI*)-encoded transferase catalyzes the first acylation step in plastid glycerolipid synthesis (Somerville et al. 2000).

Galactolipids can provide the fatty acids required for jasmonic acid (JA) biosynthesis, which is an important signaling molecule in plant response to abiotic and biotic stress. The starting precursor for the biosynthesis of JA is linolenic acid (LA) (18:3) (Somerville et al., 2000; Schaller, 2001). The polyunsaturated fatty acid is probably released from plastidic membrane lipids by the action of a lipase like enzyme (Narváez-Vásquez et al., 1999; Schaller, 2001). As the key enzymes for the initial steps of JA biosynthesis like lipoxygenase (LOX), allene oxide synthase (AOS) and allene oxide cyclase (AOC) have transit peptides for chloroplast import, and the biosynthesis of the JA precursor 12-oxo-phytodienoic acid (OPDA) occurs in the chloroplast, the major source for the LA for JA biosynthesis is likely to be the chloroplast abundant galactolipids like MGDG and DGDG (Simpson and Gardner, 1995; Schaller, 2001). OPDA is transported to the peroxisome where it is converted to JA after three rounds of  $\beta$ -oxidation. Moreover, since >80% of OPDA is thought to be esterified in complex galactolipids (Stelmach et al., 2001), these too could provide precursors for JA synthesis.

### **Systemic Acquired Resistance in Arabidopsis**

SAR is an induced response activated in the naïve distal organs of a plant due to the prior exposure of another organ to a pathogen (Ryals et al., 1996; Durrant and Dong, 2004). SAR confers resistance to a wide variety of pathogens (Ryals et al., 1996). Induction of SAR is accompanied by the increased expression of a sub-set of *PATHOGENESIS-RELATED* (*PR*) genes, some of which encode antimicrobial proteins (Klessig and Malamy, 1994; Hunt and Ryals, 1996; Kombrink and Somssich, 1997; Durrant and Dong, 2004). Elevated expression of a subset of these *PR* genes provides an excellent molecular marker for the activation of SA signaling. A signal is generated in the primary pathogen-inoculated organ, from where it moves



to rest of the plant, priming defenses to respond faster in response to subsequent pathogen attack. Petiole exudates, which are enriched in phloem sap, collected from avirulent pathogen-inoculated WT plants when applied to leaves of WT plant induce a SAR-like mechanism in the naïve leaves, suggesting that the SAR inducing signal is translocated through the petiole (Chaturvedi et al., 2008). Girdling experiments in cotton suggest that the SAR signal moves through the phloem (Guedes et al., 1980). However, experiments in *Arabidopsis* indicate that phloem may not be the exclusive conduit for this signal (Kiefer and Slusarenko, 2003). The identity of the SAR signal has been the subject of a long series of investigations (Sticher et al., 1997). SA (salicylic acid) plays an important role in plant defense, the time frame of SA induction, levels reached and its role in induction of *PATHOGENESIS-RELATED (PR)* genes, initially led to the assumption that SA was the signal that traveled from the initial site of infection to the distal parts of the plant where SAR was expressed (Malamy et al., 1990; Mettraux et al., 1990). The fact that transgenic plants overexpressing the bacterial SA hydroxylase, *NahG* that converts SA to catechol, showed low SA levels and were blocked in SAR (Gaffney et al., 1993) helped the argument for SA. This view was however challenged when it was found that the removal from cucumber plant of the primary *Pseudomonas syringae*-infected leaves did not block the induction of SAR, even though the leaves were removed before increases in SA level were observed in the petiole (Rasmussen et al., 1991). Also grafting experiments using *NahG* transgenic tobacco and WT plants suggested that SA was not the mobile signal in SAR (Vernooij et al., 1994). Root stocks expressing *NahG* and hence unable to accumulate elevated SA content were capable of synthesizing and translocating the SAR priming signal to non-transgenic WT scions, thus making the WT scions resistant to subsequent pathogen attacks. Reciprocal grafts made using non-transgenic root-stocks and transgenic scions showed that the SAR signal required SA in distal tissues to induce systemic resistance (Vernooij et al., 1994). Recently there have been suggestions that methyl salicylate (MeSA) may be a SAR signal in TMV-infected tobacco (Park et al., 2007).

The discovery of the *dir1* (*defective in induced resistance1*) mutant hinted towards the involvement of lipids or lipid derived products in the activation of SAR. The *dir1* mutant plants had normal basal or local resistance i.e. the growth of a virulent pathogen on the mutant leaves was similar to that of the WT. However, when the plants were initially inoculated with an

avirulent pathogen and subsequently the distal leaves were challenged with a virulent pathogen, growth of the virulent pathogen in the *dir1* mutant was higher compared to the WT, suggesting that SAR but not basal resistance is compromised in the *dir1* mutant (Maldonado et al., 2002). Petiole exudates from pathogen challenged leaves of *dir1* mutant plants were unable to turn on *PR1* expression (Maldonado et al., 2002) and SAR conferred-resistance in naïve WT plants (Chaturvedi et al., 2008). Conversely, petiole exudates from pathogen challenged leaves of WT plants were able to turn on SAR in naïve *dir1* mutant plants, implying that the *dir1* plants were compromised either in the generation or the transport of the SAR signal but not in its perception. The *DIR1* gene encodes a putative apoplastic lipid transfer protein with homology to non-specific lipid transfer proteins (LTP) (Lascombe et al., 2006; 2008). Two multigenic families of lipid transfer protein have been identified, LTP1 and LTP2 (Lascombe et al., 2006; 2008). LTP1 and LTP2 display low amino-acid sequence identity to each other except for the signature LTP motif of eight cysteines involved in four disulfide bridges. DIR1 shares some structural and lipid binding properties with the LTP2 family, but it displays some specific features that define DIR1 as a new type of LTP (Lascombe et al., 2008). DIR1 also shows high affinity for monoacylated phospholipids (Lascombe et al., 2008). However, whether DIR1 is involved in translocating a lipid signal associated with SAR remains to be determined.

In contrast to *dir1*, SAR is constitutively active in the Arabidopsis *ssi2* (*suppressor of SA insensitivity 2*) mutant (Shah and Chaturvedi, 2008), which exhibits heightened resistance to bacterial, oomycete and viral pathogens (Kachroo et al., 2001; Shah et al., 2001; Sekine et al., 2004; Nandi et al., 2005). *ssi2* petiole exudates constitutively accumulate a SAR activating factor (R. Chaturvedi and J. Shah, personal comm.). The *ssi2* mutant is a dwarf that spontaneously develops lesions containing dead cells (Shah et al., 2001). *SSI2* encodes a stearoyl-ACP desaturase involved in the conversion of stearoyl ACP (18:0-ACP) to oleoyl-ACP (18:1-ACP) in the plastids (Kachroo et al., 2001) thus suggesting a role for plastid lipid metabolism in SAR. A role for plastid lipid metabolism in SAR is also supported by studies of the *sfd1* (*suppressor of fatty acid desaturase deficiency 1*) mutant, which was identified in a screen for suppressors of the *ssi2*-conferred dwarf phenotype (Nandi et al., 2003). The *SFD1* gene encodes a plastidic dihydroxyacetone phosphate (DHAP) reductase (Nandi et al., 2004). SAR but not basal resistance was compromised in the *sfd1* mutant. In contrast to the wild type

plant, petiole exudates collected from avirulent pathogen-inoculated *sfd1* leaves lacked the SAR inducing activity (Chaturvedi et al., 2008). However, the *sfd1* mutant was responsive to this SAR promoting factor present in petiole exudates of avirulent pathogen inoculated WT leaves. These results suggest that the SAR defect in the *sfd1* mutant is due to its inability to accumulate the SAR promoting factor in petiole exudates. However, whether this impact of SFD1 on SAR is tied with its involvement in plastid galactolipid synthesis has not been demonstrated, neither is there any evidence confirming a role for the involvement of plastid galactolipids in SAR.

*ssi2*-conferred dwarfing and heightened disease resistance are also compromised by mutations in the *SFD2*, *FAD6* (*SFD4*) and *ACT1* (*ATS1*) genes (Nandi et al., 2003, Kachroo et al., 2003). The *ACT1* gene encodes a glycerol-3-phosphate (G3P) acyltransferase, which catalyzes the addition of an acyl chain to glycerol-3-phosphate (G3P) to yield LPA. The *ACT1* locus has been renamed *ATS1* by members of the Arabidopsis Genome Initiative to avoid confusion with the *ACT* gene symbol for the actin genes (<http://www.arabidopsis.org>). The *act1 ssi2* double mutant suppressed all of *ssi2* conferred phenotypes (Kachroo et al., 2003, 2004). However, whether like *SFD1* these other plastid lipid metabolism genes are also required for the activation of SAR is not known.

*In planta*, inducible expression of a bacterial avirulence protein resulted in the accumulation of 9- and 13-lipoxygenase-dependent oxylipins (Andersson et al., 2006). More than 90% of the oxylipins formed were found to be esterified to glycerolipids. OPDA and dinor-OPDA were found to be esterified to a novel MGDG-derived galactolipid termed Arabidopside E (Andersson et al., 2006). These galactolipid-conjugated oxylipins could be converted into JA. A recent study, suggested that JA may be a long-distance factor contributing to SAR (Truman et al., 2007), JA is known to act as a systemic signal in wound signaling in tomato (Li et al., 2002). Whether the requirement of *SFD1* and plastidic glycerolipids in SAR is tied with the requirement of galactolipids for JA synthesis during SAR remains to be determined.

In this chapter, I provide evidence for the involvement of Arabidopsis plastid glycerolipid metabolism, in particular galactolipids in SAR. I demonstrate that like *sfd1*, the *act1*, *sfd2* and *fad6* (*sfd4*) mutants, which were identified in screens for suppressors of *ssi2*, are deficient in

SAR (Fig 3.2 B; 3.3 B; 3.4 B). Furthermore, the galactolipid biosynthetic mutants *mgd1*, *dgd1*, *fad5* and *fad7* are also compromised in SAR (Fig 3.5 B; 3.6 B; 3.7 B; 3.9 B). However, SAR was not compromised in the *fad4* mutant, which has defects in the synthesis of the major phospholipid in plastids, namely phosphatidylglycerol (PG) (fig 3.8 B), implying a unique role for galactolipids in SAR. To validate our hypothesis of the role of galactolipids in SAR, I crossed *fad7*, the mutant that affects the final step of galactolipid desaturation, to *ssi2*, the constitutive SAR mutant and recorded the suppression of the constitutive SAR phenotype of *ssi2* in the *fad7 ssi2* double mutants (Fig 3.9 D), ratifying the role of *FAD7* in SAR. Further, unlike as suggested by Truman et al., 2007, I provide genetic evidence that suggests that JA synthesis and signaling is not critical for the activation of SAR (Fig 3.11).

## Materials and methods

### Cultivation of plants and pathogens

Arabidopsis plants were cultivated at 22°C in a tissue-culture chamber programmed for a 14 h light (100  $\mu$ E/m/s) and 10 h dark cycle. Seeds were germinated either in soil or on Murashige-Skoog (MS) (Sigma, St. Louis) agar supplemented with 1% sucrose. Ten days post germination, seedlings were transplanted to soil-filled pots and cultivated as described above. *Pseudomonas syringae* pv. *maculicola* ES4326 was propagated at 28°C on King's B medium (King et al., 1954) containing streptomycin (100  $\mu$ g/ml). An overnight culture was used for infecting plants. *Pseudomonas syringae* pv. *tomato* DC3000 V288 containing *avrRpt2* was propagated at 28°C on King's B medium (King et al., 1954) containing kanamycin (25  $\mu$ g/ml) and rifampicin (100  $\mu$ g/ml).

### Bacterial Inoculations

Four week old soil grown plants were used for inoculation. The overnight grown bacterial strain cultures were harvested and resuspended in 10 mM MgCl<sub>2</sub> at an optical density specific to each experiment. A 1ml syringe with out a needle was used to infiltrate the bacterial suspension in to the abaxial surface or underside of the leaf.

SAR was activated by inoculating 3-4 lower leaves (1° challenge), keeping the orthostichy of the Arabidopsis rosette in consideration, with a suspension (OD<sub>600nm</sub> = 0.01) of *Pseudomonas syringae* pv. *tomato* DC3000 V288 containing *avrRpt2* in 10 mM MgCl<sub>2</sub>. In parallel, plants that were inoculated with 10 mM MgCl<sub>2</sub> (mock challenge) provided the negative controls. The activation of SAR was monitored by quantifying the resistance in the uninoculated naive leaves of the plant. 3-4 naive leaves were challenged (2° challenge) 3 d after 1° challenge or mock challenge with a suspension of *Pseudomonas syringae* pv. *maculicola* ES4326 (OD<sub>600nm</sub> = 0.00025) and the growth of the bacteria was measured 3 d after 2° challenge. 20 (5 replications of 4 leaves in each sample) leaf discs (0.28 cm<sup>2</sup>) were harvested and samples ground in 1 ml of 10 mM MgCl<sub>2</sub> at and appropriate dilutions were plated on King's B medium containing streptomycin (100  $\mu$ g/ml). Plates were incubated at 28°C for 2 days before counting the bacterial colonies. Bacterial counts are expressed as colony-forming units per leaf disc.

### **SA and JA determination**

JA and SA levels were determined by gas chromatography-mass spectrometry as previously described (Schmelz et al., 2004).

### **Lipid extraction**

Two to three leaves of about 4 week old plants were used per each sample. The leaves were immersed into 3 ml of isopropanol with 0.01% butylated hydroxytoluene at 75°C. After 15 minutes; 1.5 ml of chloroform and 0.6 ml of water were added to the above. The tubes were shaken for about an hour, followed by removal of the extract, which was collected separately. The leaves were re-extracted with 4 ml chloroform/methanol (2:1) with 0.01% butylated hydroxytoluene four times with 30 min of agitation each time except the last round which was left overnight, until all of the leaves appeared white. The remaining leaves were heated overnight at 105°C and weighed to obtain the dry weight of the tissue used. The combined extracts were washed once with 1 ml of 1 M KCl by vortexing. The mix was then centrifuged and the upper phase was discarded. The wash was repeated with 2 ml of water and the upper phase was discarded. The remaining solvent was evaporated under nitrogen, and the lipid extract was dissolved in 1 ml of chloroform. Standards were added and the ESI-MS/MS mass spectrographic analysis was performed as mentioned in Welti et al (2002).

### **RNA extraction and RT-PCR analysis**

Leaf tissue was ground under liquid nitrogen, and RNA was extracted using acid guanidinium thiocyanate-phenol-chloroform as previously described (Chomczynski and Sacchi, 1987). The isolated RNA was purified and used in the two step reverse-transcription polymerase chain reactions (RT-PCR). 2 µg total RNA was mixed with oligo (dT) primers (Promega), and the final volume was made up to 15 µl with water. This mixture was incubated at 70°C for 5 min, and then chilled on ice for 1-2 min. To the above mix 5 µl of M-MLV RT buffer (Promega), 1.25 µl dNTP mix (10nM each), 1 µl M-MLV reverse transcriptase (Promega) and 2.75 µl of water were added. cDNA synthesis were allowed to proceed at 37°C for 1 h – 1.5 h. 1 µl aliquots of this cDNA were used in subsequent PCR. The PCR primers used for *ACT8* (At1g49240) amplification were ACT8-F 5'-ATGAAGATTAAGGTCGTGGCA-3' and ACT8-R 5'-

CCGAGTTTGAAGAGGCTAC-3'. The At-PR1-F 5'-CTCTTGTAGGTGCTCTTGTTTC-3' and At-PR1-R 5'-CAGCTCTTATTTGTATTATTTG-3' primers were used for amplification of *PR1* (At2g14610). The PCR was performed with the following conditions: 95°C for 5 min followed by 25 cycles of 95°C for 30 sec, 60°C for 45 sec, 72°C for 1 min, with final extension at 72°C for 10 min.

### **Arabidopsis mutants**

The *sfd1-1*, *sfd2-2* and *ssi2* mutants are in the transgenic line 1/8E/5, which is in the Arabidopsis Nössen (Nö). The line 1/8E/5 contains a *PR1:tms2* transgene (Nandi et al., 2003, 2004; Shah et al., 2001). The *fad7-1* mutant is in the accession Columbia (Col) with the *glabra1* mutation, the *mgd1* mutant is in the accession Col (Jarvis et al., 2000), and the *dgd1* mutant is in the accession Col-2 (Dörmann et al., 1995). The *act1*, *coi1*, *opr3*, *fad4*, *fad5* and *fad6* mutants are in the accession Col. To generate the *ssi2 fad7-1* double mutant, the *ssi2* mutant was crossed with the *fad7-1* mutant plant and the F<sub>2</sub> progeny were screened for double-mutant plants. The *ssi2* mutant allele was followed by PCR and plants homozygous for *fad7-1* allele were identified based on their lipid profile (reduction in 34:6- and 36:6-MGDG levels).

### **DNA extraction and PCR analysis**

Arabidopsis genomic DNA from the leaf tissue was isolated as previously described (Konieczny and Ausubel, 1993). A derived-cleaved amplified polymorphic sequence (dCAPS) marker was used to differentiate the *ssi2* phenotype the *SSI2* phenotype. The primers, *ssi2*dCAPS-F 5'-TTGTTTTGGT GGGGGACATGATCACAGAAGGTGCA-3' and *ssi2*dCAPS-R 5'-TCGA TCTGCCTCATGTCAACACG-3' were used in the PCR reaction. The following PCR conditions were used: 95°C for 5 min followed by 35 cycles of 95°C for 45 sec, 65°C for 45 sec, 72°C for 45 sec, with final extension at 72°C for 5 min. The 200-bp PCR product derived from WT DNA contains one *Apa*L1 (New England Biolabs) site, which on restriction with *Apa*L1 yields two products of 175 and 25 bp. In contrast, the PCR product derived from the *ssi2* allele lacks the *Apa*L1 site.

## Results

### **SAR is compromised in suppressors of *ssi2* that also impact plastid glycerolipid metabolism**

To further understand the role of lipids in SAR, SAR-conferred resistance to the bacterial pathogen *P. syringae* pv. *maculicola* ES4326 (*Psm*) and *PR1* expression were evaluated in the *sfd2*, *act1* and *fad6* mutants, all of which attenuate the *ssi2*-conferred constitutive *PR1* gene expression and enhanced resistance against *Psm* (Nandi et al., 2003; Kachroo et al., 2003, 2004). *P. syringae* pv. *tomato* DC3000 carrying the *avrRpt2* avirulence gene was infiltrated into three to four lower leaves of the *sfd2*, *act1* and *fad6* mutant plants and their respective WT parents, as a primary inoculation (1° inoculation). This treatment induces SAR in the distal leaves of WT plants. As a mock control, 10 mM MgCl<sub>2</sub> solution was inoculated in to another set of plants of the same genotypes. Three days later the upper naïve systemic leaves of these plants were challenge (2° inoculation)-inoculated with the virulent bacteria, *P. syringae* pv. *maculicola* ES4326 (*Psm*). Bacterial numbers in the challenge-inoculated leaves were determined three days after the 2° inoculation. As expected, SAR was activated in WT plants that received a 1° inoculation of the Avr bacteria (Fig 3.2 B; 3.3 B; 3.4 B). *Psm* numbers were lower in the 2° leaves of WT plants that received a 1° treatment with the Avr pathogen compared to the mock treatment. In contrast, SAR was compromised in the Avr bacteria-inoculated *sfd2*, *fad6* and *act1* mutant plants; *Psm* growth was higher in the Avr bacteria (1° inoculation)-treated plants of these mutants compared to similarly treated WT plants (Fig 3.2 B; 3.3 B; 3.4 B). Since, like *sfd1*, plastid glycerolipid composition was also altered in the *sfd2*, *act1* and *fad6* mutants, together these results provide further support implicating an important role for plastid glycerolipids in SAR.

### **Arabidopsis genes involved in plastid galactolipid biosynthesis are required for SAR signaling**

The major lipid alteration in the *sfd1* mutant was in galactolipid composition. To determine if plastid galactolipids are important for SAR, SAR associated *PR1* expression and SAR-conferred resistance to *P. syringae* were further characterized in the *mgd1*, *dgd1*, *fad5* and *fad7* mutant plants, all of which affect varied steps in the plastid galactolipid synthesis. As a control, SAR



was also characterized in the *fad4* mutant, which is defective in PG synthesis, but not in the synthesis of galactolipids. As shown in Figures 3.5 B; 3.6 B; 3.7 B; 3.9 B, *Psm* numbers were lower in the 2° leaves of WT plants that received a 1° treatment with the Avr pathogen compared to Mock treatment, indicating development of SAR. However, in case of the *mgd1*, *dgd1*, *fad5* and *fad7* mutant plants, the SAR associated reduction of bacterial count was not as pronounced as in case of the WT plants. This clearly suggested that the mutant plants were compromised in their ability to mount a SAR-like defense mechanism. In contrast, the SAR response in the *fad4* mutant was comparable to its WT (Fig 3.8 B). Taken together, these experiments show that mutants, including *mgd1*, *dgd1* and *fad5*, that are specifically affected in plastid galactolipid composition and *fad7*, which affects both galactolipid and plastidic phospholipid composition, are compromised in SAR, while SAR is not affected in the *fad4* mutant that is defective in plastidic phospholipid PG, but not galactolipid synthesis. Together, these results strongly suggest an important role for plastid galactolipid metabolism in the activation of SAR.

### ***ssi2*-conferred growth and defense phenotypes are suppressed by the *fad7* mutant allele**

FAD7 catalyzes the last desaturation step in the synthesis of trienoic acyl chain containing glycerolipids. It involves the conversion of 34:4 and 36:4 glycerolipids to 34:6 and 36:6 glycerolipids. The *fad7* mutant plants were found to be SAR compromised (Fig 3.9 B), but none of the screens used to identify the suppressors of the *ssi2* mutant-conferred dwarf phenotype recovered a *fad7* allele (Nandi et al., 2003; Kachroo et al., 2003). This raised the possibility that *FAD7* may act in a mechanism that is distinct from *SFD1*, *SFD2* and *FAD6* in SAR.

Alternatively, the *sfd* mutant screen may not be saturating or was biased towards those mutants that suppressed the *ssi2*-conferred growth defects in addition to the *ssi2*-conferred defense phenotypes.

In order to determine whether, *SFD1*, *SFD2*, *FAD6* and *FAD7* all participate in the same mechanism leading to SAR, which is also hyperactive in the *ssi2* mutant, the *fad7* mutant was crossed with the *ssi2* mutant and the *fad7 ssi2* double mutants were generated by screening the segregating generation. The *fad7 ssi2* double mutant plants were intermediate in their size compared to the WT parent and the dwarf *ssi2* single mutant plant (Fig 3.10 A). The *ssi2* mutant

has constitutive cell death unlike the *fad7* mutant, which does not show any constitutive cell death. The *fad7 ssi2* double mutant plants showed a reduced constitutive cell death phenotype (Fig 3.10 B). Finally, the *fad7 ssi2* double mutant plants suppressed the *ssi2*-conferred enhanced resistance (Fig 3.9 D) and constitutive high level expression of *PR1* (Fig 3.9 C).

### **JA mutants *opr3* and *coi1* are not SAR compromised.**

The role of JA in plant defense signaling is well studied (Creelman and Mullet, 1997; Thomma et al., 1998; Glazebrook, 2005; Shah, 2005). A recent study suggested that JA may be a systemic signal that translocates from the pathogen-inoculated organ to the distal organs where SAR is activated (Truman et al., 2007). All the mutants we looked at that were compromised in their ability to invoke SAR were also altered in their galactolipid profile. To determine if the galactolipid link to SAR was because of its involvement in providing precursors for JA, SAR was monitored in the JA biosynthesis *oxophytodienoic acid reductase3* (*opr3*) mutant, which is defective in JA synthesis. . As shown in Fig. 3.11, the SAR-conferred restriction of *Psm* growth was comparable in the *opr3* mutant and WT plants, suggesting that the *opr3* mutant is SAR competent. Pathogen infection induced increase in JA content was attenuated in the *opr3* mutant (Fig 3.12 A), confirming that the *opr3* mutant is deficient in JA synthesis in response to pathogen attack. As previously reported the *coi1* mutant exhibits heightened basal resistance to *P. syringae* pv. *maculicola* (Fig 3.11 B). However, SAR induction resulted in further reduction in the pathogen growth (Fig 3.11 B). Taken together, these results argue against JA being the critical mobile signal in SAR.

## Discussion

Since the first clear demonstration of a systemic acquired resistance phenomenon was done in tobacco against *Tobacco mosaic virus* (TMV) (Ross, 1961), the nature of the SAR signal has been speculated upon. A number of candidates have been proposed to be the elusive SAR signal with the plant hormone SA being a popular choice (Sticher et al., 1997). A couple of observations reported in the early nineties (Rasmussen et al., 1991; Vernooij et al., 1994), making use of *NahG* expressing tobacco root stocks (Vernooij et al., 1994) and timely amputation of the pathogen-infected cucumber leaves (Rasmussen et al., 1991) laid SA's candidacy as the SAR signal to rest. This said, recently there have been suggestions that methyl salicylate (MeSA) may be involved in the SAR signaling pathway in tobacco (Park et al., 2007). However, whether MeSA is involved in systemic signaling associated with SAR in other plants is not known.

Besides *sfd1*, a number of other mutants (*sfd2*, *act1*, and *fad6*) that were identified in screens for suppressors of the *ssi2*-conferred dwarf defense phenotypes were also compromised in *ssi2*-conferred enhanced resistance (Kachroo et al., 2003; Nandi et al., 2003). Interestingly, these mutants also seem affected in their galactolipid biosynthesis (Kunst et al., 1989; Nandi et al., 2003). The heightened resistance phenotype of *ssi2*, its constitutive SAR, and the SAR defects of *sfd2*, *act1* and *fad6* mutants, with altered galactolipid profiles (Fig 3.2 B; 3.3 B; 3.4 B); support the involvement of plastid glycerolipids in SAR.

Both the galactolipid specific mutants, *mdg1* that showed a 75% reduced MGDG level compared to the WT (Jarvis et al., 2000) and *dgd1* with a 90% lower DGDG levels compared to the corresponding WT (Dormann et al., 1995), were found to be compromised in SAR (Fig 3.5 B; 3.6 B). However, taking into consideration that loss of DGD1 and MGD1 activity affects chloroplast ultrastructure (Dörmann et al., 1995; Jarvis et al., 2000) and causes stunted growth in the *dgd1* mutant (Dörmann et al., 1995), there is a possibility that the impact of *mgd1* and *dgd1* on SAR is due to a general defect in plastid function and altered phenotype. Also the involvement of sulfoglycerolipid (SL) has not been tested; hence their contribution towards SAR cannot be precluded. SAR was also attenuated in plants lacking FAD5, a galactolipid specific desaturase, which affects the conversion of 16:0 MGDG species to 16:1 MGDG species, and

thus the subsequent desaturation events (Fig 3.7 B), and in plants lacking FAD7 (Fig 3.9 B), which performs the final desaturations of PG and galactolipids. But the *fad4* mutant plant appeared to be no different from the WT in its ability to turn on SAR (Fig 3.8 B). Given the fact that FAD4 is specifically involved in the desaturation of phosphatidylglycerol (PG) lipid species, I hypothesize that plastid galactolipids, and not PG, appear to be involved in the SAR mechanism (Fig 3.14).

Since *fad7* alleles were not uncovered in screens for suppressors of the constitutive SAR mutant *ssi2* (Nandi et al., 2003), its role in SAR remained unexplained. When crossed to *ssi2*, the *ssi2 fad7* double mutants were found to be intermediate in their phenotype compared to their parents (Fig 3.10 A). This intermediate morphological phenotype of the *fad7 ssi2* double mutant plants could be responsible for the non-identification of *fad7 ssi2* mutants in *ssi2* suppressor screens as the screens would be biased towards the complete suppression of *ssi2* conferred characters. Similarly, mutations in a number of other genes like *EDS1* (*ENHANCED DISEASE SUSCEPTIBILITY 1*), *PAD4* (*PHYTOALEXIN-DEFICIENT 4*), *EDS5* (*ENHANCED DISEASE SUSCEPTIBILITY 5*) and *SID2* (*SALICYLIC ACID INDUCTION-DEFICIENT 2*) are known to suppress *ssi2* conferred phenotypes (Nandi et al; Kachroo et al, 2005) and some of them like *pad4* and *eds1* are reported to be compromised in SAR (Shah, 2005). Others like *sid2* and *eds5* are essential to the SAR machinery as they are involved in the synthesis and transport of SA. But, like *fad7*, none of them were picked in *ssi2* suppression screens as they too were not capable of complete suppression of the *ssi2*-bestowed dwarf and cell death phenotype (Nandi et al; Kachroo et al., 2005) and were ignored by the stringent screens looking for complete suppression. In future it would be advisable to screen for plants across the range of suppression intensity.

Recently, we showed that the SAR defects of the *sfd1* and *fad7* mutants are due to their inability to accumulate a SAR activating factor in petiole exudates of avirulent pathogen infected leaves (Chaturvedi et al., 2008). This suggests that a plastid galactolipid is required for either the synthesis or translocation of this SAR signal into the petiole exudates. However, the *sfd1* and *fad7* mutants are sensitive to the SAR signal present in petiole exudates from avirulent pathogen infected WT leaves, suggesting that galactolipids are not required for the perception of this

signal in the distal leaves. Complementation analysis indicated that the galactolipid dependent SAR signal is required along with the DIR1 protein in the petiole exudates for the activation of SAR. It is quite likely that DIR1 translocates this galactolipid-dependent SAR signal in Arabidopsis. However, confirmation of this awaits the identification of the galactolipid-dependent SAR signal.

Unlike as suggested by Truman et al. (2007) data presented here indicates that JA does not have an important role as a mobile signal in SAR. The JA biosynthesis *oxophytodienoic acid reductase3 (opr3)* mutant and the JA insensitive *coronatine-insensitive1 (coi1)* mutant were unaffected in their ability to turn on SAR (Fig 3.11). These results confirm the observations of other researchers who found the *jar1* and *coi1* mutants to be SAR competent (Cui et al., 2005; Mishina and Zeier, 2007). The inability of co-infiltration of JA or MeJA with Avr PeXs collected from SAR compromised plant leaves to activate SAR in wild type plants (Chaturvedi et al., 2008) further argues against JA being a major component of the SAR signal. The discrepancies in results presented here and those of Truman et al. (2007) could result from the different dose of avirulent pathogen used in the experiments, as recently summarized (Shah and Chaturvedi, 2008). While Truman et al. (2007) utilized a low, non HR-inducing, dose of the pathogen, I have used a relatively high, HR inducing dose of pathogen. Although not required for SAR, the development of HR was previously shown to promote the development of SAR (Cameron et al., 1994). Since, the JA-insensitive *coi1* and *jin1* mutants used by Truman et al. (2007) have high basal resistance to *P. syringae*, the pathogen dose may not reach a threshold level to induce a strong SAR response, explaining their inability to detect HR in the JA-insensitive mutants.

In conclusion, I have shown that plastidic glycerolipid metabolism is an essential part of the SAR mechanism and provide evidence for the involvement of galactolipids in this process (Fig 3.14).

## References

- Andersson, M. X., Hamberg, M., Kourtchenko, O., Brunnström, Å., McPhail, K. L., Gerwick, W. H., Göbel, C., Feussner, I., and Ellerstrom, M.** (2006). Oxylin profiling of the hypersensitive response in *Arabidopsis thaliana*: formation of a novel oxo-phytodienoic acid-containing galactolipid, arabidopside E. J. Biol. Chem. **281**, 31528-31537.
- Awai, K., Maréchal, E., Block, M. A., Brun, D., Masuda, T., Shimada, H., Takamiya, K., Ohta, H. and Joyard, J.** (2001) Two types of MGDG synthase genes, found widely in both 16:3 and 18:3 plants, differentially mediate galactolipid syntheses in photosynthetic and nonphotosynthetic tissues in *Arabidopsis thaliana*. Proc. Natl Acad. Sci. USA **98**, 10960–10965.
- Cameron, R.K., Dixon, R.A., and Lamb, C.J.** (1994). Biologically induced systemic acquired resistance in *Arabidopsis thaliana*. Plant J. **5**, 715-725.
- Chaturvedi, R., Krothapalli, K., Makandar, R., Nandi, A., Sparks, A. A., Roth, M. R., Welti, R., and Shah, J.** (2008). Plastid omega-3-fatty acid desaturase-dependent accumulation of a systemic acquired resistance inducing activity in petiole exudates of *Arabidopsis thaliana* is independent of jasmonic acid. Plant J **54**, 106-117.
- Chomczynski, P., and Sacchi, N.** (1987). Single-step method of RNA isolation by acid guanidinium thiocyanate-phenol-chloroform extraction. Anal. Biochem. **162**, 156-159.
- Creelman, R. A., and Mullet, J. E.** (1997). Biosynthesis and action of jasmonates in plants. Annu. Rev. Plt Phy. Plt Mol Bio **48**, 355-381.
- Cui, J., Bahrami, A.K., Pringle, E.G., Hernandez-Guzman, G., Bender, C.L., Pierce, N.E., and Ausubel, F.M.** (2005). *Pseudomonas syringae* manipulates systemic plant defenses against pathogens and herbivores. Proc. Natl. Acad. Sci. USA **102**, 1891-1796.

**de Wit, P. J. G. M.** (1998). Pathogen avirulence and plant resistance: a key role for recognition. Trends Plant Sci. **2**, 452-458.

**Dörmann, P., Hoffmann-Benning, S., Balbo, I., and Benning, C.** (1995). Isolation and characterization of an Arabidopsis mutant deficient in the thylakoid lipid digalactosyl diacylglycerol. Plant Cell **7**, 1801-1810.

**Durrant, W. E., and Dong, X.** (2004). Systemic acquired resistance. Annu. Rev. Phytopathol. **42**, 185-209.

**Gaffney, T., Friedrich, L., Vernooij, B., Negrotto, D., Nye, G., Uknes, S., Ward, E., Kessmann, H., Ryals, J.** (1993). Requirement of salicylic acid for the induction of systemic acquired resistance. Science **261**, 754-756.

**Glazebrook, J.** (2005). Contrasting mechanisms of defense against biotrophic and necrotrophic pathogens. Annu. Rev. Phytopathol. **43**, 205-227.

**Guedes, M.E.M., Richmond, S. and Kuc, J.** (1980) Induced systemic resistance to anthracnose in cucumber as influenced by the location of the inducer inoculation with *Colletotrichum lagenarium* and the onset of flowering and fruiting. Physiol. Plant Pathol. **17**, 229-233.

**Hunt, M., and Ryals, J.** (1996). Systemic acquired resistance signal transduction. Crit. Rev. Plant Sci. **15**, 583 - 606.

**Jarvis, P., Dörmann, P., Peto, C. A., Lutes, J., Benning, C., and Chory, J.** (2000). Galactolipid deficiency and abnormal chloroplast development in the Arabidopsis MGD synthase 1 mutant. Proc. Natl. Acad. Sci. USA **97**, 8175-8179.

**Kachroo, A., Lapchyk, L., Fukushige, H., Hildebrand, D., Klessig, D., and Kachroo, P.** (2003). Plastidial fatty acid signaling modulates salicylic acid- and jasmonic acid-mediated defense pathways in the *Arabidopsis ssi2* mutant. *Plant Cell* **15**, 2952-2965.

**Kachroo, A., Venugopal, S. C., Lapchyk, L., Falcone, D., Hildebrand, D., and Kachroo, P.** (2004). Oleic acid levels regulated by glycerolipid metabolism modulate defense gene expression in *Arabidopsis*. *Proc. Natl. Acad. Sci. USA* **101**, 5152-5157.

**Kachroo, P., Shanklin, J., Shah, J., Whittle, E. J., and Klessig, D. F.** (2001). A fatty acid desaturase modulates the activation of defense signaling pathways in plants. *Proc. Natl. Acad. Sci. USA* **98**, 9448-9453.

**Kiefer, I. W., and Slusarenko, A. J.** (2003). The pattern of systemic acquired resistance induction within the *Arabidopsis* rosette in relation to the pattern of translocation. *Plant Physiol.* **132**, 840-847.

**King, E. O., Ward, M. K., and Raney, D. E.** (1954). Two simple media for the demonstration of phycocyanin and fluorescein. *J. Lab. Clin. Med.* **44**, 301-307.

**Klessig, D. F., and Malamy, J.** (1994). The salicylic acid signal in plants. *Plant Mol. Biol.* **26**, 1439-1458.

**Kombrink, E., and Somssich, I. E.** (1997). Pathogenesis-related proteins and plant defense. In *Plant Relationships*, e. G.C. Carroll and P. Tudzynski, ed (Berlin, Germany: Springer-Verlag), pp. 107-128.

**Konieczny, A., and Ausubel, F. M.** (1993). A procedure for mapping *Arabidopsis* mutations using co-dominant ecotype-specific PCR based markers. *Plant J.* **4**, 403-410.



**Kunst, L., Browse, J., and Somerville, C.** (1989). Altered chloroplast structure and function in a mutant of *Arabidopsis* deficient in plastid glycerol-3-phosphate acyltransferase activity. *Plant Physiol.* **90**, 846-853.

**Lascombe, M-B., Buhot, N., Bakan, B., Didier, M., Blein, J-P., Larue, V., Lamb, C., and Prangé, T.** (2006). Crystallization of DIR1, a LTP2-like resistance signalling protein from *Arabidopsis thaliana*. *Acta Cryst.* **F62**, 702-704.

**Lascombe, M-B., Bakan, B., Buhot, N., Didier, M., Blein, J-P., Larue, V., Lamb, C., and Prangé, T.** (2008). The structure of "defective in induced resistance" protein of *Arabidopsis thaliana*, DIR1, reveals a new type of lipid transfer protein. *Protein Sci.* **17**, 1522-1530.

**Li, C., Williams, M. M., Loh, Y. T., Lee, I. G., and Howe, G. A.** (2002). Resistance of cultivated tomato to cell content-feeding herbivores is regulated by the octadecanoid-signaling pathway. *Plant Physiol.* **130**, 494-503.

**M'ettraux, J. P., Signer, H., Ryals, J., Ward, E., Wyss-Benz, M., Gaudin, J., Raschdorf, K., Schmid, E., Blum, W., and Inverardi, B.** (1990). Increase in salicylic acid at the onset of systemic acquired resistance in cucumber. *Science* **250**, 1004 -1006

**Malamy, J., Carr, J. P., Klessig, D. F., and Raskin, I.** (1990). Salicylic acid a likely endogenous signal in the resistance response of tobacco to viral infection. *Science* **250**, 1002-1004.

**Maldonado, A. M., Doerner, P., Dixon, R. A., Lamb, C. J., and Cameron, R. K.** (2002). A putative lipid transfer protein involved in systemic resistance signaling in *Arabidopsis*. *Nature* **419**, 399-403.

**Mishina, T.E., and Zeier, J.** (2007). Pathogen-associated molecular pattern recognition rather than development of tissue necrosis contributes to bacterial induction of systemic acquired resistance in *Arabidopsis*. *Plant J.* **50**, 500-513.

**Nandi, A., Krothapalli, K., Buseman, C. M., Li, M., Welti, R., Enyedi, A., and Shah, J.** (2003). *Arabidopsis sfd* mutants affect plastidic lipid composition and suppress dwarfing, cell death, and the enhanced disease resistance phenotypes resulting from the deficiency of a fatty acid desaturase. *Plant Cell* **15**, 2383-2398.

**Nandi, A., Moeder, W., Kachroo, P., Klessig, D. F., and Shah, J.** (2005). The *Arabidopsis ssi2*-conferred susceptibility to *Botrytis cinerea* is dependent on EDS5 and PAD4. *Mol. Plant-Microbe Interact.* **18**, 363-370.

**Nandi, A., Welti, R., and Shah, J.** (2004). The *Arabidopsis thaliana* dihydroxyacetone phosphate reductase gene *SUPPRESSOR OF FATTY ACID DESATURASE DEFICIENCY 1* is required for glycerolipid metabolism and for the activation of systemic acquired resistance. *Plant Cell* **16**, 465-477.

**Narváez-Vásquez, J., Florin-Christensen, J., and Ryan, C. A.** (1999). Positional specificity of a phospholipase A activity induced by wounding, systemin and oligosaccharide elicitors in tomato leaves. *Plant Cell* **11**, 2249-2260.

**Park, S. W., Kaimoyo, E., Kumar, D., Mosher, S., and Klessig, D. F.** (2007). Methyl salicylate is a critical mobile signal for plant systemic acquired resistance. *Science* **318**, 113-116.

**Pieterse, C. M. J., Pelt, J. A., Ton, J., Parchmann, S., Mueller, M. J., Buchala, A. J., Metraux, J-P, and Loon, L. C.** (2000). Rhizobacteria-mediated induced systemic resistance (ISR) in *Arabidopsis* requires sensitivity to jasmonate and ethylene but is not accompanied by an increase in their production. *Physiol Mol Plant Patho* **57**, 123-134.

**Pieterse, C. M. J., Wees, S. C. M., Pelt, J. A., Knoester, M., Laan, R., Gerrits, N., Welsbeek, P. J., and Loon, L. C.** (1998). A novel signaling pathway controlling induced systemic resistance in *Arabidopsis*. *Plant Cell* **10**, 1571-1580.

**Rasmussen, J. B., Hammerschmidt, R., and Zook, M. N.** (1991). Systemic induction of salicylic acid accumulation in cucumber after inoculation with *Pseudomonas syringae* pv *syringae*. *Plant Physiol.* **97**, 1342-1347.

**Ross, A. F.** (1961). Systemic acquired resistance induced by localized virus infections in plants. *Virology* **14**, 340-358.

**Ryals, J. A., Neuenschwander, U. H., Willits, M. G., Molina, A., Steiner, H. Y., and Hunt, M. D.** (1996). Systemic acquired resistance. *Plant Cell* **8**, 1809-1819.

**Schaller, F.** (2001). Enzymes of the biosynthesis of octadecanoid-derived signalling molecules. *J. Exp. Bot.* **52**, 11-23.

**Schmelz, E. A., Engelberth, J., Tumlinson, J. H., Block, A., and Alborn, H. T.** (2004). The use of vapor phase extraction in metabolic profiling of phytohormones and other metabolites. *Plant J.* **39**, 790-808.

**Scofield, S. R., Tobias, C. M., Rathjen, J. P., Chang, J. H., Lavell, D. T., Micheltore, R. W., and Staskawicz, B. J.** (1996). Molecular basis of gene-for-gene specificity in bacterial speck disease of tomato. *Science* **274**, 2063-2065.

**Sekine, K. T., Nandi, A., Ishihara, T., Hase, S., Ikegami, M., Shah, J., and Takahashi, H.** (2004). Enhanced resistance to Cucumber mosaic virus in the *Arabidopsis thaliana* *ssi2* mutant is mediated via an SA-independent mechanism. *Mol. Plant-Microbe Interact.* **17**, 623-632.

**Shah, J., and Chaturvedi, R.** (2008) Lipid signals in plant-pathogen interaction. *Annu. Plant Rev.* (in press).

**Shah, J.** (2005). Lipids, lipases, and lipid-modifying enzymes in plant disease resistance. *Annu. Rev. Phytopathol.* **43**, 229-260.

**Shah, J., Kachroo, P., Nandi, A., and Klessig, D. F.** (2001). A recessive mutation in the *Arabidopsis* *SSI2* gene confers SA- and NPR1-independent expression of *PR* genes and resistance against bacterial and oomycete pathogens. *Plant J.* **25**, 563-574.

**Simpson, T. D., and Gardner, H. W.** (1995). Allene oxide synthase and allene oxide cyclase, enzymes of the jasmonic acid pathway, localized in *Glycine max* tissues. *Plant Physiol.* **108**, 199-202.

**Somerville, C., Browse, J., Jaworski, J. G., and Ohrologge, J. B.** (2000). Lipids. In *Biochemistry and molecular biology of plants*. B. Buchanan, W. Gruissem, and R. Jones, eds (Rockville, MD: American Society of Plant Biologists), pp. 456–527.

**Staswick, P. E., and Tiryaki, I.** (2004). The oxylipin signal jasmonic acid is activated by an enzyme that conjugates it to isoleucine in *Arabidopsis*. *Plant Cell* **16**, 2117-2127

**Stelmach, B. A., Müller, A., Hennig, P., Gebhardt, S., Schubert-Zsilavecz, M., and Weiler, E. W.** (2001). A novel class of oxylipins, sn1-O-(12-oxophytodienoyl)-sn2-O-(hexadecatrienoyl)- monogalactosyl diglyceride, from *Arabidopsis thaliana*. *J Biol Chem* **276**, 12832-12838.

**Sticher, L., Mauch-Mani, B., and Métraux, J-P.** (1997). Systemic acquired resistance. *Anal. Rev. Phytopathol.* **35**, 235-270.

**Tang, X., Frederick, R. D., Zhou, J., Halterman, D. A., Jia, Y., and Martin, G. B.** (1996). Initiation of plant disease resistance by physical interaction of Avrptoad and the Pto kinase. *Science* **274**, 2060-2063.

**Thomma, B. P. H. J., Eggermont, K., Penninckx, I. A. M. A., Mauch-Mani, B., Vogelsang, R., Cammue, B. P. A., and Broekaert, W. F.** (1998). Separate jasmonate-dependent and

salicylate-dependent defense-response pathways in Arabidopsis are essential for resistance to distinct microbial pathogens. *Proc. Natl. Acad. Sci. USA* **95**, 15107-15111.

**Truman, W., Bennett, M. H., Kubigsteltig, I., Turnbull, C., and Grant, M.** (2007).

Arabidopsis systemic immunity uses conserved defense signaling pathways and is mediated by jasmonates. *Proc. Natl. Acad. Sci. USA* **104**, 1075-1080.

**Vernooij, B., Friedrich, L., Morse, A., Reist, R., Kolditz-Jawhar, R., Ward, E., Uknes, S., Kessmann, H., and Ryals, J.** (1994). Salicylic acid is not the translocated signal responsible for inducing systemic acquired resistance but is required in signal transduction. *Plant Cell* **6**, 959-965.

**Welti, R., Li, W., Li, M., Sang, Y., Biesiada, H., Zhou, H-E., Rajashekar, C. B., Williams, T. D., and Wang, X.** (2002). Profiling membrane lipids in plant stress response. Role of phospholipase D alpha in freezing-induced lipid changes in Arabidopsis. *J. Biol. Chem* **277**, 31994-32002.

## Figure Legends

### Fig 3.1 A simplified overview of lipid biosynthesis in plastids

Shown is the simplified biosynthesis of phosphatidylglycerol (PG), the galactolipids monogalactosyldiacylglycerol (MGDG) and digalactosyldiacylglycerol (DGDG) and sulfolipid (SL) in the plastids. *SFD1* encodes a dihydroxyacetonephosphate (DHAP) reductase that provides glycerol-3-phosphate (G3P) for glycerolipid synthesis in the plastids. *ACT1* (*ATS1*) codes for an acyltransferase, that transfers an acyl chain onto diacylglycerol (DAG) to form lysophosphatidic acid (LPA). *MGD1* encodes an enzyme that transfers a D-galactose moiety onto DAG to produce MGDG. The *DGDI* gene codes for a digalactosyldiacylglycerol (DGDG) synthase. The acyl chains on PG, MGDG, DGDG and SL are desaturated by specific fatty acyl desaturases. *FAD5* encoded desaturase primarily acts on 16:0 acyl chains at the *sn2* position in MGDG to yield 16:1. *FAD4* on the other hand, encodes a desaturase that acts primarily on 16:0 acyl chains at the *sn2* position in PG to yield 16:1. The *FAD6* encodes a desaturase that catalyzes the conversion of 18:1 and 16:1 acyl chains in PG, MGDG, DGDG and SL to 18:2 and 16:2, respectively. The desaturase *FAD7* takes up the final step of converting 18:2 and 16:2 acyl chains in PG, MGDG, DGDG and SL to 18:3 and 16:3, respectively. LPA, lysophosphatidic acid; PA, phosphatidic acid

### Fig 3.2 SAR is compromised in the *sfd2* mutant

#### (A) SAR associated *PR1* expression in *sfd2*

Reverse transcription-PCR analysis for *PR1* expression in the upper leaves of WT accession 1/8E background which is the accession Nössen (Nö) and contains a *PR1:tms2* transgene and *sfd2* plants, 2 days post infiltration of three lower leaves with 10 mM MgCl<sub>2</sub> (Mock) or the avirulent pathogen (Avr).

#### (B) Growth of *Psm* in the distal leaves of WT and *sfd2* mutants that were previously inoculated with avirulent *Pst* or mock on lower leaves

Growth of the virulent pathogen *P. syringae* pv. *maculicola* (*Psm*) in WT accession 1/8E background which is the accession Nössen (Nö) and contains a *PR1:tms2* transgene and *sfd2* plants. *P. syringae* pv. *tomato* DC3000 carrying the *avrRpt2* avirulence gene was infiltrated into three lower leaves of WT and mutant plants. Plants similarly treated with 10 mM MgCl<sub>2</sub> act as

controls. Three days later, four upper leaves in each plant were infiltrated with *Psm* and bacterial numbers monitored 3 days post inoculation (dpi). White bars: Primary inoculation with 10 mM MgCl<sub>2</sub>. Black bars: Primary inoculation with Avr pathogen. The different letters above the bars indicate values that are significantly different from each other upon a student's *t*-test ( $P < 0.05$ ).

### **Fig 3.3 SAR is compromised in the *act1* mutant**

#### **(A) SAR associated *PR1* expression in *act1***

Reverse transcription-PCR analysis for *PR1* expression in the upper leaves of WT accession Columbia (Col) and *act1* plants, 2 days post-infiltration of three lower leaves with 10 mM MgCl<sub>2</sub> (Mock) or the avirulent pathogen (Avr).

#### **(B) Growth of *Psm* in the distal leaves of WT and *act1* mutants that were previously inoculated with avirulent *Pst* or mock on lower leaves**

Growth of the virulent pathogen *P. syringae* pv. *maculicola* (*Psm*) in WT accession Columbia (Col) and *act1* plants. *P. syringae* pv. *tomato* DC3000 carrying the *avrRpt2* avirulence gene was infiltrated into three lower leaves of WT and mutant plants. Plants similarly treated with 10 mM MgCl<sub>2</sub> act as controls. Three days later, four upper leaves in each plant were infiltrated with *Psm* and bacterial numbers monitored 3 days post inoculation (dpi). White bars: Primary inoculation with 10 mM MgCl<sub>2</sub>. Black bars: Primary inoculation with Avr pathogen. The different letters above the bars indicate values that are significantly different from each other upon a student's *t*-test ( $P < 0.05$ ).

### **Fig 3.4 SAR is compromised in the *fad6* mutant**

#### **(A) SAR associated *PR1* expression in *fad6***

Reverse transcription-PCR analysis for *PR1* expression in the upper leaves of WT accession Columbia (Col) and *act1* plants, 2 days post-infiltration of three lower leaves with 10 mM MgCl<sub>2</sub> (Mock) or the avirulent pathogen (Avr).

#### **(B) Growth of *Psm* in the distal leaves of WT and *fad6* mutants that were previously inoculated with avirulent *Pst* or mock on lower leaves**

Growth of the virulent pathogen *P. syringae* pv. *maculicola* (*Psm*) in WT accession Columbia (Col) and *fad6* plants. *P. syringae* pv. *tomato* DC3000 carrying the *avrRpt2* avirulence gene was

infiltrated into three lower leaves of WT and mutant plants. Plants similarly treated with 10 mM MgCl<sub>2</sub> act as controls. Three days later, four upper leaves in each plant were infiltrated with *Psm* and bacterial numbers monitored 3 days post inoculation (dpi). White bars: Primary inoculation with 10 mM MgCl<sub>2</sub>. Black bars: Primary inoculation with Avr pathogen. The different letters above the bars indicate values that are significantly different from each other upon a student's *t*-test ( $P < 0.05$ ).

### **Fig 3.5 SAR is compromised in the *mdg1* mutant**

#### **(A) SAR associated *PR1* expression in *mdg1***

Reverse transcription-PCR analysis of *PR1* expression in the upper leaves of WT accession *Col* and *mdg1* plants, 2 days post-infiltration of three lower leaves with 10 mM MgCl<sub>2</sub> (Mock) or the avirulent pathogen (Avr).

#### **(B) Growth of *Psm* in the distal leaves of WT and *mdg1* mutants that were previously inoculated with avirulent *Pst* or mock on lower leaves**

Growth of the virulent pathogen *P. syringae* pv. *maculicola* (*Psm*) in WT accession *Col* and *mdg1* plants. *P. syringae* pv. *tomato* DC3000 carrying the *avrRpt2* avirulence gene was infiltrated into three lower leaves of WT and mutant plants. Plants similarly treated with 10 mM MgCl<sub>2</sub> act as controls. Three days later, four upper leaves in each plant were infiltrated with *Psm* and bacterial numbers monitored 3 days post inoculation (dpi). White bars: Primary inoculation with 10 mM MgCl<sub>2</sub>. Black bars: Primary inoculation with Avr pathogen. The different letters above the bars indicate values that are significantly different from each other upon a student's *t*-test ( $P < 0.05$ ).

### **Fig 3.6 SAR is compromised in the *dgd1* mutant**

#### **(A) SAR associated *PR1* expression in *dgd1***

Reverse transcription-PCR analysis for *PR1* expression in the upper leaves of WT accession Columbia (Col-2) and *act1* plants, 2 days post-infiltration of three lower leaves with 10 mM MgCl<sub>2</sub> (Mock) or the avirulent pathogen (Avr).

#### **(B) Growth of *Psm* in the distal leaves of WT and *dgd1* mutants that were previously inoculated with avirulent *Pst* or mock on lower leaves**



Growth of the virulent pathogen *P. syringae* pv. *maculicola* (*Psm*) in WT accession Columbia (Col-2) and *dgd1* plants. *P. syringae* pv. *tomato* DC3000 carrying the *avrRpt2* avirulence gene was infiltrated into three lower leaves of WT and mutant plants. Plants similarly treated with 10 mM MgCl<sub>2</sub> act as controls. Three days later, four upper leaves in each plant were infiltrated with *Psm* and bacterial numbers monitored 3 days post inoculation (dpi). White bars: Primary inoculation with 10 mM MgCl<sub>2</sub>. Black bars: Primary inoculation with Avr pathogen. The different letters above the bars indicate values that are significantly different from each other upon a student's *t*-test ( $P < 0.05$ ).

### **Fig 3.7 SAR is compromised in the *fad5* mutant**

#### **(A) SAR associated *PR1* expression in *fad5***

Reverse transcription-PCR analysis for *PR1* expression in the upper leaves of WT accession Columbia (Col) and *fad5* plants, 2 days post-infiltration of three lower leaves with 10 mM MgCl<sub>2</sub> (Mock) or the avirulent pathogen (Avr).

#### **(B) Growth of *Psm* in the distal leaves of WT and *fad5* mutants that were previously inoculated with avirulent *Pst* or mock on lower leaves**

Growth of the virulent pathogen *P. syringae* pv. *maculicola* (*Psm*) in WT accession Columbia (Col) and *fad5* plants. *P. syringae* pv. *tomato* DC3000 carrying the *avrRpt2* avirulence gene was infiltrated into three lower leaves of WT and mutant plants. Plants similarly treated with 10 mM MgCl<sub>2</sub> act as controls. Three days later, four upper leaves in each plant were infiltrated with *Psm* and bacterial numbers monitored 3 days post inoculation (dpi). White bars: Primary inoculation with 10 mM MgCl<sub>2</sub>. Black bars: Primary inoculation with Avr pathogen. The different letters above the bars indicate values that are significantly different from each other upon a student's *t*-test ( $P < 0.05$ ).

### **Fig 3.8 SAR is not compromised in the *fad4* mutant**

#### **(A) SAR associated *PR1* expression in *fad4***

Reverse transcription-PCR analysis for *PR1* expression in the upper leaves of WT accession Columbia (Col) and *fad4* plants, 2 days post-infiltration of three lower leaves with 10 mM MgCl<sub>2</sub> (Mock) or the avirulent pathogen (Avr).

**(B) Growth of *Psm* in the distal leaves of WT and *fad4* mutants that were previously inoculated with avirulent *Pst* or mock on lower leaves**

Growth of the virulent pathogen *P. syringae* pv. *maculicola* (*Psm*) in WT accession Columbia (Col) and *fad4* plants. *P. syringae* pv. *tomato* DC3000 carrying the *avrRpt2* avirulence gene was infiltrated into three lower leaves of WT and mutant plants. Plants similarly treated with 10 mM MgCl<sub>2</sub> act as controls. Three days later, four upper leaves in each plant were infiltrated with *Psm* and bacterial numbers monitored 3 days post inoculation (dpi). White bars: Primary inoculation with 10 mM MgCl<sub>2</sub>. Black bars: Primary inoculation with Avr pathogen. The different letters above the bars indicate values that are significantly different from each other upon a student's *t*-test ( $P < 0.05$ ).

**Fig. 3.9 *ssi2*-conferred defense phenotypes are suppressed by *fad7***

**(A) SAR associated *PR1* expression in *fad7***

Reverse transcription-PCR analysis for *PR1* expression in the upper leaves of WT accession Columbia (Col) *glabra1* and *fad7* plants, 2 days post-infiltration of three lower leaves with 10 mM MgCl<sub>2</sub> (Mock) or the avirulent pathogen (Avr).

**(B) Growth of *Psm* in the distal leaves of WT and *fad7* mutants that were previously inoculated with avirulent *Pst* or mock on lower leaves**

Growth of the virulent pathogen *P. syringae* pv. *maculicola* (*Psm*) in WT accession Columbia (Col) *glabra1* and *fad7* plants. *P. syringae* pv. *tomato* DC3000 carrying the *avrRpt2* avirulence gene was infiltrated into three lower leaves of WT and mutant plants. Plants similarly treated with 10 mM MgCl<sub>2</sub> act as controls. Three days later, four upper leaves in each plant were infiltrated with *Psm* and bacterial numbers monitored 3 days post inoculation (dpi). White bars: Primary inoculation with 10 mM MgCl<sub>2</sub>. Black bars: Primary inoculation with Avr pathogen. The different letters above the bars indicate values that are significantly different from each other upon a student's *t*-test ( $P < 0.05$ ).

**(C) *PR1* expression in the leaves of WT, *fad7*, *ssi2* and *fad7 ssi2* mutants**

Reverse transcription-PCR analysis for *PR1* expression in the leaves of 4 week old WT, *ssi2*, *fad7* and *fad7ssi2* lines

**(D) Growth of *Psm* in the leaves of WT, *fad7*, *ssi2* and *fad7 ssi2* mutants**

Comparison between the colony forming unit (CFU) per leaf disk numbers of the bacterial pathogen *P. syringae* pv. *maculicola* ES4326, on 4 week old WT, *ssi2*, *fad7* and *fad7ssi2* lines. Each bar represents the average *Psm* count in 12 leaf discs  $\pm$  SD. The different letters above the bars indicate values that are significantly different from each other upon a student's *t*-test ( $P<0.05$ ).

**Fig. 3.10 *ssi2*-conferred growth phenotypes are suppressed by *fad7***

**(A) *fad7* partially suppresses *ssi2*'s dwarf phenotype**

The *fad7* plants are comparable to the WT, while the *ssi2* plants are dwarf in stature. The *fad7ssi2* double mutant plants are intermediate in size.

**(B) *fad7* partially suppresses *ssi2*'s constitutive cell death**

The *ssi2* plants have a constitutive cell death phenotype. The *fad7* plant, on the other hand shows no cell death. The *fad7ssi2* double mutants have an intermediate cell death phenotype.

**Fig 3.11 SAR is not compromised in the *opr3* and *coi1* mutants**

**(A) SAR is not compromised in the *opr3* mutant**

Growth of the virulent pathogen *P. syringae* pv. *maculicola* (*Psm*) in WT accession Columbia (Col) and *opr3* plants. *P. syringae* pv. *tomato* DC3000 carrying the *avrRpt2* avirulence gene was infiltrated into three lower leaves of WT and mutant plants. Plants similarly treated with 10 mM MgCl<sub>2</sub> act as controls. Three days later, four upper leaves in each plant were infiltrated with *Psm* and bacterial numbers monitored 3 days post inoculation (dpi). White bars: Primary inoculation with 10 mM MgCl<sub>2</sub>. Black bars: Primary inoculation with Avr pathogen. The different letters above the bars indicate values that are significantly different from each other upon a student's *t*-test ( $P<0.05$ ).

**(B) SAR is not compromised in the *coi1* mutant**

Growth of the virulent pathogen *P. syringae* pv. *maculicola* (*Psm*) in WT accession Columbia (Col) and *coi1* plants. *P. syringae* pv. *tomato* DC3000 carrying the *avrRpt2* avirulence gene was infiltrated into three lower leaves of WT and mutant plants. Plants similarly treated with 10 mM MgCl<sub>2</sub> act as controls. Three days later, four upper leaves in each plant were infiltrated with *Psm*

and bacterial numbers monitored 3 days post inoculation (dpi). White bars: Primary inoculation with 10 mM MgCl<sub>2</sub>. Black bars: Primary inoculation with Avr pathogen. The different letters above the bars indicate values that are significantly different from each other upon a student's *t*-test ( $P=0.05$ ).

### **Fig 3.12 JA and SA content in the WT and *opr3* mutant plants**

Four week old soil grown plants were used for inoculation. 4-5 leaves were inoculated with a suspension of *P. syringae* pv. *maculicola* ES4326 at an optical density of 0.0001 at 600 nm. 12 hours after the inoculation leaves were harvested and analysed for the JA and MeSA content. **(A) JA content in the WT and *opr3* mutant** White bars: plants inoculation with pathogen suspension. Black bars: un-inoculated plants. The different letters above the bars indicate values that are significantly different from each other upon a student's *t*-test ( $P=0.05$ ). **(B) SA content in the WT and *opr3* mutant** White bars: plants inoculation with pathogen suspension. Black bars: un-inoculated plants. The different letters above the bars indicate values that are significantly different from each other upon a student's *t*-test ( $P=0.05$ ).

### **Fig 3.13 Lipid diagrams**

- (A)** Phosphatidic Acid (PA)
- (B)** Phosphatidylglycerol (PG)
- (C)** Monogalactosyldiacylglycerol (MGDG)
- (D)** Digalactosyldiacylglycerol (DGDG)

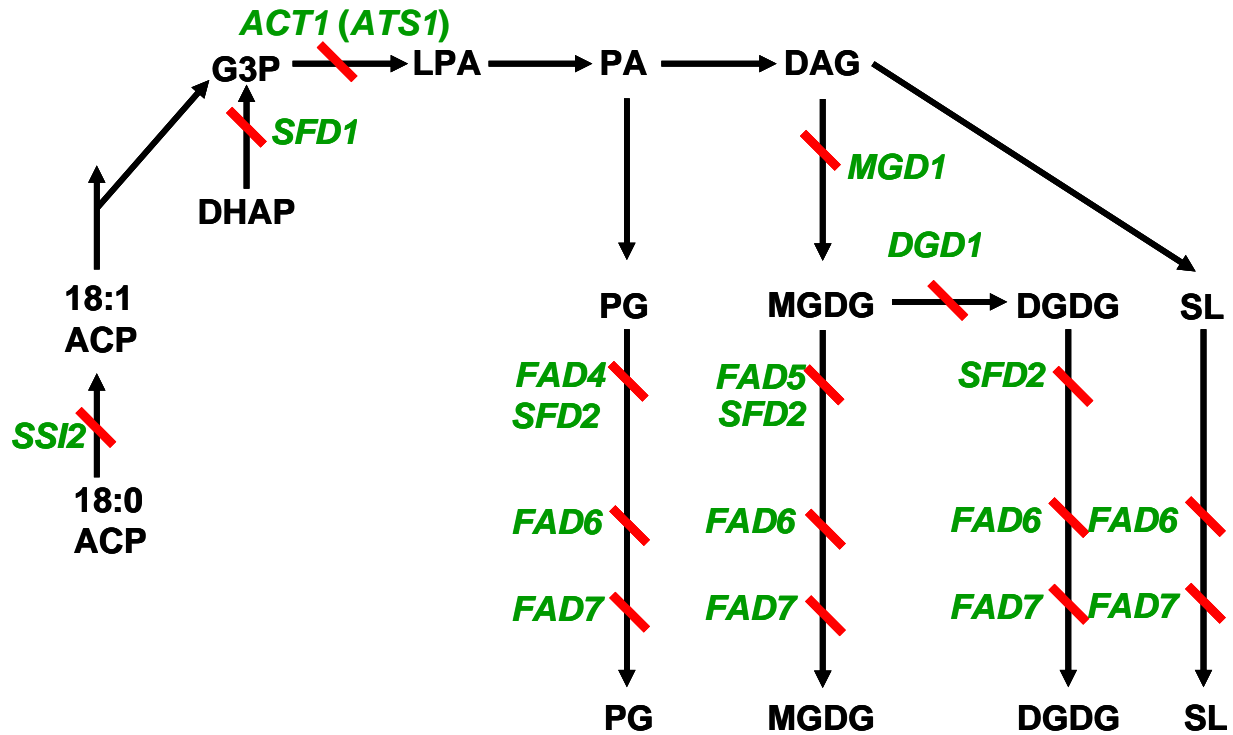
### **Fig 3.14 Schematic of SAR signaling pathway**

Steps leading to the activation of SAR in the naïve distal parts are shown here. *SFD1* codes for a dihydroxyacetonephosphate (DHAP) reductase that provides glycerol-3-phosphate (G3P) for glycerolipids synthesis in the plastids and is required for the accumulation of a SAR-inducing factor/activity in petiole exudates of a pathogen-inoculated leaf. In contrast, *SSI2* which encodes a stearyl-ACP desaturase suppresses the activation of SAR. Genetic studies indicate that the *sfd1* allele is epistatic to the *ssi2* mutant allele (Nandi et al. 2003). Lipid biosynthetic genes like *ACT1*, *FAD6*, *FAD7* and *SFD2* are also required for the accumulation of the SAR-inducing

factor/activity, as are galactolipid specific genes like *MGD1* and *DGD1* suggesting a role for galactolipids in SAR. DIR1 encodes a putative lipid transfer protein that may or may not bind to the SAR-activating factor/activity, but is required for the activation of SAR in the naïve distal parts. Petiole exudates from avirulent pathogen-inoculated *sfd1* mutant complement the SAR defect of the similar petiole exudates collected from the *dir1* mutant, suggesting that the SFD1-dependent factor and DIR1 are required together in petiole exudates for the activation of SAR.

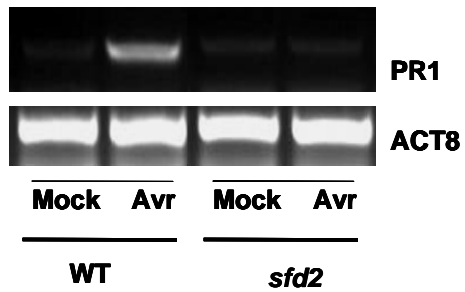
## Figures

Figure 3.1 A simplified overview of lipid biosynthesis in plastids



**Figure 3.2 SAR is compromised in the *sfd2* mutant**

**(A) SAR associated *PR1* expression in *sfd2***



**(B) Growth of *Psm* in the distal leaves of WT and *sfd2* mutants that were previously inoculated with avirulent *Pst* or mock on lower leaves.**

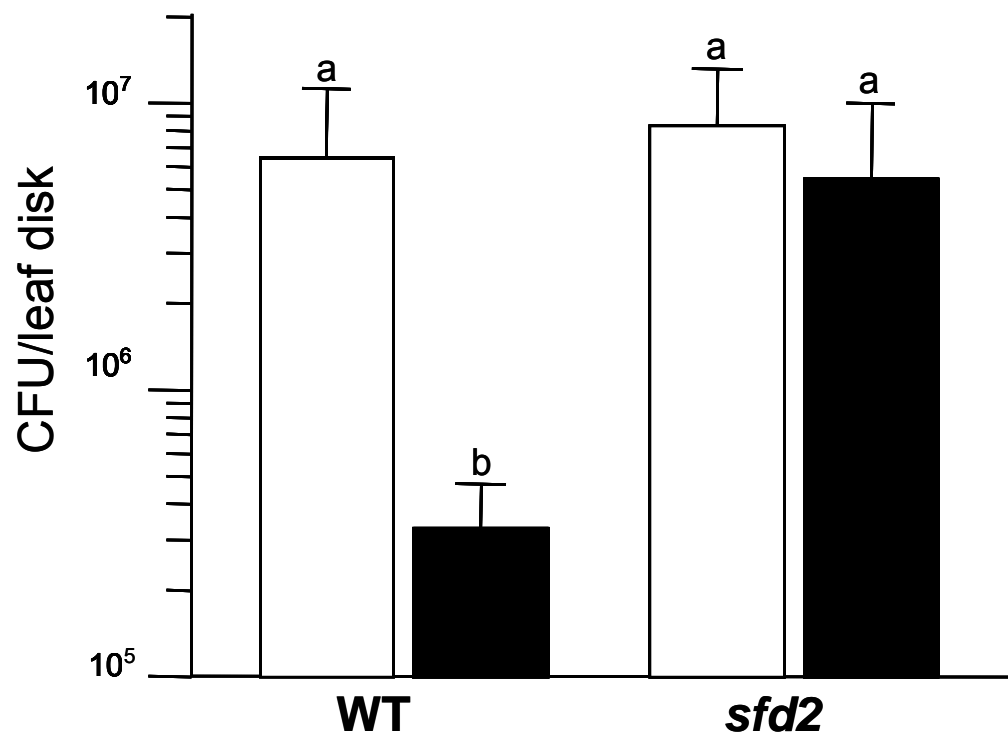
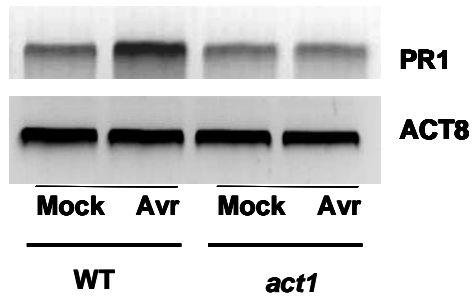


**Figure 3.3 SAR is compromised in the *act1* mutant**

**(A) SAR associated *PR1* expression in *act1***



**(B) Growth of *Psm* in the distal leaves of WT and *act1* mutants that were previously inoculated with avirulent *Pst* or mock on lower leaves.**

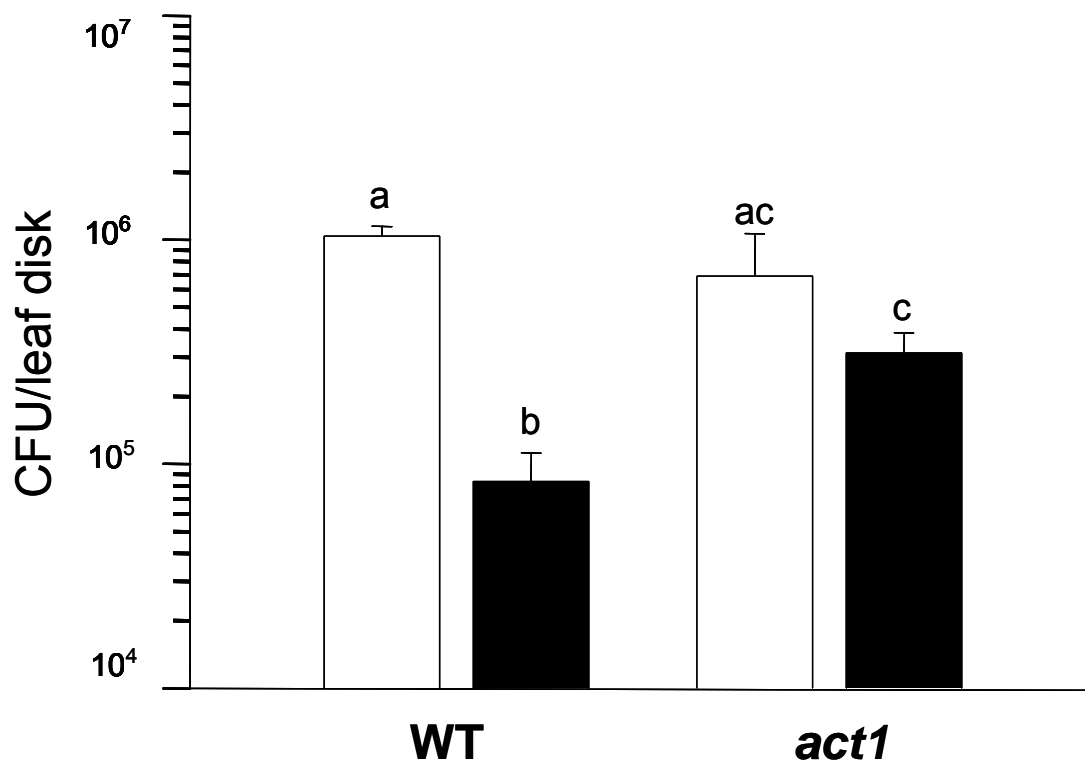
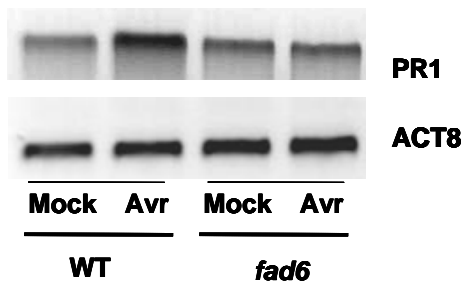




**Figure 3.4 SAR is compromised in the *fad6* mutant**

**(A) SAR associated *PR1* expression in *fad6***



**(B) Growth of *Psm* in the distal leaves of WT and *fad6* mutants that were previously inoculated with avirulent *Pst* or mock on lower leaves.**

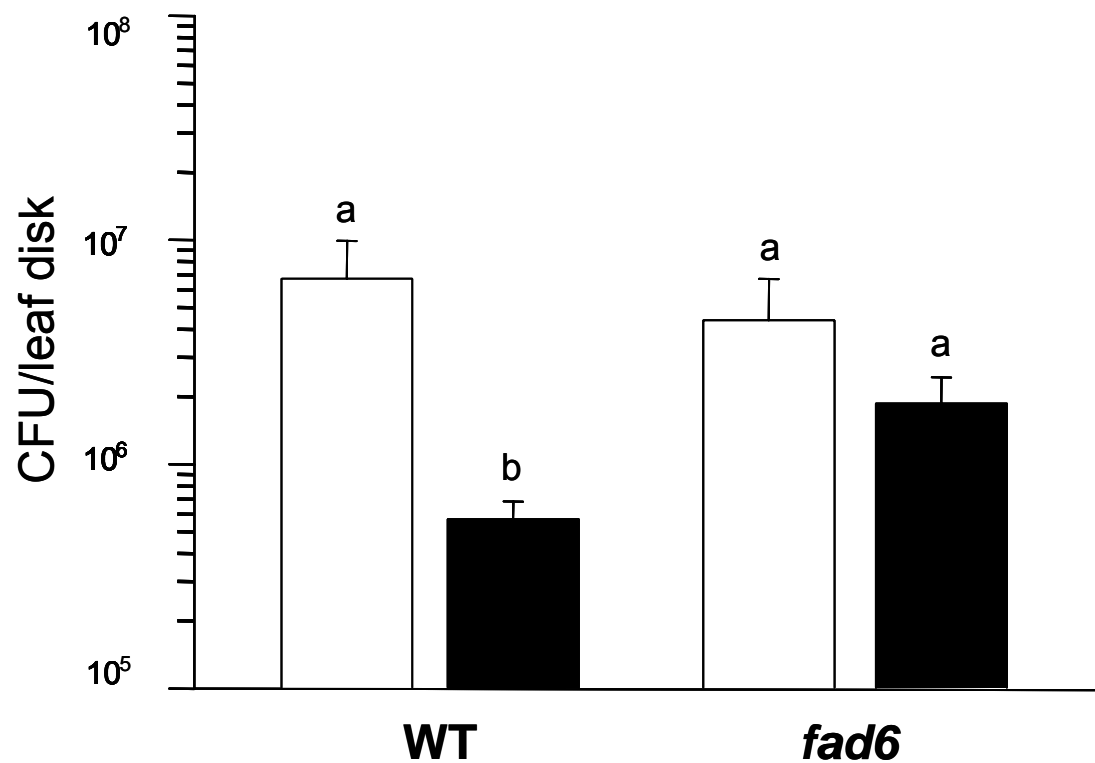
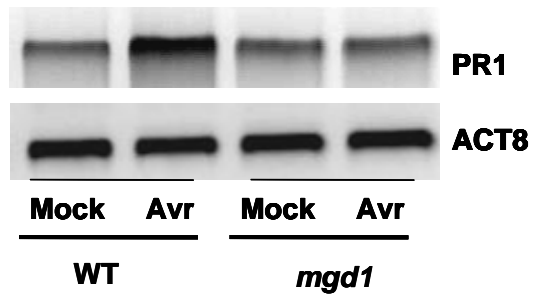


**Figure 3.5 SAR is compromised in the *mgd1* mutant**

**(A) SAR associated *PR1* expression in *mgd1***



**(B) Growth of *Psm* in the distal leaves of WT and *mgd1* mutants that were previously inoculated with avirulent *Pst* or mock on lower leaves.**

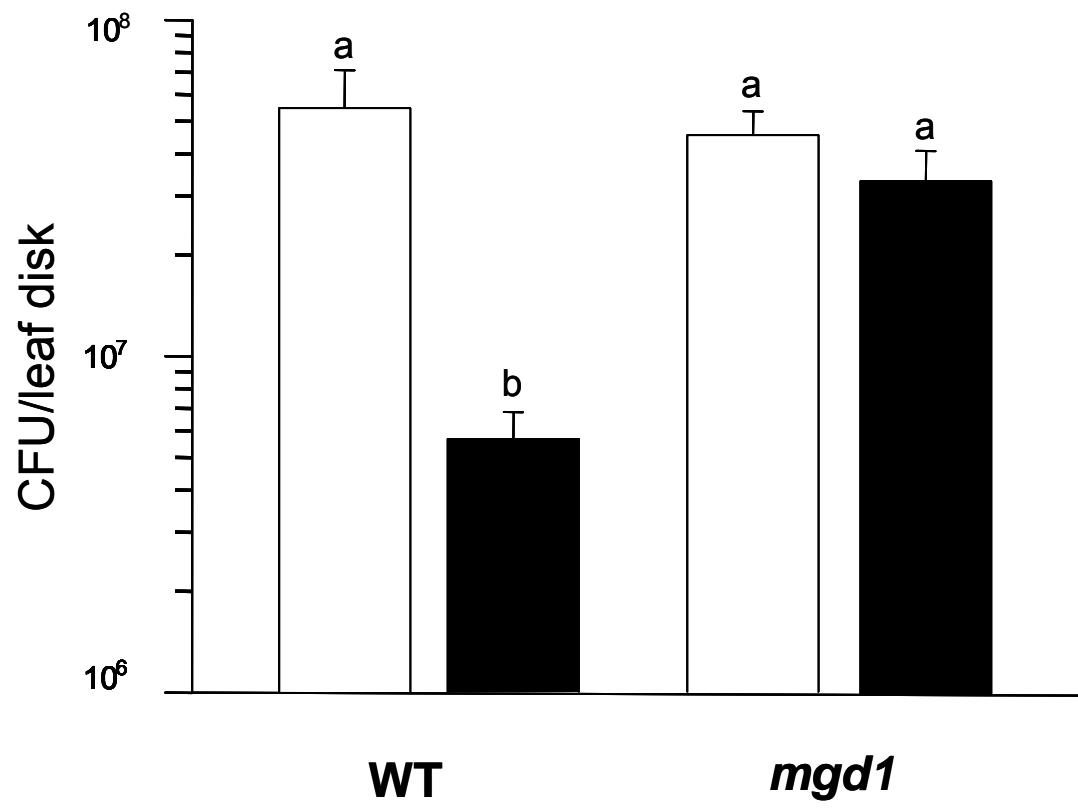
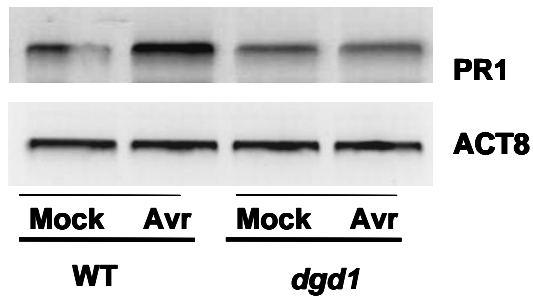


**Figure 3.6 SAR is compromised in the *dgd1* mutant**

**(A) SAR associated *PR1* expression in *dgd1***



**(B) Growth of *Psm* in the distal leaves of WT and *dgd1* mutants that were previously inoculated with avirulent *Pst* or mock on lower leaves.**

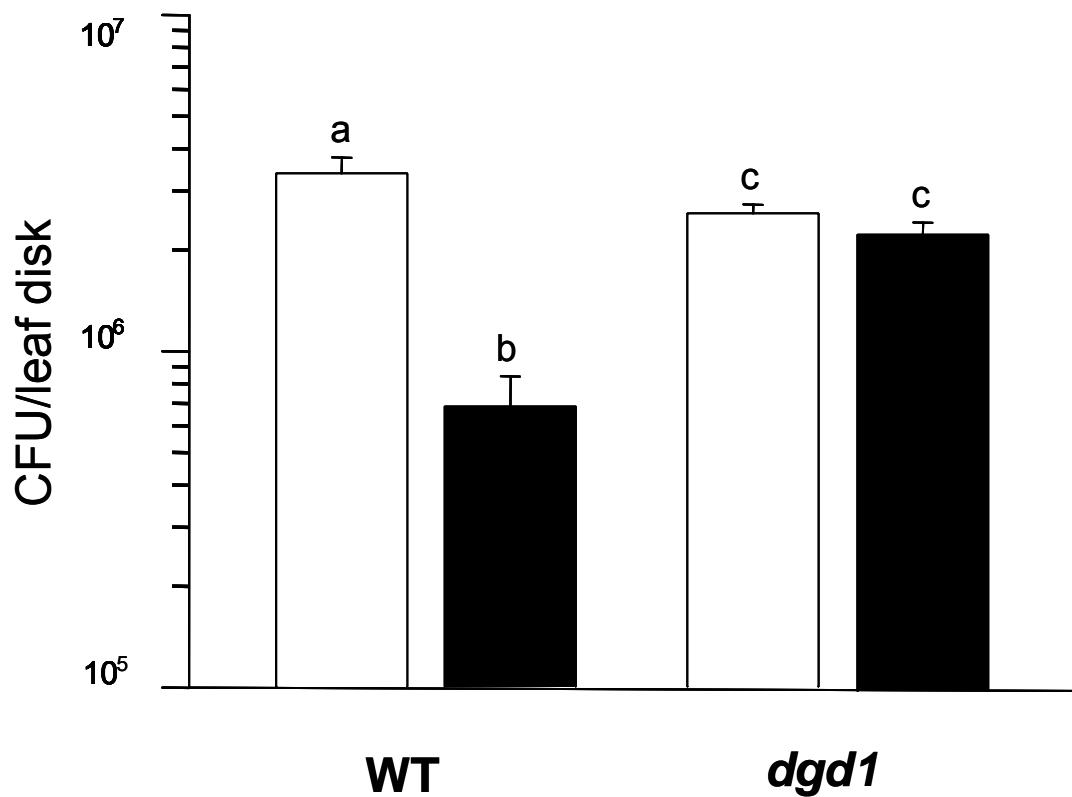
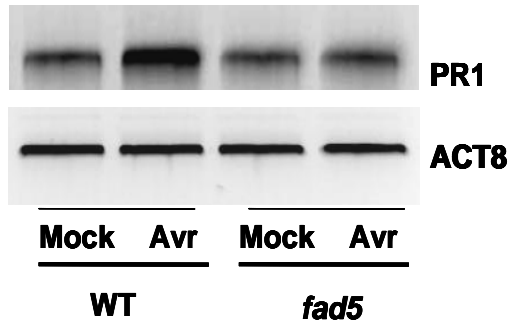


**Figure 3.7 SAR is compromised in the *fad5* mutant**

**(A) SAR associated *PR1* expression in *fad5***



**(B) Growth of *Psm* in the distal leaves of WT and *fad5* mutants that were previously inoculated with avirulent *Pst* or mock on lower leaves.**

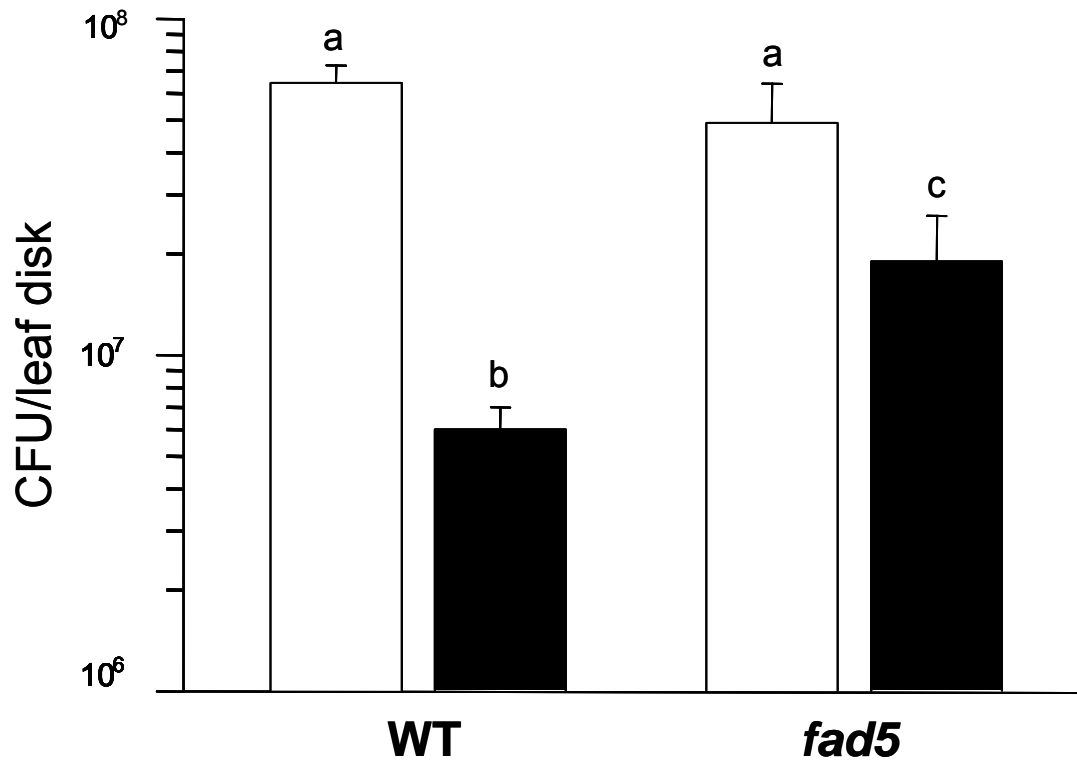
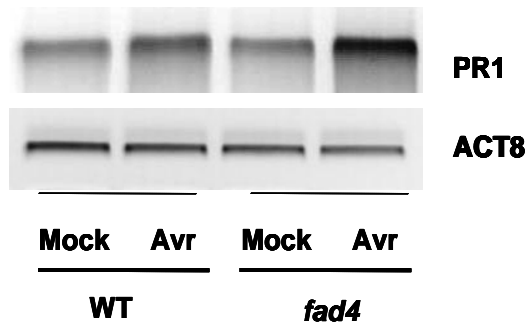


**Figure 3.8 SAR is not compromised in the *fad4* mutant**

**(A) SAR associated *PR1* expression in *fad4***



**(B) Growth of *Psm* in the distal leaves of WT and *fad4* mutants that were previously inoculated with avirulent *Pst* or mock on lower leaves.**

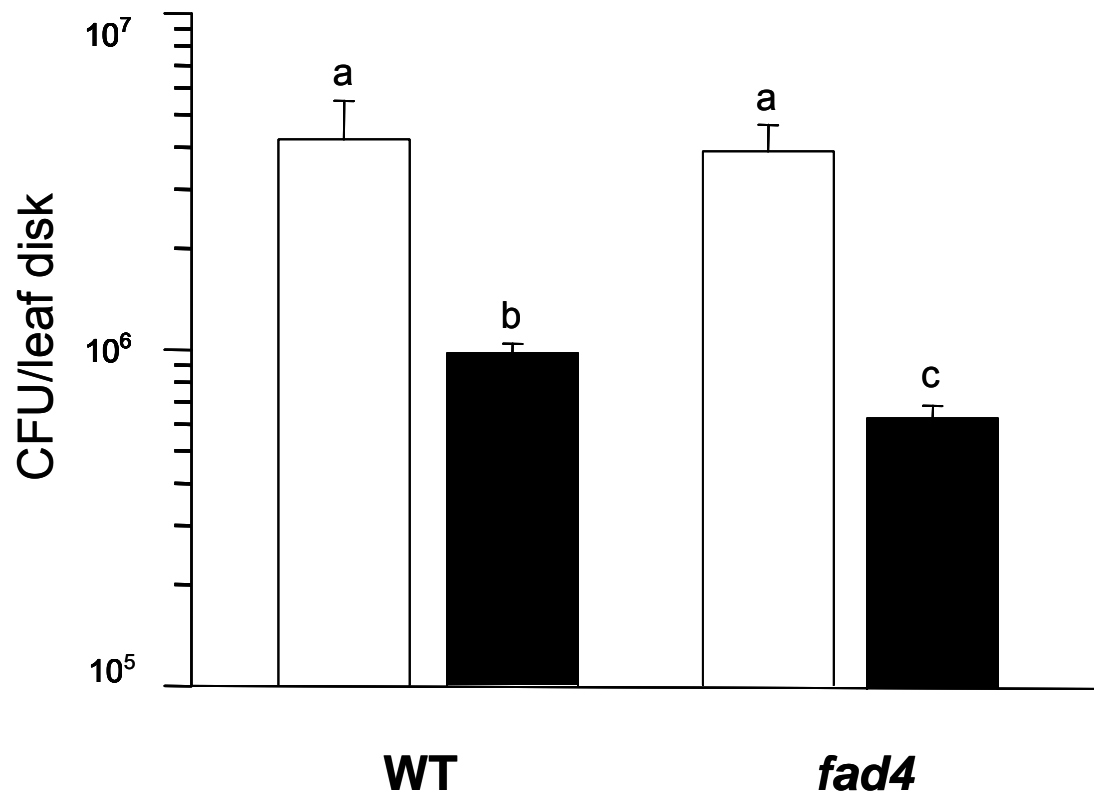
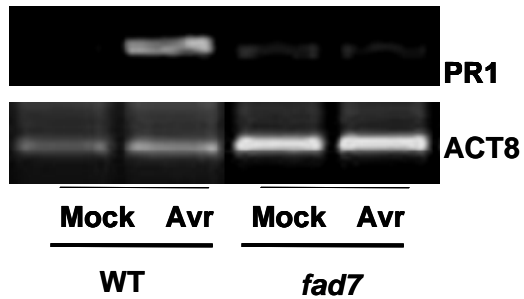
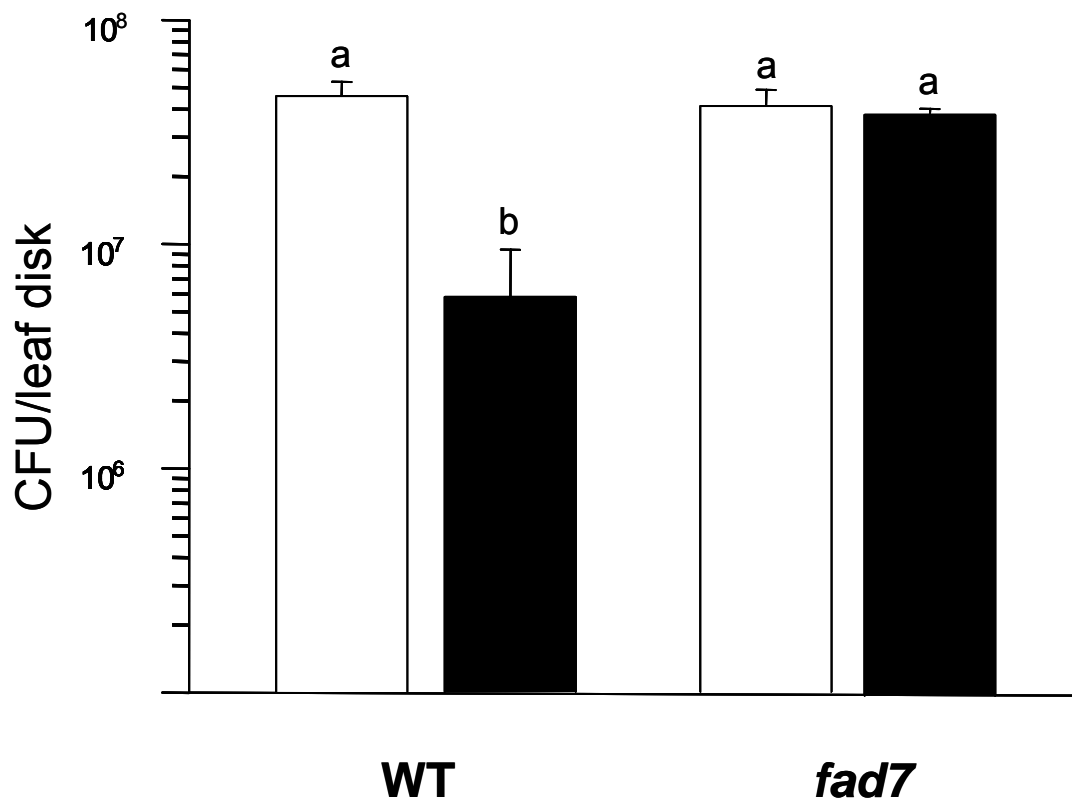


**Figure 3.9** *ssi2*-conferred defense phenotypes are suppressed by *fad7*

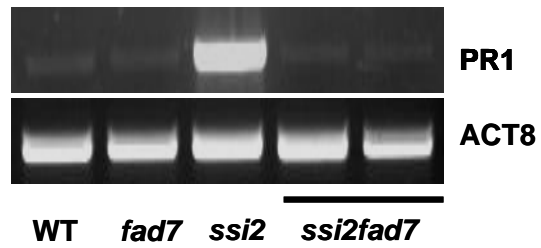
**(A)** SAR associated *PR1* expression in *fad7*



**(B)** Growth of *Psm* in the distal leaves of WT and *fad7* mutants that were previously inoculated with avirulent *Pst* or mock on lower leaves.



(C) *PR1* expression in the leaves of WT, *fad7*, *ssi2* and *fad7 ssi2* mutants



(D) Growth of *Psm* in the leaves of WT, *fad7*, *ssi2* and *fad7 ssi2* mutants

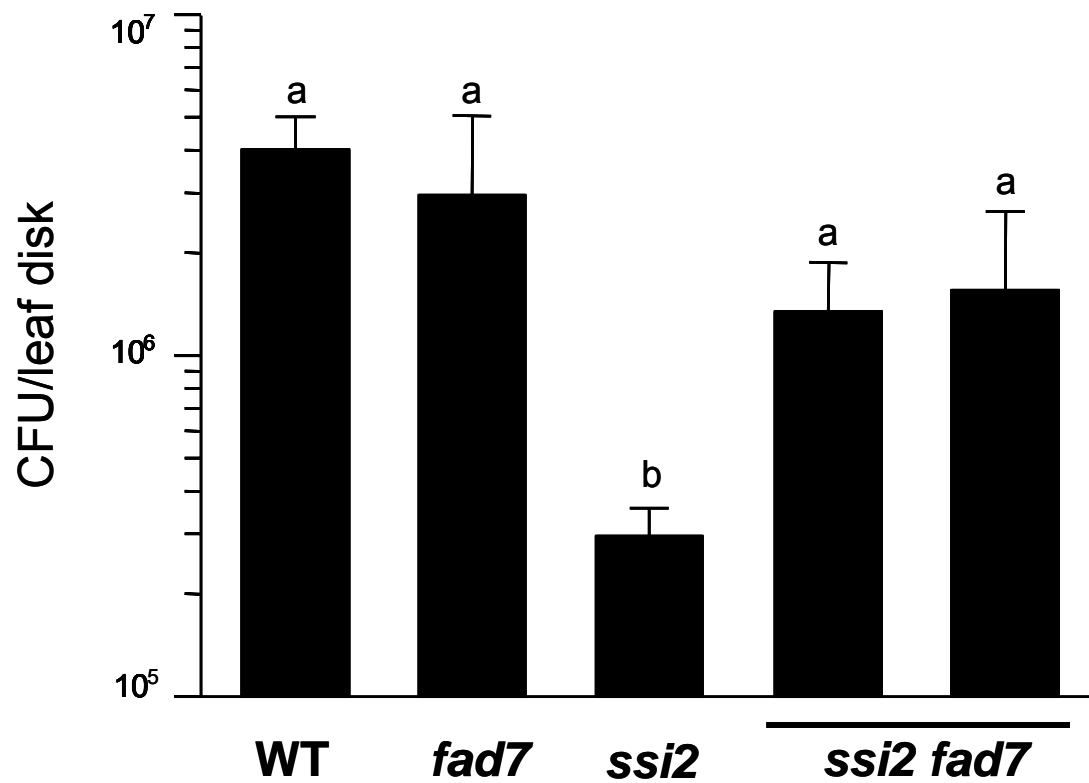
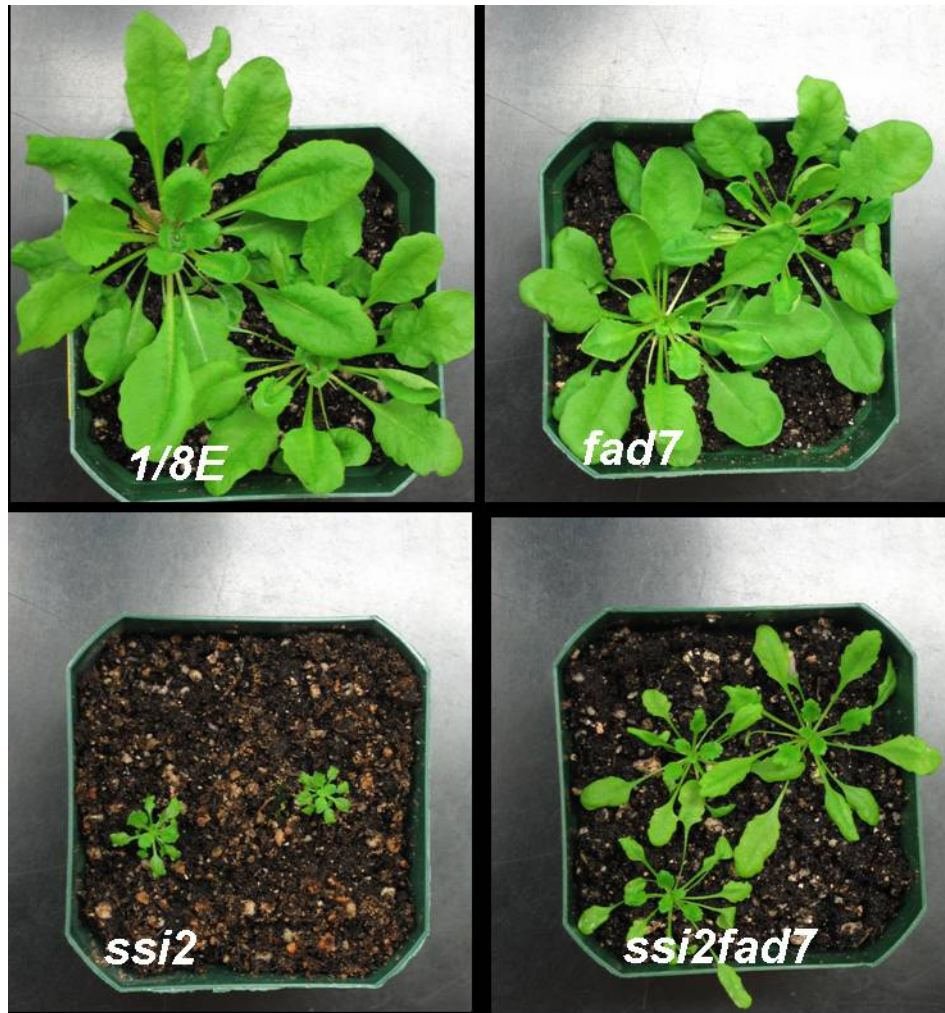




**Figure 3.10** *ssi2*-conferred growth phenotypes are suppressed by *fad7*

(A) *fad7* partially suppresses *ssi2*'s dwarf phenotype



**(B) *fad7* partially suppresses *ssi2*'s constitutive cell death**

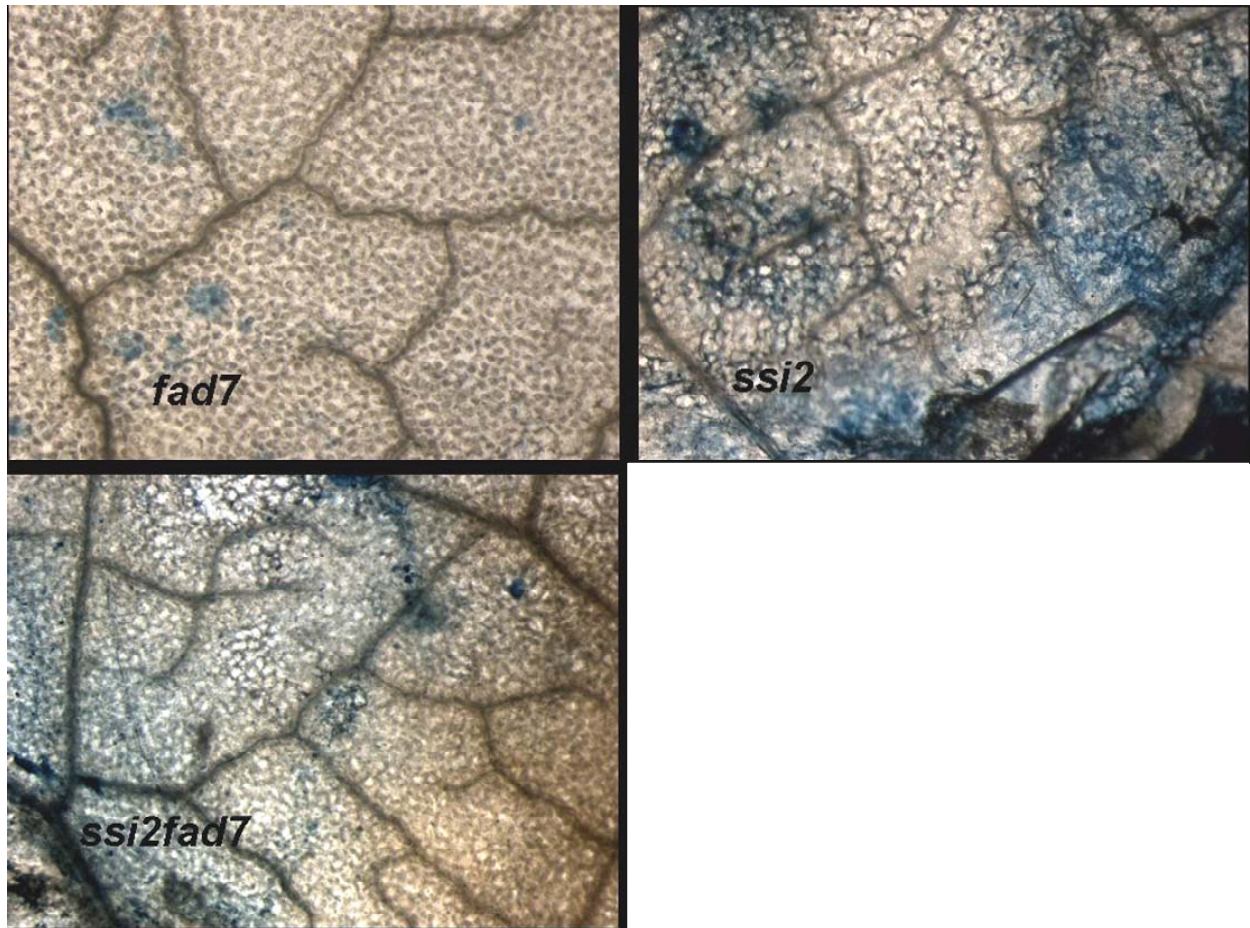
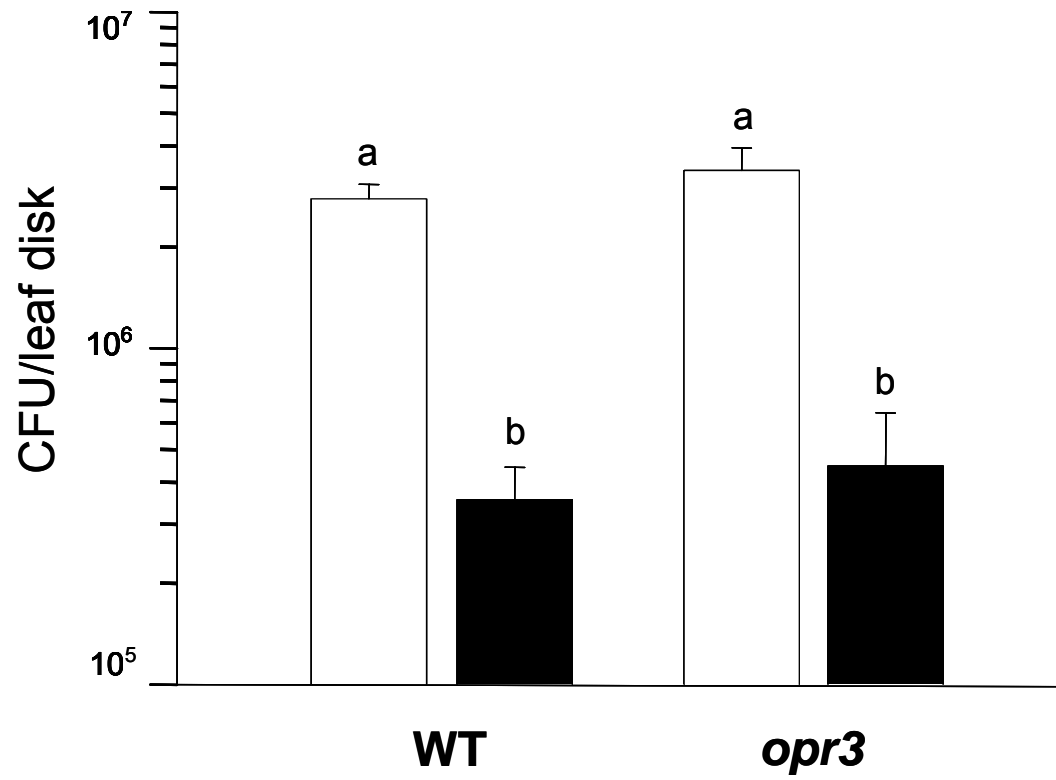


**Figure 3.11 SAR is not compromised in the *opr3* and *coil* mutants**

**(A) SAR is not compromised in the *opr3* mutant**



**(B) SAR is not compromised in the *coi1* mutant**

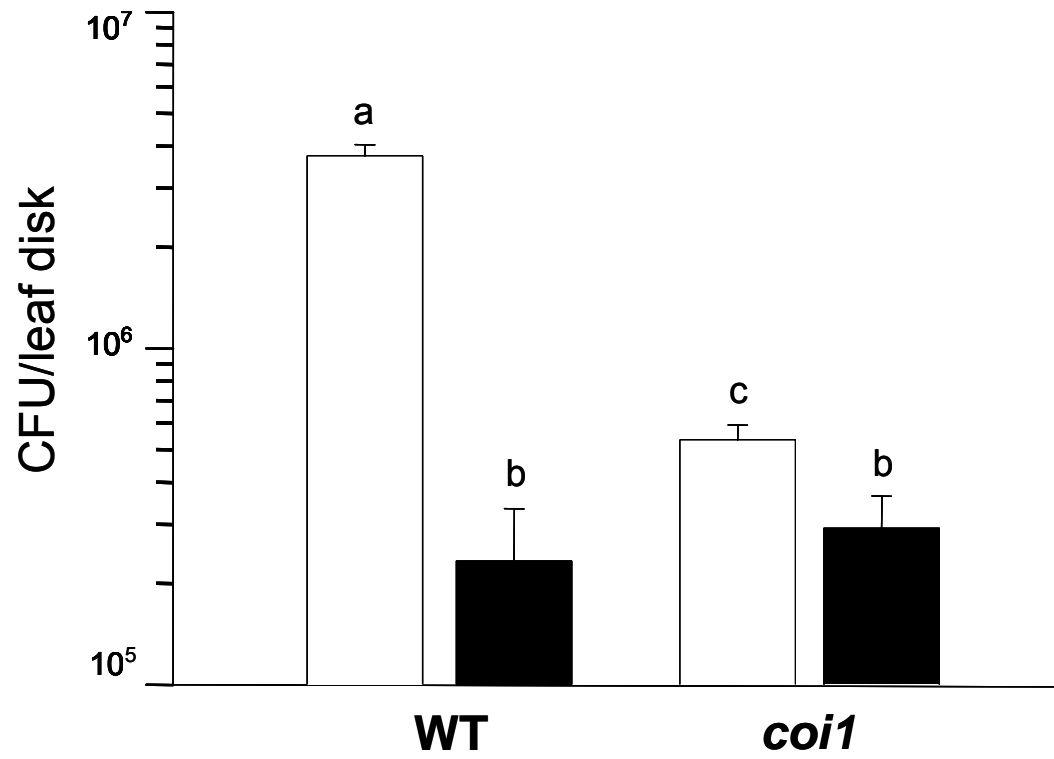
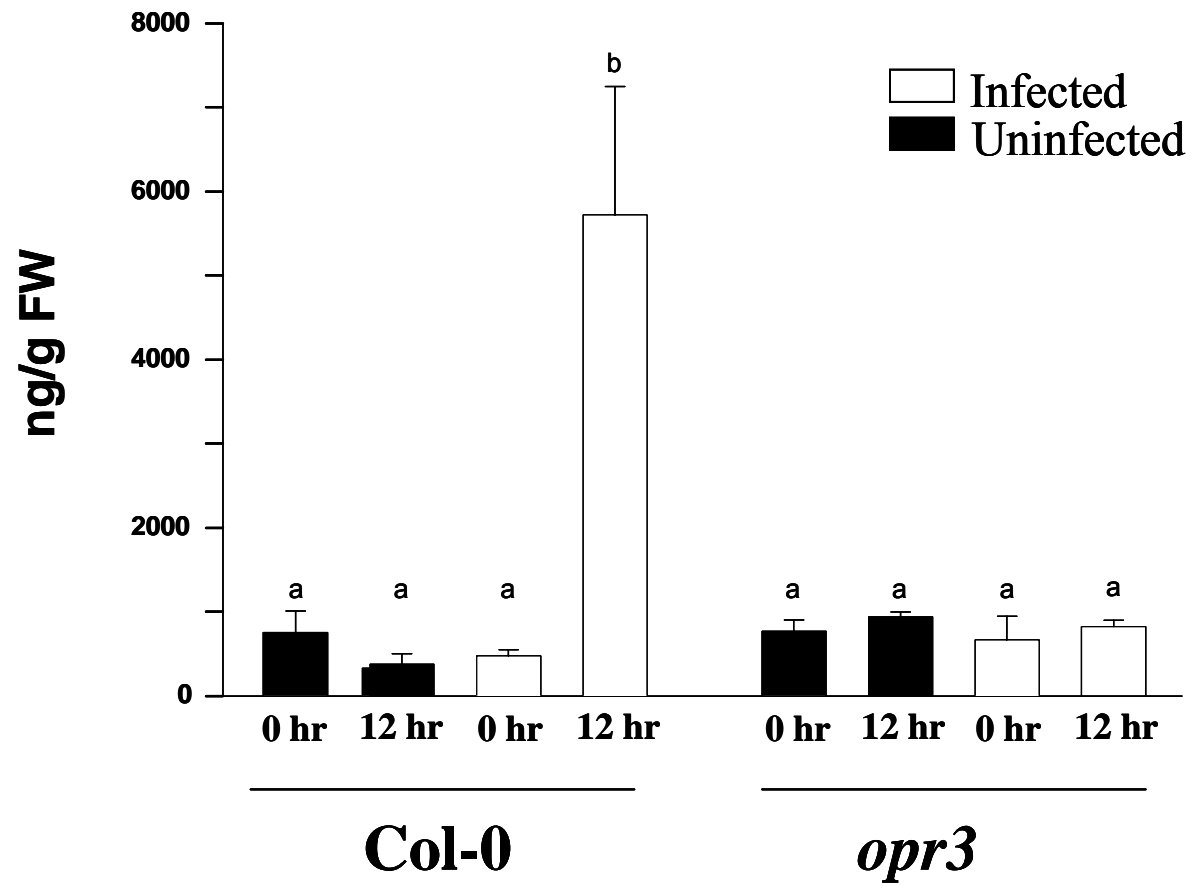


**Figure 3.12 JA and SA content in the WT and *opr3* mutant plants**

**(A) JA content in the WT and *opr3* mutant**



(B) SA content in the WT and *opr3* mutant

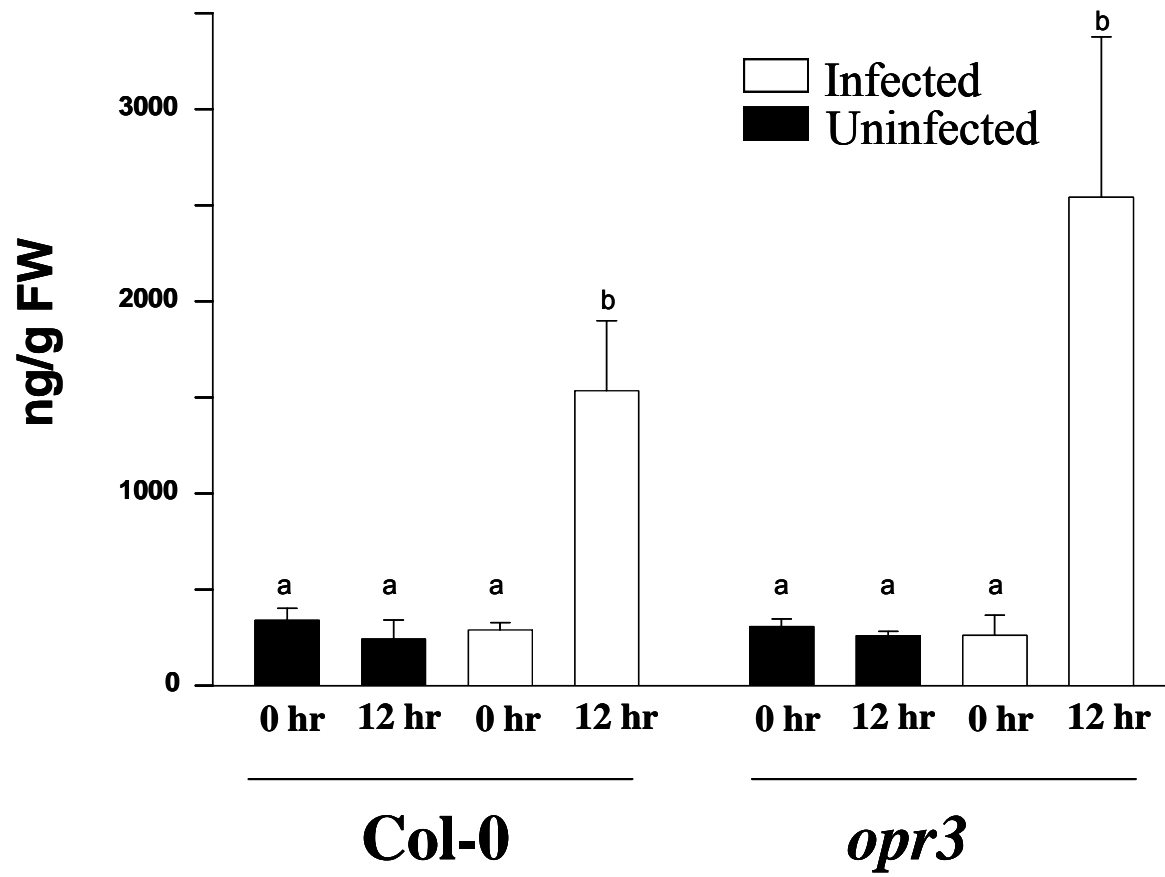
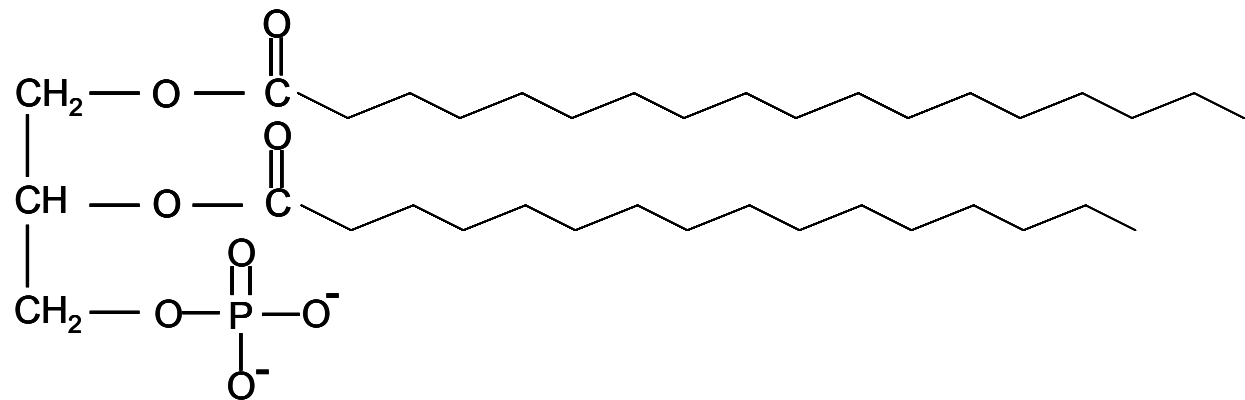
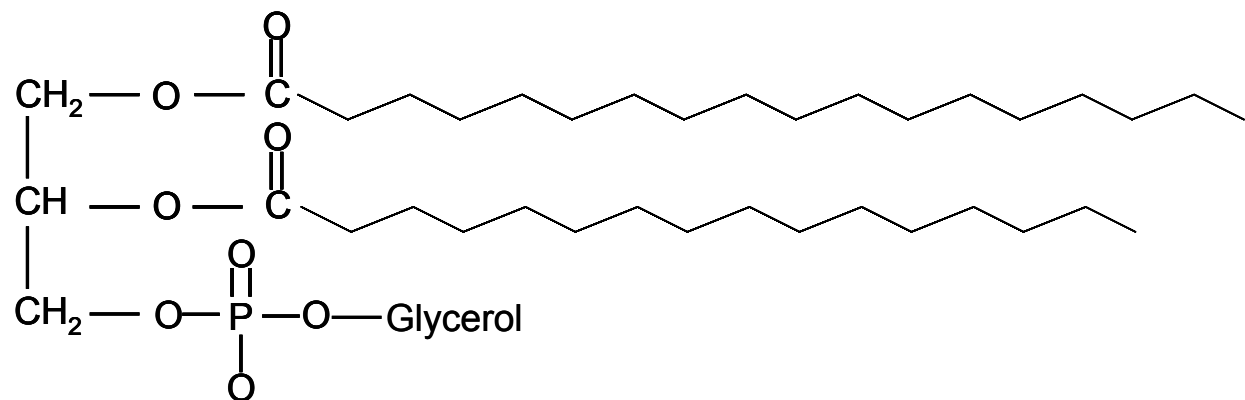


**Figure 3.13 Lipid diagrams**

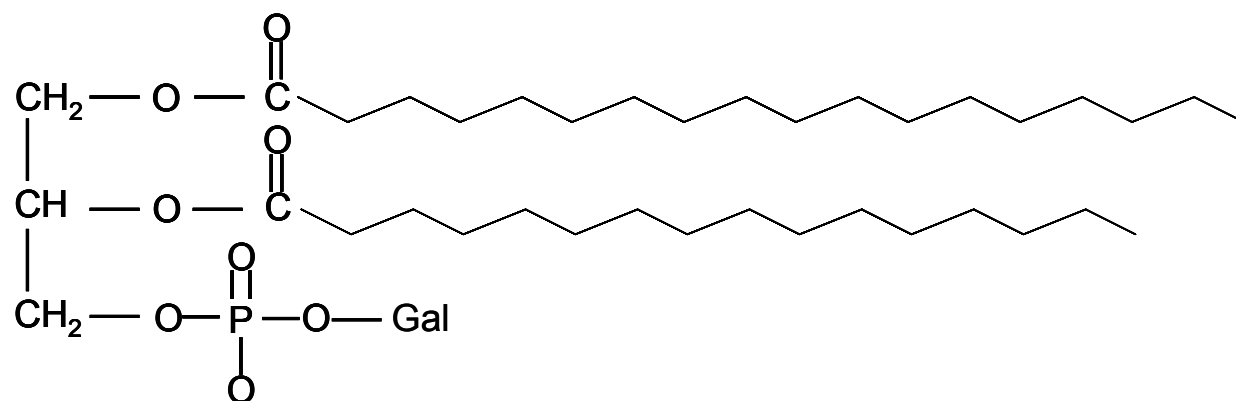
**(A) Phosphatidic Acid (PA)**



**(B) Phosphatidylglycerol (PG)**



**(C) Monogalactosyldiacylglycerol (MGDG)**



**(D) Digalactosyldiacylglycerol (DGDG)**

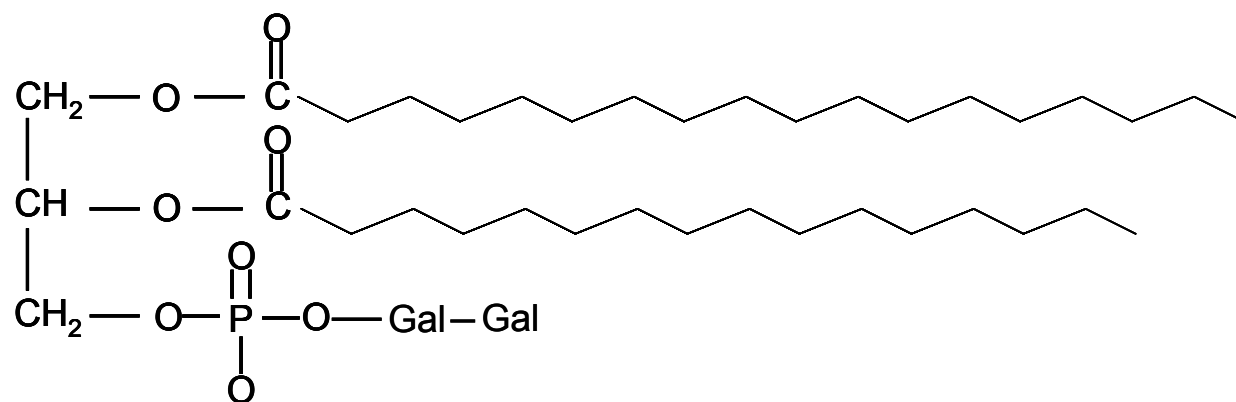
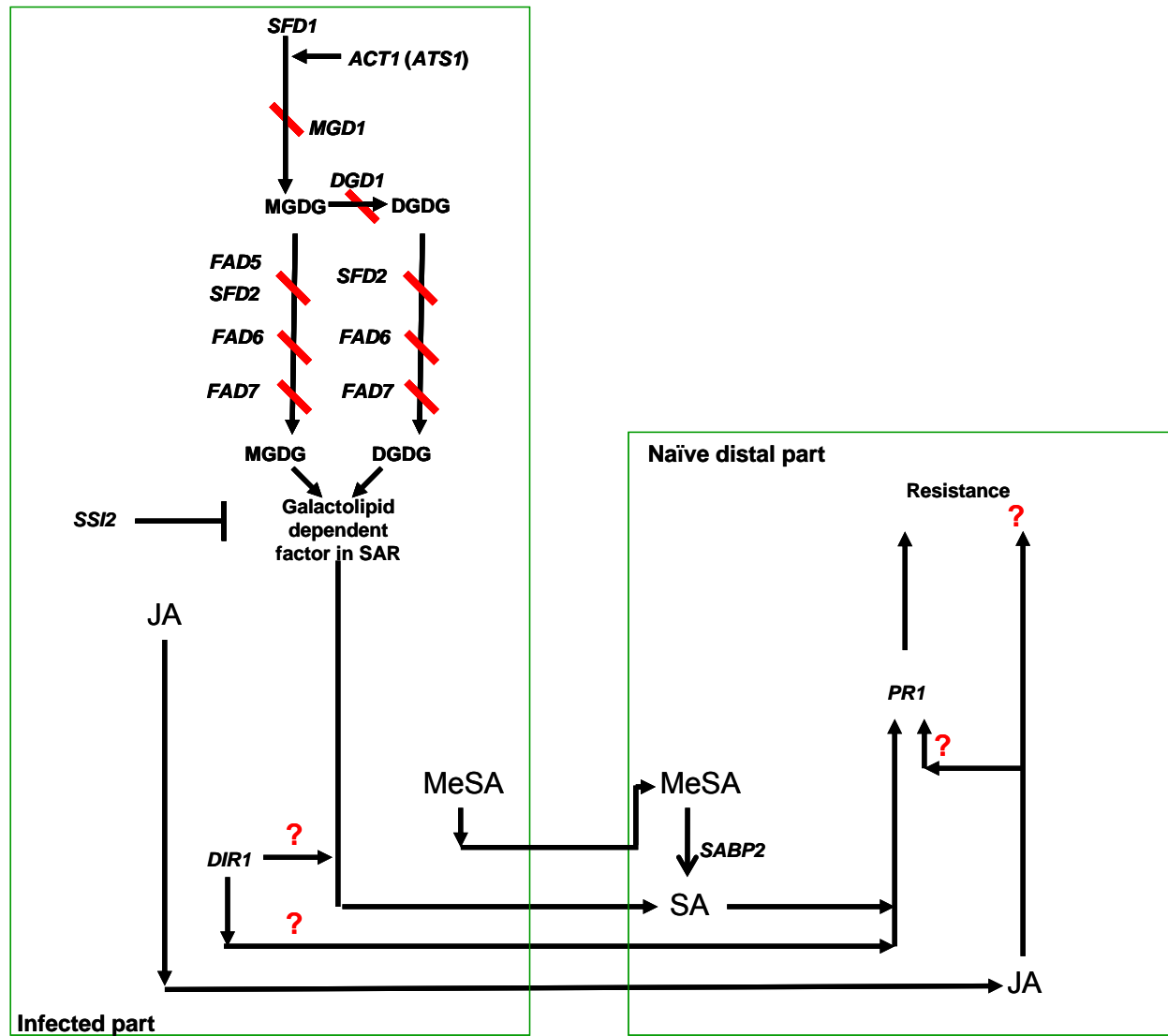




Figure 3.14 Schematic of SAR signaling pathway



## CHAPTER 4 - Genetic characterization and mapping of *sfd2*

### Introduction

#### *SFD2*

Three mutants in the single complementation group, *sfd2* (*suppressor of fatty acid desaturase 2*), were identified as suppressors of the *ssi2*-dependent dwarf phenotype in a screen of EMS mutagenized *ssi2 npr1* seeds (Nandi et al., 2003). In addition to *ssi2*-conferred dwarfing, the *ssi2*-dependent spontaneous lesion development, constitutive expression of *PR1*, and heightened resistance to *P. syringae* pv. *maculicola* ES4326 were also attenuated in the *sfd2-1*, *sfd2-2*, and *sfd2-3* allele containing plants (Nandi et al., 2003). However, the *sfd2-1* mutation was less effective than the *sfd1* mutant in attenuating *ssi2*-dependent high level accumulation of SA and in suppressing the *ssi2*-conferred NPR1-dependent expression of the *PR1* gene (Nandi et al., 2003). When crossed away from the *ssi2* allele, the *sfd2* single mutant plants were defective in the induction of SAR (Fig. 3.2). However, the *sfd2* mutations did not impact basal resistance to *P. syringae*. *SFD2* is required for the accumulation of a SAR-activating factor in the petiole exudates (enriched in phloem sap) of Arabidopsis (Chaturvedi et al., 2008).

The *sfd2* mutants exhibited a Mendelian pattern reflective of a semi-dominant mutation at a single locus (Nandi et al., 2003). Plants heterozygous for the *sfd2* locus in an *ssi2 npr1* (*sfd2/+ ssi2 npr1*) background were intermediate in size and for the level of constitutive *PR1* expression to the *ssi2 sfd2 npr1* triple mutant and the *ssi2 npr1* double mutant plants (Nandi et al., 2003). These *sfd2/+ ssi2 npr1* plants segregated in a near 1:2:1 ratio for large, intermediate and small plant phenotypes, confirming the semi-dominant nature of the *sfd2* mutant alleles (Nandi et al., 2003). Preliminary analysis indicated that the *sfd2* locus mapped to chromosome 3 (Nandi et al., 2003). Previously, it was shown that the presence of *sfd2* in the *sfd2 ssi2 npr1* and *sfd2 ssi2* mutants resulted in altered lipid composition, a phenotype that was also observed in plants containing the *sfd1* and *sfd6* mutant alleles (Nandi et al., 2003). Levels of hexadecatrienoic acid (16:3) were 82% lower in the *sfd2 ssi2 npr1* plants than the *ssi2 npr1* plant. There was an 80% reduction in the level of 34:6 MGDG (16:3+18:3) species and an increase in 36:6 MGDG

(18:3+18:3) levels (Nandi et al., 2003). The levels of 34:2, 34:3, 36:2, and 36:3 phosphatidylcholine (PC), phosphatidylethanolamine (PE) and phosphatidylinositol (PI) species in *sfd2-1 ssi2 npr1* were comparable to *ssi2 npr1* (Nandi et al., 2003).

### **FAD5**

Like *sfd1* and *sfd2*, SAR is compromised in the *fad5* (*fatty acid desaturase 5*) mutant plant (Fig. 3.7). FAD5 is a plastidial palmitoyl-monogalactosyldiacylglycerol  $\Delta^7$ -desaturase that is involved in the conversion of 16:0 in MGDG to 16:1 (Heilman et al., 2004). *fad5* mutant contained reduced content of MGDG compared to the WT. FAD5 is located on Chromosome 3. Unlike the *fad4* mutant, the *fad5* mutant is not affected in PG content, suggesting that FAD4 and FAD5 encoded 16:0 desaturases have different substrate specificity.

Although the *fad5* and *sfd2* mutants have similar SAR and lipid phenotypes, the genetic and biochemical relationship between *SFD2* and *FAD5* is not known. In this chapter, I have carried out detailed characterization of lipid composition of the *sfd2-2* and the *fad5-1* alleles. Both *fad5-1* and *sfd2-2* have qualitatively similar lipid profiles. Compared to the wild type, both mutants show a marked reduction in levels of 34:6 MGDG. The reduction in 34:6 MGDG content is more severe in *fad5* than the *sfd2* mutant. Despite the similarities in the phenotypes of the *fad5-1* and *sfd2-2* mutants, genetic and complementation experiments indicate that *sfd2-2* and *fad5-1* contain mutations in distinct genes. In an attempt to clone *SFD2*, the *sfd2* mutation was fine-mapped to a 85 kB region on chromosome 3, which contains 22 genes. Two BACs that span this region partially complemented the *sfd2-2*-dependent lipid defect, suggesting that *SFD2* is contained on these BACs.

## Materials and Methods

### Cultivation of plants

Arabidopsis plants were cultivated at 22°C in a tissue-culture chamber programmed for a 14 h light (100  $\mu$ E/m/s) and 10 h dark cycle. Seeds were germinated either in soil or on Murashige-Skoog (MS) (Sigma, St. Louis) agar supplemented with 1% sucrose. Ten days post germination; seedlings were transplanted to soil-filled pots and cultivated as described above.

### Complementation and Plant Transformation

For complementing WT plants with DNA cloned from the *sfd2-2* mutant plant, 5350 bp to 8645 bp sized PCR fragments, corresponding to different genes amplified using the *sfd2-2* genomic DNA as template, were generated with LA taq (Takara) with gene-specific primers that also contained palindrome sequences that are targets of specific restriction enzymes. The PCR products generated with these primers lead to the formation of the fragments with specific restriction enzyme target tags at the ends that simplify ligation into corresponding restriction sites in the pBI121 vector (Clontech, San Francisco, CA). Cloning into pBI121 was done with the In-fusion PCR cloning kit (Clontech, San Francisco, CA).

Construct 1: size 7259 bp: Primers used

C61640-1-F- 5'-ctctagaggatccccccatataaggcccagatca-3'  
and C61660-1-R-5'-agggactgaccaccccatctgcgcataactcaaca-3'

Construct 2: size 5350 bp: Primers used

C61670-1-F-5'-ctctagaggatccccgtctgtaacggcccatctct-3'  
and C61670-1-R-5'-agggactgaccaccccttcgactaccagacagc-3'

Construct 3: size 5835 bp: Primers used

Com61680-3-F-5'-ctctagaggatcccctagaagcggcctggttatga-3'  
and Com61680-3-R-5'- agggactgaccacccacctaggaggaggaaacga-3'

Construct 4: size 7643 bp: Primers used

Com61690-4-F-5'- ctctagaggatccccccactaattaaaccaggcgta-3'  
and Com61690-4-R-5'- agggactgaccaccaaccattgcttcaggaccac-3'

Construct 5: size 7963 bp: Primers used

Com61700-5-F-5'-ctctagaggatccccaggggaaaaagcaagcaagt-3'  
and Com61715-5-R-5'- agggactgaccaccccacgtgcattgtgaagtttg-3'

Construct 6: size 8110 bp: Primers used

Com61720-6-F-5'- ctctagaggatcccccaatgcacgtgaacttcgat-3'  
and Com61730-6-R-5'- agggactgaccaccccacactcactgggaccctct -3'

Construct 7: size 7345 bp: Primers used

Com61740-7-F-5'- ctctagaggatccccCCAATTTTCTCTTCCGTCCA-3'  
and Com61740-7-R-5'- agggactgaccacccaagtggaaatcggtcttgg-3'

Construct 8: size 8310 bp: Primers used

Com61750-8-2F-5'- ctctagaggatccccATGTCGTCAAGGTCCGTTTC-3'  
and Com61760-8-2R-5'- agggactgaccaccTCGAATGATTGGACGCAATA-3'

Construct 9: size 7580 bp: Primers used

Com61770-9-F-5'- ctctagaggatccccTCACAAGCGCAATCAAATC-3'  
and Com61780-9-R-5'- agggactgaccaccccagcttttggaaacttgga-3'

Construct 10: size 7740 bp: Primers used

Com61790-10-F-5'- ctctagaggatccccccaaaagctgggtttaaca-3'  
and Com61810-10-R-5'- agggactgaccaccgcgtatttagtggcgcatgt-3'

Construct 11: size 8645 bp: Primers used

Com61820-11-3F-5'- ctctagaggatcccctaataccacgggcttacttg-3'  
and Com61820-11-3R-5'- agggactgaccaccccacatcgtcttgtgtcttg-3'

Construct 12: size 8065 bp: Primers used

Com61830-12-F-5'-ctctagaggatccccgagaatatccgcagcagctc-3'

and Com61840-12-R-5'-agggactgaccacccccacatttcgtgtcgttttg-3'

The recombinant constructs cloned within the T-DNA borders of pBI121 were transformed into the *Agrobacterium tumefaciens* strain GV3101 by electroporation. Transformants were selected on LB (Luria-Bertani) agar media containing kanamycin (50 mg/L), gentamycin (25 mg/L) and rifampicin (10 mg/L). Presence of the recombinant insert in the transformants was confirmed by sequencing ends of the inserts. The recombinant plasmid containing GV3101 transformants were subsequently utilized to transform the WT ecotype Nössen plant by the floral dip method (Clough and Bent, 1998). The T1 seeds from the transformed plants were harvested and screened for kanamycin-resistant transformants on MS agar plates (Gibco BRL, Bethesda, MD) supplemented with kanamycin (50 mg/L).

For complementing the *sfd2-2* mutant plants with WT DNA, two bacterial artificial chromosome (BAC) clones, JAtY69J17 and JAtY52G17 (John Innes Center, Norwich, UK) were first transformed into *Agrobacterium tumefaciens* GV3101 by electroporation, as described above. GV3101 containing the above BAC clones were used to transform *sfd2-2* plants by the floral dip method (Clough and Bent, 1998). T1 seeds were harvested and screened on MS agar plates supplemented with the herbicide BASTA (50 µg/ml) for transgenic plants resistant to BASTA (Bayer CropScience). The BAC clones contain a selection marker that confers resistance to BASTA. BAC clones JAtY69J17 and JAtY52G17 together contain DNA spanning the 85 kb region from chromosome 3 to which *sfd2* was mapped. The plant DNA insert in JAtY69J17 is 70,082 bp spanning Arabidopsis chromosome 3 nucleotides 22,815,897 bp to 22,885,979 bp. The genes represented in JAtY69J17 span the interval between At3g61630 and At3g61790. BAC clone JAtY52G17 is 85,851 bp in size, spanning Arabidopsis chromosome 3 nucleotides 22,881,598 bp to 22,967,449 bp. The genes represented in JAtY52G17 span the interval between At3g61790 and At3g61980.

To determine if FAD5 complements the *sfd2-2* mutant phenotype, a full-length *FAD5* cDNA (obtained from ABRC) was cloned into the pBI121 vector such that FAD5 expression is driven from the *Cauliflower mosaic virus* 35S promoter. The primers FAD5-F- *Sma*I-*Xba*I: 5'-CCCGGGTCTAGAATGGCTTCTC TTCTAAC-3' and FAD5-R- *Sac*I-*Sma*I: 5'-CCCGGGGAGCTCACTTTAGGCATAACCATGTAGTT-3' were used to amplify the *FAD5* cDNA such that the *Sma*I and *Xba*I restriction sites are incorporated at the 5' end and the *Sac*I and *Sma*I restriction sites are incorporated at the 3' end. The resultant PCR product was digested with *Xba*I and *Sma*I and ligated into *Xba*I and *Sma*I digested vector pBI121 (Clontech, San Francisco, CA). The pBI121-*FAD5* construct was electroporated into the *Agrobacterium tumefaciens* strain GV3101. Drug (kanamycin + gentamycin + rifampicin) resistant colonies were identified on LB agar plates containing kanamycin (50 mg/L), gentamycin (25 mg/L) and rifampicin (10 mg/L). Ends of the inserts were sequenced to confirm presence of recombinant plasmids in the transformants. GV3101 transformants containing these inserts were used to transform *sfd2-2* mutant plants by the floral dip method (Clough and Bent, 1998). The kanamycin-resistant positive transformants were selected on MS agar plates (Gibco BRL, Bethesda, MD) supplemented with kanamycin (50 mg/L).

### **Arabidopsis mutants**

*sfd2 ssi2* and *sfd2 SSI2* were in the 1/8E/5 background which is in the accession Nössen (Nö) and contains a *PR1:tms2* transgene (Shah et al., 1997). The *fad5-1* mutant was in the accession Columbia (Col). *sfd2 SSI2* plants were crossed with Nössen WT plants to segregate the *sfd2-2* allele from the *PR1:tms2* insertion that contains the neomycin phosphotransferase gene, which confers resistance to kanamycin. F2 plants which were susceptible to kanamycin were identified from their seed growth on kanamycin plates and the *sfd2-2* phenotype was followed by lipid analysis. To determine if *fad5* and *sfd2* are allelic, *fad5-1* plants were crossed to *sfd2-2* to generate F1 plants that have one copy of each mutant allele (*fad5-1* and *sfd2-2*). In parallel, the *sfd2-2* mutant plant was crossed to WT Columbia plants to obtain F1 plants that had been heterozygous for the *sfd2-2* allele.

## Fine mapping

The following markers were developed between the ecotypes Columbia (Col) and Nössen (Nö) to follow the mutant phenotype.

	Position on chr 3 in MB	Type	cuts	sequence	enzyme
NGA6-F	23.042167	SSLP		atggagaagcttacactgatc	
NGA6-R				tggatttcttcctctctctac	
F21F14-936 F	22.969623	CAPS	Nö	cataaaggcgaggagtgaga	<i>Tsp451</i>
F21F14-936 R				gagttttgattaagcttttgtgat	
Decap61920 F	22.944333	dCAPS	Nö	cgtaaagaaaaatgaaaatagc	<i>Alu1</i>
61920capmark- R				tgtaggacatggatccacaca	
FAM 61830-40 F	22.902503	6 FAM fluorescent dye	Nö	6cgggcatcatatgaaagtca	
M61830-40 R				gatggtcctatggatgttcgtt	
dcap61700-5u- 1 F	22.846102	dCAPS	Nö	tgcaaatattgtctttacatatttactc	<i>Xba1</i>
M61700-5u R				cctgaagcctttgaagaacg	
F15G16-8864 F	22.817444	CAPS	Col	ggggaaattttgtgtggtgatgatgacgtgg	<i>BsmA1</i>
F15G16-8864 R				actgcttcctaccgttgagacagtct	



Sld-3	22.799980	CAPS	Col: twice; Nö: once	tcacgattctggtcattacg	<i>Bsr1</i>
Sld-4				gcaacgtttcgtggttacg	
F2a19 468547 F	22.789285	CAPS	Nö	tccgagcacgagaaacca	
F2a19 468547 R				ctcagtgcagaaacaatacataa	<i>Nde1</i>
T27I15 F	22.617164	CAPS	Col	cgcaaccaagattcatcaac	<i>Hinf-1</i>
T27I15 R				tctccctcaaacaatggcag	
T8B10-F	22.394908	CAPS	Nö	ccacaataaaacccactggaac	<i>Bcl 1</i>
T8B10-R				aatagcaccaggactccac	
F24G16-F	22.146068	CAPS	Col: twice	ctcccaaactcatttctctacg	<i>Hae2</i>
F24G16-R				ctcattacagtatcaaaggcgg	
NGA 707-F	21.763494	SSLP		ctctctgcctctcgtcg	
NGA 707-R				tgaatgcgtccagtgagaag	

## **Lipid Extraction**

Two to three leaves of about 4 week-old plants are used per sample. The leaves are immersed into 3 ml of isopropanol with 0.01% butylated hydroxytoluene at 75°C. After 15 minutes; 1.5 ml of chloroform and 0.6 ml of water were added to the above. The tubes were shaken for about an hour, followed by removal of the extract, which is collected separately. The leaves were re-extracted with 4 ml chloroform/methanol (2:1) with 0.01% butylated hydroxytoluene four times with 30 min of agitation each time except the last round which were left overnight, until all of the leaves appeared white. The remaining leaves were heated overnight at 105°C and weighed to obtain the dry weight of the tissue used. The combined extracts were washed once with 1 ml of 1 M KCl by vortexing. The mix was then centrifuged and the upper phase was discarded. The wash was repeated with 2 ml of water and the upper phase was discarded. The remaining solvent was evaporated under nitrogen, and the lipid extract was dissolved in 1 ml of chloroform. Standards were added and the ESI-MS/MS mass spectrographic analysis was performed as mentioned previously (Wolti et al., 2002).

## **DNA extraction and PCR analysis**

Arabidopsis genomic DNA from leaf tissue was isolated as previously described (Konieczny and Ausubel, 1993). A medium sized leaf (approx 30 mg) was placed in a 1.5 ml microfuge tube and frozen in liquid nitrogen. A plastic pestle was used to grind the frozen sample. 200 µl of extraction buffer (200 mM Tris-HCl pH 7.5, 250 mM NaCl, and 25 mM EDTA pH 8.0, 0.5% SDS) was added to the still frozen ground sample. 100 µl of Tris-saturated phenol: chloroform (1:1) solution was then added and the contents mixed by vortexing. The sample was centrifuged at 13,000 rpm for 10 min. The supernatant was added to 150 µl of isopropanol in a fresh 1.5 ml microfuge tube, the contents mixed by vortexing and then centrifuged at 13,000 rpm for 10 min. The supernatant was discarded and the pellet, which contains the DNA, was washed with 70% ethanol. The washed DNA pellet was suspended in 200 µl of HPLC grade water.

A derived-cleaved amplified polymorphic sequence (dCAPS) marker was used to differentiate the *ssi2* and *SSI2* alleles. The primers, *ssi2*dCAPS-F 5'-TTGTTTTGGTGGGGGACATGATCACAGAAGGTGCA-3' and *ssi2*dCAPS-R 5'-TCGATCTGCCTCATGTCAACACG-3' were used in the PCR reaction. The following PCR

conditions were used: 95°C for 5 min followed by 35 cycles of 95°C for 45 sec, 65°C for 45 sec, 72°C for 45 sec, with final extension at 72°C for 5 min. The 200-bp PCR product derived from WT DNA contains one *Apa*L1 (New England Biolabs) site, which on restriction with *Apa*L1 yields two products of 175 and 25 bp. In contrast, the PCR product derived from the *ssi2* allele lacks the *Apa*L1 site.

### **RNA extraction and RT-PCR analysis**

Leaf tissue was ground under liquid nitrogen, and RNA was extracted using acid guanidinium thiocyanate-phenol-chloroform as previously described (Chomczynski and Sacchi, 1987). The isolated RNA was purified and used in the one step real time polymerase chain reactions (RT-PCR). 2 µg total RNA from each plant was mixed with master mix (Qiagen one step RT-PCR kit), and the final volume was made up to 25 µl. The PCR primers used to amplify for the *ACT8* gene (At1g49240) were ACT8-F 5'-ATGAAGATTAAGGTCGTGGCA-3' and ACT8-R 5'-CCGAGTTTGAAGAGGCTAC-3'. The PCR primers used to amplify for the *FAD5* gene (At3g15850) were FAD5-RT-F 5'- TCACCAAAGCTTGCTCCTT-3' and FAD5-RT-R 5'-CCATTCTCTCTCCCACCAA-3'. The following PCR conditions were used: 50°C for 30 min for reverse transcription to occur then 95°C for 15 min to allow for initial PCR activation followed by 25 cycles of 95°C for 30 sec, 65°C for 30 sec, 72°C for 60 sec, with final extension at 72°C for 10 min.

## Results

### *sfd2*'s lipid profile resembles *fad5*

Leaves of the *fad5-1* and *sfd2-2* mutant plants contained reduced levels of MGDG compared to the corresponding WT (Fig 4.1A, 4.1B). In particular, levels of 34:6 (18:3 + 16:3) MGDG (Fig 4.1C, D) were very low in the *fad5-1* and *sfd2-2* mutants compared to the WT. In contrast, 36:6 (18:3 + 18:3) MGDG content was higher in the mutants than the WT (Fig 4.1C, D). However, the extent of reduction in 34:6 MGDG content in *sfd2-2* plants was not as severe as in the *fad5* plants (Fig 4.1C, D). In contrast to the negligible content of 34:6 MGDG in the *fad5* mutant, the *sfd2-2* mutant contained only an 8-fold lower content of 34:6 MGDG than the WT plant.

### *FAD5* and *SFD2* are different genes

The above results suggested that *sfd2-2* could be a weak allele of *fad5*. A complementation test was conducted in which the *fad5* mutant was crossed with the *sfd2-2* mutant. The *fad5* mutant is recessive to the WT *FAD5*, while the *sfd2-2* allele is semi-dominant to the WT *SFD2*. The F<sub>1</sub> plants derived from this cross will have one copy of each, the *fad5* and *sfd2-2* mutant alleles. As a control the *sfd2* mutant was also crossed with the WT plants to obtain plants that were heterozygous at the *SFD2* locus. If *fad5* and *sfd2* were allelic then it is expected that the two mutant alleles would not complement each other and thus the 34:6 MGDG content would be intermediate to that in the *sfd2-2* and *fad5* mutant plants. However, if *fad5* and *sfd2-2* were at separate loci, and therefore not allelic, then the levels of 34:6 MGDG would be similar to the heterozygous *sfd2-2* plant. Lipids were extracted from the F<sub>1</sub> progeny derived from the *sfd2-2* x *fad5* and *sfd2* x WT cross and 34:6 MGDG content in leaves determined. The 34:6 MGDG content in the F<sub>1</sub> plants derived from both crosses were similar (Fig 4.2), suggesting that *sfd2-2* and *fad5* are not allelic. As shown later, *FAD5* and *sfd2-2* map to different loci, thus confirming that the *sfd2-2* mutant does not contain a mutation in the *FAD5* gene.

An alternative explanation for the weak *fad5*-like lipid composition phenotype of the *sfd2-2* allele is that the *SFD2* protein modulates *FAD5* expression. To test this hypothesis, real time RT-PCR analysis was conducted on RNA extracted from the WT, *fad5* and *sfd2-2* plants. The Ct (cycle threshold) values were calculated. As expected, the Ct value for *FAD5* transcript was

higher in the *fad5* mutant compared to WT indicating that *FAD5* transcript abundance is low in the *fad5* mutant (Fig 4.3). In contrast, the Ct value for *FAD5* transcript abundance in the *sfd2-2* mutant was similar to that in the WT plant, indicating that *sfd2-2* mutation does not affect *FAD5* transcript abundance. If the *sfd2-2* defect was due to reduced accumulation of *FAD5* transcript then it is anticipated that constitutive overexpression of *FAD5* would complement the *sfd2-2* lipid defect. *FAD5* cDNA was used to create a 35S:*FAD5* chimera in which expression of the *FAD5* transcript is driven by the CaMV 35S promoter. The 35S:*FAD5* chimera was introduced into the *sfd2* plants by *Agrobacterium*-mediated transformation. Kanamycin resistant transformants that contain the transformed DNA were identified and 34:6 MGDG content compared to that of the *sfd2-2* mutant plant. As shown in Fig 4.4 the 34:6 MGDG content in the *FAD5* overexpressing *sfd2-2* mutant plants was comparable to that in the non-transgenic *sfd2-2* plant, indicating that constitutive overexpression of *FAD5* is not sufficient to overcome the *sfd2-2* defect. These results provide further support to our conclusion that the *sfd2-2* mutant phenotype is not due to reduced accumulation of the *FAD5* transcript. However, these results do not rule out the possibility that the *sfd2-2* mutant affects *FAD5* protein content and/or enzyme activity.

### **Mapping strategy and generation of the mapping population**

The mapping strategy adopted to fine map *sfd2* was adopted from a previous publication (Konieczny and Ausubel, 1993). It is based on the variation in the genetic sequence among the different accessions of Arabidopsis. Initially, a mapping population was generated by crossing the *sfd2-3 ssi2* double mutant plant with the *fab2* mutant plants. F<sub>2</sub> seeds collected from these F<sub>1</sub> plants were used for mapping *sfd2-3*. The *sfd2-3 ssi2* plant is in the accession Nössen (Nö), while *fab2*, which is allelic to *ssi2*, is in the accession Columbia (Col). This cross of *fab2* in Col background with *sfd2-3 ssi2* in Nö background allows the utilization of the sequence variation between Col and Nö to map the *sfd2-3* allele in a *fab2/ssi2* genetic background. The *sfd2-3* allele renders the *ssi2 (fab2) sfd2-3* plants a paler appearance compared to the *ssi2* and *fab2* single mutant plants. This pale green phenotype was utilized for initial mapping of *sfd2-3*. The DNA sequence polymorphism between accessions Col and Nö was exploited to develop PCR-based molecular markers that distinguish between the two accessions. A wide variety of such polymorphic markers were utilized for mapping *sfd2-3*. For example, the simple sequence length

polymorphisms (SSLP) (Bell and Ecker, 1994) polymorphic marker NGA6 utilizes the difference in the length of the amplified sequence between the two accessions. The cleaved amplified polymorphic sequence (CAPS) (Konieczny and Ausubel, 1993), SLD3 that relies upon the differences in restriction enzyme digestion patterns of PCR amplified fragments. In contrast, the derived cleaved amplified polymorphic sequence (dCAPS) (Michaels and Amasino, 1998) dcap61920 utilizes primer altered additions to generate restriction enzyme polymorphisms in the PCR products derived from the two accessions. This initial mapping analysis that utilized over 600 *sfd2-3/sfd2-3* segregants mapped *sfd2-3* to a 1.3 Mb region between the markers NGA6 and NGA707. However, the pale green phenotype due to *sfd2-3* allele was difficult to follow in the mapping population. Furthermore, the differences in the severity of the dwarf stature of *fab2* as compared to *ssi2* also contributed to variance in the morphological phenotypes amongst the F<sub>2</sub> segregants, making it difficult to conclusively identify the *sfd2-3/sfd2-3* homozygous segregants. To overcome these problems, we crossed the *sfd2-2* single mutant in the Nö accession with WT Col and followed the very distinct low 34:6 MGDG lipid phenotype of the *sfd2-2* single mutant. F<sub>2</sub> plants were used to fine map *sfd2* using molecular markers (Table 4.1). The *sfd2* mutation was mapped to an 85,059 bp region with 22 genes (At3g61640- At3g61830), between the markers 8864 (22.817444 Kb) and FAM (22.902503 Kb) on the third chromosome of *Arabidopsis*.

### **Genetic and complementation analysis**

If the *sfd2-2* allele was a dominant negative allele then the *sfd2-2* mutant allele when transformed into a WT plant is expected to yield a *sfd2-2*-like lipid composition phenotype. Twelve DNA fragments covering the approx 85 Kb region spanning the markers 8864 and FAM were generated by long-range PCR with *sfd2* DNA as the template. These 12 fragments were individually ligated in to the pBI121 vector using the In-fusion PCR cloning kit (Clontech). This vector contains the neomycin phosphotransferase gene that functions as a selection marker in plants by conferring resistance to kanamycin. The resulting construct were electroporated into the *Agrobacterium tumefaciens* strain GV3101. Kanamycin resistant *Agrobacterium* that contained the recombinant insert were used to transform WT (Nö) plants by the floral dip method (Clough and Bent, 1998). Kanamycin resistant transformants were selected on MS agar plates containing kanamycin. The kanamycin resistant transformants were screened for changes

in their lipid profile compared to the WT and *sfd2-2* mutant plant. Kanamycin resistant transformants obtained with all twelve constructs showed a WT lipid profile implying that none of these genes contain Arabidopsis DNA that could confer a dominant negative *sfd2*-like phenotype when introduced into WT plants (Fig 4.6 A, B).

In a parallel approach, WT genomic DNA spanning the 85 Kb region to which *sfd2-2* was mapped were transformed into the *sfd2-2* mutant plant to identify clones that complement the *sfd2-2* lipid defect. The two BAC clones JAtY69J17 and JAtY52G17 span this region. JAtY69J17 is 70,082 bp and spans the Arabidopsis chromosome 3 from nucleotides 22,815,897 to 22,885,979. This region contains 18 genes from At3g61630 to At3g61790. The second clone JAtY52G17 is 85,851 bp and spans the Arabidopsis chromosome 3 from nucleotides 22,881,598 to 22,967,449. This region contains 22 genes from At3g61790 to At3g61980. The clones were transformed into the *Agrobacterium tumefaciens* strain GV3101, which were then used to transform the *sfd2-2* plants by the floral dip method (Clough and Bent, 1998). As the JAtY clones have a phosphinothricin acetyl transferase gene that confers resistance to phosphinothricin, the active ingredient in herbicides like BASTA (Bayer), phosphinothricin resistant transformants were selected on plates containing BASTA. The positive transformants were analyzed for changes in their lipidome. Transformants obtained with both JAtY clones had a distinct alteration in 34:6 MGDG levels compared to the *sfd2-2* mutant (Fig 4.7). 34:6 MGDG levels, in all transformants were significantly higher than the *sfd2-2* mutant plants, but markedly lower than in WT Nö plants (Fig 4.7).

The two JAtY BAC clones had an overlap of 4,381 bp between them which contained the gene At3g61790, annotated as an E3 ubiquitin-protein ligase. These enzymes regulate a number of biological processes by the transfer of ubiquitin to the target protein. The At3g61790 gene was sequenced from all three *sfd2* alleles. However, no sequence alterations in comparison to the WT were detected in this gene in the *sfd2* mutant plants.





## Discussion

Although *SFD2* and *FAD5* are different genes, the *sfd2* mutants have a lipid pattern that qualitatively is similar to that of the *fad5* mutant. Since *FAD5* transcript level was not affected in the *sfd2* mutant plants, the *sfd2-2* lipid defect is unlikely to result from any changes in *FAD5* transcript accumulation. The inability of *35S:FAD5* chimera to complement the *sfd2-2* lipid defect supports this conclusion. However, we cannot rule out the possibility that *sfd2* mutants affect *FAD5* protein accumulation and/or enzyme activity.

The 85 Kb region that *sfd2* maps to has 22 genes, 6 genes that encode proteins of unknown function, 5 genes that have protein-protein interacting domains, three putative transcription factors, a lipase-like gene, a GTPase-like gene and a gene that codes for a protein with a lipid-binding motif, amongst others. Many of these genes may be involved in a wide variety of roles from transcriptional regulation to post translational modification and signal transduction. Both JAtY BAC clones containing WT DNA spanning the 85 kb region to which *sfd2* was mapped partially restored 34:6 MGDG levels in the *sfd2-2* mutant background. A 4381 bp region that is common to the two JAtY clones contains a gene At3g61790, which is predicted to encode a putative E3 ubiquitin ligase. These enzymes are involved in the ubiquitin mediated proteolysis of target proteins. There are about 1,300 genes that correspond to E3 ubiquitin ligases in the Arabidopsis genome that modulate a number of biological processes in plants like reproduction, light response, biotic and abiotic stress tolerance, hormonal control of vegetative growth and DNA repair (Mazzucotelli et al., 2006; Delauré et al., 2008).

A defect in the At3g61790 gene or encoded activity could impact the turnover of *FAD5* protein or another protein that regulates *FAD5* activity thus contributing to the *sfd2* mutant phenotype. However, in comparison to the WT plant, no sequence changes were detected in this gene in the *sfd2* mutant plants, suggesting that if At3g61790 is *SFD2* then the *sfd2* phenotype is most likely due to epigenetic changes that impact activity of At3g61790. There is evidence showing that methylation of upstream promoter regions of E3 ubiquitin ligase genes can result in phenotypic changes, for example, cancer in humans (Erson et al., 2004; Cheung et al., 2005; Chen et al., 2006). The methylation event in this area can be a result of a mutation that has taken place elsewhere on the genome (Bender, 2004). However, since RT-PCR was unable to detect

changes in expression of the At3g61790 transcript, it is unlikely that epigenetic changes impacting expression of this gene are responsible for the *sfd2-2* phenotypes. However, additional experiments are needed to determine if minor changes in expression level of this gene could contribute to the *sfd2* mutant phenotype.

The 4,381 bp region that is common to the two JAtY clones may contain additional non-annotated genes, or other non-gene sequences that could be responsible for the *sfd2* phenotypes. Indeed, very recently re-annotation of the Arabidopsis genome (<http://www.arabidopsis.org>) has annotated additional genes in this region. These include, At3g61721, which is annotated as a pseudogene of protein binding/zinc ion binding/RING-H2 finger protein, At3g61723, which encodes a putative protein with similarity to DNA binding motif containing protein encoded by the At3g61740 gene, and At3g61678, At3g61763 At3g61826, At3g61827 and At3g61829 all of which encode for unknown proteins. Since, only annotated genes in this region were sequenced from the *sfd2* mutants, alterations in any of these seven newly annotated genes, or the still non-annotated and non-gene regions would have been missed in my analysis. Sequencing of the non-gene and non-annotated regions of the *sfd2* mutants will allow us to address these possibilities.

In conclusion I show that although *sfd2* has a lipid phenotype similar to *fad5*, *sfd2* is not allelic nor does it affect the accumulation of *FAD5* transcript. *sfd2* maps to an 85 kb region on the third chromosome of Arabidopsis and the *sfd2-2* mutant phenotype is partially complemented by two overlapping BAC clones. However, the identity of the *SFD2* gene remains elusive.

## References

- Bell, C. J., and Ecker, J. R.** (1994). Assignment of 30 microsatellite loci to the linkage map of *Arabidopsis*. *Genomics* **19**, 137-144.
- Bender, J.** (2004). DNA methylation and epigenetics. *Annu. Rev. Plant Biol.* **55**, 41-68.
- Chaturvedi, R., Krothapalli, K., Makandar, R., Nandi, A., Sparks, A. A., Roth, M. R., Welti, R., and Shah, J.** (2008). Plastid omega-3-fatty acid desaturase-dependent accumulation of a systemic acquired resistance inducing activity in petiole exudates of *Arabidopsis thaliana* is independent of jasmonic acid. *Plant J.* **54**, 106-117.
- Chen, C., Seth, A. K., and Aplin, A. E.** (2006). Genetic and expression aberrations of E3 ubiquitin ligases in human breast cancer. *Mol. Cancer Res* **4**, 695-707
- Cheung, H., W., Ching, Y-P., Nicholls, J. M., Ling, M-T., Wong, Y. C., Hui, N., Cheung, A., Tsao, S. W., Wang, Q., Yeun, P. W., Lo, K. W., Jin, D-Y., and Wang, X.** (2005). Epigenetic inactivation of CHFR in nasopharyngeal carcinoma through promoter methylation. *Molecular Carcinogenesis* **43**, 237-245.
- Chomczynski, P., Sacchi, N.** (1987). Single-step method of RNA isolation by acid guanidinium thiocyanate-phenol-chloroform extraction. *Anal. Biochem.* **162**, 156-159.
- Clough, S. J., and Bent, A. F.** (1998). Floral dip: A simplified method for *Agrobacterium*-mediated transformation of *Arabidopsis thaliana*. *Plant J.* **16**, 735-743.
- Delaure, S. L., Van Hemelrijck, W., De Bolle, M. F. C., Cammue, B. P. A., and De Coninck, B. M. A.** (2008). Building up plant defenses by breaking down proteins. *Plant Sci.* **174**, 375-385.
- Erson, A. E., and Petty, E. M.** (2004). CHFR-associated early G2/M checkpoint defects in breast cancer cells. *Mol. Carcinog.* **39**, 26-33.

**Heilmann, I., Mekhedov, S., King, B., Browse, J., and Shanklin, J.** (2004). Identification of the Arabidopsis palmitoyl-monogalactosyldiacylglycerol 7-desaturase gene *FAD5-1*, and effects of plastidial retargeting of Arabidopsis desaturases on the *fad5-1* mutant phenotype. Plant Physiol. **136**, 4237-4245.

**Konieczny, A., and Ausubel, F. M.** (1993). A procedure for mapping Arabidopsis mutations using co-dominant ecotype-specific PCR based markers. Plant J. **4**, 403-410.

**Mazzucotelli, E., Belloni, S., Marone, D., De Leonardis, A. M., Guerra, D., Di Fonzo, N., Cattivelli, L., and Mastrangelo, A. M.** (2006). The E3 ubiquitin ligase family in plants: regulation by degradation. Curr. Genomics **7**, 509-522.

**Michaels, S. D., and Amasino, R. M.** (1998). A robust method for detecting single-nucleotide changes as polymorphic markers by PCR. Plant J. **14**, 381-385.

**Nandi, A., Krothapalli, K., Buseman, C. M., Li, M., Welti, R., Enyedi, A., and Shah, J.** (2003). Arabidopsis *sfd* mutants affect plastidic lipid composition and suppress dwarfing, cell death, and the enhanced disease resistance phenotypes resulting from the deficiency of a fatty acid desaturase. Plant Cell **15**, 2383-2398.

**Shah, J., Tsui, F and Klessig, D. F.** (1997). Characterization of a salicylic acid-insensitive mutant (*sai1*) of *Arabidopsis thaliana*, identified in a selective screen utilizing the SA-inducible expression of the *tms2* gene. Mol. Plant-Microbe Interact. **10**, 69-78.

**Welti, R., Li, W., Li, M., Sang, Y., Biesiada, H., Zhou, H-E., Rajashekar, C. B., Williams, T. D., and Wang, X.** (2002). Profiling membrane lipids in plant stress response. Role of phospholipase D alpha in freezing-induced lipid changes in Arabidopsis. J. Biol. Chem **277**, 31994-32002.

## Figure legends

### Fig 4.1 DGDG, MGDG and PG profiles of *fad5* and *sfd2*

(A) **DGDG, MGDG and PG content of *fad5*.** The graph shows the nmol per mg dry weight of the plastidic glycerolipids monogalactosyldiacylglycerol (MGDG), digalactosyldiacylglycerol (DGDG) and phosphatidylglycerol (PG) in the WT and *fad5* plants.

(B) **DGDG, MGDG and PG content of *sfd2*.** The graph shows the nmol per mg dry weight of the plastidic glycerolipids monogalactosyldiacylglycerol (MGDG), digalactosyldiacylglycerol (DGDG) and phosphatidylglycerol (PG) in the WT and *sfd2* plants.

(C) **MGDG species profile of *fad5*** shows the nmol per mg dry weight of MGDG species containing 34:6, 34:3 and 36:6 acyl chain composition in the WT and *fad5* plants.

(D) **MGDG species profile of *sfd2*** shows the nmol per mg dry weight of MGDG species containing 34:6, 34:3 and 36:6 acyl chain composition in the WT and *sfd2* plants.

The different letters above the bars indicate values that are significantly different ( $P < 0.05$ ) from each other as determined by student's *t*-test.

### Fig 4.2 34:6 MGDG content in leave of WT, *sfd2*, *fad5*, *sfd2/+* and *fad5/+ sfd2/+* plants

The graph shows the nmol per mg dry weight of the 34:6 monogalactosyldiacylglycerol (MGDG) in the WT, *sfd2*, *fad5*, *sfd2/+* and *fad5/+ sfd2/+* plants. The levels in the *fad5* mutant are extremely low. The lipid extraction was done by Dr. Ashis Nandi.

### Fig 4.3 Real time PCR data for *FAD5* expression in the *sfd2* and *fad5* mutant and the corresponding wild type plants

The real time PCR Ct (cycle threshold) values are plotted on a log scale as a ratio of *FAD5* and actin expression. The RNA from leaves of four week old *sfd2* and *fad5* mutants, and the corresponding wild type 1/8E/5 and Col-0 plants, respectively, was used. The Ct value has an inverse relation to the transcript availability.

#### **Fig 4.4 Lipid profiles of WT, *sfd2* and *FAD5-sfd2* plants**

The graph shows the mol % values of the chief monogalactosyldiacylglycerol (MGDG) species 34:6, 34:3 and 36:6 in the WT, *sfd2* and *FAD5-sfd2* plants. The similar letters above the bars indicate values that are no different from each other upon a student's *t*-test ( $P=0.05$ ).

#### **Fig 4.5 Chromosome 3 of Arabidopsis with *FAD5* and *sfd2* region**

Chromosome 3 of Arabidopsis showing position of *FAD5* (At3g15850) and the fine mapped region of *sfd2* in between the markers 8864 (22.817444 Mb) and FAM (22.902503 Mb).

#### **Fig 4.6 34:6 MGDG content of WT, *sfd2*WT and *sfd2* plants**

**(A) 34:6 MGDG levels in WT, *sfd2*-WT and *sfd2* plants.** The graph shows the mol % values of the 34:6 monogalactosyldiacylglycerol (MGDG) species in the WT, *sfd2*-WT and *sfd2* plants.

**(B) 36:6 MGDG levels in WT, *sfd2*-WT and *sfd2* plants.** The graph shows the mol % values of the 36:6 monogalactosyldiacylglycerol (MGDG) species the WT, *sfd2*-WT and *sfd2* plants.

Leaf samples were harvested from 2 week old plants grown on MS agar plates.

Black bars represent WT levels. Gray bars represent the levels in the WT plants that were transformed with fragments of DNA cloned from the *sfd2*-2 mutant (constructs 1 to 12). White bar represents the levels in the *sfd2* mutant.

#### **Fig 4.7 34:6 MGDG content of WT, WT-*sfd2* and *sfd2* plants**

The graph shows the mol% values of the 34:6 monogalactosyldiacylglycerol (MGDG) species in the WT, JAtY69J17 transformed *sfd2*-2, JAtY52G17 transformed *sfd2*-2, and the *sfd2*-2 mutant plants. The different letters above the bars indicate values that are significantly different ( $P<0.05$ ) from each other upon a student's *t*-test. Leaf samples were harvested from 2 week old plants grown on MS agar plates.

#### **Table 4.1 Recombination data of *sfd2*-2 X WT (Col) mapping population**

The table shows the critical recombination break points in the *sfd2*-2 X WT accession Col mapping population. Around 250 plants were analyzed using the very distinct low 34:6 MGDG lipid phenotype of the *sfd2*-2 single mutant. The *sfd2* gene maps to an 85,059 bp region with 22

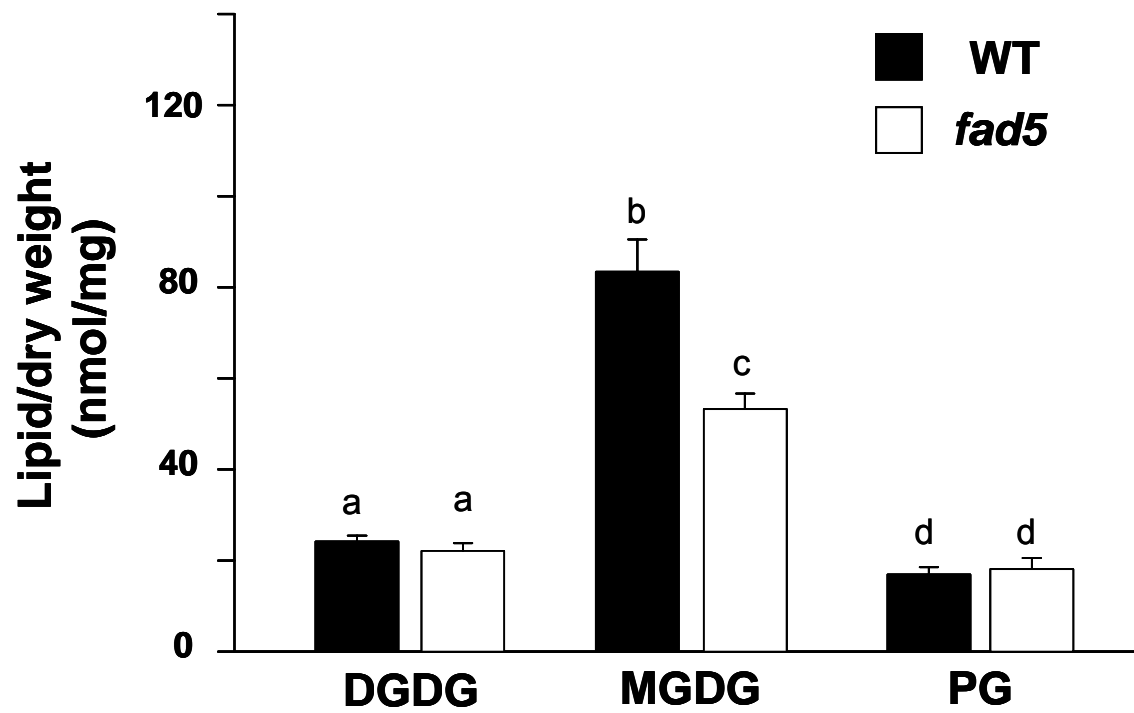
genes (At3g61640- At3g61830), between the markers 8864 (22.817444 Kb) and FAM (22.902503 Kb) on the third chromosome of Arabidopsis. The critical recombination break points in lines # 84 and 124, which place *sfd2* in the region between the markers 8864 and FAM are highlighted in yellow.

S: homozygous accession Nö pattern; H: heterozygous Col/Nö pattern.

## Figures

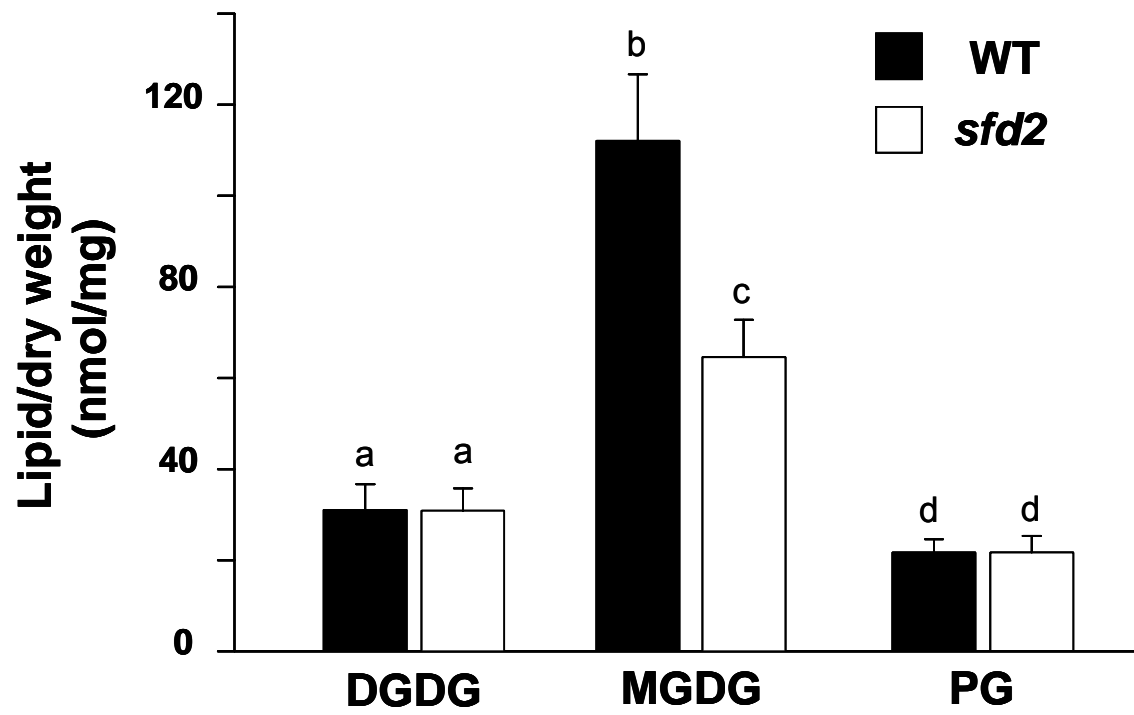
Figure 4.1 Lipid profiles of WT, *fad5* and *sfd2*

(A) DGDG, MGDG and PG content of *fad5*

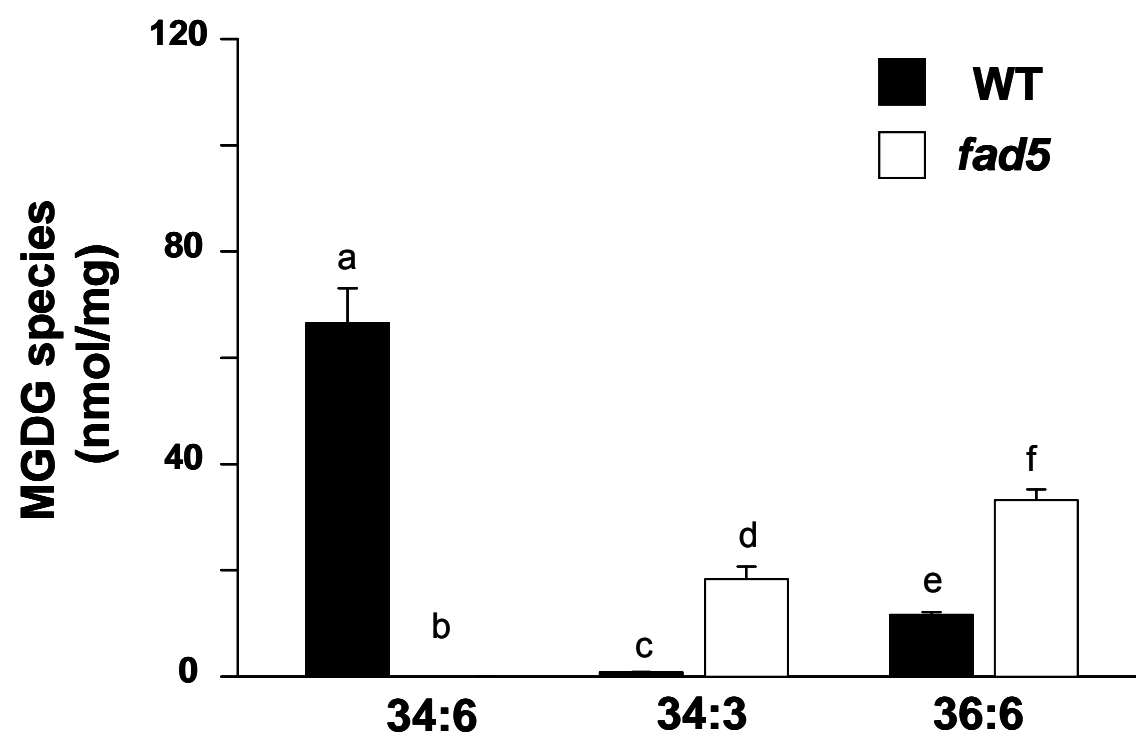




(B) DGDG, MGDG and PG content of *fad5*.



(C) MGDG species profile of *fad5*



D) MGDG species profile of *sfd2-2*

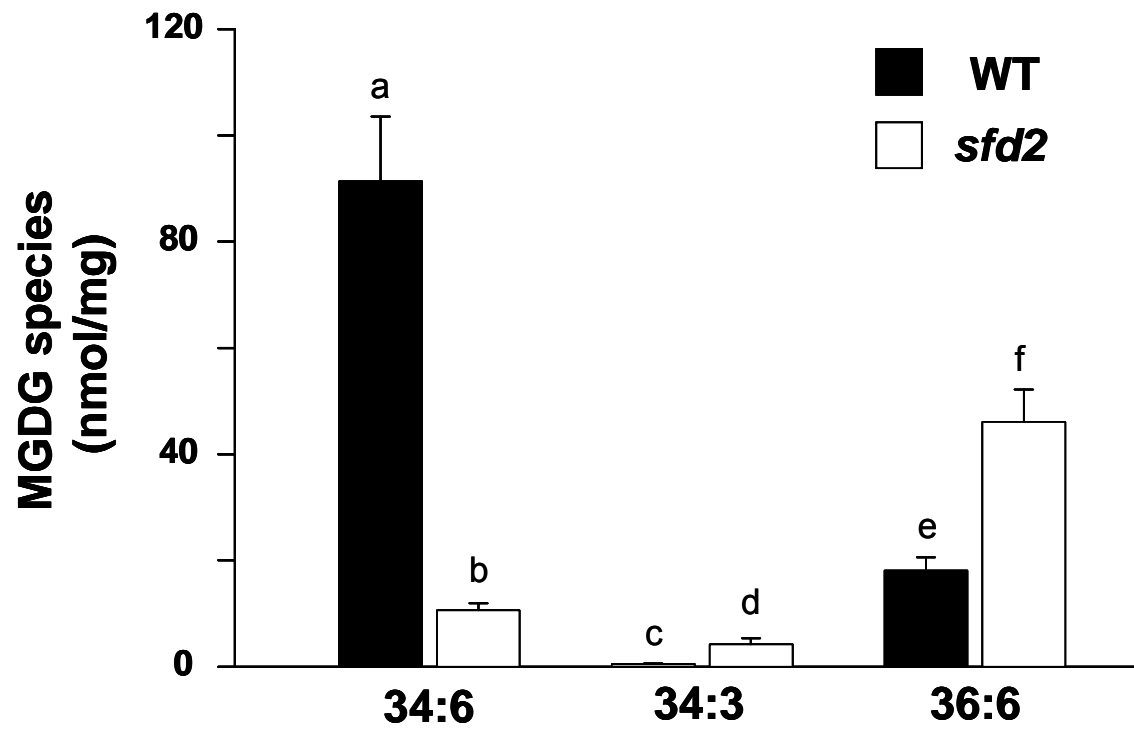


Figure 4.2 Lipid profiles of WT, *sfd2*, *fad5-1*, *sfd2/+* and *fad5/+ sfd2/+* plants

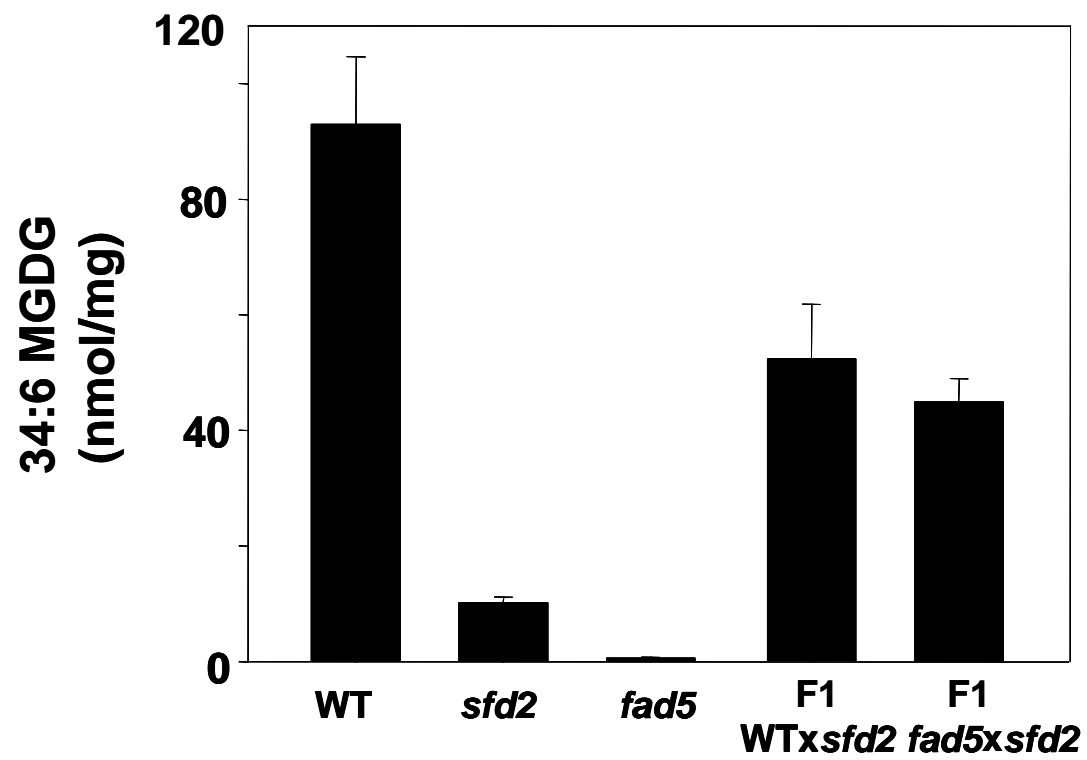


Figure 4.3 Real time PCR data for *FAD5* expression in the *sfd2* and *fad5* mutants and the corresponding WT plants

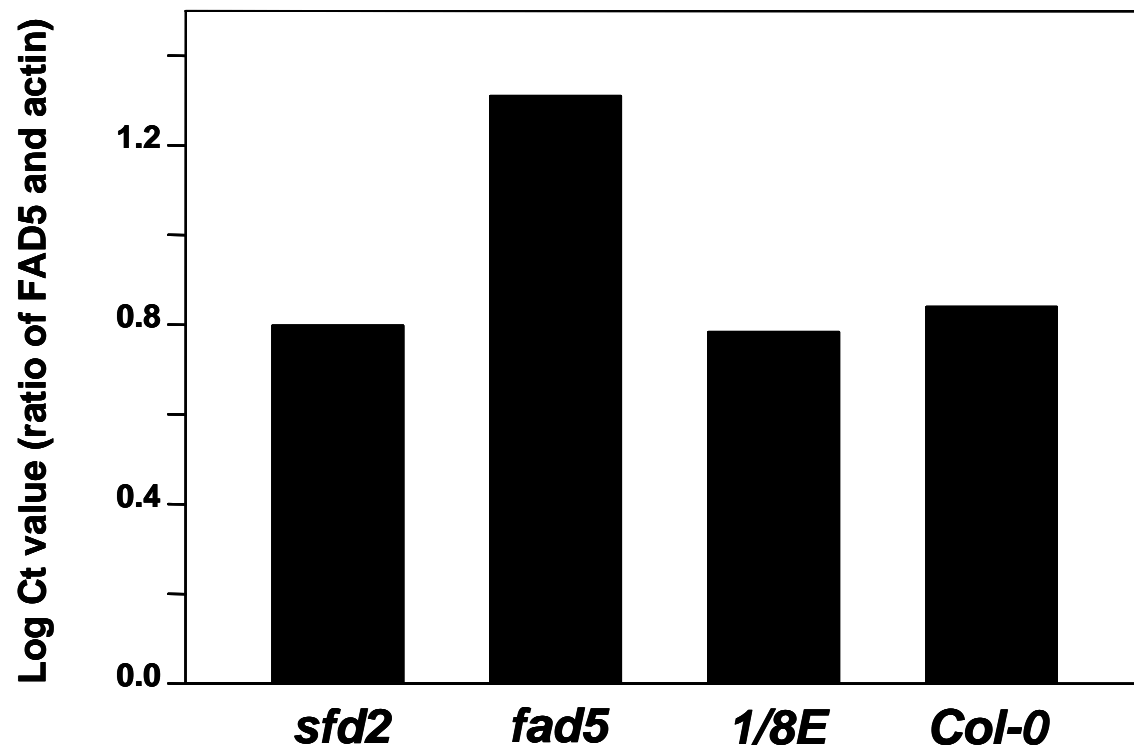


Figure 4.4 Lipid profiles of WT, *sfd2* and *FAD5-sfd2* plants

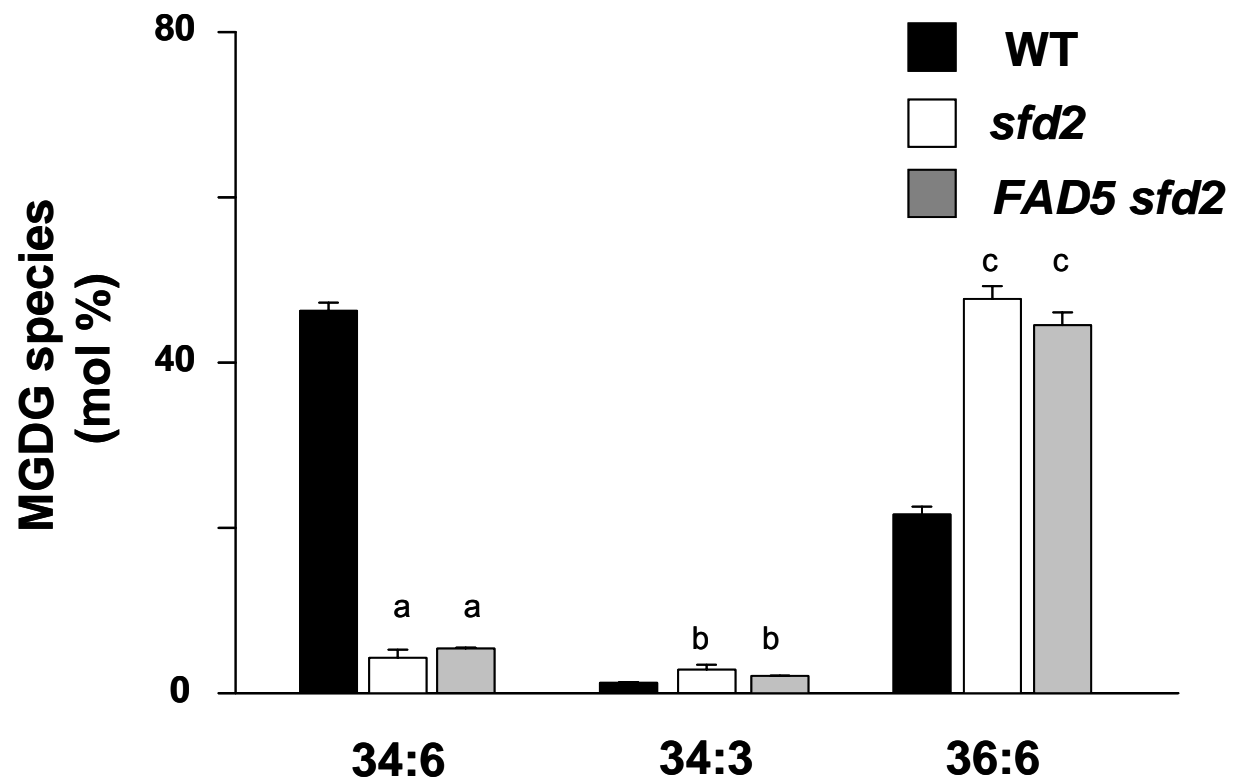


Figure 4.5 Chromosome 3 of Arabidopsis with *FAD5* and *sfd2* region

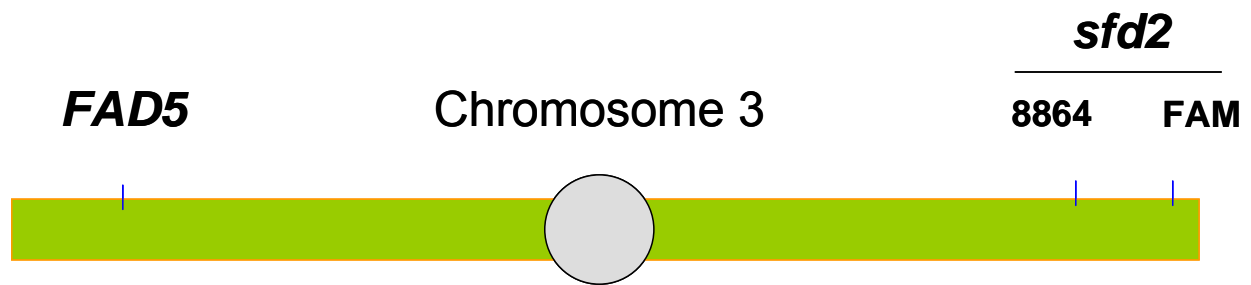
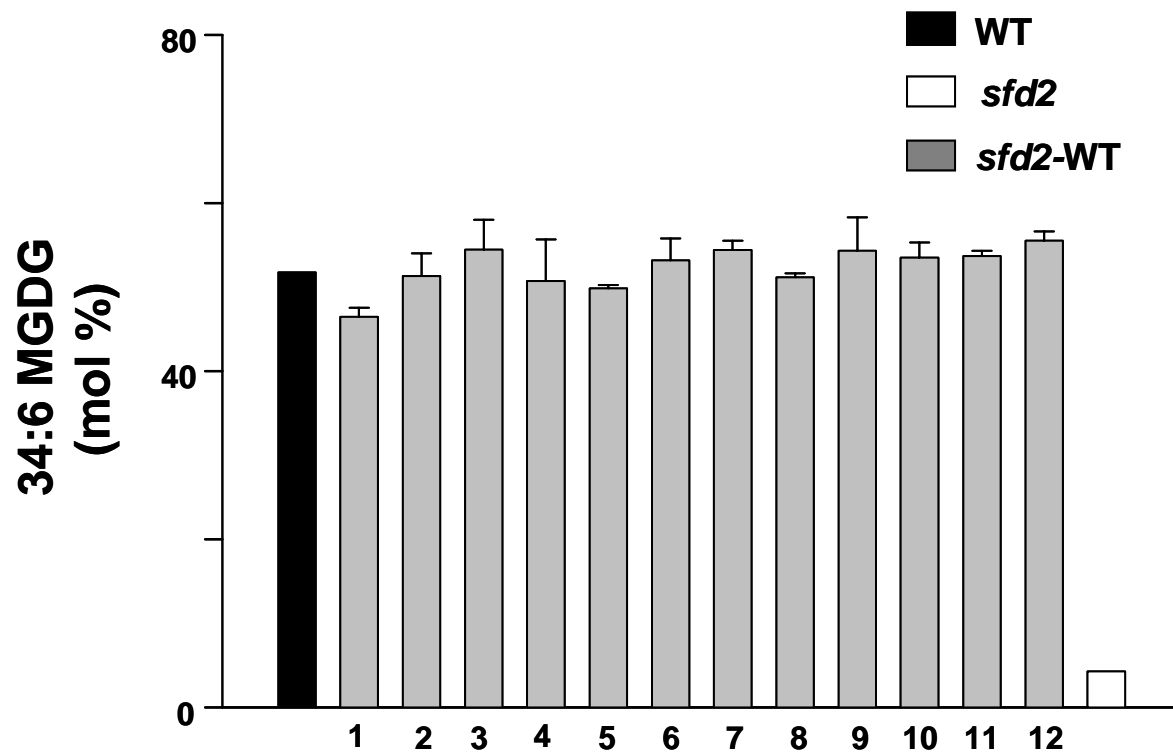


Figure 4.6 34:6 MGDG content of WT, *sfd2*-WT and *sfd2* plants

(A) 34:6 MGDG content in WT, *sfd2*-WT and *sfd2*





(B) 36:6 MGDG content in WT, *sfd2*-WT and *sfd2*

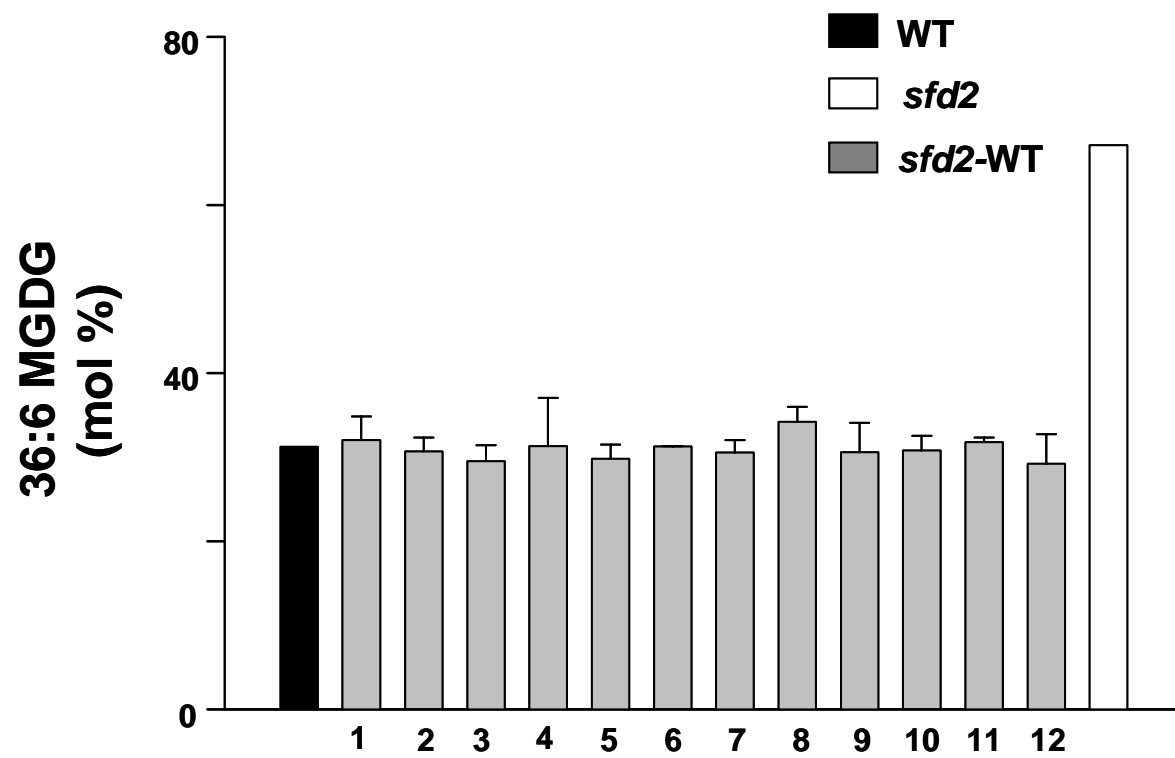
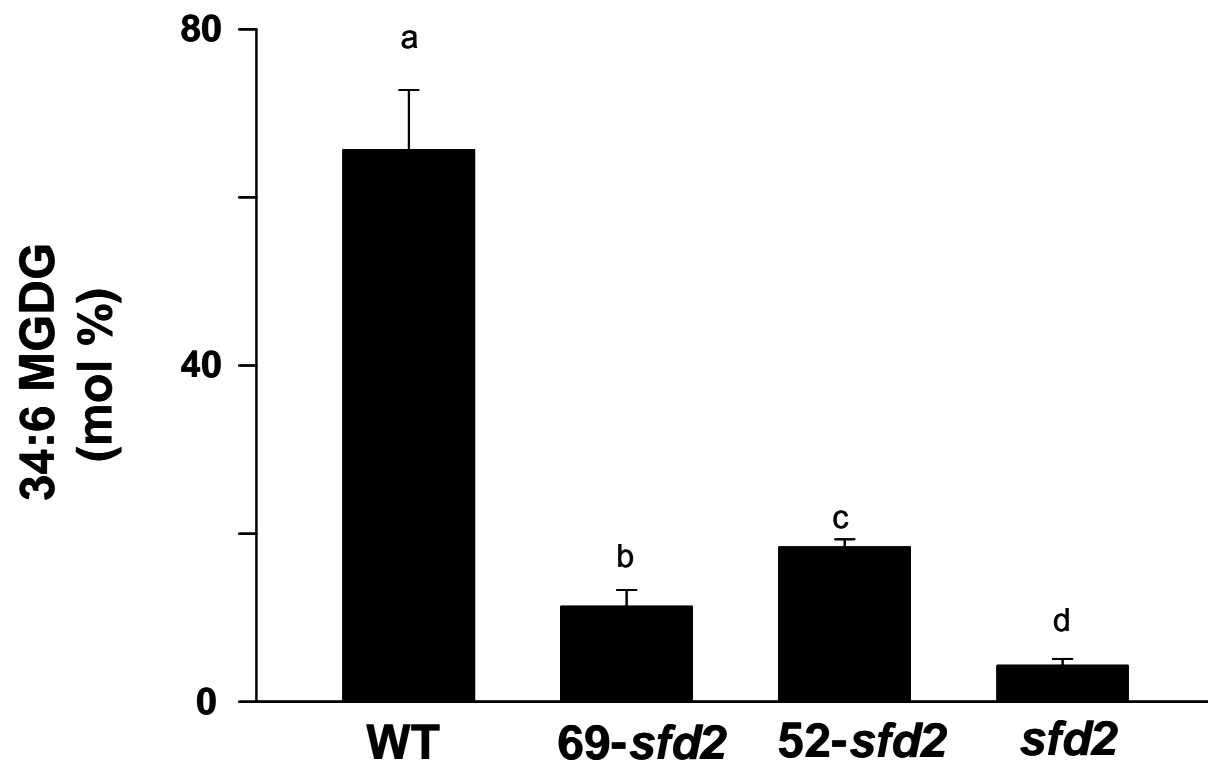


Figure 4.7 34:6 MGDG content of WT, WT-sfd2 and *sfd2* plants



**Table 4-1 Recombination data of *sfd2-2* X *Col-0* mapping population**

line#	F24G16 [22.1]	T8B10 [22.3]	T27115 [22.6]	547 [22.7]	SLD3 [22.7]	8864 [22.8]	61700 [22.8]	FAM [22.9]	61920 [22.9]	936 [22.9]	NGA6 [23.0]
47	S	S	S	S	S	S					S
49	S	S	S	S	S	S					S
50	H	H	H	S	S	S					S
75	S	S	S	S	S	S					S
78	S	S		S	S	S					S
82	S	S	S	S	S	S					S
83	S	S	S	S	S	S	S	S	H	H	H
84	H	H	H	H	H	H	S	S	S	S	S
88	S	S	S	S	S	S					S
90	H	H	H	H	H		S	S	S	S	S
91	H	H	S	S	S	S	S	S	S	S	S
98	S	S	S	S	S	S					S
106	S	S	S	S	S	S					S
114						S					S
122						S					S
124						S	S	H	H	H	H
127						S					S
133						S	S	S	H	H	H
139						S					S

## CHAPTER 5 - Other Observations and Future directions

In this study, it was observed that although *SFD1*, a plastidic dihydroxyacetone phosphate (DHAP) reductase, played a significant role in SAR (Nandi et al., 2004). Two other genes that encode proteins with homology to *SFD1* were not involved in SAR. DHAP reductases are involved in the conversion of DHAP to glycerol-3-phosphate (G3P). But there is another pathway for the creation of G3P in plants. It involves the conversion of glycerol to G3P by glycerol kinase. At1g80460 (*NHO1*) is the only *Arabidopsis* gene encoding glycerol kinase and it had been shown to be involved in non-host resistance mechanism in *Arabidopsis* (Kang et al., 2003). Although, *nho1* is susceptible to a number of non-host bacterial pathogens of *Arabidopsis* like *Pseudomonas syringae* pv. *phaseolicola* NPS3121, *P. s. tabaci* and *P. fluorescens*; it shows no effect on the growth of the virulent bacteria *P. s. maculicola* ES4326 and *P. s. tomato* DC3000 (Lu et al., 2001). Moreover, *nho1* appears to suppress some of *ssi2*-conferred phenotypes in an age-dependent manner (Kachroo et al., 2005). However, studies in our lab indicate that SAR is not affected in the *nho1* mutant (A. Nandi and J. Shah, unpublished), suggesting that G3P synthesized in the cytosol via the glycerol kinase route may not contribute to the development of SAR. Thus the involvement of *SFD1* in SAR is unique amongst the different G3P synthesizing enzymes that have been investigated to date.

In *Arabidopsis*, sulfolipids might be of conditional importance, the ratio of nonphosphorous glycerolipids to phospholipids drastically increases after phosphate deprivation (Essigmann et al., 1998). The relative amount of sulfolipids rises several fold because of an active process based on the increased expression of at least one of the sulfolipid genes, *SQD1* (Essigmann et al., 1998; Yu et al., 2002). One concern of our study is that we have not specifically characterized the role of the sulfolipid sulfoquinovosyldiacylglycerol (SQDG) in SAR. The biosynthesis of this lipid proceeds in two steps first, the assembly of UDP-sulfoquinovose from UDP-glucose and sulfite catalyzed by *SQD1*, a sulfolipid synthase, and second step, the transfer of the sulfoquinovose moiety from UDP-sulfoquinovose to diacylglycerol is catalyzed by the enzyme *SQD2*, a sulfoquinovosyl transferase. The *sqd2* plants show a complete lack of sulfolipids and

are morphologically similar to the wild type plants (Yu et al., 2002). As the lack of a SAR compromised phenotype in the phospholipid phosphatidylglycerol (PG) specific *fad4* mutant plants indicated that the plastidic phospholipids might not have a role in SAR, analysis of the SAR phenotype of sulfoquinovosyldiacylglycerol specific *sqd2* would permit addressing any contribution of sulfolipids to SAR.

As this study provides evidence for the role of glycerolipids, most likely galactolipids, or their derived products in SAR, It would be useful to examine the lipid phenotypes of SAR compromised mutants like *dir1* (*defective in induced resistance 1*), *eds1* (*enhanced disease susceptibility 1*) and *pad4* (*phytoalexin-deficient 4*), as all them seem to show homology to genes that may be involved in lipid metabolism. DIR1 shares some structural and lipid binding properties with the LTP2 family, but it displays some specific features that define DIR1 as a new type of LTP (Lascombe et al., 2008). The EDS1 protein shows homology to acyl-hydrolases (Falk et al., 1999), while *PAD4* encodes a lipase like gene (Jirage et al., 1999). DIR1 shows high affinity to two species of long-chain fatty acid derivatives like monoacylated phospholipids (Lascombe et al., 2008). The authors used model lipids lysophosphatidylcholines (LPC) with various fatty acid chain lengths to understand lipid protein interactions. They also state that the DIR1 protein displays higher affinities (nanomolar range) than LTP1s (micromolar range) for lysophospholipids with a chain length greater than 14 carbon atoms and was capable of binding up to two lipids. It would be an interesting to evaluate DIR1's affinity to galactolipids as it would shed light on the role of galactolipids in SAR.

SAR is compromised in suppressors of *ssi2* (Fig 3.2 B; 3.3 B; 3.4 B), but a number of suppressors of *ssi2* like *FAD7*, *EDS1*, *PAD4*, *EDS5* (*ENHANCED DISEASE SUSCEPTIBILITY 5*) and *SID2* (*SALICYLIC ACID INDUCTION-DEFICIENT 2*) were not identified from suppression screens. The *ssi2 fad7* double mutants were found to be intermediate in their dwarf phenotype compared to their parents (Fig 3.10 A). This intermediate morphological phenotype of the *fad7 ssi2* double mutant plants could be responsible for the non-identification of *fad7* in screens for suppressors of *ssi2* as the screens were biased towards the complete suppression of *ssi2* conferred dwarf phenotype. Similarly, mutations in *eds1*, *pad4*, *eds5* and *sid2* are known to partially suppress *ssi2* conferred dwarf phenotype (Nandi et al; Kachroo et al, 2005) but are

known to suppress the *ssi2*-conferred enhanced resistance and also SAR. Setting up a screen for suppressors of *ssi2* that does not eliminate partial suppressors the *ssi2* conferred phenotypes is likely to throw up a number of candidate genes that might be involved in the SAR mechanism. Such a screen should try to saturate the entire range of suppression phenotypes.

To determine if epigenetic changes associated with changes in methylation pattern are responsible for the *sfd2* mutant phenotypes, the *sfd2* mutants can be grown on plates containing 5-aza-2'-deoxycytidine, an inhibitor of methyltransferases. If hypermethylation was responsible for the *sfd2* phenotype, then it would result in restoration of wild type phenotype in the *sfd2* plants. Bisulfite sequencing of the overlap region could also be done to identify nucleotides in the 85 kb region that exhibit differences in methylation pattern between the WT and *sfd2* plants.

Recently re-annotation of the Arabidopsis genome (arabidopsis.org) has led to the addition of seven new genes into the 85 kb region to which *SFD2* was mapped. These genes are, At3g61721 annotated as a pseudogene of protein binding/zinc ion binding/RING-H2 finger protein, At3g61723 with similarity to DNA binding motif containing At3g61740 gene, and the At3g61678, At3g61763 At3g61826, At3g61827 and At3g61829 genes that encode for unknown proteins. As all these genes were not specifically sequenced from the *sfd2* mutant plants, there is a probability of any of them might be harboring the *sfd2* mutations. These genes should be sequenced from the *sfd2* mutant plants to determine if they contain alterations compared to the WT plant.

## References

- Essigmann, B., Güler, S., Narang, R. A., Linke, D., and Benning, C.** (1998). Phosphate availability affects the thylakoid lipid composition and the expression of *SQD1*, a gene required for sulfolipid biosynthesis in *Arabidopsis thaliana*. *Proc. Natl. Acad. Sci. USA* **95**, 1950-1955.
- Falk, A., Feys, B. J., Frost, L. N., Jones, J. D. G., Daniels, M. J., and Parker, J. E.** (1999). EDS1, an essential component of R gene-mediated disease resistance in *Arabidopsis* has homology to eukaryotic lipases. *Proc. Natl. Acad. Sci. USA* **96**, 3292-3297.
- Jirage, D., Tootle, T. L., Reuber, T. L., Frost, L. N., Feys, B. J., Parker, J. E., Ausubel, F. M., and Glazebrook, J.** (1999). *Arabidopsis thaliana* *PAD4* encodes a lipase-like gene that is important for salicylic acid signaling. *Proc. Natl. Acad. Sci. USA* **96**, 13583-13588.
- Kachroo, P., Venugopal, S. C., Navarre, D. A., Lapchyk, L., and Kachroo, A.** (2005). Role of salicylic acid and fatty acid desaturation pathways in *ssi2*-mediated signaling. *Plant Physiol.* **139**, 1717-1735.
- Kang, L., Li, J., Zhao, T., Xiao, F., Tang, X., Thilmony, R., He, S., and Zhou, J. M.** (2003). Interplay of the *Arabidopsis* nonhost resistance gene *NHO1* with bacterial virulence. *Proc. Natl. Acad. Sci. USA* **100**, 3519-3524.
- Lascombe, M-B., Bakan, B., Buhot, N., Didier, M., Blein, J-P., Larue, V., Lamb, C., and Prangé, T.** (2008). The structure of "defective in induced resistance" protein of *Arabidopsis thaliana*, DIR1, reveals a new type of lipid transfer protein. *Protein Sci.* **17**, 1522-1530.
- Lu, M., Tang, X., and Zhou, J. M.** (2001). *Arabidopsis* *NHO1* Is Required for General Resistance against *Pseudomonas* Bacteria. *Plant Cell* **13**, 437-447.
- Mazzucotelli, E., Belloni, S., Marone, D., De Leonardis, A. M., Guerra, D., Di Fonzo, N., Cattivelli, L., and Mastrangelo, A. M.** (2006). The E3 ubiquitin ligase family in plants: regulation by degradation. *Curr. Genomics* **7**, 509-522.

**Nandi, A., Moeder, W., Kachroo, P., Klessig, D. F., and Shah, J.** (2005). The *Arabidopsis* *ssi2*-conferred susceptibility to *Botrytis cinerea* is dependent on EDS5 and PAD4. *Mol. Plant-Microbe Interact.* **18**, 363-370.

**Nandi, A., Welti, R., and Shah, J.** (2004). The *Arabidopsis thaliana* dihydroxyacetone phosphate reductase gene *SUPPRESSOR OF FATTY ACID DESATURASE DEFICIENCY 1* is required for glycerolipid metabolism and for the activation of systemic acquired resistance. *Plant Cell* **16**, 465-477.

**Yu, B., Xu, C., and Benning, C.** (2002). *Arabidopsis* disrupted in *SQD2* encoding sulfolipid synthase is impaired in phosphate-limited growth. *Proc. Natl. Acad. Sci. USA* **99**, 5732-5737.



## Appendix A - Lipid profiles

Table 5-1 Lipid profiles of WT (Col), *fad5*, WT (1/8E/5) and *sfd2* in mol % of total lipids

Sample description	WT(Col)		<i>fad5</i>		WT (1/8E/5)		<i>sfd2-2</i>	
	ave	stdev	ave	stdev	ave	stdev	ave	stdev
DGDG 34:6	1.350	0.118	0.001	0.002	1.389	0.136	0.422	0.027
DGDG 34:5	0.069	0.026	0.000	0.000	0.149	0.047	0.258	0.063
DGDG 34:4	0.129	0.020	0.096	0.035	0.093	0.007	0.149	0.016
DGDG 34:3	2.589	0.213	10.582	0.879	2.704	0.383	4.794	0.575
DGDG 34:2	0.567	0.080	0.000	0.000	0.571	0.087	0.000	0.000
DGDG 34:1	0.243	0.018	0.065	0.051	0.137	0.024	0.064	0.012
DGDG 36:6	9.181	0.407	5.174	0.540	9.609	0.377	11.947	1.098
DGDG 36:5	0.000	0.000	0.000	0.000	0.000	0.000	0.000	0.000
DGDG 36:4	0.266	0.023	0.113	0.061	0.197	0.024	0.325	0.046
DGDG 36:3	0.107	0.023	0.372	0.050	0.136	0.025	0.447	0.202
DGDG 36:2	0.001	0.002	0.000	0.000	0.003	0.005	0.024	0.029
DGDG 36:1	0.000	0.000	0.000	0.000	0.000	0.001	0.014	0.009
DGDG 38:6	0.113	0.020	0.178	0.058	0.043	0.024	0.169	0.028
DGDG 38:5	0.000	0.000	0.002	0.005	0.004	0.009	0.001	0.003
DGDG 38:4	0.022	0.019	0.002	0.004	0.009	0.008	0.045	0.039
DGDG 38:3	0.001	0.002	0.000	0.000	0.001	0.002	0.009	0.011
<b>Total DGDG</b>	<b>14.636</b>	<b>0.648</b>	<b>16.585</b>	<b>1.401</b>	<b>15.046</b>	<b>0.933</b>	<b>18.669</b>	<b>0.948</b>
MGDG 34:6	40.382	3.584	0.032	0.030	44.629	1.679	6.495	0.866
MGDG 34:5	0.000	0.000	0.013	0.029	0.000	0.000	0.385	0.165
MGDG 34:4	1.327	0.184	0.210	0.054	0.263	0.067	0.346	0.087
MGDG 34:3	0.478	0.070	13.733	1.096	0.266	0.028	2.538	0.573
MGDG 34:2	0.356	0.076	0.000	0.000	0.042	0.015	0.007	0.015
MGDG 34:1	0.200	0.333	0.226	0.221	0.065	0.094	0.022	0.049
MGDG 36:6	7.026	0.217	25.028	2.419	8.825	0.347	27.967	1.673
MGDG 36:5	0.053	0.063	0.000	0.000	0.000	0.000	0.000	0.000
MGDG 36:4	0.711	0.108	0.343	0.049	0.479	0.101	0.833	0.148
MGDG 36:3	0.032	0.034	0.224	0.095	0.001	0.003	0.219	0.214
MGDG 36:2	0.011	0.012	0.003	0.007	0.000	0.000	0.050	0.038
MGDG 36:1	0.002	0.004	0.028	0.030	0.003	0.004	0.002	0.005
MGDG 38:6	0.000	0.000	0.010	0.016	0.013	0.015	0.076	0.058
MGDG 38:5	0.000	0.000	0.000	0.000	0.000	0.000	0.006	0.009
MGDG 38:4	0.019	0.018	0.245	0.054	0.036	0.027	0.324	0.122
MGDG 38:3	0.009	0.013	0.012	0.027	0.087	0.083	0.001	0.002
<b>Total MGDG</b>	<b>50.605</b>	<b>3.835</b>	<b>40.106</b>	<b>2.209</b>	<b>54.709</b>	<b>1.345</b>	<b>39.271</b>	<b>2.298</b>
PC 32:0	0.006	0.001	0.007	0.000	0.011	0.001	0.017	0.004

PC 34:4	0.079	0.012	0.034	0.003	0.075	0.004	0.062	0.009
PC 34:3	1.635	0.264	1.652	0.148	1.720	0.031	2.886	0.530
PC 34:2	2.094	0.254	2.739	0.233	1.540	0.054	1.788	0.271
PC 34:1	0.333	0.048	0.467	0.022	0.076	0.011	0.078	0.024
PC 36:6	1.225	0.230	1.185	0.098	1.428	0.087	1.767	0.253
PC 36:5	2.955	0.451	2.996	0.166	2.499	0.095	2.070	0.445
PC 36:4	2.247	0.315	3.085	0.189	1.506	0.074	1.125	0.276
PC 36:3	0.919	0.117	1.444	0.034	0.372	0.018	1.213	0.287
PC 36:2	0.369	0.056	0.548	0.024	0.189	0.010	0.727	0.179
PC 36:1	0.000	0.000	0.000	0.000	0.001	0.001	0.000	0.000
PC 38:6	0.008	0.002	0.009	0.001	0.007	0.001	0.012	0.002
PC 38:5	0.030	0.004	0.035	0.004	0.018	0.001	0.028	0.006
PC 38:4	0.047	0.005	0.070	0.007	0.029	0.003	0.048	0.008
PC 38:3	0.052	0.005	0.070	0.004	0.027	0.002	0.044	0.005
PC 38:2	0.030	0.003	0.046	0.005	0.011	0.002	0.022	0.003
PC 40:5	0.002	0.001	0.002	0.001	0.004	0.000	0.004	0.002
PC 40:4	0.003	0.000	0.003	0.001	0.005	0.001	0.005	0.002
PC 40:3	0.003	0.000	0.004	0.001	0.002	0.000	0.005	0.001
PC 40:2	0.002	0.000	0.004	0.000	0.003	0.001	0.005	0.001
<b>Total PC</b>	<b>12.038</b>	<b>1.748</b>	<b>14.402</b>	<b>0.860</b>	<b>9.523</b>	<b>0.301</b>	<b>11.905</b>	<b>1.598</b>
LysoPC 16:1	0.000	0.000	0.000	0.000	0.000	0.000	0.000	0.000
LysoPC 16:0	0.005	0.001	0.008	0.000	0.005	0.001	0.013	0.004
LysoPC 18:3	0.010	0.001	0.014	0.002	0.008	0.002	0.012	0.006
LysoPC 18:2	0.013	0.002	0.020	0.003	0.007	0.001	0.012	0.005
LysoPC 18:1	0.002	0.000	0.005	0.001	0.000	0.000	0.001	0.001
LysoPC 18:0	0.002	0.000	0.005	0.001	0.001	0.001	0.011	0.005
<b>Total LysoPC</b>	<b>0.032</b>	<b>0.004</b>	<b>0.052</b>	<b>0.004</b>	<b>0.021</b>	<b>0.003</b>	<b>0.048</b>	<b>0.016</b>
LysoPE 16:1	0.000	0.000	0.000	0.000	0.000	0.000	0.000	0.001
LysoPE 16:0	0.023	0.002	0.034	0.006	0.016	0.002	0.031	0.007
LysoPE 18:3	0.013	0.002	0.016	0.003	0.009	0.003	0.016	0.002
LysoPE 18:2	0.021	0.003	0.035	0.003	0.014	0.001	0.021	0.003
LysoPE 18:1	0.001	0.001	0.003	0.001	0.000	0.001	0.001	0.001
<b>Total LysoPE</b>	<b>0.059</b>	<b>0.007</b>	<b>0.089</b>	<b>0.010</b>	<b>0.039</b>	<b>0.003</b>	<b>0.069</b>	<b>0.008</b>
PE 34:4	0.033	0.004	0.020	0.002	0.027	0.002	0.034	0.002
PE 34:3	1.881	0.279	2.039	0.166	1.624	0.072	3.097	0.466
PE 34:2	2.668	0.356	3.673	0.264	2.029	0.085	2.712	0.224
PE 34:1	0.000	0.000	0.000	0.000	0.001	0.001	0.000	0.000
PE 36:6	0.508	0.089	0.457	0.036	0.336	0.031	0.595	0.103
PE 36:5	1.470	0.239	1.607	0.114	1.024	0.050	1.384	0.159
PE 36:4	1.511	0.207	2.129	0.147	0.990	0.034	1.180	0.132
PE 36:3	0.370	0.052	0.573	0.045	0.217	0.009	0.765	0.162
PE 36:2	0.184	0.025	0.253	0.006	0.163	0.006	0.640	0.158
PE 36:1	0.005	0.002	0.007	0.001	0.001	0.001	0.000	0.000
PE 38:6	0.011	0.002	0.014	0.001	0.009	0.001	0.014	0.002
PE 38:5	0.021	0.003	0.030	0.004	0.012	0.000	0.027	0.002
PE 38:4	0.027	0.004	0.048	0.005	0.018	0.001	0.035	0.006
PE 38:3	0.043	0.008	0.052	0.004	0.021	0.002	0.056	0.008
PE 38:2	0.057	0.006	0.076	0.004	0.027	0.002	0.074	0.018
PE 40:3	0.030	0.004	0.033	0.003	0.025	0.001	0.065	0.010
PE 40:2	0.060	0.009	0.080	0.009	0.066	0.004	0.129	0.014

PE 42:4	0.014	0.002	0.014	0.001	0.017	0.001	0.016	0.004
PE 42:3	0.055	0.007	0.069	0.008	0.037	0.001	0.049	0.007
PE 42:2	0.059	0.012	0.080	0.006	0.060	0.005	0.087	0.017
<b>Total PE</b>	<b>9.006</b>	<b>1.296</b>	<b>11.253</b>	<b>0.756</b>	<b>6.703</b>	<b>0.240</b>	<b>10.960</b>	<b>1.169</b>
PG 32:1	0.414	0.069	0.390	0.034	0.458	0.049	0.366	0.026
PG 32:0	0.186	0.051	0.200	0.047	0.174	0.025	0.349	0.064
PG 34:4	5.976	0.545	8.776	0.850	7.440	0.625	6.851	0.796
PG 34:3	1.595	0.184	1.977	0.196	1.551	0.183	3.021	0.404
PG 34:2	1.290	0.133	1.409	0.065	0.732	0.089	1.539	0.095
PG 34:1	0.789	0.065	0.772	0.090	0.244	0.055	0.752	0.119
PG 34:0	0.011	0.011	0.016	0.015	0.004	0.006	0.236	0.064
<b>Total PG</b>	<b>10.261</b>	<b>0.944</b>	<b>13.541</b>	<b>1.097</b>	<b>10.604</b>	<b>0.870</b>	<b>13.113</b>	<b>1.032</b>
lysoPG 16:1	0.005	0.002	0.010	0.003	0.001	0.001	0.002	0.004
lysoPG 16:0	0.004	0.002	0.009	0.002	0.001	0.001	0.001	0.002
lysoPG 18:3	0.024	0.003	0.033	0.005	0.010	0.002	0.012	0.007
lysoPG 18:2	0.002	0.001	0.001	0.001	0.001	0.002	0.000	0.000
lysoPG 18:1	0.003	0.002	0.004	0.004	0.000	0.000	0.000	0.000
<b>Total lysoPG</b>	<b>0.038</b>	<b>0.003</b>	<b>0.057</b>	<b>0.006</b>	<b>0.013</b>	<b>0.003</b>	<b>0.015</b>	<b>0.008</b>
PA 34:6	0.001	0.001	0.000	0.000	0.000	0.001	0.000	0.000
PA 34:4	0.003	0.004	0.000	0.000	0.005	0.005	0.067	0.084
PA 34:3	0.112	0.032	0.080	0.010	0.133	0.050	0.645	0.769
PA 34:2	0.115	0.027	0.095	0.023	0.125	0.033	0.484	0.628
PA 34:1	0.051	0.013	0.126	0.045	0.001	0.002	0.018	0.014
PA 36:6	0.033	0.010	0.015	0.005	0.038	0.013	0.182	0.251
PA 36:5	0.067	0.024	0.039	0.008	0.074	0.027	0.291	0.424
PA 36:4	0.069	0.022	0.046	0.006	0.052	0.025	0.198	0.284
PA 36:3	0.022	0.008	0.014	0.007	0.015	0.005	0.153	0.170
PA 36:2	0.005	0.002	0.006	0.004	0.003	0.004	0.083	0.080
<b>Total PA</b>	<b>0.477</b>	<b>0.125</b>	<b>0.422</b>	<b>0.041</b>	<b>0.446</b>	<b>0.147</b>	<b>2.121</b>	<b>2.662</b>
PI 34:4	0.011	0.004	0.004	0.001	0.007	0.003	0.005	0.002
PI 34:3	0.976	0.200	1.057	0.055	1.108	0.094	1.526	0.043
PI 34:2	1.102	0.195	1.468	0.121	1.054	0.083	1.187	0.110
PI 34:1	0.000	0.000	0.002	0.004	0.000	0.000	0.000	0.000
PI 36:6	0.050	0.012	0.067	0.017	0.059	0.011	0.052	0.011
PI 36:5	0.074	0.011	0.077	0.005	0.051	0.006	0.043	0.013
PI 36:4	0.082	0.014	0.106	0.008	0.036	0.008	0.030	0.015
PI 36:3	0.099	0.017	0.124	0.010	0.066	0.013	0.179	0.032
PI 36:2	0.066	0.013	0.084	0.003	0.046	0.007	0.137	0.037
PI 36:1	0.005	0.003	0.010	0.002	0.005	0.007	0.015	0.015
<b>Total PI</b>	<b>2.464</b>	<b>0.446</b>	<b>2.999</b>	<b>0.192</b>	<b>2.433</b>	<b>0.189</b>	<b>3.172</b>	<b>0.134</b>
PS 34:4	0.000	0.000	0.000	0.000	0.000	0.001	0.000	0.000
PS 34:3	0.048	0.009	0.059	0.006	0.074	0.002	0.097	0.010
PS 34:2	0.049	0.005	0.077	0.010	0.076	0.003	0.083	0.010
PS 34:1	0.000	0.000	0.000	0.000	0.001	0.001	0.000	0.000
PS 36:6	0.002	0.000	0.002	0.001	0.002	0.000	0.002	0.001
PS 36:5	0.004	0.001	0.006	0.001	0.006	0.001	0.006	0.002
PS 36:4	0.007	0.002	0.009	0.002	0.007	0.001	0.009	0.002
PS 36:3	0.026	0.004	0.032	0.003	0.031	0.001	0.061	0.008
PS 36:2	0.020	0.002	0.026	0.005	0.023	0.002	0.034	0.004
PS 36:1	0.000	0.000	0.001	0.001	0.000	0.001	0.001	0.001

PS 38:6	0.000	0.000	0.000	0.000	0.000	0.000	0.000	0.000
PS 38:5	0.000	0.000	0.001	0.001	0.000	0.001	0.001	0.001
PS 38:4	0.003	0.001	0.003	0.001	0.001	0.000	0.002	0.001
PS 38:3	0.024	0.004	0.026	0.004	0.021	0.001	0.035	0.005
PS 38:2	0.023	0.001	0.029	0.005	0.020	0.003	0.029	0.004
PS 38:1	0.000	0.000	0.000	0.000	0.000	0.000	0.000	0.000
PS 40:4	0.000	0.001	0.001	0.001	0.001	0.000	0.002	0.001
PS 40:3	0.030	0.006	0.034	0.004	0.025	0.002	0.057	0.006
PS 40:2	0.037	0.004	0.050	0.006	0.031	0.003	0.054	0.006
PS 40:1	0.000	0.000	0.001	0.001	0.000	0.000	0.000	0.001
PS 42:4	0.010	0.001	0.010	0.001	0.012	0.001	0.015	0.004
PS 42:3	0.051	0.008	0.060	0.010	0.069	0.003	0.091	0.017
PS 42:2	0.045	0.008	0.063	0.009	0.054	0.002	0.070	0.011
PS 42:1	0.000	0.000	0.000	0.000	0.001	0.001	0.000	0.000
PS 44:3	0.001	0.001	0.001	0.001	0.002	0.000	0.003	0.001
PS 44:2	0.003	0.001	0.003	0.001	0.003	0.001	0.003	0.001
<b>Total PS</b>	<b>0.383</b>	<b>0.047</b>	<b>0.495</b>	<b>0.039</b>	<b>0.461</b>	<b>0.008</b>	<b>0.656</b>	<b>0.049</b>
	<b>100.000</b>	<b>0.000</b>	<b>100.000</b>	<b>0.000</b>	<b>100.000</b>	<b>0.000</b>	<b>100.000</b>	<b>0.000</b>

Table 5-2 Lipid profiles of WT (Col), *atgpdhc* and *atgpdhp* mutants in mol % of total lipids

Sample description	WT (Col)		<i>atgpdhc</i>		<i>atgpdhp</i>	
	ave	stdev	ave	stdev	ave	stdev
DGDG 34:6	1.407	0.042	1.275	0.163	1.403	0.124
DGDG 34:5	0.082	0.025	0.090	0.045	0.123	0.056
DGDG 34:4	0.118	0.011	0.110	0.017	0.144	0.041
DGDG 34:3	2.779	0.175	3.070	0.189	3.152	0.198
DGDG 34:2	0.491	0.036	0.466	0.041	0.527	0.072
DGDG 34:1	0.236	0.025	0.197	0.027	0.225	0.059
DGDG 36:6	9.024	0.293	9.436	0.600	9.555	0.502
DGDG 36:5	0.000	0.000	0.000	0.000	0.000	0.000
DGDG 36:4	0.255	0.042	0.226	0.028	0.286	0.057
DGDG 36:3	0.126	0.011	0.137	0.034	0.106	0.027
DGDG 36:2	0.010	0.006	0.004	0.009	0.008	0.008
DGDG 36:1	0.003	0.004	0.004	0.009	0.000	0.001
DGDG 38:6	0.082	0.032	0.096	0.050	0.084	0.014
DGDG 38:5	0.003	0.004	0.001	0.001	0.000	0.000
DGDG 38:4	0.002	0.002	0.009	0.011	0.006	0.011
DGDG 38:3	0.001	0.002	0.000	0.000	0.000	0.000
<b>Total DGDG</b>	<b>14.620</b>	<b>0.495</b>	<b>15.121</b>	<b>0.670</b>	<b>15.620</b>	<b>0.814</b>
MGDG 34:6	39.112	2.353	35.845	3.434	34.405	1.720
MGDG 34:5	0.000	0.000	0.000	0.000	0.000	0.000
MGDG 34:4	0.987	0.129	0.961	0.148	1.013	0.148
MGDG 34:3	0.367	0.044	0.286	0.103	0.340	0.076
MGDG 34:2	0.182	0.042	0.110	0.088	0.177	0.082
MGDG 34:1	0.095	0.099	0.141	0.106	0.126	0.075
MGDG 36:6	7.437	0.483	8.642	1.429	7.531	0.531
MGDG 36:5	0.006	0.014	0.068	0.113	0.005	0.010
MGDG 36:4	0.663	0.163	0.723	0.276	0.772	0.092
MGDG 36:3	0.031	0.031	0.042	0.071	0.057	0.055
MGDG 36:2	0.002	0.005	0.000	0.000	0.022	0.020
MGDG 36:1	0.001	0.002	0.000	0.000	0.003	0.006
MGDG 38:6	0.000	0.000	0.000	0.000	0.000	0.000
MGDG 38:5	0.001	0.002	0.000	0.000	0.000	0.000
MGDG 38:4	0.042	0.021	0.062	0.106	0.063	0.065
MGDG 38:3	0.006	0.013	0.008	0.018	0.000	0.000
<b>Total MGDG</b>	<b>48.932</b>	<b>1.902</b>	<b>46.888</b>	<b>3.260</b>	<b>44.511</b>	<b>1.841</b>
PG 32:1	0.371	0.012	0.384	0.076	0.436	0.024
PG 32:0	0.196	0.025	0.267	0.023	0.205	0.030
PG 34:4	6.874	0.239	6.567	0.679	7.140	0.315
PG 34:3	1.692	0.198	2.210	0.195	1.931	0.083
PG 34:2	1.272	0.074	1.227	0.129	1.344	0.060
PG 34:1	0.650	0.071	0.691	0.093	0.750	0.052
PG 34:0	0.017	0.019	0.021	0.008	0.006	0.008
<b>Total PG</b>	<b>11.073</b>	<b>0.393</b>	<b>11.367</b>	<b>0.978</b>	<b>11.811</b>	<b>0.401</b>
lysoPG 16:1	0.003	0.001	0.004	0.002	0.001	0.001
lysoPG 16:0	0.002	0.001	0.001	0.001	0.001	0.001
lysoPG 18:3	0.017	0.003	0.017	0.003	0.020	0.004
lysoPG 18:2	0.001	0.001	0.000	0.001	0.001	0.001
lysoPG 18:1	0.000	0.001	0.001	0.000	0.001	0.001
Total lysoPG	0.023	0.002	0.024	0.004	0.023	0.006
LysoPC 16:1	0.000	0.000	0.000	0.000	0.000	0.000

LysoPC 16:0	0.004	0.001	0.004	0.000	0.004	0.000
LysoPC 18:3	0.005	0.001	0.005	0.001	0.006	0.001
LysoPC 18:2	0.006	0.001	0.007	0.001	0.007	0.001
LysoPC 18:1	0.001	0.000	0.001	0.001	0.001	0.000
LysoPC 18:0	0.001	0.001	0.001	0.001	0.001	0.001
Total LysoPC	0.017	0.002	0.018	0.002	0.019	0.002
LysoPE 16:1	0.000	0.000	0.000	0.000	0.000	0.000
LysoPE 16:0	0.018	0.003	0.018	0.002	0.020	0.003
LysoPE 18:3	0.007	0.001	0.009	0.000	0.009	0.002
LysoPE 18:2	0.014	0.002	0.015	0.002	0.016	0.002
LysoPE 18:1	0.001	0.001	0.001	0.001	0.001	0.000
Total LysoPE	0.041	0.004	0.043	0.002	0.046	0.004
PC 32:0	0.006	0.001	0.006	0.001	0.006	0.001
PC 34:4	0.092	0.005	0.096	0.009	0.101	0.009
PC 34:3	1.777	0.057	2.021	0.178	2.046	0.170
PC 34:2	2.321	0.123	2.448	0.219	2.642	0.157
PC 34:1	0.286	0.056	0.289	0.056	0.311	0.034
PC 36:6	1.204	0.051	1.434	0.135	1.386	0.122
PC 36:5	3.158	0.171	3.447	0.240	3.527	0.209
PC 36:4	2.261	0.193	2.359	0.327	2.484	0.183
PC 36:3	0.870	0.124	0.866	0.145	0.895	0.110
PC 36:2	0.357	0.043	0.343	0.049	0.378	0.036
PC 36:1	0.000	0.000	0.000	0.000	0.000	0.000
PC 38:6	0.009	0.001	0.011	0.001	0.011	0.002
PC 38:5	0.029	0.002	0.031	0.003	0.031	0.002
PC 38:4	0.048	0.004	0.052	0.006	0.053	0.005
PC 38:3	0.055	0.003	0.057	0.005	0.057	0.006
PC 38:2	0.032	0.002	0.034	0.003	0.032	0.002
PC 40:5	0.003	0.000	0.005	0.001	0.004	0.000
PC 40:4	0.007	0.001	0.007	0.001	0.007	0.001
PC 40:3	0.006	0.001	0.007	0.002	0.007	0.001
PC 40:2	0.003	0.000	0.004	0.001	0.004	0.000
Total PC	12.524	0.798	13.516	1.105	13.980	0.560
PE 34:4	0.036	0.003	0.036	0.003	0.039	0.003
PE 34:3	1.908	0.087	1.986	0.159	2.090	0.114
PE 34:2	2.991	0.152	2.979	0.260	3.262	0.203
PE 34:1	0.000	0.000	0.000	0.000	0.000	0.000
PE 36:6	0.364	0.017	0.412	0.041	0.424	0.036
PE 36:5	1.408	0.081	1.453	0.120	1.552	0.083
PE 36:4	1.752	0.074	1.714	0.128	1.896	0.063
PE 36:3	0.349	0.045	0.363	0.046	0.396	0.037
PE 36:2	0.208	0.025	0.192	0.018	0.225	0.017
PE 36:1	0.004	0.003	0.004	0.004	0.004	0.003
PE 38:6	0.010	0.000	0.012	0.001	0.012	0.001
PE 38:5	0.022	0.001	0.022	0.002	0.023	0.001
PE 38:4	0.025	0.002	0.027	0.004	0.029	0.003
PE 38:3	0.035	0.002	0.039	0.004	0.038	0.005
PE 38:2	0.055	0.002	0.058	0.004	0.055	0.004
PE 40:3	0.029	0.002	0.030	0.003	0.037	0.003
PE 40:2	0.075	0.008	0.071	0.007	0.083	0.007
PE 42:4	0.015	0.001	0.016	0.001	0.017	0.003
PE 42:3	0.063	0.006	0.060	0.004	0.071	0.005
PE 42:2	0.076	0.007	0.067	0.004	0.079	0.005
Total PE	9.425	0.487	9.539	0.743	10.328	0.485
PI 34:4	0.010	0.002	0.012	0.005	0.012	0.002
PI 34:3	1.004	0.070	1.078	0.154	1.179	0.157

PI 34:2	1.272	0.069	1.257	0.111	1.403	0.172
PI 34:1	0.000	0.000	0.000	0.000	0.000	0.000
PI 36:6	0.045	0.006	0.054	0.006	0.052	0.009
PI 36:5	0.065	0.005	0.070	0.004	0.077	0.004
PI 36:4	0.067	0.007	0.063	0.007	0.067	0.004
PI 36:3	0.078	0.010	0.082	0.014	0.097	0.013
PI 36:2	0.063	0.007	0.066	0.014	0.073	0.006
PI 36:1	0.004	0.002	0.006	0.003	0.001	0.001
<b>Total PI</b>	<b>2.610</b>	<b>0.124</b>	<b>2.688</b>	<b>0.209</b>	<b>2.961</b>	<b>0.321</b>
PS 34:4	0.000	0.000	0.000	0.000	0.000	0.000
PS 34:3	0.050	0.005	0.049	0.004	0.053	0.006
PS 34:2	0.055	0.004	0.057	0.004	0.062	0.005
PS 34:1	0.001	0.000	0.000	0.000	0.000	0.000
PS 36:6	0.002	0.000	0.002	0.001	0.002	0.001
PS 36:5	0.005	0.001	0.005	0.001	0.004	0.001
PS 36:4	0.007	0.001	0.007	0.002	0.007	0.001
PS 36:3	0.025	0.005	0.028	0.004	0.028	0.001
PS 36:2	0.025	0.004	0.027	0.004	0.030	0.004
PS 36:1	0.000	0.000	0.000	0.000	0.000	0.000
PS 38:6	0.000	0.000	0.000	0.000	0.000	0.000
PS 38:5	0.000	0.000	0.001	0.000	0.001	0.000
PS 38:4	0.002	0.001	0.002	0.001	0.002	0.001
PS 38:3	0.022	0.005	0.025	0.003	0.025	0.003
PS 38:2	0.026	0.005	0.027	0.003	0.028	0.002
PS 38:1	0.000	0.000	0.000	0.001	0.000	0.000
PS 40:4	0.000	0.000	0.000	0.001	0.001	0.000
PS 40:3	0.027	0.003	0.030	0.003	0.031	0.002
PS 40:2	0.039	0.008	0.041	0.005	0.039	0.002
PS 40:1	0.000	0.001	0.000	0.001	0.000	0.000
PS 42:4	0.009	0.001	0.011	0.002	0.010	0.001
PS 42:3	0.051	0.003	0.058	0.006	0.058	0.009
PS 42:2	0.056	0.007	0.055	0.007	0.058	0.009
PS 42:1	0.000	0.000	0.000	0.000	0.000	0.000
PS 44:3	0.001	0.001	0.002	0.001	0.001	0.000
PS 44:2	0.002	0.001	0.003	0.000	0.003	0.001
<b>Total PS</b>	<b>0.406</b>	<b>0.045</b>	<b>0.431</b>	<b>0.032</b>	<b>0.443</b>	<b>0.022</b>
PA 34:6	0.001	0.001	0.000	0.000	0.001	0.001
PA 34:4	0.000	0.000	0.006	0.005	0.003	0.006
PA 34:3	0.090	0.026	0.095	0.015	0.073	0.022
PA 34:2	0.096	0.020	0.105	0.016	0.085	0.008
PA 34:1	0.029	0.008	0.037	0.008	0.000	0.000
PA 36:6	0.020	0.005	0.020	0.006	0.020	0.004
PA 36:5	0.037	0.008	0.040	0.007	0.033	0.011
PA 36:4	0.038	0.015	0.039	0.008	0.031	0.004
PA 36:3	0.015	0.004	0.015	0.004	0.009	0.005
PA 36:2	0.005	0.003	0.005	0.004	0.002	0.002
<b>Total PA</b>	<b>0.330</b>	<b>0.071</b>	<b>0.364</b>	<b>0.041</b>	<b>0.258</b>	<b>0.040</b>
<b>Total</b>	<b>100.000</b>	<b>0.000</b>	<b>100.000</b>	<b>0.000</b>	<b>100.000</b>	<b>0.000</b>